M. LORENZ

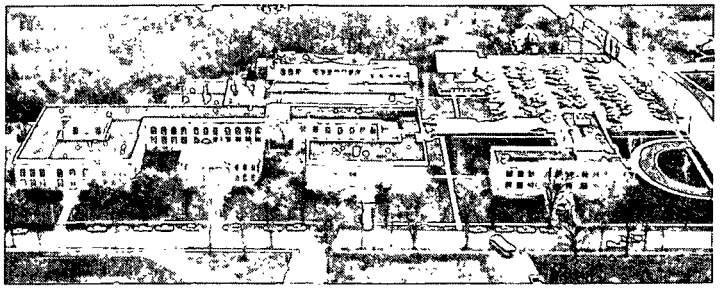

THE INSTITUTE OF PAPER CHEMISTRY, APPLETON, WISCONSIN

STATUS REPORTS

To The

PAPER PROPERTIES AND USES

PROJECT ADVISORY COMMITTEE

March 22-23, 1989

The Institute of Paper Chemistry
Continuing Education Center
Appleton, Wisconsin

NOTICE & DISCLAIMER

The Institute of Paper Chemistry (IPC) has provided a high standard of professional service and has exerted its best efforts within the time and funds available for this project. The information and conclusions are advisory and are intended only for the internal use by any company who may receive this report. Each company must decide for itself the best approach to solving any problems it may have and how, or whether, this reported information should be considered in its approach.

IPC does not recommend particular products, procedures, materials, or services. These are included only in the interest of completeness within a laboratory context and budgetary constraint. Actual products, procedures, materials, and services used may differ and are peculiar to the operations of each company.

In no event shall IPC or its employees and agents have any obligation or liability for damages, including, but not limited to, consequential damages, arising out of or in connection with any company's use of, or inability to use, the reported information. IPC provides no warranty or guaranty of results.

This information represents a review of on-going research for use by the Project Advisory Committees. The information is not intended to be a definitive progress report on any of the projects and should not be cited or referenced in any paper or correspondence external to your company.

Your advice and suggestions on any of the projects will be most welcome.

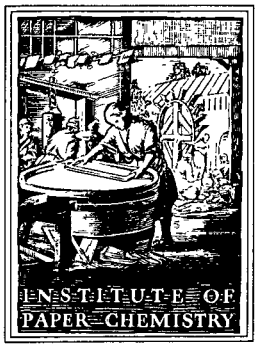

THE INSTITUTE OF PAPER CHEMISTRY
Post Office Box 1039
Appleton, Wisconsin 54912
Phone: 414/734-9251
FAX: 414/738-3448
Telex: 469289

March 2, 1989

TO: MEMBERS OF PAPER PROPERTIES AND USES PROJECT ADVISORY COMMITTEE

Attached for your review are the Status Reports for the projects to be discussed at the Paper Properties and Uses PAC meeting scheduled for March 22-23, 1989, in Appleton. A meeting agenda can be found inside the booklet.

For those of you staying at the Continuing Education Center, the attached pink card gives the combination to the front door so that you may gain entrance if you arrive after the doors are locked. Room schedules are posted in the lobby. If you have not indicated whether you will be attending the meeting or have not yet reserved a room, please do so by notifying Sheila Burton at 414/738-3259.

We look forward to seeing you on March 22-23. Best regards.

Sincerely yours,

Maclin S. Hall
Acting Director
Paper Materials Division

MSH/sb
Enclosure

March 16, 1989

INFLUENCE OF RETENTION AID POINT OF ADDITION ON RETENTION AND SHEET PROPERTIES

BACKGROUND

Previous studies on the addition of cationic polymers to the components of papermaking furnishes have shown that the distribution of adsorption of these polymers onto the components is related to the charge, as well as the surface areas of the components. In sample wood pulp furnishes, the major components are long fibers and fines. Although the surface charge is usually similar for both the long fiber and the fines, the much larger surface area of the fines usually results in the predominant adsorption onto fines. The preferential adsorption onto fines has been demonstrated for cationic starches, cationic wet strength resins, as well as other cationic polyelectrolytes.

Stratton previously studied the influence of cationic polymer addition on sheet properties with polyamine-polyamide-epichlorohydrin wet strength resin. Addition of this cationic polymer to the long fiber fraction, followed by addition of fines and subsequent formation into handsheets resulted in sheets with enhanced strength properties relative to sheets made with polymer addition to the whole furnish. Dry strength increased 12%, while wet strength increased 14%. It was concluded that addition of the wet strength resin to only the long fiber would provide

improved strength properties; however, in order to apply this in a mill situation, it would require fractionation of the pulp. The expense of fractionation most likely precludes mill application of this method for improving the strength of paper.

Goulet has studied the adsorption of retention aids onto the components of pulp. His work showed that, once again, the fines adsorb more polymer on a weight basis than the long fiber fraction. This study, however, did not look at the influence this adsorption would have on retention or sheet properties.

While the mechanism by which retention aids improve retention of fines and fillers is still under debate, it is generally assumed that adsorption of the polymer onto one or more of the components of the furnish is necessary for them to be effective. Since studies of wet strength resin addition to fiber components showed differences in sheet properties depending on where the polymer was adsorbed, it was of interest to determine whether adsorption of retention aid onto the components of pulps would influence the sheet properties.

EXPERIMENTAL

A southern pine fully bleached kraft pulp was beaten to three different freeness levels; 600 CSF, 400 CSF, and 200 CSF. These were then individually run over the IPC web former to separate the fines from the long fiber. The fines were collected and were allowed to settle to increase the consistency. The long fiber fractions were kept separate and stored in plastic bags in

a cold room for later use. Simulated pulps were made by adding fines to the long fiber fractions. For both the 600 CSF and 400 CSF long fiber fractions, 10% and 30% fines additions were used.

Retention studies were done using the Britt Dynamic Draining Jar (DDJ). Initially, the long fiber, the appropriate amount of fines and polymer (either 1/2 lb/ton or 1 lb/ton) were added to the slurry, and the suspension was agitated for 5 minutes at 0.25% consistency. The turbulence level was then increased, and approximately 100 ml of sample were drained from the jar. The fines content of the sample was determined. Addition of polymer to the components of the pulp was done by adding the polymer to a suspension of either the long fiber or the fines in the DDJ. This was agitated for three minutes; then the appropriate amounts of either long fiber or fines were added, and agitation continued for two more minutes before obtaining a retention sample. The retentions obtained with the different permutations are shown in Table 1.

The same sequence was repeated to obtain samples of fines for determination of electrophoretic mobility. These determinations were made with the Malvern Zetasizer. The results of these measurements are shown in Table 2.

The determination of the influence of retention aid on sheet properties was done by making handsheets where the retention aid was added to the fines, allowed sufficient time to adsorb, then

the long fiber was added, and handsheets were formed. Addition of retention aid to the long fiber prior to mixing with fines was not done because it is unlikely that this type of fractionation would be carried out in a mill. In addition, the retention levels determined with the DDJ for this sequence gave poorer retention, in general, than addition to the whole furnish. The physical properties of these sheets are shown in Table 3.

RESULTS AND DISCUSSION

The physical properties of the handsheets made by adding retention aid either to the whole furnish or just to the fines show that there is little influence on the sheet characteristics. There is some reduction in breaking length, as well as slight increases in the density when the retention aid is added to the fines relative to addition to the whole furnish. Interestingly, while the strength goes down and density increases, the porosity either stays the same or increases. It is suspected that the location of the fines in the sheet is altered by addition of the retention aid to the fines, and this causes the changes in strength, density, and porosity. This aspect is under continuing investigation.

When cationic polymers are added to whole beaten pulps, the cationic materials will absorb onto the components of the pulp in amounts roughly proportional to the surface areas of the components. The surface area of the fines portion can be many times the surface area of the long fiber fractination (0.5 to 1.5

m^2/g). Consequently, the fines will adsorb cationic polymers in relation to their overall surface area contribution to the whole furnish. This has been amply demonstrated in studies with cationic starches, polyethylenimines, and cationic polyacrylamides. When cationic wet strength resin (a polyamine-polyamide-epichlorohydren polymer) is added to the long fiber fraction of pulp and the treated long fibers are then mixed with fines, the resulting strength properties of sheets made from this furnish are improved over the strength properties of sheets made by the addition of polymer to a mixture of long fiber and fines. Adsorption of polymer onto the long fiber and the fines in relation to their weight fraction in the furnish (as opposed to the surface area contributions) provided increases in strength relative to controls, but these increases were not as great as when the polymer was preferentially adsorbed onto the long fiber only. These results suggest that adsorption of polymers onto different components of pulp will influence their performance.

Retention aids are cationic polymers added to papermaking furnishes to improve the retention of fines and fillers. It is generally assumed that these polymers adsorb onto the surfaces of fibers or fines and bring about improved retention either through attachment of the fines to the long fibers or through agglomeration of the fines to form larger, more easily retained particles.

The present study was designed to investigate whether addition of retention aid to the components of pulp will influence the retention or the sheet properties. A single pulp was used in this investigation, and although it is suspected that not all pulps will respond in the same manner, it has been assumed that similar results would be obtained with other pulps.

The retention studies using the Britt Dynamic Drainage Jar (DDT) show that addition of retention aid to the fines only provides as good, if not better, retention than addition of polymer to the whole furnish. If it is assumed that adsorption of retention aid onto fines is important to overall retention, then this result is easily understood. Simple addition of polymer to the whole furnish should result in adsorption of between 50 and 95% of the polymer onto the fines depending on the amount of fines present as well as the amount of polymer added. Addition of polymer to the fines only will result in higher levels of polymer adsorbed onto the fines. This could be from 70 to 99+%, again depending on the amounts of fines and polymer. On the average, addition of polymer to the fines only improves retention (63% avg. retention @ 1/2 pound/ton polymer vs. avg. of 54% retention by addition to whole furnish; with one pound of polymer, the average retentions are 73% and 60% respectively). The poorest retention was observed when polymer was added to the long fiber fraction (52% retention with 1/2 pound polymer and 56% retention with 1 pound of polymer).

In general, the electrophoretic mobility of the fibers closely paralleled the retention of the fines. It was expected that increasing polymer dosage would provide a more positive electrophoretic mobility. The electrophoretic mobilities of the fines from addition of polymer to the whole furnish and to just the fines were more positive than the mobilities of fines treated with 1/2 lb. of polymer. It would be expected that fines from addition of polymer to the fines only should be more positive than fines from polymer addition to the whole furnish. This is true at the 1 lb/ton level, but at the lower dosage, the opposite is true. It is not clear why this occurs, but it may relate to the system, such that not all of the fines surfaces contain adsorbed cationic polymer. Addition of polymer to the long fiber fraction provides very little change in the electrophoretic mobility of unretained fines. This is not unreasonable if one assumes that all of the polymer has been adsorbed onto the long fiber.

Finally, the handsheet data indicates that addition of the polymer to the fines provides slight decreases in breaking length (overall average of 3.5%), small increases in density (overall average of 3.5%) and indications of sheets with higher porosity when adjusted to similar density. Whether the differences in porosity indicate differences in the way the fines are retained in the sheet is not known but is under investigation.

Interestingly, there appears to be little influence of retention and point of addition on formation. In general, sheets formed after addition of polymer to the fines only had very similar formation to the corresponding sheets made by addition to the whole furnish.

The conclusions resulting from this study are that point of addition of retention aid can influence the retention of fines without significant changes in the overall properties of the sheet. This implies that, if possible, to obtain maximum efficiency of retention aids in papermaking operations, the retention aid should be added to the fines. This is not easy to do in many papermaking operations but could be done in some twin wire formed tissue operations where first pass retention may be only 50-60%. Addition of retention aid to the fines laden recycle from the Saveall could substitute for addition to the whole furnish, thereby either improving overall retention or reducing the amount of retention aid necessary to obtain a given level of retention.

Table 1

BRITT JAR RETENTION*

	No Polymer	Polymer To Whole Furnish	Polymer To Fines	Polymer To Long Fiber
600 CSF				
10% Fines	59			
30% Fines	48			
10% Fines + 1/2#/T		69	79	57
10% Fines + 1#/T		67	82	70
30% Fines + 1/2#/T		59	62	49
30% Fines + 1#/T		63	71	62
400 CSF				
10% Fines	32			
30% Fines	46			
10% Fines + 1/2#/T		34	62	49
10% Fines + 1#/T		47	75	52
30% Fines + 1/2#/T		54	51	52
30% Fines + 1#/T		62	63	42

* Percent of Fines Retained

D. Hollenberg 3/89

Table 2

ZETASIZER ELECTROPHORETIC MOBILITY
(μ-cm/v-sec.)

	No Polymer	Polymer To Long Fiber	Polymer To Fines	Polymer To Whole Furnish
Fines Only				
Fines (10%)	-1.24			
Fines (30%)	-1.08			
Fines (10%) + 1/2#/T			-0.64	
Fines (10%) + 1#/T			+0.15	
Fines (30%) + 1/2#/T			-0.89	
Fines (30%) + 1#/T			-0.71	
Fines + Long Fiber (600 CSF)				
Fines (10%) + 1/2#/T		-1.09	-0.98	-0.90
Fines (10%) + 1#/T		-0.95	-0.54	-0.65
Fines (30%) + 1/2#/T		-1.15	-1.00	-0.91
Fines (30%) + 1#/T		-0.99	-0.86	-0.95
Fines (10%)	-1.21			
Fines (30%)	-1.00			

D. Hollenberg 3/89

Table 3

HANDSHEET DATA

	Retention Aid	Density (g/cm^3)	Breaking Length (km)	Gurley Porosity (sec.)	Rel. Formation**
600 CSF					
Whole Pulp		.591	3.70	0	4
	+ 1/2#/T	.592	3.63	0	2
	+ 1#/T	.606	3.63	0	3
Control-Classified		.547	2.76	0	7
	+ 1/2 #/T	.560	2.73	0	10
	+ 1#/T	.562	2.82	0	11
10% Fines		.615	4.04	1	11
	+ 1/2#/T	.620 (.644)*	4.11 (3.85)	1 (1)	5 (6)
	+ 1#/T	.629 (.641)	4.25 (3.98)	1 (0)	15 (16)
30% Fines		.741	5.82	149	19
	+ 1/2#/T	.763 (.780)	5.35 (5.47)	295 (250)	24 (26)
	+ 1#/T	.750 (.775)	5.57 (5.42)	284 (305)	29 (28)
400 CSF					
Control-Classified		.614	3.29	0	1
	+ 1/2#/T	.604	3.32	0	14
	+ 1#/T	.589	3.22	0	19
10% Fines		.638	4.69		9
	+ 1/2#/T	.660 (.687)	4.47 (4.25)	6 (3)	17 (8)
	+ 1#/T	.684 (.698)	4.54 (4.63)	5 (2)	11 (17)
30% Fines		.785	6.39	744	25
	+ 1/2#/T	.805 (.841)	6.19 (5.84)	537 (373)	22 (21)
	+ 1#/T	.815 (.871)	5.69 (5.80)	364 (528)	27 (23)

* Numbers in parentheses are for sheets made with polymer added to fines.

** Ranked according to formation index obtained from Robotest formation tester.

D. Hollenberg 3/89

TABLE OF CONTENTS

AGENDA

PAPER PROPERTIES AND USES
PROJECT ADVISORY COMMITTEE

March 22-23, 1989
The Institute of Paper Chemistry
Continuing Education Center (CEC)
Appleton, WI

Wednesday -- March 22

		Staff
7:15 a.m.	BREAKFAST (CEC Dining Room)	
8:30	Welcome/Introductions	Betz/Hall
8:45	Status of IPC Move to Atlanta	Yeske
9:15	PROJECT REVIEWS	
	Board Properties and Performance	Whitsitt/ Halcomb/Dees
	Internal Strength Enhancement	Stratton/ Hollenberg
	Student Presentation	Miller
12:00 noon	LUNCH (CEC Dining Room)	
1:00	PROJECT REVIEWS	
	Strength Improvement and Failure Mechanisms	Waterhouse/ Students
	Process, Properties, Product Relationships	Habeger/Pan
	Board Optical Transmission Meter	Hardacker
	Fundamentals of Paper Surface Wettablity	Etzler
	On-Line Measurement of Paper Mechanical Properties	Hall
5:15	SOCIAL TIME	
6:00	DINNER (CEC Dining Room)	

Thursday -- March 23

7:15 a.m.	BREAKFAST (CEC Dining Room)
8:00	COMMITTEE DISCUSSION OF PROJECTS (Krannert 108/109)
11:30	ADJOURNMENT/LUNCH (CEC Dining Room)

NEXT MEETING: October 18-19, 1989

PAPER PROPERTIES AND USES
PROJECT ADVISORY COMMITTEE

Mr. Dennis Betz, Chairman -- 6/90*
Assistant Research Director
P. H. Glatfelter Co.
228 S. Main Street
Spring Grove, PA 17362
(717) 225-4711

Dr. Keith A. Bennett -- 6/91
Senior Research Scientist
Weyerhaeuser Paper Company
WTC 2B42
Tacoma, WA 98477
(206) 924-6714

Dr. Robert L. Beran -- 6/89
Research Director
Westvaco Corporation
Covington Research Center
Washington Avenue
Covington, VA 24426
(703) 962-2111

Dr. Keith E. Bradway -- 6/91
Senior Research Scientist
Union Camp Corporation
P.O. Box 3301
Princeton, NJ 08543
(609) 896-1200

Dr. Von L. Byrd -- 6/91
Manager, End-Use Performance
Mead Corporation
Central Research Laboratories
8th & Hickory Streets
Chillicothe, OH 45601
(614) 772-3539

Mr. Richard P. Grant -- 6/89
Senior Engineer
Eastman Kodak Company
1669 Lake Avenue
Bldg. 36
Rochester, NY 14650
(716) 477-6537

Mr. Keith A. Kraft -- 6/91
Development Engineering Specialist
Minnesota Mining & Manufacturing Company
Carbonless Products Dept.
3M Center, Bldg 235 1E-33
St. Paul, MN 55144
(612) 736-4545

Mr. Thomas L. Lord -- 6/89
Director Communication Papers
James River Corporation
Neenah Technical Center
1915 Marathon Avenue
Neenah, WI 54956
(414) 729-8091

Dr. Leslie L. Martin -- 6/91
Senior Research Engineer
Potlatch Corporation
Fiber R & D, East End
Cloquet, MN 55720
(218) 879-2387

Dr. James J. Nault -- 6/90
Assistant Papermill Superintendent
Stone Container Corporation
P.O. Box 201
Hopewell, VA 23860
(804) 541-9754

Dr. Robert J. Niebauer -- 6/91
Project Manager, R&D
Crane & Co., Inc.
30 South St.
Dalton, MA 01226
(413) 684-2600

Mr. Lowell Schleicher -- 6/89
Director of Basic Research
Appleton Papers Inc.
P.O. Box 359
Appleton, WI 54912
(414) 735-8857

*Date of retirement from committee.

PAC Project Advisory Committee continued.

Mr. Robert L. Smathers -- 6/89
Manager, Technical Services
MacMillan Bloedel Inc.
P.O. Box 336
Pine Hill, AL 36769
(205) 963-4391

Mr. David South -- 6/89
Director of Market Planning & Prod. Dev.
Chesapeake Corporation
P.O. Box 311
West Point, VA 23181
(804) 843-5252

Mr. Quinton W. Vancleave -- 6/90
Technical Manager
Kraft Paper and Paperboard Kraft
Georgia Pacific Corporation
133 Peachtree Street
Atlanta, GA 30303
(404) 521-5903

Mr. Dale C. Woodward -- 6/91
Mgr., Process Control Technology
Nekoosa Packaging
1660 Indian Wood Circle
P.O. Box 697
Toledo, OH 43694-0697
(419) 891-5990

THE INSTITUTE OF PAPER CHEMISTRY

Appleton, Wisconsin

Status Report

to the

PAPER PROPERTIES AND USES

PROJECT ADVISORY COMMITTEE

Project 3571

BOARD PROPERTIES AND PERFORMANCE

March 22-23, 1989

PROJECT SUMMARY

PROJECT NO. 3571: BOARD PROPERTIES AND PERFORMANCE February 13, 1989

PROJECT STAFF: W. J. Whitsitt, R. A. Halcomb, J. Dees

PROGRAM GOAL:

Develop relationships between critical paper and board property parameters and how they are achieved in terms of raw material selection, principles of sheet design, and processing conditions.

PROJECT OBJECTIVE:

- To develop relationships between container performance, combined board and component properties.

- To improve the performance/cost ratios of combined board (including medium).

- The short term goals are directed to (1) using structural models to assess the impact of papermaking factors on combined board and box performance and (2) improving liner and medium end-use and converting performance properties.

PROJECT RATIONALE, PREVIOUS ACTIVITY AND PLANNED ACTIVITY FOR FISCAL 1988-89 are on the Project Form that follows.

SUMMARY OF RESULTS LAST PERIOD: (March 1988 - October 1988)

Section 1 - Combined Board Warp -- Liner Orientation Effects

(1) Past Institute research shows that the shape, elastic stiffness vs. orientation diagrams (termed polar plots) can vary greatly across paper machines depending on wet-end conditions. These variations of shape, area, and angle of lean are known to correlate with converting or end-use performance of some papers. For example, variations in the polar angle of lean could affect the development of twist warp in the manufacture of combined board.

(2) Therefore, a study is being carried out to determine the effects of combining single- and double-face (SF and DF) liners with polar angles ranging up to 15 degrees from the MD of the corrugated board on warp development.

(3) When SF and DF liners with polar angles deviating in opposite directions were combined into corrugated board, major twist warp occurred as moisture content changed. The degree of twist warp increased steadily as the polar angle increased from 0 to 15 degrees. Thus such combined boards will be dimensionally unstable as they pick-up or lose moisture.

(4) When the liners had polar angles deviating in the same direction from the MD, little twist warp developed as moisture content changed.

(5) These results indicate that information on ways to reduce stiffness variations on the paper machine can help the box plants reduce warp and hence, productivity.

(6) Further tests at other RH levels are in progress and additional work on other moisture effects is planned.

Section 2 - Liner and Medium Improvement -- Chemical Additives

(1) Past work showed that surface treatments with PAE type materials enhanced compressive strength and other corrugating runnability properties. However, such treatments greatly reduced wettability, and hence, reduced bonding strength on the corrugator.

(2) The Surface Science Group is now screening other additives for surface application which will increase strength without making major reductions in wettability. These trials will be completed for the March meeting.

Section 3 - Runnability Modeling -- Strength Losses

(1) Application of our runnability model shows that the losses in tensile strength of the medium during fluting are well related to the applied stresses predicted from the model. When the stress ratio approaches unity, flute fracture should occur.

(2) When the applied stress ratio was below about 0.75 the tensile strengths of the fluted mediums ranged from about 75 to 85% of their original strength for 33-lb mediums. At higher stress ratios above 0.90 the tensile strengths rapidly declined and fractures were observed. We believe this is an excellent confirmation of the theory used in developing the model.

(3) Similar results were observed with 40-lb mediums but more extreme losses and fracturing were observed.

(4) This completes the planned work on tensile strength losses during fluting.

Section 4 - Runnability Modeling -- High Temperature Furnish Effects.

(1) A study to determine the effects of varying medium chemical composition on high temperature tensile property behavior and runnability is in process.

(2) For this purpose experimental sheets are being prepared from furnishes with varying degrees of delignification and, in some cases, with synthetic fiber/polymer blends incorporated in the outer layers. The sheets will be tested to determine how the furnish chemical and fiber composition affect the high temperature tensile properties and, hence runnability.

Section 5 - Runnability Modeling -- Speed and Strain-Rate Effects

(1) A simple viscoelastic model to represent the medium tensile properties is being developed to be used with our runnability model to (a) study ways to optimize tensile characteristics for high speed runnability and (b) explain speed and strain rate effects on runnability and strength retention. It should also help explain moisture and temperature effects during corrugating.

(2) An initial summary of the model concept is summarized in this report.

Section 6 - Flat Crush and Flute Formation Modeling

(1) Examination of medium specimens, which had been subjected to bending around a radius similar in size to that of a flute tip, showed that damage occurred to the fibers on the compression side of the bend at regular intervals. The damage appeared to be primarily fiber buckling, however some shear delamination of the sheet was observed. In general, the fibers in the tension zone of the bend and the fibers between the buckled areas appeared to be undamaged.

(2) A laboratory study to determine the factors which affect the location and extent of damage to the medium during bending is being conducted.

(3) The results of the testing program are being used to refine the finite element model of flat crush loads on a flute. Nonlinear finite element methods are being used in a parameter study of flat crush load resistance.

Section 7 - Commercial Box Abuse Study

(1) A testing program has been started which will study the effects of simulated service abuse on box performance. The abuse conditions include precrush of the combined board and elevated relative humidity conditions.

SUMMARY OF RESULTS THIS PERIOD: (October 1988 - March 1989)

Section 1 - Combined Board Warp -- Liner Orientation Effects

(1) When liners having oppositely oriented polar angles and equal moisture contents are made into combined board, large twist warps occur as the combined board moisture is changed. For this case:

   a) The degree of twist warp increases as the polar angle difference between liners increases.

   b) Relative to 50% RH, the degree of twist warp increases as RH (moisture) increases.

   c) At RH levels lower than 50% (condition at time of glueing) the direction of twist warp reverses but is still large.

   d) Thus, such combined boards are dimensionally unstable as they pick up or lose moisture.

(2) Elastic theory for composite structures indicates that a moment is generated when liners having opposite polar angle deviations are combined and, subsequently, are stressed. The moment causes twist warp when the liners expand or contract as moisture content is changed. This concept explains why twist warp occurs.

(3) When liners having polar angles deviating in the same direction from the MD and equal moisture contents are made into combined board, little twist warp develops as moisture content is changed.

(4) With liners having oppositely oriented polar angles, large amounts of twist warp can occur depending on the ambient RH. The twist warp is superimposed on CD warp (and some MD warp) which is caused by the unbalance in SF/DF moisture contents at time of glueing. For this case:

a) The amount of twist warp increases as the polar angle difference increases

b) The direction of the twist warp changes depending on which liner component is dryest at time of glueing.

Section 2 - Liner and Medium Improvement -- Chemical Additives

(1) In cooperation with the Surface Science Group, various chemical agents for surface application to linerboard and medium are being studied. These efforts are directed to studying agents to improve strength without greatly reducing the water receptivity of the board for glueing and printing.

(2) For this report two agent combinations were tried: (a) high charge density cationic flocculant in combination with a high charge density anionic agent and (b) low charge density cationic starch in combination with a low charge density anionic agent.

(3) Modest improvements in compressive strength were obtained with these surface treatments without making the medium or linerboard too impervious to aqueous liquids. More effective agents or higher application levels are needed to achieve significant strength improvements.

Section 3 - Runnability Modeling -- High Temperature Furnish Effects

(1) A study to determine the effects of varying medium chemical composition on high temperature tensile and stretch performance and runnability is in progress.

(2) Experimental Formette sheets have been made using three furnishes with differing chemical composition and blends thereof.

(3) Lignin content ranged from <0.5% for the bleached kraft furnish to 16.4% for the NSSC furnish; hemicellulose content ranged from 16.9% for unbleached kraft to 24.2% for the NSSC; cellulose content ranged from 57.6% for NSSC to 79.3% for bleached kraft. These composition differences should affect the high temperature tensile properties and, hence runnability.

(4) Testing of the sheets made from these furnishes is in process.

Section 4 - Runnability Modeling -- Temperature/moisture/strain-rate.

(1) Viscoelastic and other stress-strain models are being used to represent medium tensile properties under various conditions. These models are being

used with our runnability model to study ways to optimize tensile characteristics for high speed runnability.

(2) The Halsey, White and Eyring non-linear viscoelastic model can successfully model loading rate changes in medium tensile properties. Other options are also being considered.

(3) Computer simulations have suggested that additional medium stretch may be required during fluting due to the driving action of the lower corrugating roll.

(4) The above models will be used to relate speed, temperature and moisture effects on the medium stress-strain behavior to runnability and strength retention.

Section 5 - Flat crush and Flute Formation Modeling

(1) An apparatus was designed and constructed for the purpose of applying uniform bending to a MD strip of medium. The medium specimens were bent around a radius similar in size to that of a flute tip, using various wrap angles and web tensions.

(2) A significant reduction in MD STFI compressive strength occurred when the mediums were subjected to wrap angles between 30 and 90 degrees.

(3) A significant reduction in the tensile strength of the mediums was also observed in the mediums subjected to wrap angles between 30 and 90 degrees.

(4) Physical damage to the mediums was found to be periodic and located primarily in the compression zone of the bend. Some sheet damage was apparent in specimens subjected to wrap angles of 30 degrees. Damage, in the form of localized fiber buckling and delamination, was more apparent in mediums subjected to wrap angles of 90 and 180 degrees.

(5) Web tension did not have a significant effect on the amount of compression strength reduction during bending.

Section 6 - Commercial Box Abuse Study

(1) Testing is proceeding in this study, which is examining the effects of precrush of the combined board and elevated RH conditions.

PROJECT TITLE: Board Properties and Performance

PROJECT STAFF: W. Whitsitt/R. Halcomb/J. Dees

PRIMARY AREA OF INDUSTRY NEED: Properties related to end uses.

PROGRAM AREA: Performance and Properties of Paper and Board

Date: 2/3/88
Budget: $180,000
Period Ends: 6/30/89
Project No: 3571

PROGRAM GOAL:

Develop relationships between critical paper and board property parameters and determine how they are achieved in terms of raw materials, sheet structure and processing conditions.

PROJECT OBJECTIVE:

- To develop relationships between container performance, combined board properties, and component properties.
- To improve the performance/cost ratios of combined board, linerboard, and medium.
- The short term goals are to (1) use structural models to assess the impact of papermaking factors on combined board and box performance and (2) improve medium end-use and converting performance properties.

PROJECT RATIONALE:

There are many aspects of container and component performance which have not been adequately related to board properties through sound structural models. Such models would identify the critical board properties needed for end use performance. They would be used to select papermaking approaches to maintain or improve box performance at less cost. An important step is to incorporate the elastic stiffnesses of the board into such models, if possible. This will enable us to use our knowledge on how papermaking factors affect the elastic stiffnesses to make board improvements.

RESULTS TO DATE:

Our Rayleigh-Ritz analyses of box failure under several types of load indicated that compressive strength (ECT) is the limiting property governing performance. Further analyses of the ECT behavior of corrugated board showed that present local buckling models fail to properly predict ECT strength when the strength of the liners or medium is changed by certain papermaking operations, e.g. wet pressing. Therefore new models have been developed which show that ECT is primarily dependent on the compressive strength and/or elastic stiffnesses of the liners and medium. The bending stiffness of the liners appears to have only a minor effect on ECT. The importance of linerboard bending stiffness has been a point of concern to our industry and these results indicate that it is much less important than compressive strength. We are extending this work to combined board flexural stiffness and box compression.

Finite element techniques are being used to study the effects of the high stresses imposed on the medium during fluting on the subsequent flat crush strength of the board. Initial results demonstrate that the leading and trailing sides of the flute are stressed differently which, if too extreme, can cause leaning flutes and poor flat crush.

Our forming models indicate that satisfactory high speed runnability on the corrugator is dependent on at least four medium properties as well as nip geometry and medium web tension. Better runnability is obtained as MD tensile and stretch are increased and the coefficient of friction of medium and medium thickness are decreased.

Our research has shown that fluting reduces the compressive strength of medium and hence reduces flat crush and ECT. Densification via wet pressing is one way to reduce these losses. Current work shows that the tensile characteristics of medium are also reduced by forming. It appears that these reductions can be predicted from our runnability model.

PLANNED ACTIVITY FOR FY 1988-89:

Our activities during the next fiscal year will be directed to include research on end-use performance and the converting process. In both areas we are developing and using models to relate component compression and elastic properties to performance. The models are being used to determine ways to improve performance/cost ratios via better material selection and papermaking.

During 1988 we will be validating our structural models for ECT and flexural stiffness to show that they properly predict box strengths under various conditions. Our box modeling work will be extended to take into account the effects of moisture and abuse during storage/transportation. Commercial boxes will be used for the initial phases of this work.

Our analyses of forming and flat crush will be expanded to take non-linear elasticity effects into account. Experimental work to measure forming stress effects is underway.

For further applications of our runnability model we need to consider moisture/temperature effects during fluting. Current work for the FKBG is showing how the steam showers and preheating affect finished board qualities such as ECT, flat crush and high-lows. We plan to show how high temperatures, coupled with the moistures in the process, affect the basic stiffnesses of the medium and hence formability. Incorporating these effects in the model will allow better optimization of the process.

In the area of liner/medium improvement surface additive treatments are and will be studied as a way to enhance compressive strength without impairing corrugator runnability. Some work on bonding at high speeds will be included in this phase.

Status Report

BOARD PROPERTIES AND PERFORMANCE

Project 3571

The objectives of this project are to: (1) develop relationships between container performance, combined board and component properties, and (2) determine ways to improve the cost/performance ratios of medium and linerboard. To fulfill these objectives both end-use performance and runnability on the corrugator are being considered. Our current work is divided into several parts, namely; (1) combined board warp vs. liner directionality effects, (2) liner and medium improvement, (3) runnability modeling, (4) finite element analysis of flat crush and fluting stresses and (5) ECT and box compression performance.

Two papers were presented at the fall meeting of the TAPPI Corrugated Container conference; copies of these papers were attached to the October status report. An article was written for the Institute publication "Paperlink". It is entitled "Recent Box Compression Developments" and is appended to this report. Two summary reports on projects sponsored by the Fourdrinier Kraft Board Group have been drafted and a third report has been planned.

COMBINED BOARD WARP -- LINER ORIENTATION EFFECTS

Past institute research shows that elastic stiffness vs. orientation diagrams (termed polar plots) can vary greatly across paper machines depending on wet end conditions. Figure 1 shows one example of polar angle changes across a paper machine. These variations of shape, area, and polar angle are known to correlate with converting and end-use conditions.

As discussed in the October status report, combined board twist warp is generated when two linerboard webs having dissimilar polar angles are glued

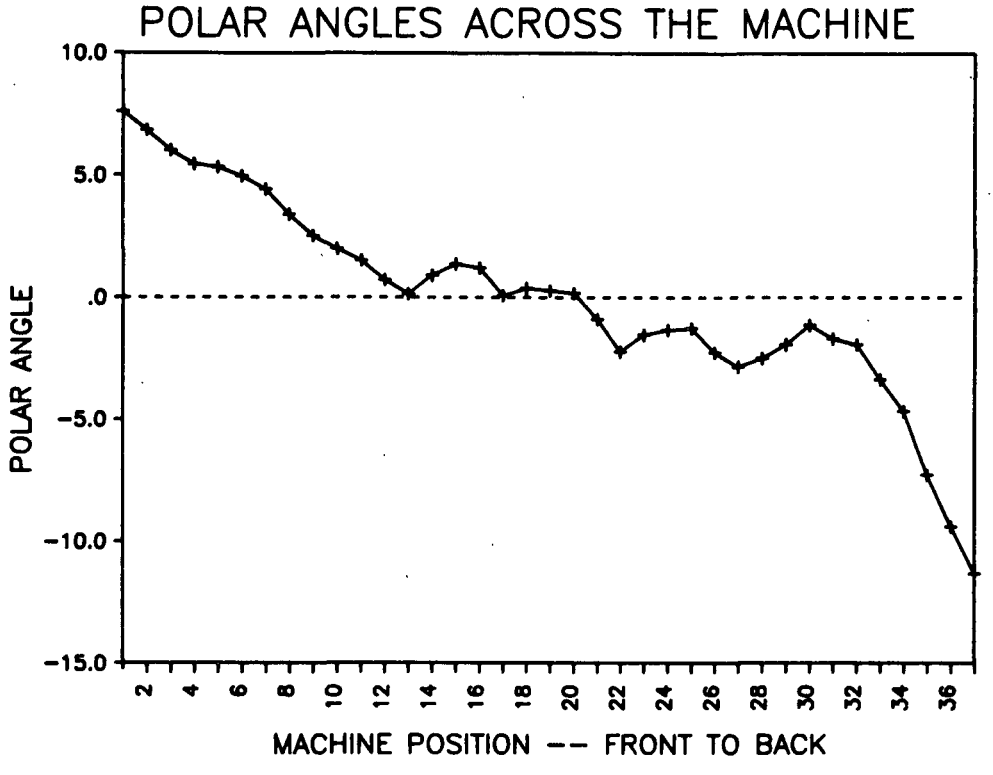

Figure 1. Large changes in polar angle can occur across a linerboard machine and, hence affect quality. factors.

to the fluted medium. Two extreme cases can occur. In one case the polar angles of the two liners deviate in the same direction in the corrugated board (Fig 2a). Less twist warp occurs with this configuration because the polar angle misorientations of the liners match each other. In the other case the polar angles of the liners deviate in opposite directions from the machine direction of the corrugated board (Fig. 2b). Major twist warp is obtained in this case because the dimensional changes of the liners tend to twist the flutes as moisture content is changed and the liners expand or contract.

When stresses are applied to an orthotropic material along the orthotropic axes, the shear and normal components of strain are uncoupled, that is, the normal stresses produce only normal strains and shear stresses produce

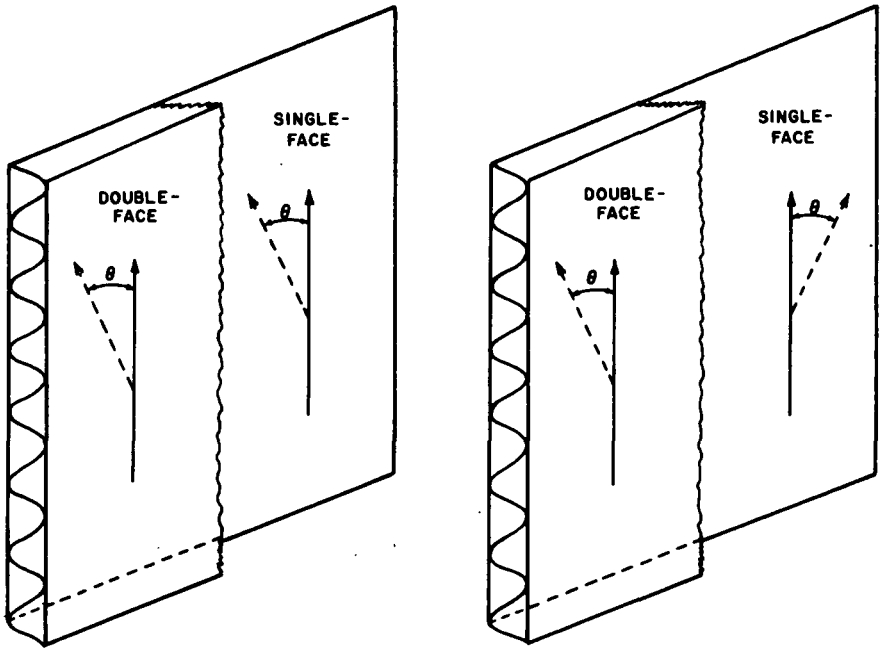

a) Liner polar angles in same direction

b) Liner polar angles in opposite direction

Figure 2. Two opposite cases of liner polar angle misalignment. Case (b) promotes twist warp.

only shear strain. However, when the stresses are applied at angles to the orthotropic axes, the shear and normal stresses are coupled. For example, in Fig. 3 combining the two plies shown with opposite angles, results in a moment which acts to twist the composite structure[1]. This concept helps explain the generation of twist warp in combined board and will provide the basis for a theoretical treatment of twist warp generation.

Warp is very dependent on the moisture conditions of the single-face web and double-back liner at time of bonding, because it is a manifestation of the hygroexpansivity of the liners. Therefore, papermaking factors which cause

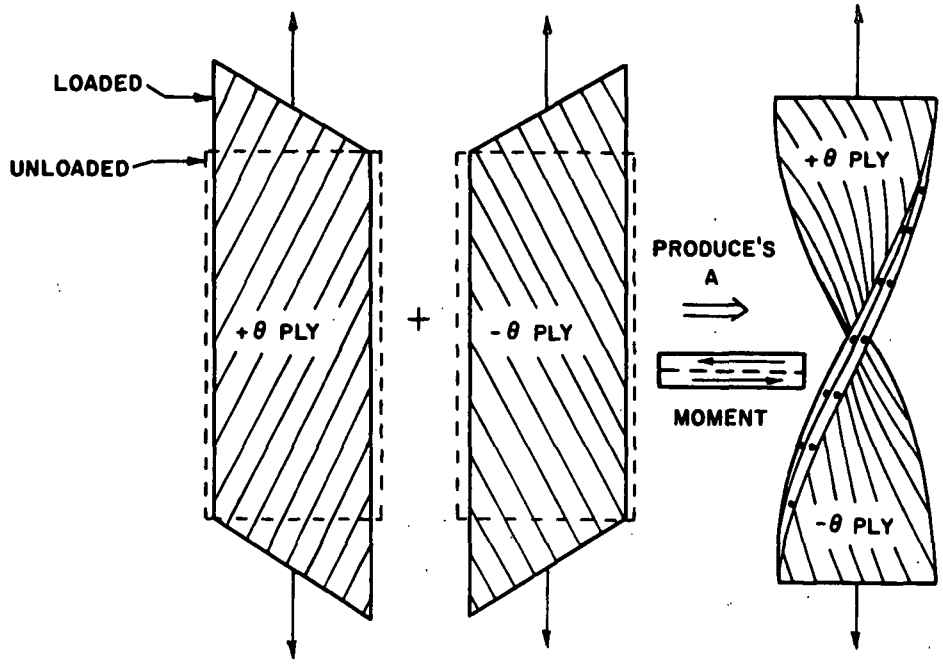

Figure 3. Shear coupling deformation associated with combining two lamina with opposite angular axes produces twist in the composite structure. (From J. C. Halpin, reference 1.)

differences in hygroexpansivity of the liners can be expected to affect the proclivity to warp and the kind of warp. Figures 4 and 5 compare the absorption and desorption hygroexpansivity curves at various angles from the machine direction for the 42-lb liner sample used in this study. Much greater changes in sheet dimensions are obtained in the CD as expected. Thus, combining liners with opposite polar angle deviations results in strong CD hygroexpansion differences and, hence, promotes twist warp.

For the last report we prepared combined board sheets as follows:

1. Polar angles of SF and DF liners in the same direction (case a) in the combined board: 0, 5, 10, and 15 degrees.
2. Polar angles of SF and DF liners in opposite direction (case b) in the combined board: 0, 5, 10, and 15 degrees.

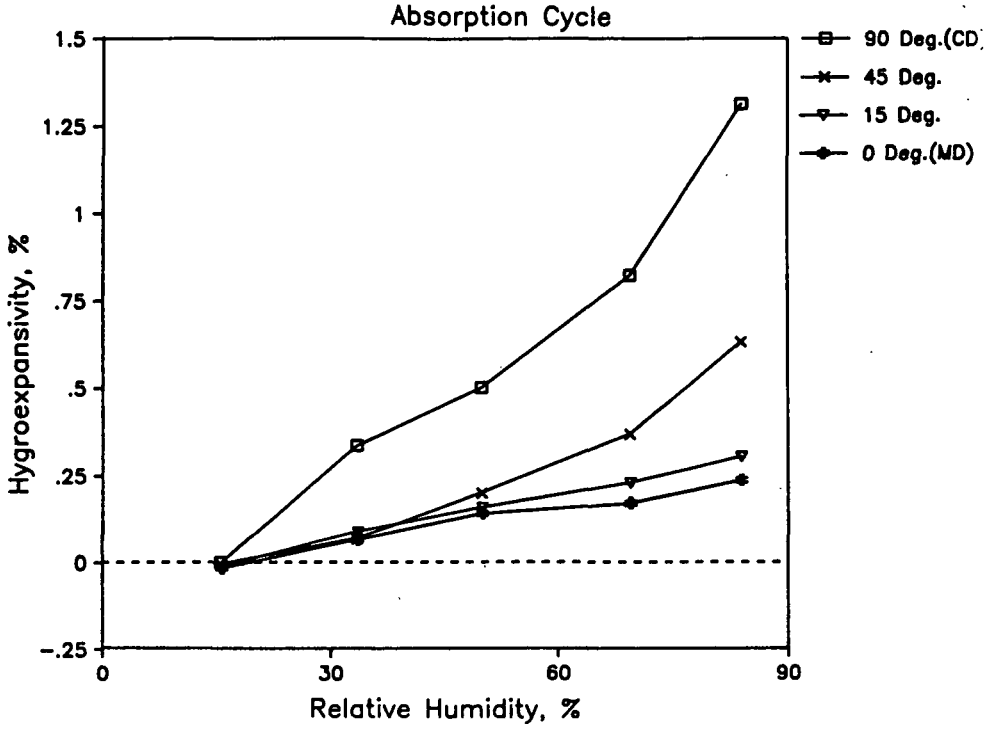

Figure 4. Absorption cycle hygroexpansivity curves show large differences with orientation.

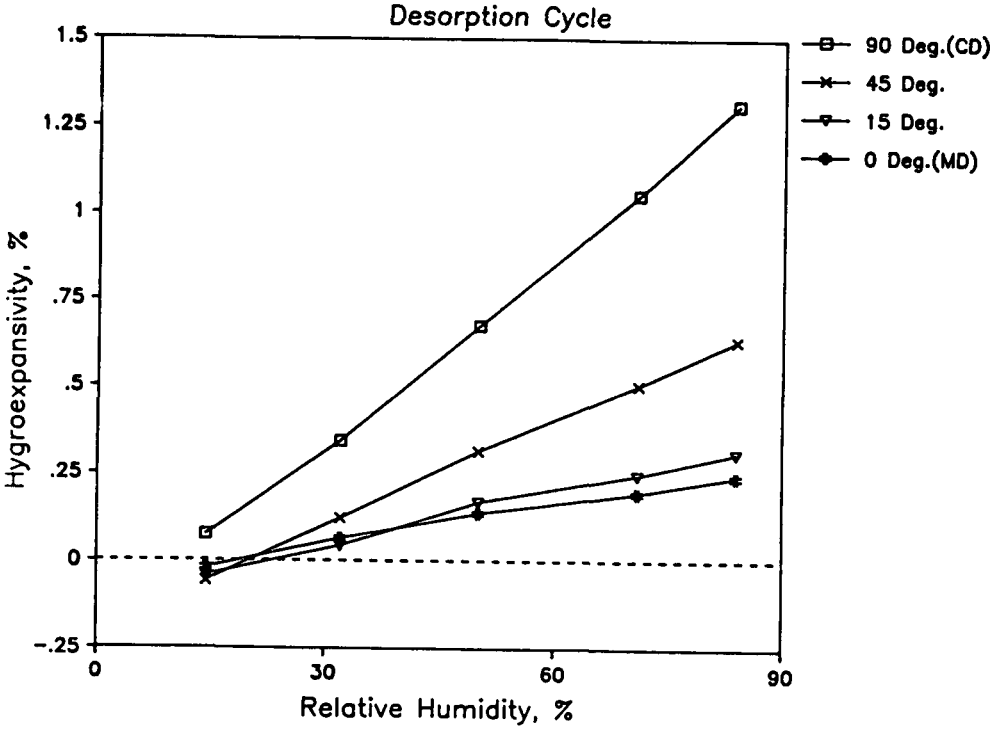

Figure 5. Desorption cycle hygroexpansivity curves show large differences with orientation.

The single-face board and DF liners were conditioned at 50% RH prior to double-backing so the components were at the same moisture content at time of glueing. After double-backing, the sheets were reconditioned at 50% RH and then exposed to RH levels of 20, 70 and 90% RH.

As discussed in the October report, combined boards made with liner polar angles deviating in opposite directions (case b) from the MD of the combined board exhibited large twist warps (Fig. 6). The amount of twist warp increased steadily as the polar angle deviations increased from 0 to 15 degrees. Figures 7 and 8 show that the sheets exposed at 70 and 20% RH also exhibited significant amounts of twist warp and the amounts of warp were proportional to the polar angle deviation. However, the warp magnitudes were less than obtained at 90% RH because the dimensional changes were less. Note that the direction of warp changed from high to low RH; for example, a high corner at 70 or 90% RH is a low corner at 20% RH. This change in warp would be expected because the liners try to expand at high RH and contract at low RH.

Figure 9 and 10 show that the combined boards made with liner polar angles deviating in the same direction from the MD of the combined board exhibit only small changes in warp when exposed to 20 or 70% RH. Similar results were obtained at 90% RH as noted in the October report.

To simulate the combined effects of liner polar angle deviations and unbalanced SF and DF liner moisture content levels two additional sets of combined boards were prepared as follows:

1. SF web at 90% RH; DF liner at 50% RH. Liner polar angles in opposite directions: 0, 5, 10 and 15 degrees
2. SF web at 50% RH; DF liner at 90% RH. Liner polar angles in opposite directions: 0, 5 and 10 degrees.

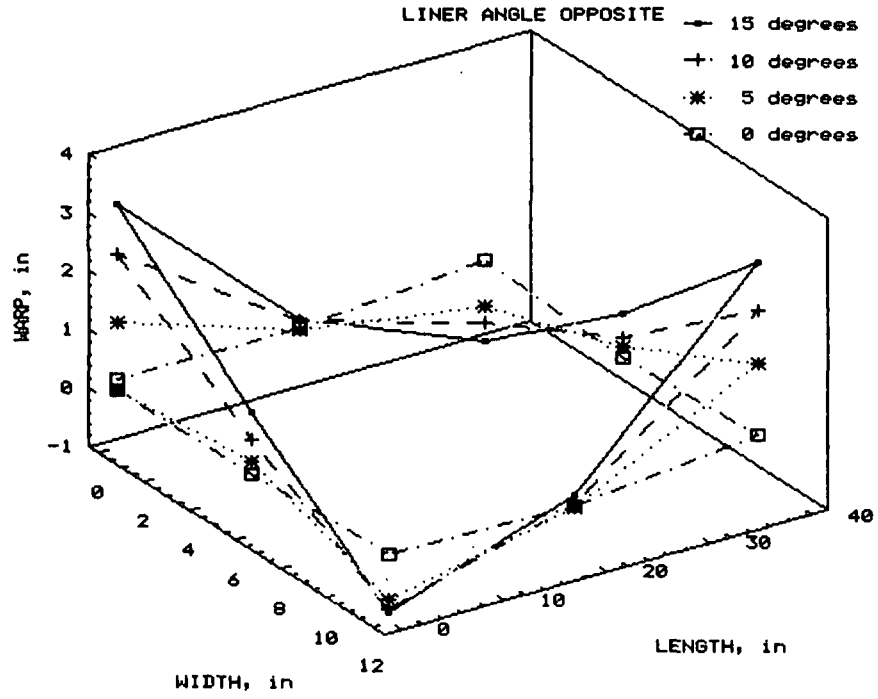

Figure 6. The amount of twist warp at 90% RH increased steadily with increasing liner polar angle deviation in opposite directions from the MD of the combined board.

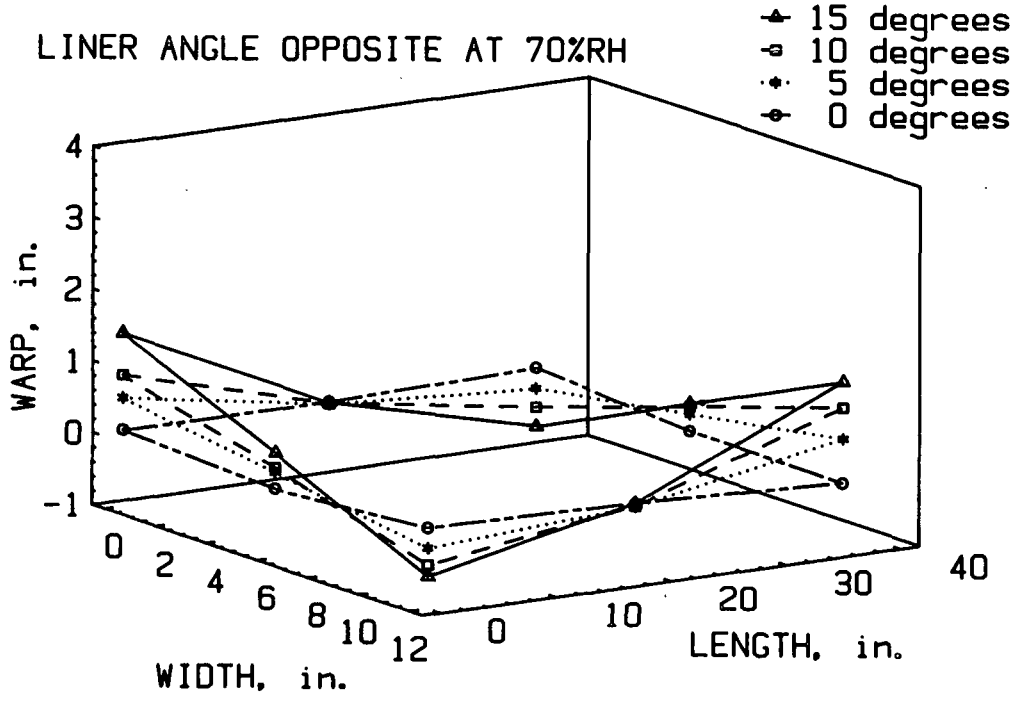

Figure 7. The twist warp obtained with opposite liner polar angle deviations at 70% RH are similar to those obtained at 90% RH but smaller in magnitude.

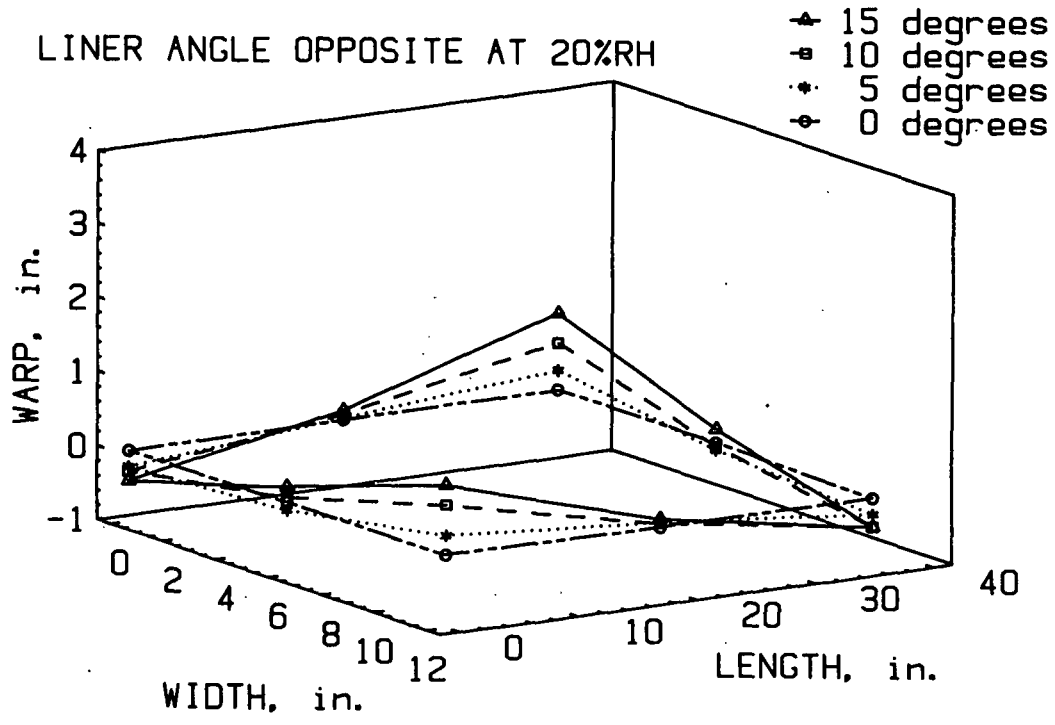

Figure 8. At 20% RH significant amounts of twist warp are obtained but the direction of warp is reversed from that obtained at high RH.

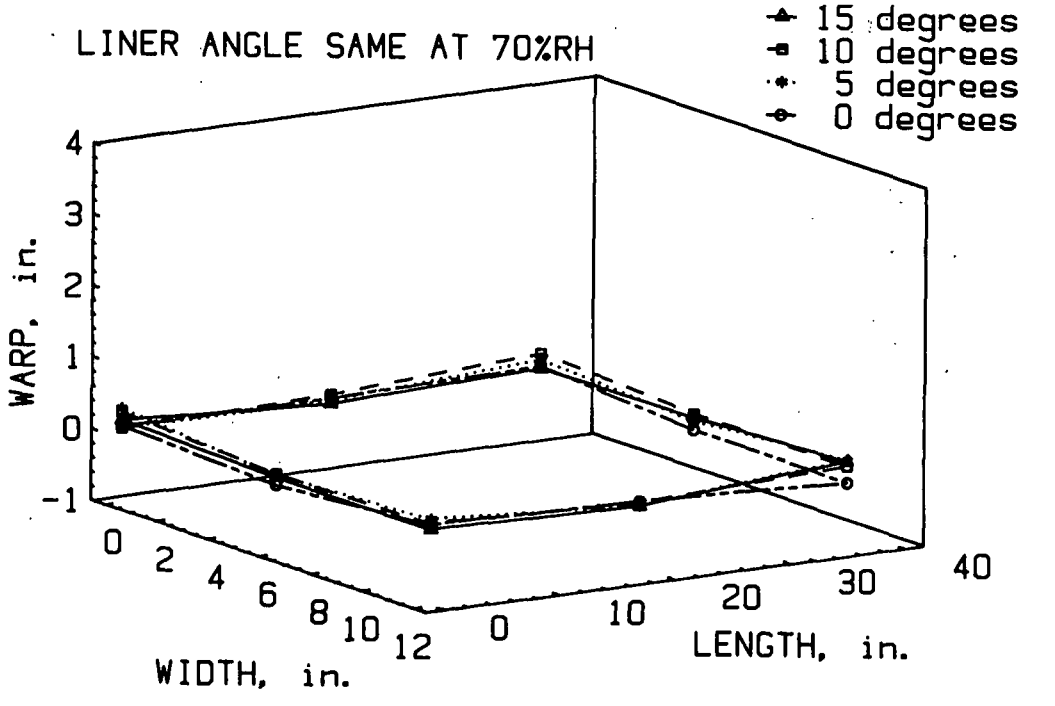

Figure 9. Combined board warp profiles for board made with SF and DF liner polar angles in the same directions show little warp at 70% RH.

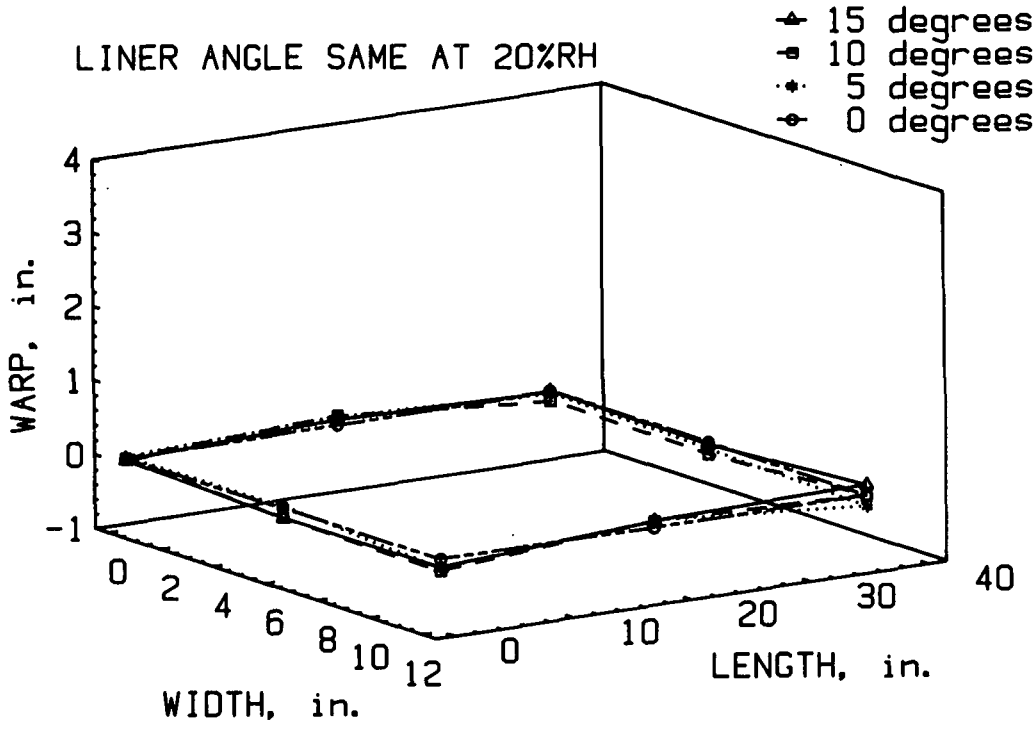

Figure 10. Combined board warp profiles for board made with SF and DF liner polar angles in the same directions show little warp at 20% RH.

The above sheets were double-backed at 50% RH and warp measurements were made after conditioning the sheets using the following sequence: 50%, 20%, 50% and 90% RH.

Figures 11-13 illustrate the degrees of warp obtained with the moist SF web combination at 20, 50 and 90% RH respectively. At 20% RH very large amounts of twist warp were obtained as the polar angles were increased from 0 to 15 degrees (Fig. 11). This increase in twist warp would be expected based on the previous discussion. The twist warp is superimposed on CD warp (and some MD warp) which is caused by the unbalance in SF/DF moisture contents. In this case the CD warp is toward the SF side which was initially at a higher moisture content. Figure 12 shows that the twist warp is still very pronounced at 50% RH.

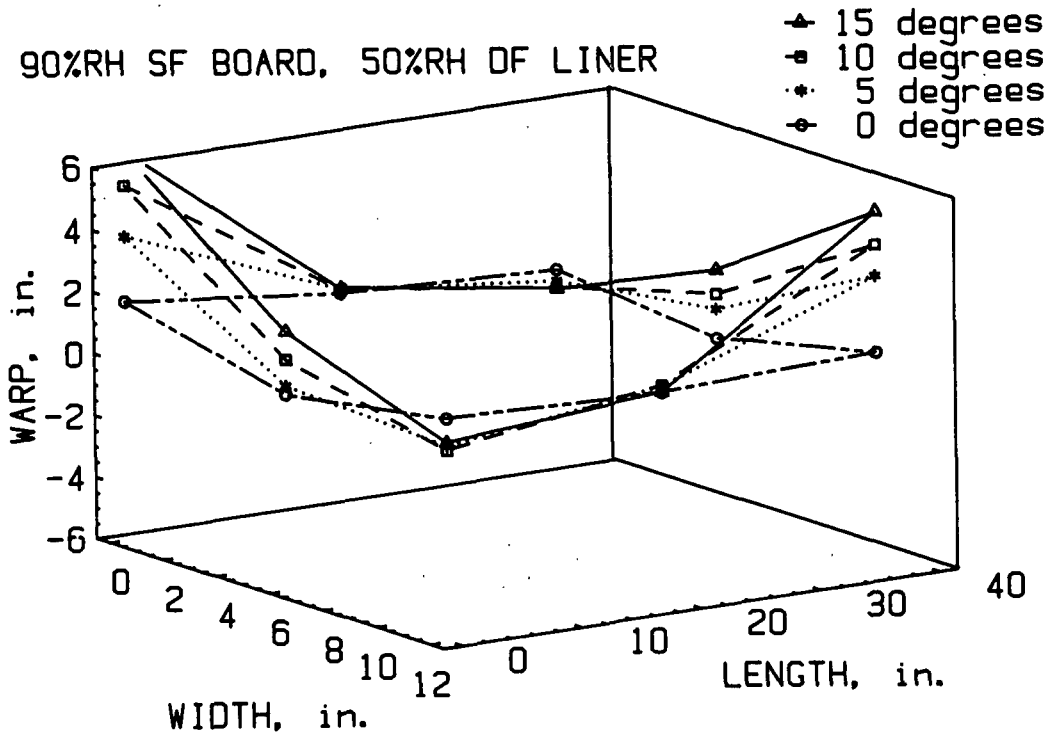

Figure 11. AT 20% RH large twist warps are obtained due to liner polar angle differences. CD warp is also present due combining a moist SF web with a dryer DF liner.

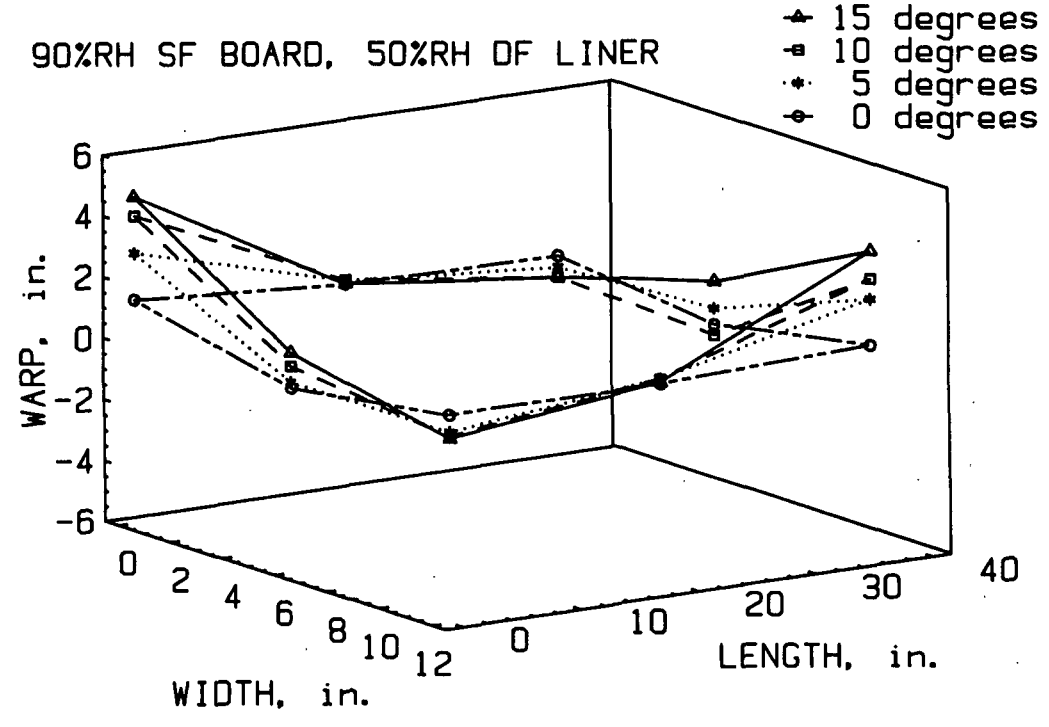

Figure 12. Twist warp and CD warp are present at 50% RH due to polar angle differences and unbalanced moisture content at time of glueing.

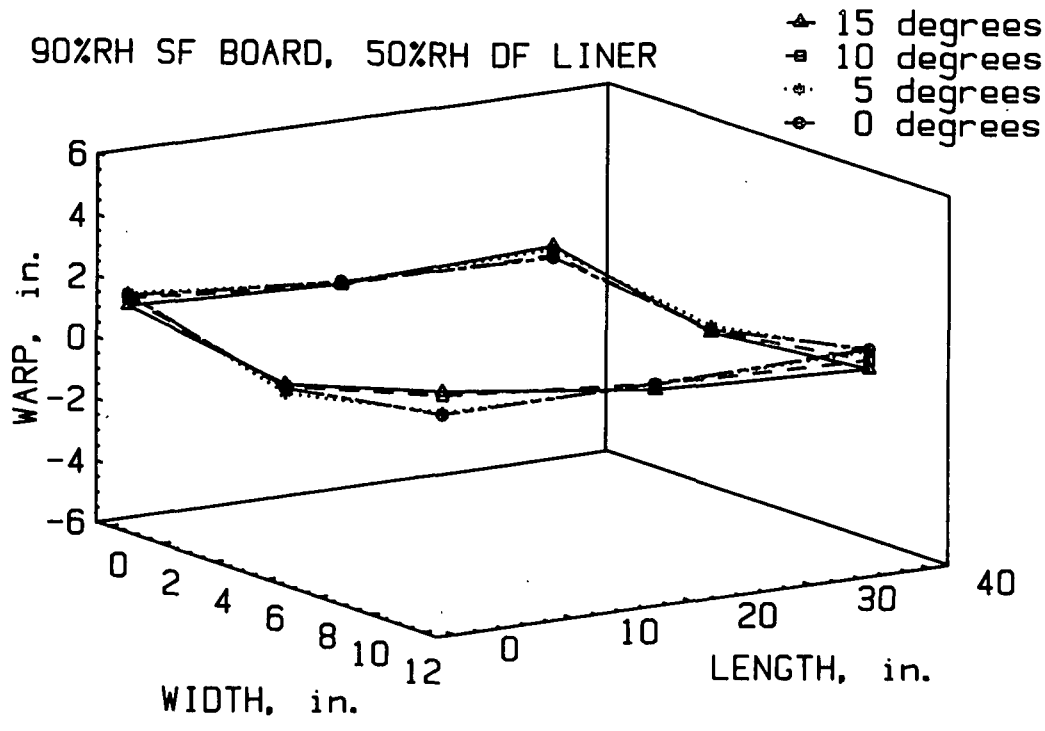

Figure 13. Less twist warp was present at 90% RH but CD warp was still evident due to the moister SF web at time of glueing.

At 90% RH the amount of twist warp is less than obtained at 20 and 50% RH but the CD warp due to the initial unbalance in moisture content is still present.

Figures 14-16 illustrate the warp obtained for the reverse case, that is, a high moisture DF liner combined with a dryer SF web. At 20% RH large amounts of twist warp due to polar angle deviations were obtained as above but the twist is opposite from the moist SF case (Fig. 14). The twist warp is superimposed on a significant CD warp due to the unbalance in liner moistures. In this case the CD warp is toward the DF liner side because it was the moister liner at time of glueing. Figure 15 shows that the twist warp is less evident at 50% RH along with a large CD warp. However at 90% RH the twist warp due to polar angle deviations became larger and the CD warp due to moisture unbalance is also large.

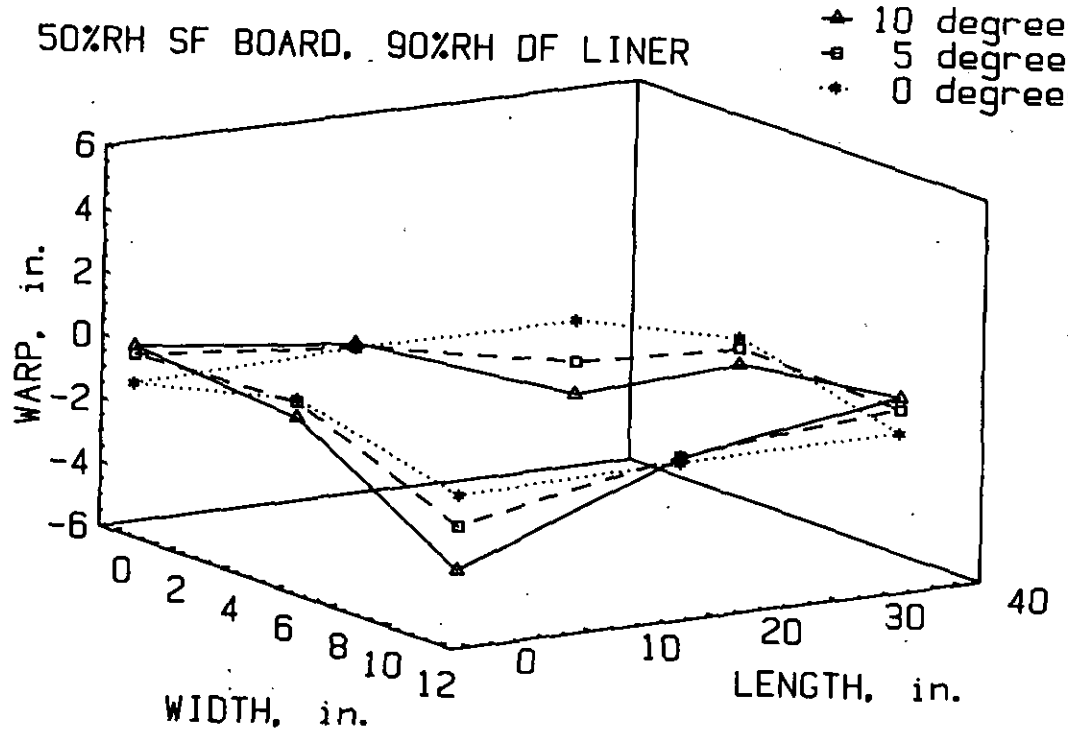

Figure 14. At 20% RH large twist warps are obtained due to polar angle differences. CD warp toward DF side is also present due to combining a dryer SF web with a wetter DF liner.

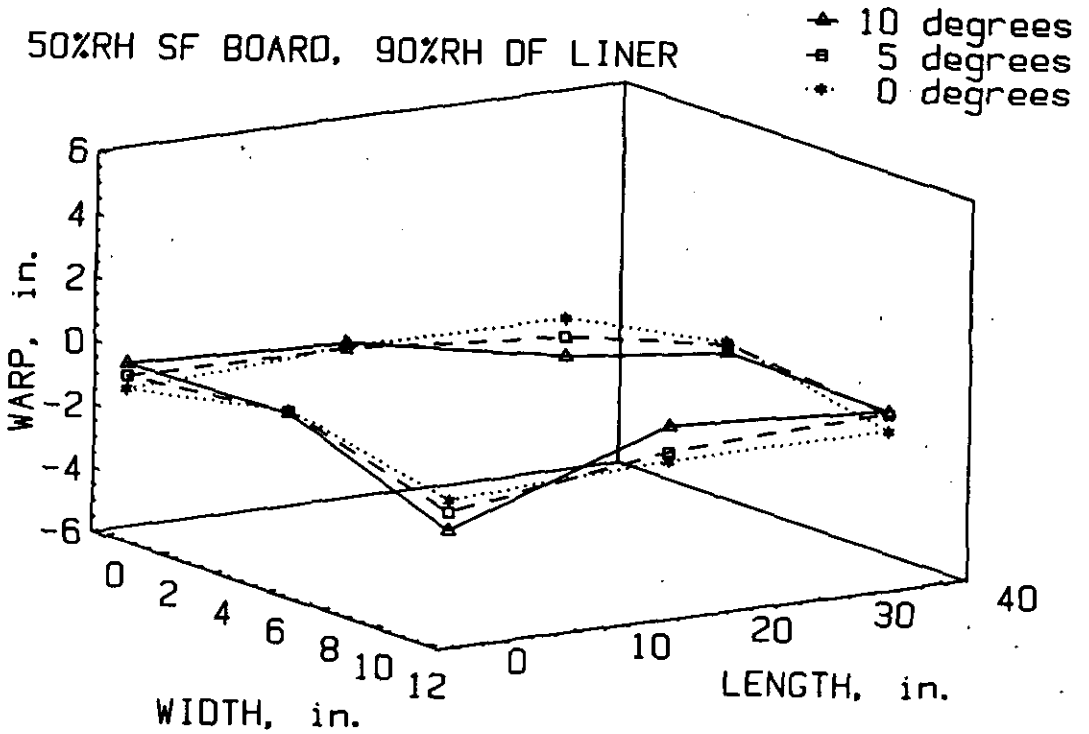

Figure 15. Less twist warp was present at 50% RH due to polar angle differences but CD warp was present due to moisture unbalance.

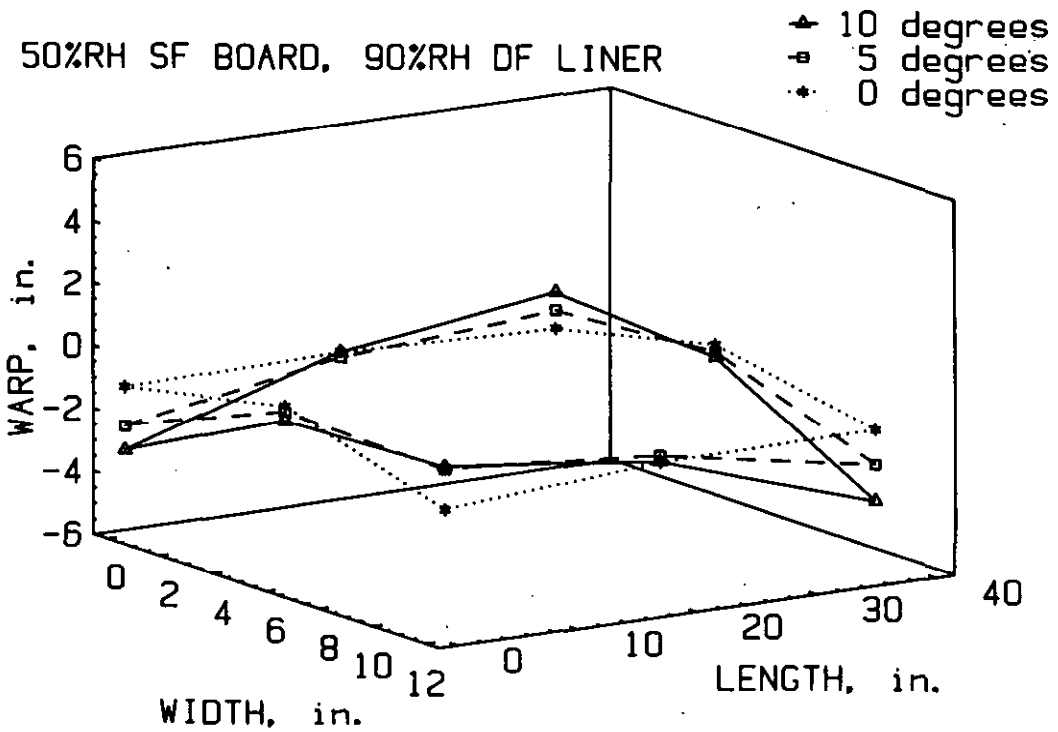

Figure 16. At 90% RH the twist warp directions reversed from the 20% RH results. CD warp toward DF side was large due to combining dryer SF web with a wetter DF liner.

Another series of sheets were prepared after conditioning the SF web and DF liner at 90% RH. The warp results were similar to those obtained when both sheets were conditioned at 50% RH taking the RH differences into account.

The initial planned experimental work on this phase is complete. Further analysis to quantify the concepts and effects of liner properties and moisture effects is planned.

These results indicate that improvements in liner uniformity should help box plants minimize warp problems. A current FKBG study is directed to evaluating liner and medium paper machine stiffness profiles. It will also develop information on paper machine causes of variations and possible control measures. Based on the present results it appears that, it may be possible

to reduce twist warp by turning one of the liner rolls around to bring the polar angles into the same orientation.

Briefly summarizing the results indicate:

1. When liners having oppositely oriented polar angles and equal moisture contents are made into combined board, large twist warps occur as the combined board moisture is changed. For this case:
   a. The degree of twist warp increases as the polar angle difference between liners increases.
   b. Relative to 50% RH, the degree of twist warp increases as RH (moisture) increases.
   c. At RH levels lower than 50% (condition at time of glueing) the direction of twist warp reverses but is still large.
   d. Thus such combined boards are dimensionally unstable as they pick up or lose moisture.

2. Elastic theory for composite structures indicates that a moment is generated when liners having opposite polar angle deviations are combined and, subsequently, are stressed. The moment causes twist warp when the liners expand or contract as moisture content is changed. This concept explains why twist warp occurs.

3. When liners having polar angles deviating in the same direction from the MD and equal moisture contents are made into combined board, little twist warp develops as moisture content is changed.

4. With liners having oppositely oriented polar angles and unequal moisture content at time of glueing, large amounts of twist warp can occur depending on the ambient RH. The twist warp is

superimposed on CD warp (and some MD warp) which is caused by the unbalance in SF/DF moisture contents. For this case:

a. The amount of twist warp increases as the polar angle difference increases

b. The direction of the twist warp changes depending on which liner component is dryest at time of glueing.

LINER AND MEDIUM IMPROVEMENT -- CHEMICAL ADDITIVES

In Project 3526 various wet end additives are under study as a means to increase fiber-to-fiber bonding strength under normal and humid conditions. Duopolymer systems comprised of CMC/PAE and PAA/PAE have been found to be effective strength agents for a variety of bleached and unbleached, conventional kraft and high yield cooks. However, these treatments reduce wettability and, hence, affect converting operations.

As an alternative to wet-end treatments we are studying the merits of chemical surface treatments to improve converting and end-use performance. This approach is being pursued jointly under this project and Project 3526. The Surface Science Group selects and applies the selected agents; the converting and end-use tests are being carried out by the Container Group.

As discussed in the October report, the Surface Science Group has been screening a number of additives which potentially could increase strength with less effect on wettability. For recent trials two agent combinations were selected:

1. 0.5% of high charge density cationic flocculant and 0.5% of a high charge density anionic agent, combination termed HCDA.

2. 1.0% of low charge density cationic starch and 0.5% of a low charge density anionic agent (LCDA).
3. Water treated control.

For each type of treatment strips of commercial medium and liner were treated using a two step process. Each strip was dipped in the cationic agent, the excess was doctored off, the strip was dried and the process was repeated with the anionic agent.

A portion of the strips from each treatment were corrugated at speeds of 600 and 800 fpm to check runnability, adhesion, and combined board properties.

Medium Treatments

Tables 1 and 2 summarize the results for the treated mediums. Figure 17 shows that both treatments effected increases in cross direction STFI short span compressive strength of about 13-15% at 50% RH relative to the water control. At 92% RH the starch treatment combination LCDA maintained a 13% advantage over the water control. The high charge density agent HCDA treatment was less effective at 92% RH. These differences in behavior also show up in the effects of the agents on the tensile stiffness ET, one of the factors on which compressive strength is dependent[2]. The low charge density agent LCDA increased CD ET more than the high charge density agents and some of the improvement was maintained at high RH.

The CD ring crush strengths were also increased by both treatments but the low charge density starch treatment LCDA was more effective than the high

Table 1. Physical characteristics of mediums.

		Controls		Liner Treatments			
		Untreated	Water @ pH5	HCDA Agent		LCDA Agent	
		Average	Average	Average	% Diff.	Average	% Diff.
Sample code:		6553	FF	CC		DD	
Basis Weight							
Grammage, gm/M^2		121	118	121	+2.5	120	+1.7
$lbs/1000\ ft^2$		24.9	24.3	24.8	+2.1	24.5	+0.8
Caliper							
TAPPI Thickness, mil		10.9	12.1	12.1	-0-	12.2	+0.8
IPC Thickness, mil		8.5	8.9	9.1	+2.2	8.9	-0-
Density							
TAPPI, kg/m^3		436	386	394	+2.1	386	-0-
IPC, kg/m^3		564	524	524	-0-	526	+0.4
Ring Crush							
MD, lb/6 in.	50% RH	48	38	41	+7.9	50	+31.6
	92% RH	34	22	32	+45.5	29	+31.8
CD, lb/6 in.	50% RH	40	32	34	+6.3	38	+18.8
	92% RH	18	17	18	+5.9	19	+11.8
STFI							
MD, lbF/in.	50% RH	20.18	18.34	19.47	+6.2	20.16	+9.9
	92% RH	9.50	8.76	8.23	-6.1	8.96	+2.3
CD, lbF/in.	50% RH	12.90	11.76	13.32	+13.3	13.46	+14.5
	92% RH	6.58	5.88	6.36	+8.2	6.66	+13.3
Tensile							
MD, lb/in.	50% RH	29.6	25.7	26.7	+3.9	28.4	+10.5
	92% RH	15.1	12.8	13.2	+3.1	16.0	+25.0
	WET	2.3	2.1	2.9	+38.1	2.3	+9.5
CD, lb/in.	50% RH	15.1	13.0	14.6	+12.3	16.1	+23.8
	92% RH	7.4	7.2	7.6	+5.6	8.3	+15.3
	WET	1.0	1.1	1.4	+27.3	1.2	+9.1
Stretch							
MD, %	50% RH	1.05	1.28	1.31	+2.3	1.01	-21.1
	92% RH	1.66	1.85	1.89	+2.2	1.76	-4.9
	WET	0.90	0.96	1.13	+17.7	1.02	+6.3
CD, %	50% RH	1.81	1.30	1.73	+33.1	1.48	+13.8
	92% RH	2.95	2.48	3.01	+21.4	2.29	-7.7
	WET	1.78	1.70	2.07	+21.8	1.76	+3.5

Table 1 continued. Physical characteristics of mediums.

		Controls		Liner Treatments			
		Untreated	Water @ pH5	HCDA Agent		LCDA Agent	
		Average	Average	Average	% Diff.	Average	% Diff.
Sample code:		6553	FF	CC		DD	
TEA							
MD,ft lb/ft^2	50% RH	2.41	2.61	2.76	+5.7	2.21	-15.3
	92% RH	2.13	1.93	2.06	+6.7	2.31	+19.7
	WET	0.19	0.18	0.29	+61.1	0.21	+16.7
CD,ft lb/ft^2	50% RH	2.39	1.40	2.23	+59.3	1.99	+42.1
	92% RH	2.03	1.69	2.10	+24.3	1.67	-1.2
	WET	0.16	0.18	0.25	+38.9	0.19	+5.6
ET							
MD, lb/in.	50% RH	4294	3516	3591	+2.1	4401	+25.2
	92% RH	2122	1634	1686	+3.2	2073	+26.9
	WET	481	403	512	+27.0	62	-84.6
CD, lb/in.	50% RH	1930	1844	1884	+2.2	2118	+14.9
	92% RH	960	916	894	-2.4	985	+7.5
	WET	147	148	158	+6.8	142	-4.1
Concora							
lbs	50% RH	54	45	52	+15.6	54	+20.0
Gurley Porosity							
sec/100cc	50% RH	6.2	4.2	4.4	+4.8	4.0	-4.8
Water Drop, T 819A							
Seconds							
Wire side up	50% RH	4	439	>600	+36.7	428	-2.5
Felt side up	50% RH	2	282	437	+55.0	353	+25.2
Friction, Hot Coef.							
Wire side up	50% RH	0.37	0.41	0.38	-7.3	0.39	-4.9
Felt side up	50% RH	0.35	0.27	0.37	+37.0	0.33	+22.2

Table 2. Physical characteristics of combined board made with treated medium.

		Controls		Liner Treatments			
		Untreated Average	Water @ pH5 Average	HCDA Agent Average	HCDA Agent % Diff.	LCDA Agent Average	LCDA Agent % Diff.
Sample code:		6706/6553	6706/FF		6706/CC		6706/DD
Singlefaced Board							
High-Lows,							
% > 3 mils	600 fpm	9.5	9.8	7.1	-27.6	8.3	-15.3
	800 fpm	8.2	11.5	4.3	-62.6	7.7	-33.0
% > 4 mils	600 fpm	2.8	2.6	2.3	-11.5	2.9	+11.5
	800 fpm	2.2	3.7	0.8	-78.4	2.4	-35.1
Caliper, mils							
Single face	600 fpm	154.6	154.7	154.3	-0.3	154.4	-0.2
	800 fpm	154.9	156.0	155.8	-0.1	155.4	-0.4
Flat Crush, psi							
50% RH	600 fpm	27.5	25.8	25.7	-0.4	29.0	+12.4
92% RH	600 fpm	15.0	13.8	14.1	+2.2	15.6	+13.0
50% RH	800 fpm	28.8	25.6	26.4	+3.1	30.9	+20.7
92% RH	800 fpm	16.0	13.9	14.2	+2.2	15.4	+10.8
Pin Adhesion, lb							
	600 fpm	76CC	77CC	75CC	-2.6	79CC	+2.6
	800 fpm	78CC	80CC	77CC	-3.8	81CC	+1.3
ECT, lb/in.							
50% RH	600 fpm	44.1	39.9	38.8	-2.8	39.3	-1.5
92% RH	600 fpm	19.8	19.4	18.6	-4.1	17.7	-8.8
50% RH	800 fpm	40.3	39.3	40.5	+3.1	40.3	+2.5
92% RH	800 fpm	18.6	18.6	18.5	-0.5	18.5	-0.5

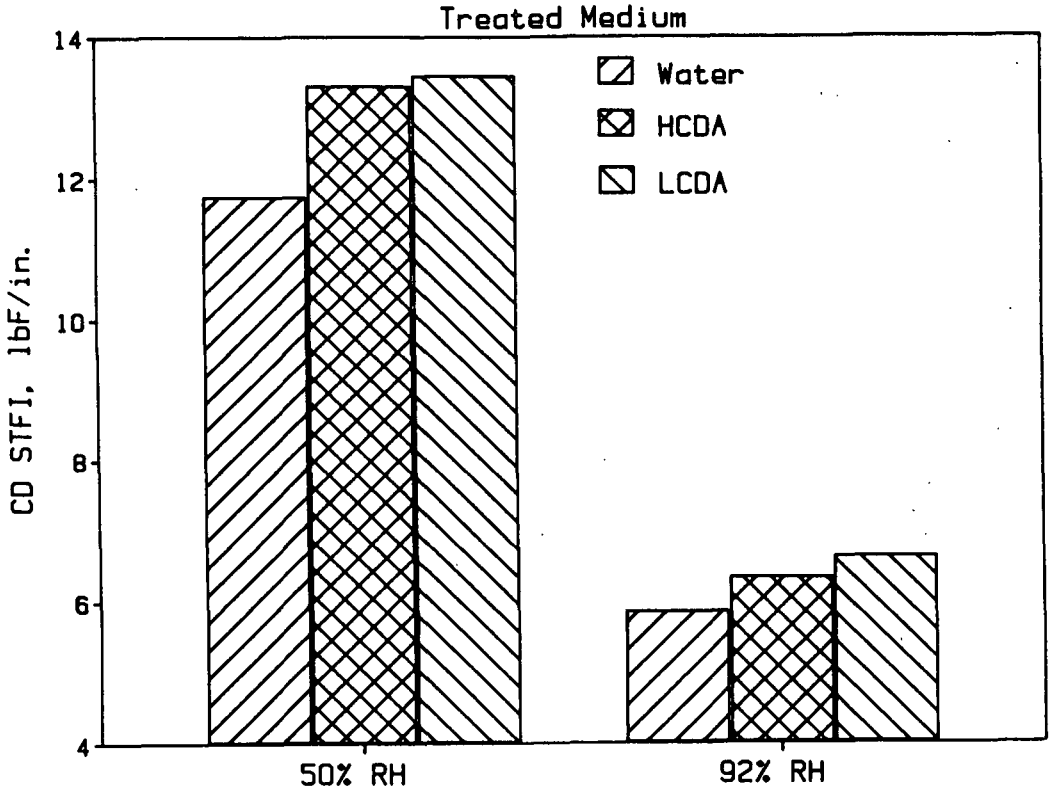

Figure 17. Effects of surface treatments on CD STFI short span compressive strength.

charge density agents (Fig. 18). The percentage improvements in CD ring strength with the LCDA agents were about the same as in the case of CD STFI strength.

The low charge density starch treatments LCDA increased MD and CD tensile strength relative to the water control and made only small changes in the hot friction coefficient. The increases in MD tensile should promote better corrugator runnability after taking the minor friction changes into account.

In past work PAE agents were found to greatly increase the water drop of the medium, making it less receptive to the aqueous starch adhesive used in corrugating. As a result it appeared to be more difficult to bond medium

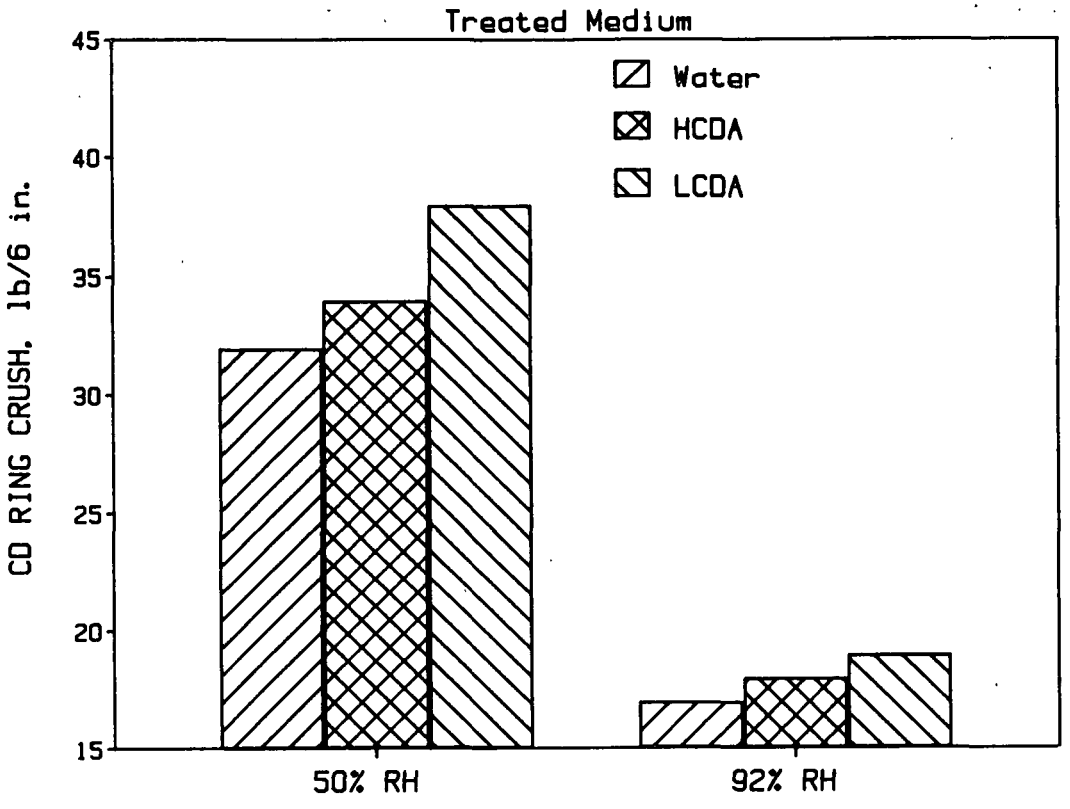

Figure 18. Effects of surface treatments on CD ring compression strength.

treated with PAE agents at high corrugating speeds. One of the objectives of the current work was to find agents which would increase strength but which would have less effect on wettability.

Figure 19 shows that the water drop results for the low charge density starch treatment LCDA were about equal to the water control on the wire side and only slightly higher than the water control on the felt side. Somewhat higher water drop values were obtained with the high charge density agent treatment. From this standpoint it appears that these treatment types have potentials for increasing strength without making the medium too unreceptive to aqueous liquids. However, we noted that the water control exhibited much higher water

drop values than the untreated medium. The reasons for this are not clear but we speculate that the change in water drop may be due to a combination of effects such as ageing and the wetting and redrying during treatment.

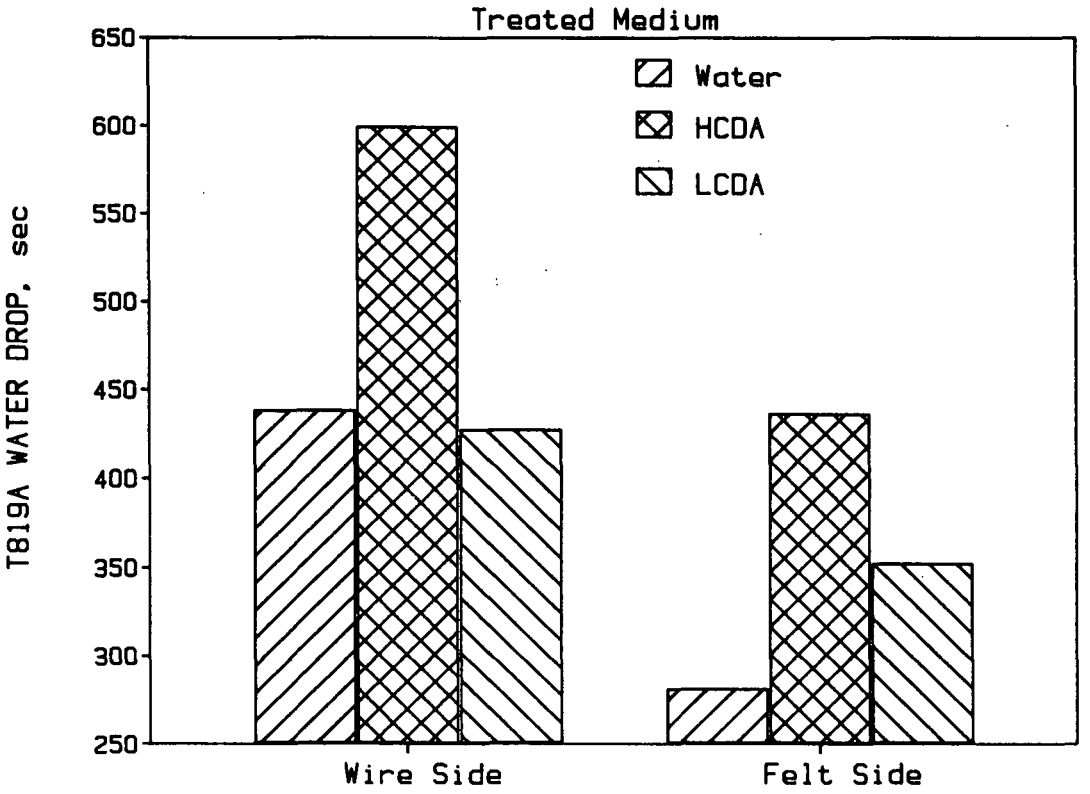

Figure 19. Effects of surface treatments on the water drop of medium.

We corrugated the treated mediums with no difficulty and the pin adhesion strengths of the treated mediums were comparable to those obtained with the water control and the untreated medium (Fig. 20). The pin adhesion strengths for all combinations were lower than usually obtained, however, this is dependent on the characteristics of the starch formulation, amount applied and the machine conditions.

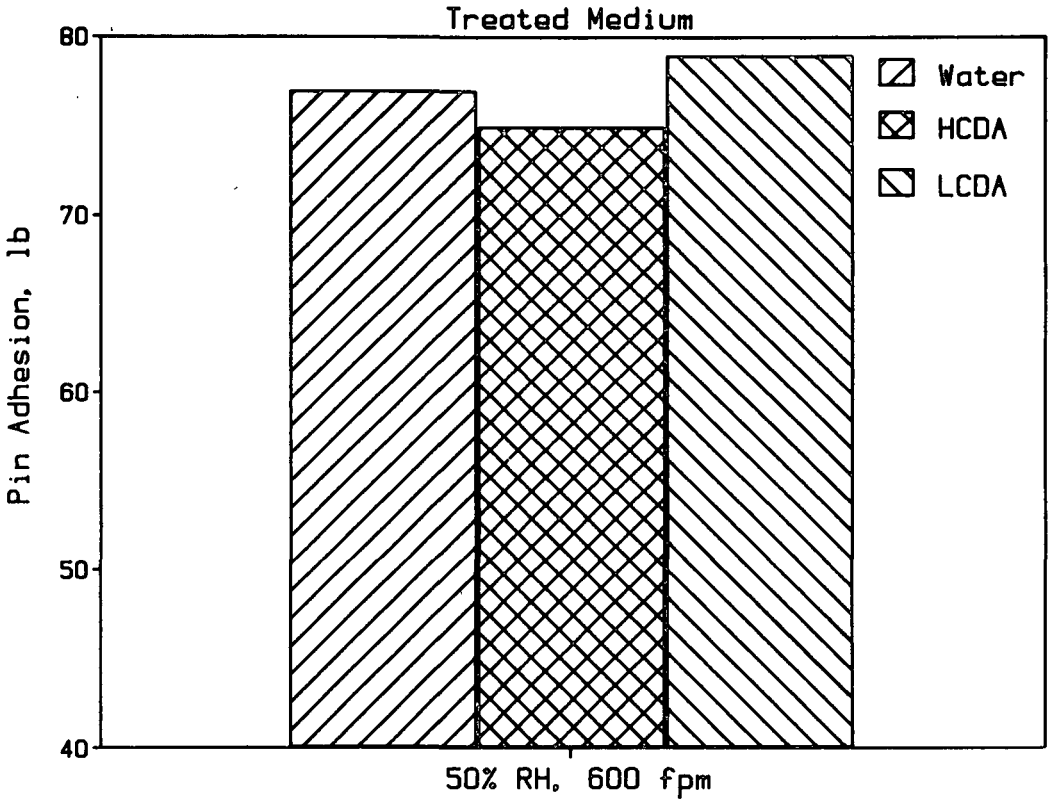

Figure 20. The pin adhesion strengths of the treated mediums are comparable to those obtained with the water control.

Figure 21 shows that the low charge density starch, LCDA, substantially increased the flat crush strength of the combined board relative to the water control. This increase reflects the increases in STFI and ring crush achieved with this treatment. On the other hand neither treatment appeared to have much effect on ECT (Fig. 22). In part, this reflects the fact that the medium makes up only about one-third of the combined board so larger increases in CD strength are needed than were achieved at these treatment levels. Possibly, the low pin adhesion strengths are another factor because we know that ECT strengths are reduced when pin adhesion is low.

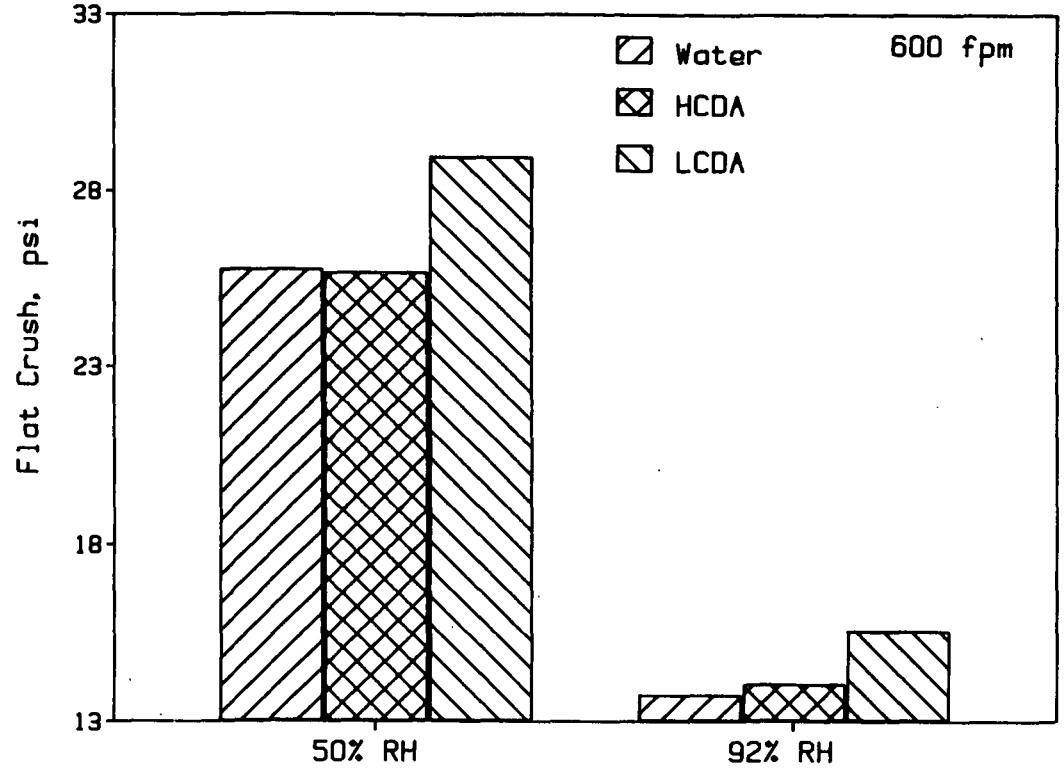

Figure 21. Flat crush results for treated mediums.

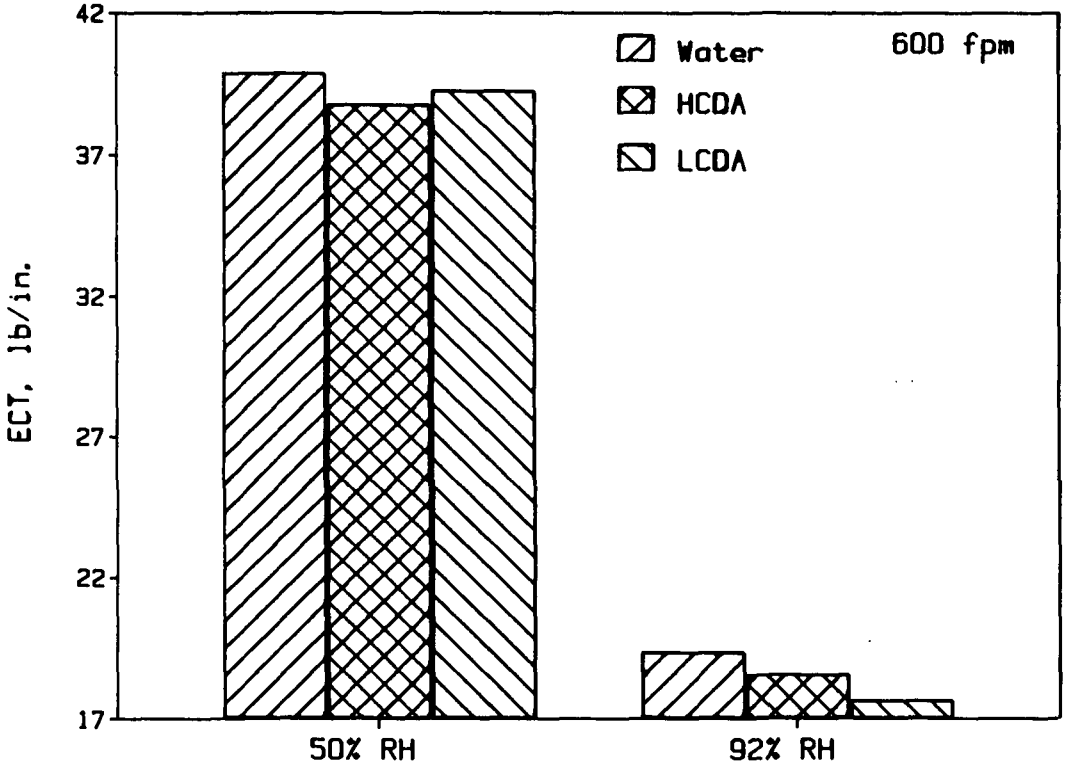

Figure 22. ECT results for treated mediums.

Linerboard Treatments

Tables 3 and 4 summarize the results for the treated liners. Figure 23 shows that both treatments effected small increases in cross direction STFI short span compressive strength of about 6-7.4% at 50% RH relative to the water control. Thus these treatments appeared to have less effect on the CD liner STFI strength than on medium.

The CD ring crush strengths were also increased by both treatments but the low charge density starch treatment LCDA was more effective than the high charge density agents (Fig. 24) at 50% RH. However, at 92% RH both agents gave equal improvements of 6.7%.

ECT strengths were generally improved by the low charge density starch treatments (Fig. 25) which reflects the compressive strength improvements noted above. However, the improvements were relatively modest, ranging from 5.7 to 7.2% at 50% RH.

Briefly summarizing, modest improvements in compressive strength tended to be obtained with these surface treatments without making the medium or linerboard too impervious to aqueous liquids. More effective agents or higher application levels are needed to achieve significant strength improvements.

The data show evidence of erratic changes in properties which may be related to the dipping and drying techniques used in this work. The application procedures may be causing differences in amount of pick-up and location of the additives within the sheet which increase test variability.

Table 3. Physical characteristics of liners.

		Controls		Liner Treatments			
		Untreated	Water @ pH5	HCDA Agent		LCDA Agent	
		Average	Average	Average	% Diff.	Average	% Diff.
Sample code:		6706	EE	AA		BB	
Basis Weight							
Grammage, gm/M^2		204	206	208	+1.0	210	+1.9
$lbs/1000\ ft^2$		41.9	42.2	42.6	+1.0	43.0	+1.9
Caliper							
TAPPI Thickness, mil		12.7	13.8	14.1	+2.2	14.2	+2.9
IPC Thickness, mil		10.9	11.8	12.0	+1.7	11.6	-1.7
Density							
TAPPI, kg/m^3		632	588	580	-1.4	580	-1.4
IPC, kg/m^3		739	688	683	-0.7	714	+3.8
Ring Crush							
MD, lb/6in.	50% RH	108	96	72	-25.0	103	+7.3
	92% RH	49	42	44	+4.8	48	+14.3
CD, lb/6in.	50% RH	73	66	72	+9.1	83	+25.8
	92% RH	32	30	32	+6.7	32	+6.7
STFI							
MD, lbF/in.	50% RH	37.88	34.76	36.11	+3.9	37.80	+8.7
	92% RH	14.75	13.31	12.87	-3.3	13.69	+2.9
CD, lbF/in.	50% RH	21.80	20.74	22.01	+6.1	22.27	+7.4
	92% RH	8.22	8.01	8.61	+7.5	8.24	+2.9
Tensile							
MD, lb/in.	50% RH	83.7	80.6	84.5	+4.8	88.3	+9.6
	92% RH	43.2	44.8	45.1	+0.7	49.1	+9.6
	WET	8.1	8.8	10.0	+13.6	9.3	+5.7
CD, lb/in.	50% RH	36.9	34.1	36.3	+6.5	37.0	+8.5
	92% RH	19.2	19.3	20.2	+4.7	21.8	+13.0
	WET	3.5	3.8	4.5	+18.4	4.2	+10.5
Stretch							
MD, %	50% RH	1.56	1.84	1.83	-0.5	2.15	+16.8
	92% RH	1.89	2.53	2.42	-4.3	2.61	+3.2
	WET	1.17	1.18	1.36	+15.3	1.48	+25.4
CD, %	50% RH	4.33	4.09	4.33	+5.9	3.78	-7.6
	92% RH	5.80	5.50	5.78	+5.1	6.10	+10.9
	WET	3.99	3.89	4.13	+6.2	4.20	+8.0

Table 3 continued. Physical characteristics of liners.

		Controls		Liner Treatments			
		Untreated	Water @ pH5	HCDA Agent		LCDA Agent	
		Average	Average	Average	% Diff.	Average	% Diff.
Sample code:		6706	EE	AA		BB	
TEA							
MD,ft lb/ft^2	50% RH	10.79	11.72	12.21	+4.2	15.34	+30.9
	92% RH	6.76	8.74	8.98	+2.7	10.06	+15.1
	WET	1.04	1.01	1.42	+40.6	1.45	+43.6
CD,ft lb/ft^2	50% RH	14.30	12.74	14.18	+11.3	12.56	-1.4
	92% RH	9.02	8.82	9.32	+5.7	10.47	+18.7
	WET	1.16	1.21	1.49	+23.1	1.46	+20.7
ET							
MD, lb/in.	50% RH	9890	8729	8862	+1.5	9285	+6.4
	92% RH	4569	3657	4096	+12.0	4004	+9.5
	WET	1269	1202	1292	+7.5	1054	-12.3
CD, lb/in.	50% RH	3545	3329	3243	-2.6	3592	+7.9
	92% RH	1382	1290	1352	+4.8	1039	-19.5
	WET	171	175	188	+7.4	185	+5.7
Gurley Porosity							
sec/100 cc	50% RH	21.2	14.4	14.6	+1.4	15.6	+8.3
Water Drop, T 492 - 10% Lactic Acid							
Seconds							
Wire side up	50% RH	251	223	314	+40.8	270	+21.1
Felt side up	50% RH	>600	>600	>600	-0-	>600	-0-
Friction, Hot Coef.							
Wire side up	50% RH	0.36	0.40	0.35	-12.5	0.40	-0-
Felt side up	50% RH	0.31	0.37	0.34	-8.1	0.35	-5.4

Table 4. Physical characteristics of combined board.

Sample code:		Controls: Untreated Average 6706/6553	Controls: Water @ pH5 Average EE/6553	Liner Treatments: HCDA Agent Average AA/6553	HCDA Agent % Diff.	Liner Treatments: LCDA Agent Average BB/6553	LCDA Agent % Diff.
Singlefaced Board							
Caliper, mils							
Singleface	600 fpm	154.6	155.0	155.1	+0.1	155.0	-0-
	800 fpm	154.9	156.2	156.8	+0.4	156.2	-0-
Flat Crush, psi							
50% RH	600 fpm	27.5	28.5	29.0	+1.8	29.4	+3.2
92% RH	600 fpm	15.0	15.1	14.5	-4.0	14.6	-3.3
50% RH	800 fpm	28.8	29.8	30.8	+3.4	30.4	+2.0
92% RH	800 fpm	16.0	15.3	15.2	-0.7	15.3	-0-
Pin Adhesion, lb							
	600 fpm	76CC	74CC	74CC	-0-	74CC	-0-
	800 fpm	78CC	77CC	75CC	-2.6	76CC	-1.3
ECT, lb/in							
50% RH	600 fpm	44.1	40.5	41.5	+2.5	43.4	+7.2
92% RH	600 fpm	19.8	18.6	20.1	+8.1	20.1	+8.1
50% RH	800 fpm	40.3	40.2	40.1	-0.2	42.5	+5.7
92% RH	800 fpm	18.6	18.9	19.9	+5.3	17.2	-9.0

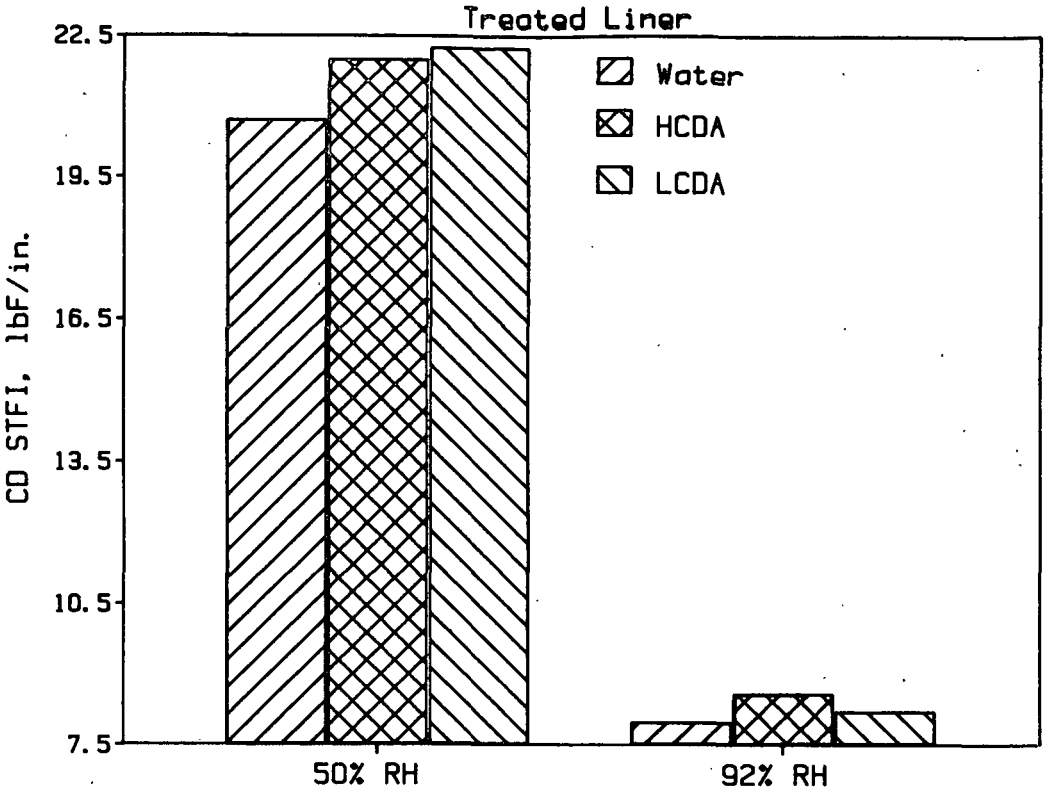

Figure 23. CD STFI short span compressive strength results for the treated linerboards.

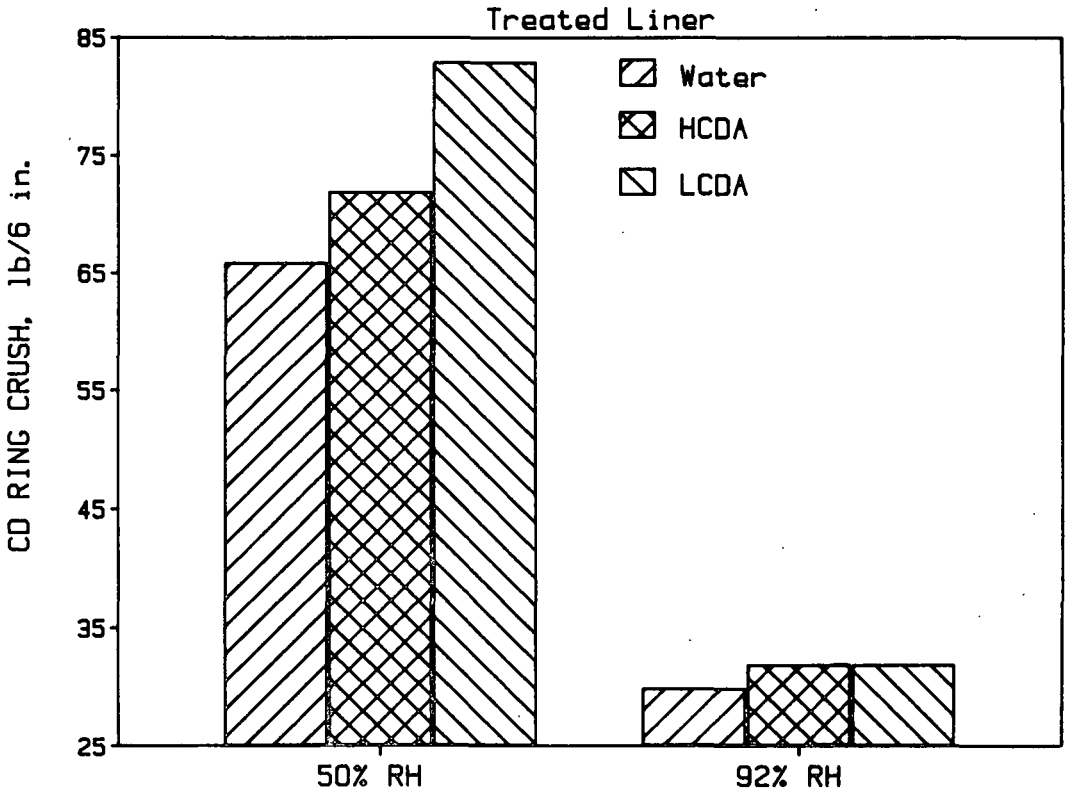

Figure 24. CD ring crush strengths for the treated linerboards.

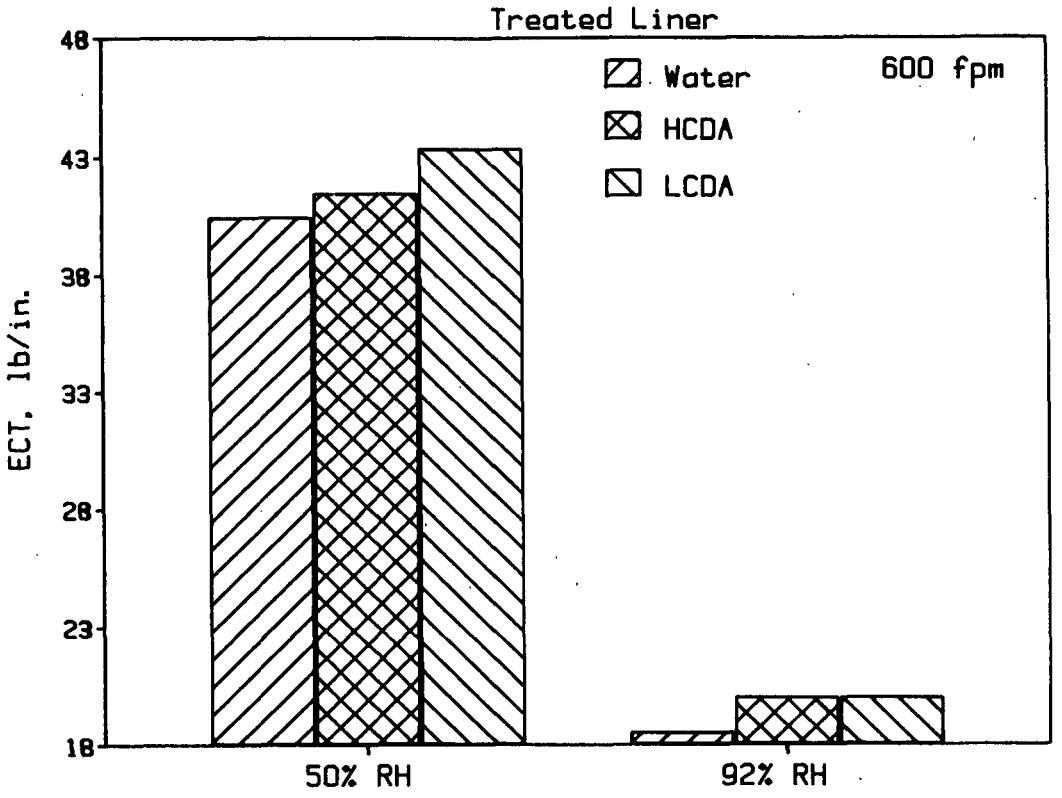

Figure 25. ECT strengths for treated linerboards.

RUNNABILITY MODELING -- HIGH TEMPERATURE FURNISH EFFECTS

As discussed in the October status report, we have initiated a study to determine the effects of medium composition on high temperature tensile property behavior and runnability. During fluting the medium is exposed to high temperatures at various moisture contents. Higher temperatures and moisture contents lower tensile strength and generally increase stretch. Differences in high temperature behavior of medium may help explain some aspects of runnability behavior which are not revealed by tests at standard conditions.

A schematic plan for material selection is shown in Figure 26. This work is being carried out cooperatively under Projects 3571 and 3469. Experimental mediums are being made on the Formette sheet former and wet pressed

at two levels from these furnishes:

1. NSSC/unbleached softwood: 100/0%, 50/50% and 0/100%
2. NSSC/bleached softwood: 50/50% and 0/100%
3. NSSC with synthetic fiber/polymer blends in outer layers.

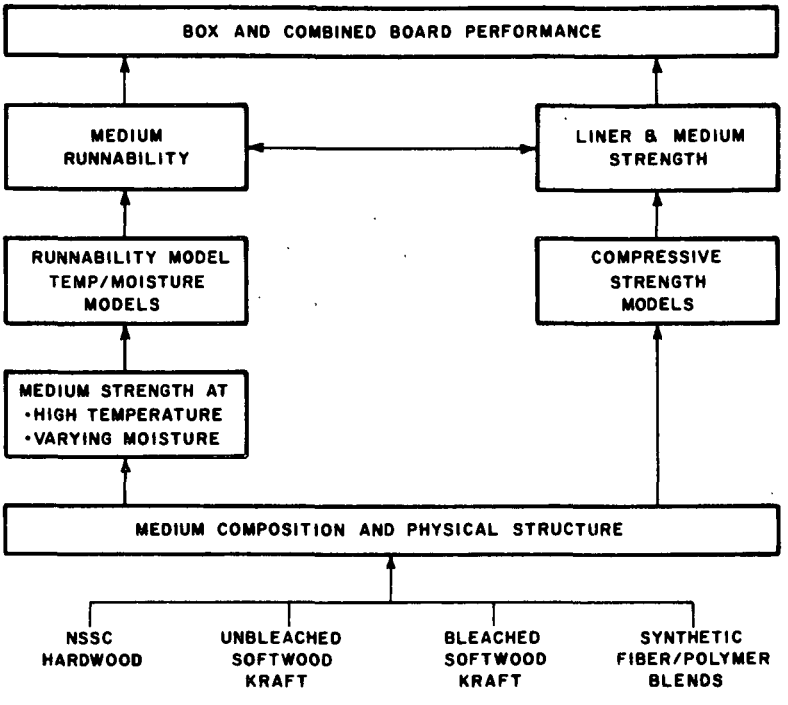

Figure 26. Schematic plan for high temperature medium furnish study.

We have just completed preparation of the bleached softwood sheet combinations; the NSSC and unbleached softwood sheet combinations are also made. The sheets with synthetic fiber are in process.

The chemical compositions of the base furnishes are shown in Table 5. Compositions range from the high lignin, low cellulose content of the NSSC furnish to the low lignin, high cellulose content of the bleached softwood kraft. Hemicellulose contents also vary greatly.

Table 5. Chemical composition of furnishes.

	NSSC	Unbl. Kraft	Bl. Kraft
Lignin, %	16.4	15.0	<0.5
Araban, %	4.4	1.0	1.0
Xylan, %	17.3	8.3	8.6
Mannan, %	2.0	6.5	8.6
Galactan, %	0.5	1.1	0.8
Glucan, %	57.6	66.4	79.3

Table 6 summarizes the ultrasonic stiffness tests on the NSSC and softwood kraft furnishes. Figure 27 shows that the base furnishes exhibit significant differences in MD specific stiffness and hence, will exhibit significant differences in strength and runnability properties. Taken in conjunction with the chemical content, the high temperature tensile behavior of the furnishes should be quite different.

The physical properties of the base furnishes and blends are being evaluated at present and should be completed during the next month. The high temperature tensile tests will be carried out at temperatures of 200, 250 and 300°F using a heating time of 1 second. The specimens will be conditioned to 50% and 80-85% RH prior to test. These tests will start in the near future along with the corrugating trials.

Table 6. Base furnish properties.

	100% Unbl. NSSC	100% Unbl. NSSC	100% Unbl. Softwood Kraft	100% Unbl. Softwood Kraft	50/50 NSSC/ Unbl. Kr.	50/50 NSSC/ Unbl. Kr.	100% Bl. Softwood Kraft	100% Bl. Softwood Kraft	50/50 NSSC/ Bl. Kr.	50/50 NSSC/ Bl. Kr.
Sample No.:	77-1	79-1	86-1	84-1	88-1	90-1	139-1	143-1	146-1	144-1
Wet Pressing:	Low	High	Low	High	Low	High	Low	High	Low	High
IN-PLANE SONIC TESTS										
MD-CD Geom. Mean V^2 $(km/sec)^2$	9.71	10.05	9.97	10.05	9.68	9.78	10.37	10.51	9.54	9.95
Stiffness Ratio	2.37	2.26	2.08	1.96	2.22	2.22	2.52	2.30	2.46	2.38
NUXY	0.18	0.15	0.21	0.21	0.19	0.18	0.19	0.19	0.18	0.17
NUYX	0.43	0.34	0.44	0.40	0.41	0.41	0.48	0.43	0.44	0.40
Geom. Mean Nu	0.28	0.23	0.30	0.29	0.28	0.27	0.30	0.29	0.28	0.26
Ex/Rho, $(km/sec)^2$	13.77	14.31	12.80	12.87	13.29	13.43	14.94	14.64	13.80	14.30
Ey/Rho, $(km/sec)^2$	5.81	6.32	6.16	6.58	6.00	6.06	5.93	6.37	5.60	6.01
G/Rho, $(km/sec)^2$	3.16	3.36	3.26	3.38	3.23	3.48	3.49	3.77	3.32	3.49
MD-CD G. Mean E/Rho, $(km/sec)^2$	8.94	9.51	8.88	9.20	8.93	9.02	9.41	9.66	8.79	9.27
E_x, TAPPI, Gpa	6.21	6.95	7.01	7.59	6.35	6.92	8.96	9.85	6.69	7.22
E_y, TAPPI, Gpa	2.62	3.07	3.38	3.88	2.87	3.12	3.56	4.29	2.72	3.04
G, TAPPI, Gpa	1.43	1.63	1.79	2.00	1.55	1.79	2.09	2.54	1.61	1.76
E_x, IPC, Gpa	11.30	13.51	9.66	11.08	10.50	11.89	12.65	14.11	11.44	13.48
E_y, IPC, Gpa	4.77	5.97	4.65	5.67	4.74	5.37	5.02	6.14	4.64	5.67
G, IPC, Gpa	2.60	3.17	2.46	2.91	2.56	3.08	2.96	3.64	2.75	3.29
OUT-OF-PLANE SONIC TESTS										
$V^2(LZ)$, $(km/sec)^2$	--	--	--	--	--	--	0.219	0.236	0.214	0.223
st. dev.	--	--	--	--	--	--	0.011	0.011	0.016	0.030
Caliper, micrometers	--	--	--	--	--	--	149.8	133.1	162.7	150.4
st. dev.	--	--	--	--	--	--	2.1	1.7	9.8	19.6
PHYS. TEST RESULTS										
Basis wt., g/m^2	119.2	124.9	126.7	125.6	125.8	127.9	124.8	123.2	124.3	124.5
Caliper, (TAPPI), micrometers	264.4	257.0	231.1	212.9	263.1	248.2	207.8	183.1	256.3	246.6
st. dev.	18.3	20.3	6.1	5.8	25.4	16.2	27.0	2.5	27.9	50.3
Caliper (soft pl.), micrometers	145.2	132.3	167.9	145.9	159.2	144.5	147.3	127.8	150.0	132.1
st. dev.	3.9	2.8	2.8	2.1	3.1	2.5	2.1	1.2	1.8	2.3
Density (TAPPI), g/cm	0.451	0.486	0.548	0.590	0.478	0.515	0.600	0.673	0.485	0.505
Density (soft pl.), g/cm	0.821	0.944	0.755	0.861	0.790	0.885	0.847	0.964	0.829	0.943

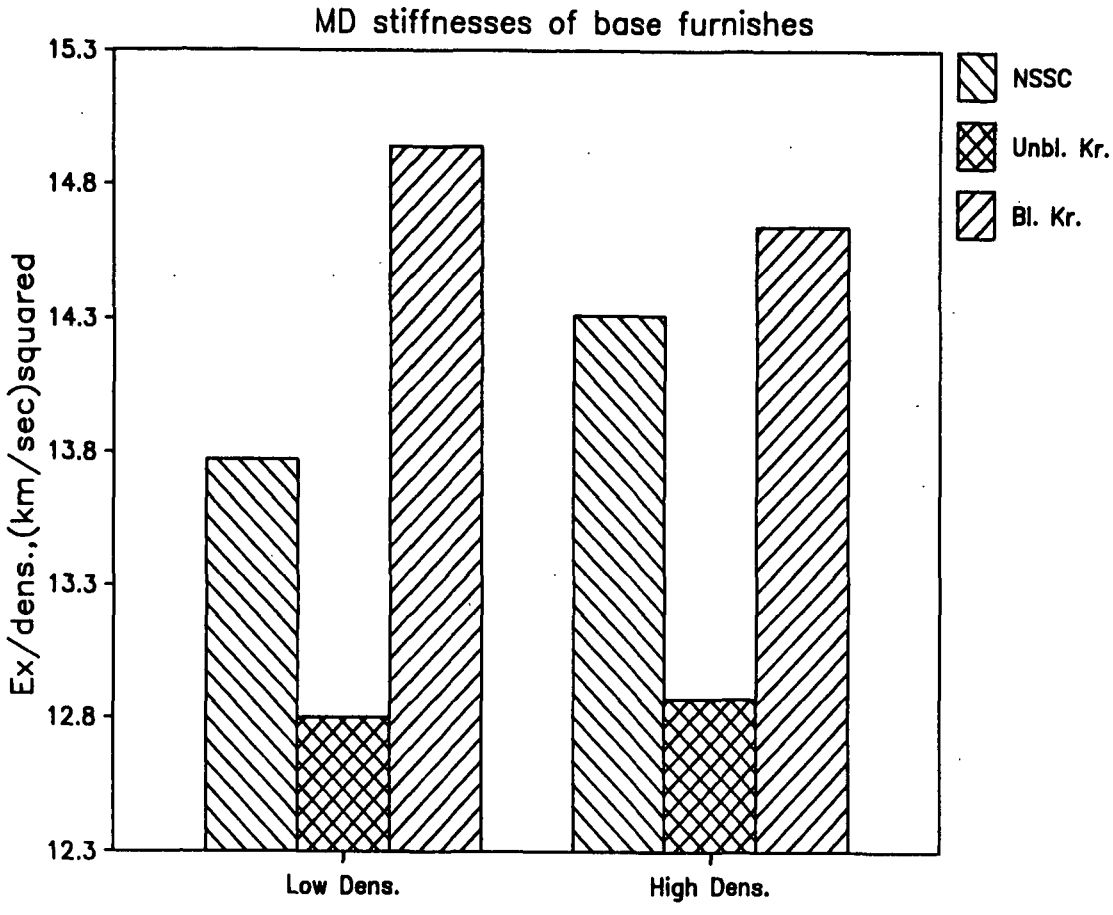

Figure 27. MD Elastic specific stiffnesses of base furnishes.

RUNNABILITY MODELING - SPEED, TEMPERATURE AND MOISTURE EFFECTS

The influence of corrugating speed on combined board properties such as flat crush and ECT are well recognized. For most mediums high lows increase with corrugating speed and some mediums even fracture at moderate or high speeds. Whitsitt has developed an empirical model to predict a medium's runnability from its stretch, tensile, friction and thickness properties. Complications arise with the stretch and tensile properties because they are affected by rate of loading, moisture and temperature. The property values measured under normal laboratory testing conditions are not the values governing the medium's runnability in a high speed corrugating operation with preheaters and showers.

One approach to dealing with the rate of loading problem is to represent the medium's deformation behavior with a mechanical model which characterizes the material as viscoelastic with rheological parameters. The list of previous investigators using mechanical models to describe paper include Steenberg[3], Kubat[4], Agbezuge[5], Skowronski[6], and Nissan[7]. The power of using a mechanical model for the current problem is that the rheological parameters can be obtained from tests carried out in the laboratory and then the model's performance can be extrapolated to the high loading rates of the corrugator.

In the previous report, preliminary results were presented for a linear mechanical model. Improved results have now been obtained using the HWE (Halsey, White and Erying) model shown in Fig. 28 with two linear spings and a non Newtonian dashpot. (For a discussion of the HWE model see Agbezuge[5].) The dominant feature of the HWE model is the nonlinear dash pot whose behavior is described by:

$$\dot{\varepsilon}_D = K \sinh a \sigma_D$$

where sinh is hyperbolic sine,

$\dot{\varepsilon}_D$ is the derivative of the dashpot strain with respect to time

σ_D is the dashpot stress

K, a are the dashpot parameters.

This form was suggested by Erying. The governing differential equation for the HWE model is:

$$(E_1 + E_2)\,\dot{\varepsilon} - \dot{\sigma} = E_2 K \sinh a(\sigma - E_1\varepsilon)$$

where E_1, E_2 are the linear spring constants

σ is the total stress

$\dot{\sigma}$ is the derivative of total stress

ε is the total strain

$\dot{\varepsilon}$ is the derivative of total strain.

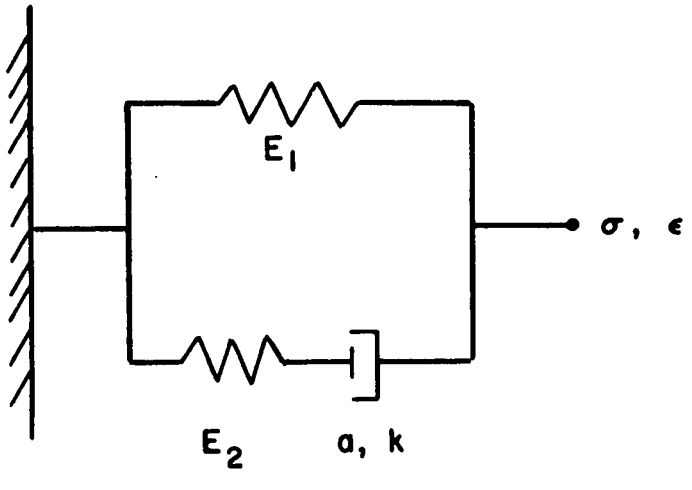

Figure 28. HWE viscoelastic model with a non Newtonian dashpot.

The HWE model was found to be well suited for characterizing the constant strain rate deformations of a sample from commercial medium 6799. The procedures followed for this characterization were:

1. Constant strain rate curves were obtained for medium 6799 using the Instron with head speeds of 0.2 in./min. and 1.0 in./min.
2. Ten pairs of stress-strain points were selected from each of the two load curves.
3. A computer program was used to obtain the optimal values for the 4 HWE parameters so as to minimize the squared residuals between the 20 experimental points and a set of 20 corresponding points from the model.

   The optimal values obtained in this way were

   E_1 = 2049 lb/in.

   E_2 = 3472 lb/in.

   K = 2.99×10^{-5} min^{-1}

   a = 0.463 in./lb

Figures 29 and 30 show how successfully the HWE model was able to match the two experimental curves.

It has been estimated that running the pilot corrugator at 1000 ft/min corresponds roughly to a strain rate of 6000 in./min. The HWE model predicted a tensile strength for medium 6799 at this strain rate of 57 lb/in. and a corresponding stretch of 1.05%. These predictions were based on the above mentioned parameters and the assumption that the areas under the constant strain rate curves are independent of strain rate.

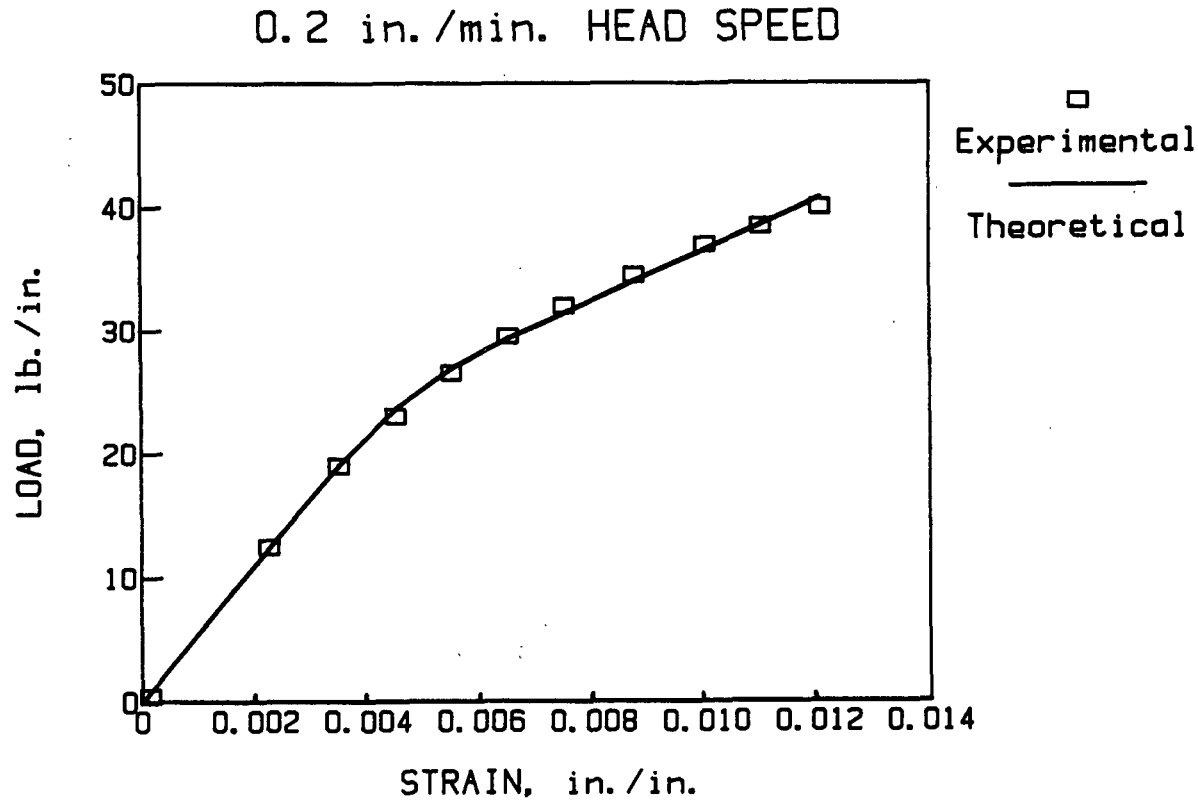

Figure 29. Comparison of experimental stress-strain points against HWE model theoretical curve.

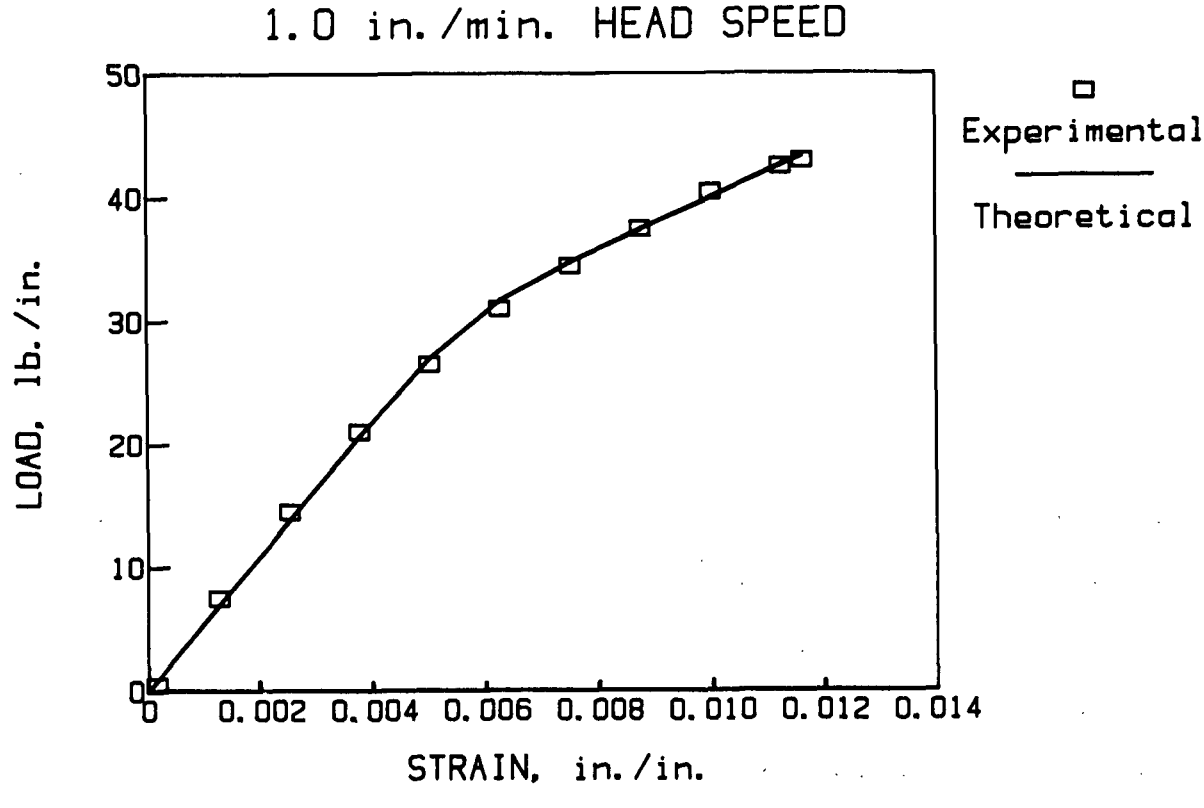

Figure 30. Comparison of experimental stress-strain points against HWE model theoretical curve.

The tensile properties which govern a medium's runnability are influenced not only by loading rate but also by the temperature and moisture conditions in the labyrinth. See Waterhouse[8] for a review of findings concerning how physical properties of paper and board are influenced by environmental conditions. Recently an apparatus was constructed at the Institute to study the tensile load-elongation properties of mediums under typical corrugating temperature and moisture conditions. Medium specimens can be preconditioned to various levels of moisture content and then heated for controlled periods of time just prior to a tensile test.

The following table gives some results for medium 6799 obtained with this new hot tensile apparatus.

Table 7. High temperature test data for medium 6799.

Platen Temp.	Tensile, lb/in.		Stretch, %	
Conditioning RH:	50	70	50	70
73	41.7	35.9	1.15	1.51
150	33.0	29.4	1.61	1.86
200	29.1	24.4	1.80	2.15
250	24.4	18.6	1.87	2.01

Note: Test speed was 20 in./min.

The tensile falls off with increasing temperature and increasing RH conditioning. Stretch on the other hand increases with increasing temperature and increasing RH conditioning. It is probable that changes in tensile properties due to changes in corrugating speed are attributable not only to loading rate effects but also to changes in moisture and temperature indirectly caused

by speed changes. How the medium moisture and temperature are influenced by corrugating speed are currently under investigation.

Computer simulation of the labyrinth geometry suggests that the medium may have to undergo about 0.5 % stretch in the final stage of its journey towards the labyrinth centerline. This is because the medium may be pinched tight between the upper and lower rolls due to the driving action of the bottom roll about one flute away from the centerline. If the medium can no longer slip because of this pinching, the remaining bit of deformation of the medium must be accomplished through stretch.

We are currently exploring how this final stretch along with the brake tension and bending tension are related to the medium's stress-strain curve. The latter is influenced by furnish, papermaking factors, corrugating speed and moisture and temperature conditions. These results should lead to a better understanding of flute fractures, high lows and strength retention.

FLAT CRUSH AND FLUTE FORMATION MODELING

This portion of the project is directed toward studying ways to reduce the compressive strength losses that occur in a medium during the flute forming process. It has been shown, in past research, that the medium experiences a considerable reduction in the MD compression strength during corrugating. The properties of the medium after corrugating play a key role in the performance of the combined board. Damage to the medium decreases the combined board's flat crush strength, edgewise compression strength, flexural stiffness and box compression strength. This research has focused on building a greater understanding of the physical damage to the medium during flute formation. Effective ways of reducing the damage may be developed, if the failure mechanisms are understood.

During the flute forming process, the medium is subjected to stresses which include tension, bending, shear and thickness direction compression. Past research has shown that a significant portion of the strength reduction during flute formation resulted from bending. Our research indicated that damage occurred periodically to fibers in the compression zone of the bend. The damage appeared to be primarily fiber buckling with some shear delamination between buckled areas. In general, the fibers in the tension zone of the bend and the fibers between buckled areas appeared undamaged.

Presently, a testing program is being conducted to study the effects of bending on damage to the medium. The objective of the testing is to determine the extent and type of damage to the medium resulting from various degrees of bend and amounts of initial web tension. The extent of damage was determined from STFI compression tests, tension tests and observation under the microscope, after bending.

A bending test apparatus was designed and constructed for the purpose of applying uniform bending to a medium specimen. The basic components of the apparatus are shown in Fig. 31. In the apparatus, the medium was bent around a radius, similar in size to that of a flute tip (approximately a 0.062-inch radius). The radius was mounted on a plate, which could move horizontally to achieve the desired amount of wrap. A wrap angle range from 0 to 180 degrees was possible. The bending test apparatus was mounted on the base of a tensile tester with the medium specimen strip attached to the load cell of the tester. Test specimens were pulled around the radius at a speed of 20 in./min. The medium specimens were subjected to wrap angles of 0, 30, 90, and 180 degrees in the bending test apparatus. The felt side of the medium was placed on the inside of the bend (compression zone) for this set of tests. Preload levels of 1 lb/in. and 3 lb/in. were applied to the specimens.

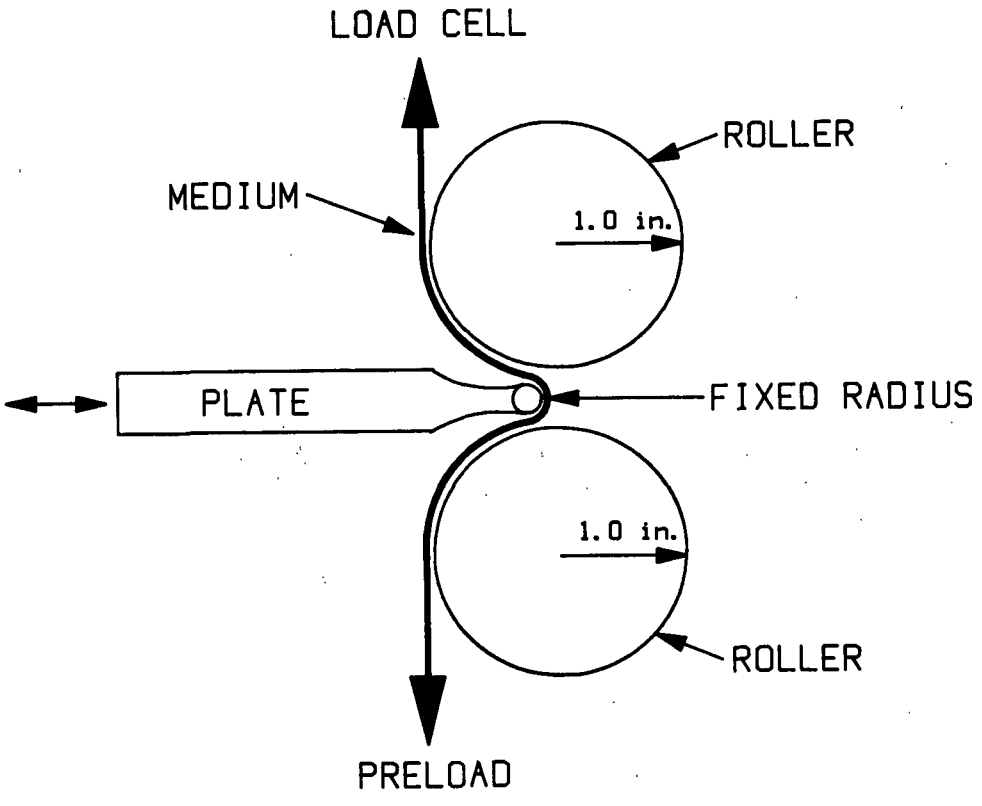

Figure 31. Basic components of the bending test apparatus.

Two different 40-lb medium specimens were tested. Their physical properties are shown on Table 8.

Table 8. Physical properties of mediums.

Medium	A	B
Basis Weight, lb/msq ft	40.5	38.6
Caliper (TAPPI), mil	12.7	14.6
Caliper (IPC), mil	10.2	11.9
MD Tensile, lb/in.	63.3	68.8
CD Tensile, lb/in.	28.0	31.6
MD Stretch, %	1.37	1.09
CD Stretch, %	2.54	2.18
MD-ET, lb/in.	8540	9830
CD-ET, lb/in.	3550	4020
MD TEA, ft lb/sq ft	6.67	5.32
CD TEA, ft lb/sq ft	6.38	5.98
MD-STFI, lb/in.	37.0	37.4
CD-STFI, lb/in.	22.7	23.0
Concora, lb	89.0	92.2
Friction (hot), felt	0.380	0.500
Friction (hot), wire	0.360	0.510

An important physical property of the medium, affecting the performance of the combined board, is the compression strength after corrugating. In this testing, STFI compression tests were conducted on the medium specimens after bending. The results, showing the relationship between the medium's STFI compression strength and the degree of wrap around a radius, are plotted on Fig. 32. A small reduction in compression strength occurred for mediums subjected to a 30 degree wrap around the radius. A significant compression

strength loss (approximately 30%) was observed when the mediums were subjected to a wrap angle of 90 degrees. A wrap angle of 180 degrees did not produce significant further damage. This data indicates that most of the damage to the medium occurred between wrap angles of 30 and 90 degrees. The results of this testing are in close agreement with past research relating compression strength loss to bending of the medium.

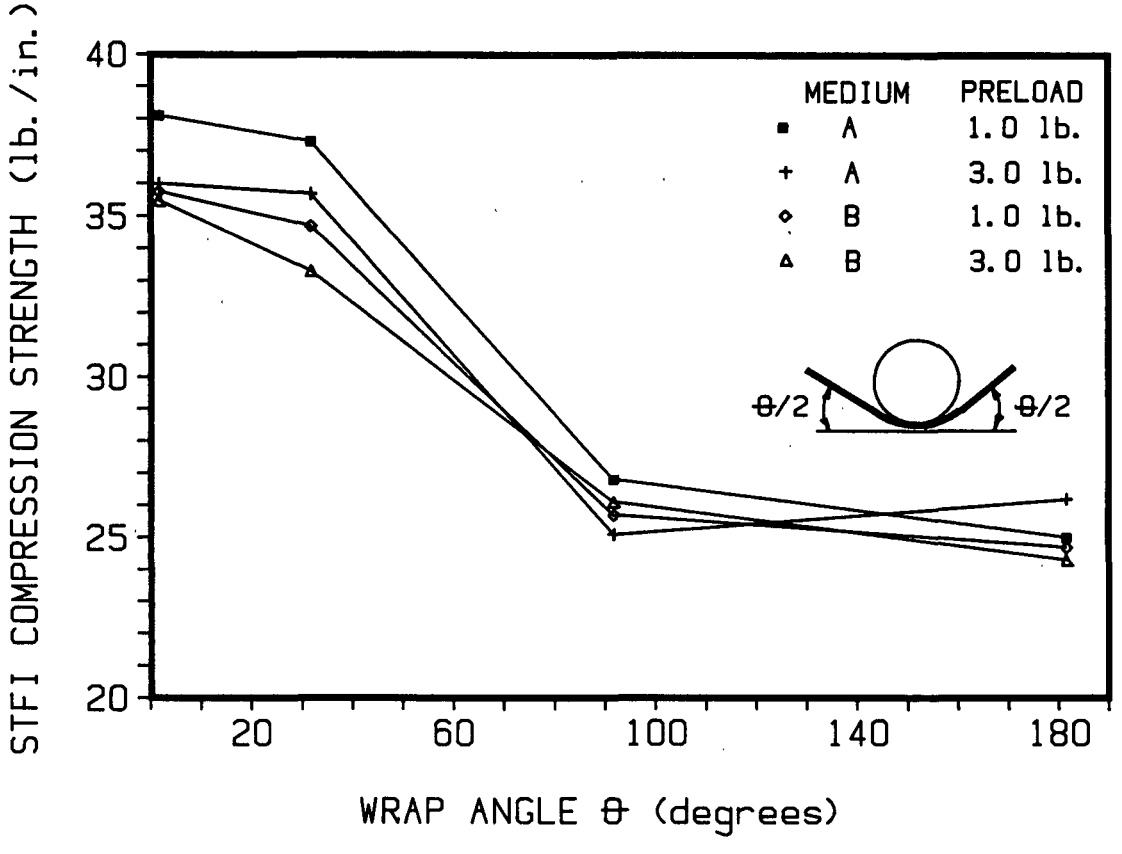

Figure 32. The relationship between the MD STFI compression strength of the medium after bending and the degree of wrap around the radius.

The STFI compression strength of the mediums, after bending, was not significantly affected by an increase in preload during bending. The tension force required to pull the mediums around the radius increased in approximately

the same proportion as the preload. The increased tension force was apparently due to greater frictional forces between the medium and the radius. However, the increased tension stresses on the medium did not lower the strains in the compression zone of the bend to the point of reducing losses in compression strength.

The tensile strength of the medium is an important factor affecting the speed at which fracture takes place during corrugating. In the flute forming process, tension in the medium increases as the medium is pulled into the labyrinth. As the tension stresses increase, bending is also occurring. Therefore, the tensile strength of the medium after bending would be an important property for runnability of the medium. In this program, tensile tests were conducted on the specimens after bending. Reductions in the tensile strengths were observed. The trends were similar to that of the compression strength loss, with the greatest damage occurring between wrap angles of 30 and 90 degrees. The magnitude of the tensile strength loss was between 15% and 30%, for specimens subjected to a 90 degree or greater wrap. However, the magnitude of the tensile strength loss was not as consistent as the compression strength reduction. A greater number of tests need to be conducted to make any conclusions about the tensile strength losses due to bending. Also, it is possible that further tensile strength losses would be observed if tension tests could be conducted on the specimens in their bent state. Straightening of the specimens after bending may allow some of the buckled fibers to contribute to the tensile strength. In the bent state, the buckled fibers may not be effective in resisting tension.

Examination the medium specimens under the microscope, after bending, provided visual evidence of sheet damage. The first indication of physical

damage was observed in the specimens subjected to a 30 degree wrap, as shown in Fig. 33. The specimen in Fig. 33 was reformed to approximately the 30 degree wrap and localized fiber buckling was evident on the compression side of the bend. Damage was more apparent in the specimens which had been subjected to a 90 degree wrap, as shown in Fig. 34. Buckled fibers, in the localized damaged area, extent deeper into the sheet and some shear delamination near the middle of the thickness can be observed. Significant damage was seen in the specimens subjected to a 180 degree wrap, as shown in Fig. 35. Localized fiber buckling and shear delamination can be observed in the specimen shown in Fig. 36 which had been subjected to a 180 degree wrap angle. From this testing it was not possible to determine if the delamination preceded the fiber buckling. Observation of the damage in the process of occurring would be necessary to fully understand the failure mechanism. The spacing of the localized fiber buckling was found to be at approximately 0.030 inches.

Further research into the failure mechanisms in medium due to bending is necessary to provide a better understanding of the causes and to find possible ways of reducing them. Testing of 26 lb and 33-lb mediums should be conducted to determine if the failure mechanisms are similar to that of the 40-lb mediums. Also, the effects of temperature, moisture and radius of bend should be examined.

Nonlinear finite element modeling of the flute forming process, flat crush loads and other combined board properties may provide a better understanding of the stresses and strains produced in the medium. A finite element model of the flat crush loading on a flute, with the approximate damage pattern found in the laboratory study of bending, produced results similar to the flat crush tests. The model also indicated the potential for increased

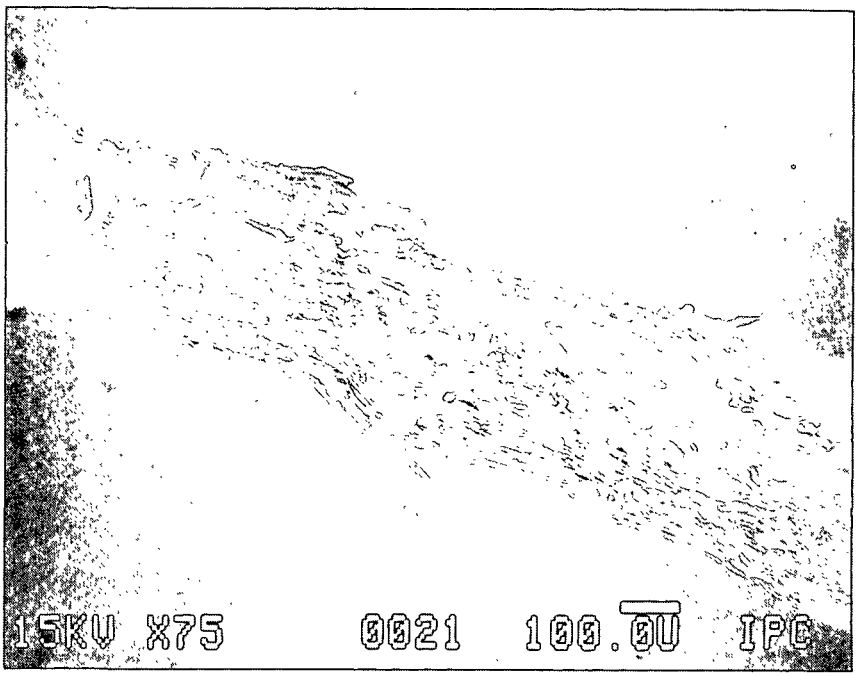

Figure 33. Some damage was evident in the compression zone of the bend, after bending to a wrap angle of 30 degrees.

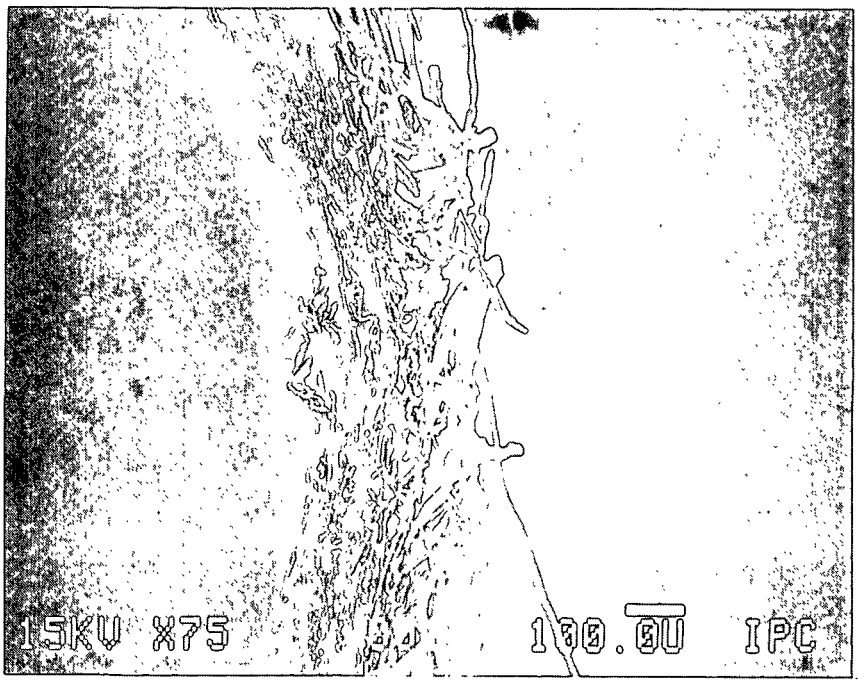

Figure 34. Localized damage was apparent, after bending to a wrap of 90 degrees.

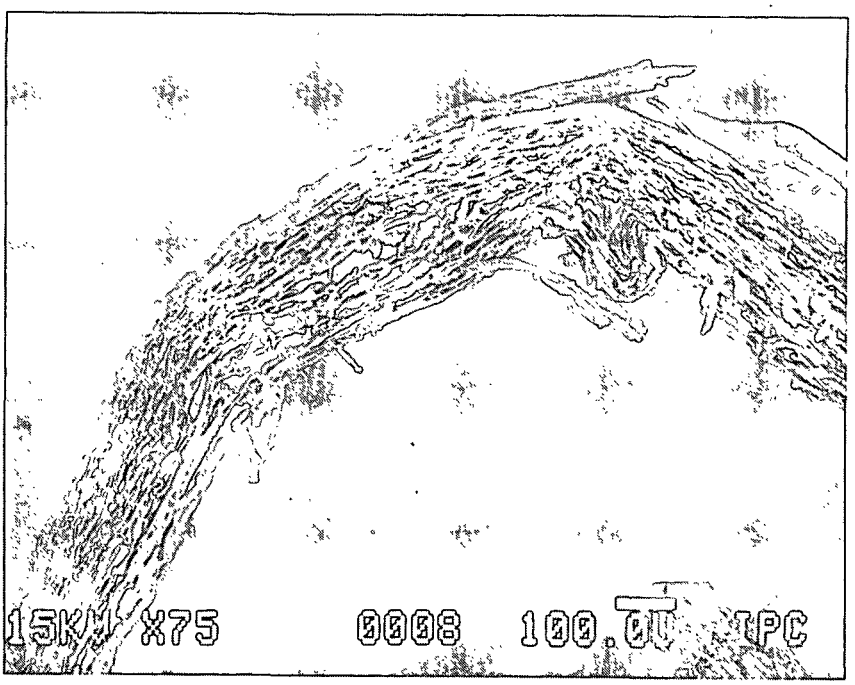

Figure 35. Buckled fibers were be observed in the damaged area, after bending to a 180 degree wrap angle. The damage extends through a significant portion of the sheet.

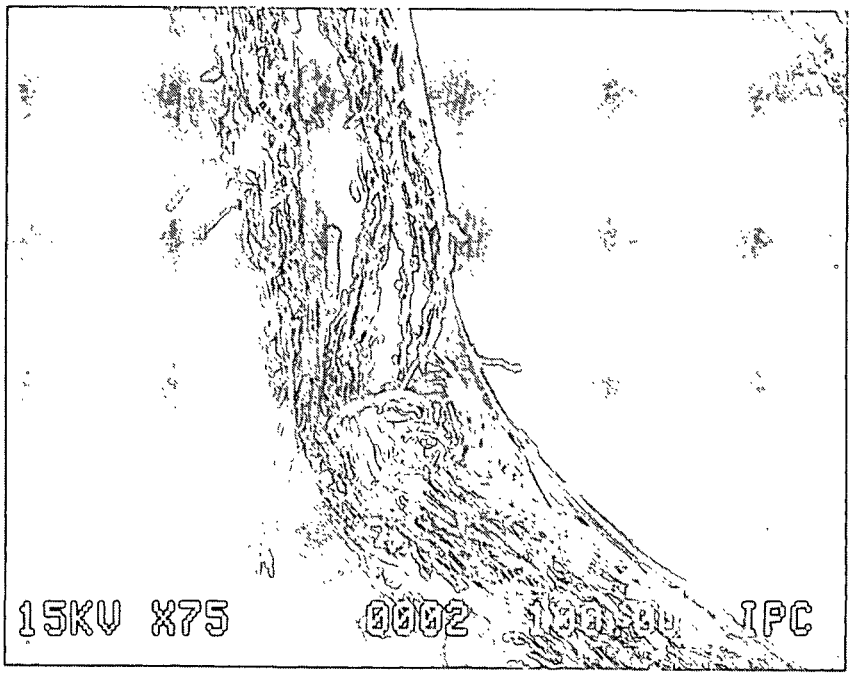

Figure 36. Delamination and localized fiber buckling was observed in the damaged area, of a specimen which had been subjected to a 180 degree wrap angle.

strength, if the damage to the medium could be reduced. Further use of laboratory results, concerning the material properties of the medium, in the finite element modeling may provide a better understanding of the role of the medium in the combined board performance.

COMMERCIAL BOX ABUSE STUDY

During the manufacture and working life of a corrugated container, the combined board is many times subjected to conditions which are less than ideal for optimum performance of the box. Feeder rolls on the manufacturing line may compress the board in the thickness direction past the elastic limit. Excessive thickness direction compression (precrush) may adversely affect the flat crush load resistance, flexural stiffness, ECT, and box compression strength. After manufacture, the container may be subjected to elevated relative humidities in a warehouse. Therefore, this portion of the project is directed toward determining the effects of simulated service abuse conditions on commercial board and boxes. The simulated service abuse conditions that are being examined include the following:

1. Thickness direction compression (precrush) of the board.
2. Exposure to elevated relative humidity conditions.
3. Combined effects of precrush and elevated relative humidities.

The testing program is also developing baseline results for ECT, flexural stiffness and box compression strength with commercial board.

Corrugated board blanks were obtained for use in the testing program. The boards were C-flute with 69-lb liners and 26-lb and 33-lb mediums.

The simulated service abuse conditions used in this testing were as follows:

1. The boards were subjected to two levels of precrush. The precrush levels were determined in a pilot study. In addition, a set of control samples with no precrush was tested. All precrushing was conducted at 50% RH and 73°F. Precrushing of the corrugated board blanks was done with a roll press.
2. The boards were subjected to relative humidity conditions of 50% and 85-90% at a temperature of 73°F.

Combining the two service abuse conditions (3 precrush levels and 2 relative humidity conditions) resulted in a total of six different conditions.

The tests which are being conducted on the board specimens include basis weight, flat crush load deformation curves, ECT, MD and CD flexural stiffness, and top load box compression.

The pilot testing portion of this project has been completed and testing is proceeding on the remainder of the program.

LITERATURE CITED

1. Halpin, J. C. Primer on Composite Materials: Analysis Technomic Publishing Co., Inc., Lancaster, PA (1984).
2. Habeger, C. C. and Whitsitt, W. J. Fibre Sci. & Techn. 19(3):215(1983).
3. Steenberg, B.: Svensk Papperstidn. 50 (1947): 15, 346.
4. Kubat, J.: Svensk Papperstidn. 56 (1953): 17, 670.
5. Agbezuge, L.: Polymer Engineering & Science 21 (1981): 9, 538.
6. Skowronski, J. and Robertson, A. A.: Preprint TAPPI International Paper Physics Conference, Harwichport, MA, 1983.
7. Nissan, A. and Batten, G. L.: Nordic Pulp and Paper Research Journal. Special Issue - B. Steenberg 75.
8. Waterhouse, J. TAPPI Notes, Management Techniques for Optimizing Laboratory Operations Seminar, September 1985.

THE INSTITUTE OF PAPER CHEMISTRY

Appleton, Wisconsin

Status Report

to the

PAPER PROPERTIES AND USES

PROJECT ADVISORY COMMITTEE

Project 3467

PROCESS, PROPERTIES, PRODUCT RELATIONSHIPS

March 22-23, 1989

PROJECT SUMMARY

PROJECT NO. 3467: PROCESS, PROPERTIES, PRODUCT RELATIONSHIPS

PROJECT STAFF: C. Habeger, K. Hardacker, Y. Pan February 13, 1989

PROGRAM GOAL:

Develop relationships between the critical paper and board property parameters and how they are achieved in terms of raw material selection, principles of sheet design, and processing conditions.

PROJECT OBJECTIVE:

(1) To improve our capability of characterizing paper and board materials,
(2) to relate measured parameters to end-use performance (especially in the case of Z-direction measurements), and
(3) to relate measured parameters to machine and process variables.

PROJECT RATIONALE, PREVIOUS ACTIVITY, AND PLANNED ACTIVITY FOR FISCAL 1988-89 are on the attached 1988-89 Project Form.

SUMMARY OF RESULTS LAST PERIOD: (March 1988 - October 1988)

(1) The robotic in-plane tester has been refined and tested, and it is ready for routine operation. Commercialization by RoboTest appears to be on schedule.

(2) Using the additional computing capabilities available with the IBM PC AT on the robotic tester, an improved technique was developed to measure in-plane elastic constants. This provides better estimates for in-plane Poisson ratios and the first ever measurement of C_{16} and C_{26}.

(3) New out-of-plane longitudinal ultrasonic transducers, which are capable of pulse-echo measurements, were constructed. These give a much improved method for determining out-of-plane acoustic losses in paper. Also, they allowed the development of a new technique that provides an ultrasonic measure of surface properties.

(4) An investigation of the ability of out-of-plane ultrasonic measurements to predict softness in tissue was promising.

(5) Papers for publication concerning the in-plane robot and the effect of environment on in-plane velocities were prepared.

(6) A suitable flash lamp was obtained and installed on the Board Optical Transmission Meter (BOTM), the instrument being developed for determining the optical scattering coefficient of heavy-weight papers.

(7) The optical and electronic systems for measuring the peak intensities of the source and transmitted light have been completed and put in working order.

(8) Good agreement has been observed between values of the transmittance of light-weight papers determined from R_0 and R_∞ measured on the TB-1 Brightness Tester and from R_0 and the transmittance determined with the BOTM.

SUMMARY OF RESULTS THIS PERIOD: (October 1988 - March 1989)

(1) The ultrasonic technique for measuring shear coupling coefficients in polymeric sheets has been verified by experiments with laminates. A paper has been written.

(2) The use of ultrasonic reflection coefficients on paper has been investigated. This resulted in a new, one-sided, easily administered measurement. However, we found that the transmission coefficients could not be inferred from the reflection coefficients, and they therefore could not be used for rigorous loss coefficient calculations. A paper, whose subject is the transducers used in the reflection measurements, has been written.

(3) An investigation of the effects of tissue manufacturing variables on out-of-plane ultrasonic measurements was conducted. A paper has been written on the empirical relations between out-of-plane ultrasonic parameter and tissue softness.

(4) An aperture wheel has been installed on the transmission detector of the Board Optical Transmission Meter (BOTM) for easy selection of port sizes to cover the full range of measurable transmittances.

(5) After calibration, it was demonstrated that transmission measurements could be made on a 39.2 g/m^2 white bond paper in stacks containing 1 to 23 sheets. The calculated transmittances extended to a low of about 7×10^{-8}. It was also demonstrated that the specific scattering coefficients of a range of papers from ordinary bond to a heavy unbleached kraft linerboard could be obtained easily.

(6) The BOTM may be used to measure R_0 with the specimen either bare or in the Teflon sandwich needed for transmittance measurement. This requires a specific calibration for the particular specimen type being measured. Best accuracy is obtained using R_0 values from the TB-1 brightness tester.

(7) The design, construction, and calibration of the instrument have now been completed, and it is ready for use.

PROJECT TITLE: Process, Properties, Product Relationships

PROJECT STAFF: C. Habeger

PRIMARY AREA OF INDUSTRY NEED: Properties related to end uses

PROGRAM AREA: Performance and Properties of Paper and Board

Date: 2/3/88
Budget: $175,000
Period Ends: 6/30/89
Project No: 3467

PROGRAM GOAL:

Develop relationships between the critical paper and board property parameters and how they are achieved in terms of raw material selection, principles of sheet design, and processing conditions.

PROJECT OBJECTIVE:

- Improve our ability to characterize the physical properties of paper and board materials.
- Relate measured parameters to end-use performance.
- Relate measured parameters to machine and process variables.

PROJECT RATIONALE:

It is important to understand the relationships between process variables, end-use performance, and paper and board properties in order to improve these products or maintain performance within close tolerances while effectively utilizing available raw materials, minimizing energy requirements, and minimizing environmental impacts.

RESULTS TO DATE:

The major activities and results can be separated into three areas: development of instrumentation; the impact of process variables on elastic properties; and the relationships between elastic properties and the end-use performance of paper.

Ultrasonic techniques and instruments have been developed which enable us to measure all four of the in-plane elastic stiffnesses of paper and three of the five out-of-plane elastic stiffnesses. These instruments also are suitable for measurements on other planar materials. Some of the equipment has been automated, so that the measurements are carried out under computer control with appropriate calculations made and results printed out in a report format. An automated in-plane ultrasonic measuring apparatus, which is made from a standard robot and off-the-shelf electronics, has been designed and constructed. A microwave technique for determining fiber orientation has also been developed. A soft rubber platen caliper system was developed under this project to provide accurate caliper and density measurements.

The ability to measure the three dimensional elastic behavior of paper has led to an extensive study of how process variables affect the elastic response. To date, process variables examined include wood species, pulping method, yield, refining, jet-to-wire speed ratios, wet pressing, wet stretching, drying

restraints, and calendering. The effects of coatings, fillers, sheet composition, sheet structure, and environmental factors (temperature and relative humidity) have also been investigated. Several useful relationships between the elastic stiffnesses have been discovered.

Finally, the elastic stiffnesses have been shown to be related to a number of the parameters now used to predict end-use performance and/or convertability. The elastic stiffnesses are fundamental properties of a material, and are good indicators of operating conditions on the paper machine and of final product quality.

PLANNED ACTIVITY FOR FY 1988-89:

In recent years this project has been concerned with measuring the elastic properties of paper, and relating these to process variables and end use performance, where possible. These activities will continue in FY 1988-89.

The feasibility of using out-of-plane ultrasonic measurements for nondestructive testing on tissue will be explored.

Software development will continue on the in-plane ultrasonic robot. Procedures for supplying duplicate instruments to member companies will be established.

The use of out-of-plane loss measurement for studying weak bonding in multi-ply sheets will continue.

Publications on using soft neoprene to couple ultrasonic transducers to paper, ZD ultrasonic loss processes in paper, the effect of the environment on of equilibrium ultrasonic velocity measurements, the moisture transient effect in cellulose, and the relationship between fiber properties and sheet elastic properties will be completed in FY 1989.

The possibility of using airborne ultrasound to measure air permeability in paper will be studied.

Construction of a device that can measure specific scattering coefficients in heavy board materials will be completed and used to test boards differing in composition and structure.

The use of polar diagrams to evaluate machine operating characteristics will continue.

STUDENT RELATED RESEARCH:

B. F. Berger, Ph.D.-1988; B. J. Berger, Ph.D.-1988; R. R. Willhelm, M.S.-1988; W. E. Myers, M.S.-1989.

Status Report

PROCESS, PROPERTIES, PRODUCT RELATIONSHIPS

Project 3467

I. PROGRESS ON THE ROBOTIC IN-PLANE TESTER

An instrument which uses a commercial laboratory robotic to make automated measurements of ultrasonic in-plane elastic parameters of paper has been developed and is described in detail in the appendix of the October 1988 PAC report. During the last period, a number of minor hardware and software improvements have been introduced. The couplings to the air cylinders, which rotate the transducers between shear and longitudinal operation, have been modified to preclude a tendency of the rotational assembly to occasionally lock-up. The slides for separating the transducers have also been modified to reduce friction. The software changes have been basically to facilitate user interface and to report additional parameters of interest in special cases. The instrument has been transferred from the ultrasonic research laboratory to the paper testing laboratory, where it is being used solely for routine testing. It is operating reliably and is well accepted by all users.

In the last PAC report, some preliminary work, using the asymmetries in polar plots to measure shear coupling coefficients and to assess the applicability of the orthotropic symmetry assumption, was discussed. As stated there, machine-made papers conform, within experimental error, to the orthotropic assumption. This appears to be true even when the specimen's principal axes are at relatively large angles to the machine axes. Nonetheless, it was possible to find commercial plastic sheets whose behavior deviated significantly from that predicted by orthotropic symmetry. In the last period, much work was done to verify the approach. A technique was developed for laminating plastic sheets without the bonded interface affecting the elastic response. Laminates, with

known amounts of non-orthotropic response, were fabricated, and the expected modifications in the polar plots were observed. This demonstrated self-consistency in the technique, and confirmed some very interesting results for extruded plastic sheets. A paper describing this work has been authored and is included in the appendix.

II. PROGRESS WITH LABORATORY OUT-OF-PLANE INSTRUMENTATION

In the last PAC report, we discussed the construction of special PVDF, pulse-echo transducers. For a more up-to-date account, see the paper included in the appendix. The purpose of these transducers was to improve out-of-plane loss measurements by quantifying the coupling efficiency at the paper-transducer interface. The signal reflection from the sample was to be compared with that reflected from an air interface, and the reflection coefficient would be calculated at both sample-transducer interfaces. After choosing a logical relation between the transmission coefficient and the reflection coefficient, the portion of energy transferred into (and out of) the sample could be determined, and losses in the sample could then be calculated from the amplitude of the time-of-flight signal through the sample. This was envisioned to be part of an automated test which determined the real and imaginary parts of the specific out-of-plane stiffness of paper.

Our first step toward incorporating the pulse-echo transducers was to devise a test solely for measuring the reflection coefficient. This proceeds in the following manner. A pulse echo transducer is mounted to the upper platen of the ZD longitudinal tester. The standard out-of-plane instrumentation is connected to a pulse-echo transducer with one electrode acting as the transmitter and the other as the receiver. Under computer control, the upper platen is

lifted, so that the transducer is in contact with air. The signal reflecting from the neoprene-air interface is digitized, and a Fast Fourier Analysis is performed. A sample is then placed on the lower platen, the jaws close and, after a prescribed time has elapsed, the reflected signal from the neoprene-sample interfaces is digitized and Fourier analyzed. Since the reflection coefficient at the air interface is very nearly -1, the reflection coefficient at the neoprene-sample interface can be determined by comparison with the air reflection signal. This is done for each Fourier component, and the average results for the chosen number of tests is reported. If the air reference signal is automatically updated between samples, this test is very repeatable. It provides an opportunity for detecting two-sidedness in mechanical properties by making measurements from the felt and wire sides separately. Compared to the through-transmission attenuation determinations, it is more straightforward, as it is not influenced by the uncertainties and variabilities of the coupling of signals through an aluminum foil reference.

Results of the reflection testing of a 42-lb linerboard with 125 kPa loading pressure are presented in Fig. 1. The phase shift for each Fourier component is listed in the third column, while the magnitude of the reflection coefficient is in column 7 (it is given a minus sign if, as in this case, the phase angle is between 90°and 270°). The signal amplitudes at each frequency are given for the air reference and for the sample in columns 5 and 6.

If the coupling were perfect, the complex reflection coefficient, R, could be related to the impedances of the neoprene, Z_N, and the sample, Z_S, as

$$R = (Z_S - Z_N)/(Z_S + Z_N) \ . \qquad (1)$$

THE INSTITUTE OF PAPER CHEMISTRY
OUT OF PLANE LONGITUDINAL REFLECTION COEFFICIENT

OPERATOR: Y-L. PAN IMPEDANCE & REFLECTION
DATE: JANUARY 23, 1989
TIME: 15:8:11

PROJECT: 3467
SAMPLE: F B LB 42# . 125 kPa, 5 min. CLEAN

NUMBER OF TESTS = 3

STABILIZATION DELAY (sec) = 2
INTEGRATION WINDOW = 352

HARM	FREQ (MHz)	PHASE SHIFT (deg)	TIME SHIFT (ns)	AMP REF (mv)	AMP SAMPLE (mv)	REFLECT COEF	STD DEV	Z AMP	Z PHASE (deg)
1	0.49	170.5	53.6	447.6	332.3	-0.742	0.001	0.29	28.69
2	0.73	170.1	38.0	578.2	415.6	-0.719	0.001	0.32	27.06
3	0.98	169.6	29.6	546.5	378.8	-0.693	0.001	0.34	25.74
4	1.22	168.8	25.1	455.5	307.3	-0.675	0.001	0.37	25.64
5	1.46	168.2	22.6	356.0	231.5	-0.650	0.004	0.40	24.82
6	1.71	168.2	19.5	239.3	147.3	-0.615	0.003	0.44	22.09
7	1.95	168.0	16.1	154.2	91.1	-0.591	0.002	0.47	20.71
8	2.20	168.3	13.5	93.1	54.5	-0.585	0.008	0.47	19.89
9	2.44	171.2	10.4	40.0	22.8	-0.571	0.014	0.48	14.59

Average Reflection Coef = -0.6979
Average Frequency = 0.9462 (MHz)
Average Time = 34.3 (ns)

Average Phase Shift = 169.58 (deg)
Average Z Amp = 0.340 (10^6 kg/sm^2)
Average Z Phase = 26.34 (deg)

Reference Predelay (μs) = 17.600

Ref gain = 0.893
Paper gain = 0.600

FFT window position = 356
Ref value at window = -3
Paper value at window = 4
Paper baseline value = 8

Figure 1. Typical reflection coefficient report.

Knowing the impedance of the neoprene, this equation could then be inverted to calculate the complex impedance of the sample from the reflection coefficient. These results are presented in the last two columns of Fig. 1. Remember this assumes perfect coupling, which is not generally the case. However, as loading pressure and time increase, coupling improves the values of Z_S calculated from the reflection should approach those made from transmission measurements. (The impedance is equal to the velocity of sound times the density and can easily be calculated from transmission measurements as the basis weight divided by the time-of-flight.) Since the phase angle of the impedance is one-half the loss angle, a complete determination of the ZD longitudinal elastic response could be obtained from one-sided reflection measurements, if coupling were perfect.

If the reflection technique is a valid approach, it should, at least, give correct impedances under ideal conditions. This was demonstrated by testing a set of four smooth, clean plastic disks at a 125 kPa loading pressure. The results are presented in Table 1. The first two columns list the amplitude and phase of the impedance as determined by reflection measurements. The third column is the impedances found from IPC time-of-flight measurements, and the final column is the reference book results.

Table 1. Reflection and transmission impedances for plastic shapes.

Sample type	Impedance refl. (kg/m^2s)	Phase refl. (°)	Impedance t.o.f. (kg/m^2s)	Impedance refer. (kg/m^2s)
PVDF	$3.24\ 10^6$	-4	$3.45\ 10^6$	$3.46\ 10^6$
Teflon	$2.68\ 10^6$	0	$2.78\ 10^6$	
Plexiglass	$3.00\ 10^6$	-4	$3.21\ 10^6$	$3.19\ 10^6$
Polystyrene	$2.31\ 10^6$	-4	$2.42\ 10^6$	$2.48\ 10^6$

Knowing the impedance of the neoprene, this equation could then be inverted to calculate the complex impedance of the sample from the reflection coefficient. These results are presented in the last two columns of Fig. 1. Remember this assumes perfect coupling, which is not generally the case. However, as loading pressure and time increase, coupling improves the values of Z_S calculated from the reflection should approach those made from transmission measurements. (The impedance is equal to the velocity of sound times the density and can easily be calculated from transmission measurements as the basis weight divided by the time-of-flight.) Since the phase angle of the impedance is one-half the loss angle, a complete determination of the ZD longitudinal elastic response could be obtained from one-sided reflection measurements, if coupling were perfect.

If the reflection technique is a valid approach, it should, at least, give correct impedances under ideal conditions. This was demonstrated by testing a set of four smooth, clean plastic disks at a 125 kPa loading pressure. The results are presented in Table 1. The first two columns list the amplitude and phase of the impedance as determined by reflection measurements. The third column in the impedances found from IPC time-of-flight measurements, and the final column is the reference book results.

Table 1. Reflection and transmission impedances for plastic shapes.

Sample type	Impedance refl. (kg/m^2s)	Phase refl. (°)	Impedance t.o.f. (kg/m^2s)	Impedance refer. (kg/m^2s)
PVDF	3.24 10^6	-4	3.45 10^6	3.46 10^6
Teflon	2.68 10^6	0	2.78 10^6	
Plexiglass	3.00 10^6	-4	3.21 10^6	3.19 10^6
Polystyrene	2.31 10^6	-4	2.42 10^6	2.48 10^6

Notice that the reflection determinations are about 5% lower than the actual values. This is because there is still some slippage at the interface, making the sample impedance appear less than it actually is. The values are, however, reasonably close to correct numbers and the phase angles are small. This demonstrates that on a smooth plastic sample the test is indicative of the nature of the material, with minor influences from the coupling conditions.

The next test of the reflection measurements is to make similar impedance comparisons on paper samples. Some typical results are presented in Table 2.

Table 2. Reflection and transmission impedances for paper samples.

Sample	Ref. Imped. felt side (kg/m^2s)	Ref. Imped. wire side (kg/m^2s)	T.O.F. Imped. (kg/m^2s)
Linerboard	$0.41\ 10^6$	$0.26\ 10^6$	$0.17\ 10^6$
Unpressed Handsheet	$0.15\ 10^6$	$0.15\ 10^6$	$0.07\ 10^6$
Pressed Handsheet	$0.23\ 10^6$	$0.22\ 10^6$	$0.20\ 10^6$

The reflection values are of the right order of magnitude; they show the expected trend with pressing; and they are sensitive to the two-sidedness in commercial linerboard. However, there are some very disturbing results in Table 2. For low impedance paper samples, poor coupling should lead to greater than expected reflections, which would cause the impedance, calculated for reflection amplitudes, to be lower than the actual value. Notice that in Table 2 the reflection numbers are, instead, greater than the time-of-flight numbers. This is particularly true for the unpressed handsheet and linerboard

samples, that are presumably rougher than the pressed handsheet. If these reflection coefficients were used to determine the transmission ratios, arbitrarily large values would be obtained. However, the transmission cannot be any better than in the perfect coupling case. The measured reflections are less than would result for perfect coupling, leading one to infer a larger than possible transmission.

The source of the lower than expected reflection coefficients in paper may be the irregularities in the geometry of the neoprene-paper interface. Energy, scattered at a rough surface, may not contribute to the reflected signal, and thus it might lead to an overestimate of the transmitted energy. These considerations throw serious doubt on the viability of our original goal: using reflection measurements to infer transmission coefficients and thereby to make interface-independent attenuation calculations. Since interface structure has not been characterized independently, we are not yet able to infer transmission directly from reflection measurements.

Even though rigorous measurements of out-of-plane loss coefficients in paper still are not within reach, the reflection coefficient measurement does provide a new nondestructive test for paper. The results depend on bulk mechanical properties and on surface irregularities in a complex manner. Moreover, since it is one-sided, the test is particularly simple, and it can be directly applied with much less procedure than a two-sided, through-transmission test.

III. EMPIRICAL RELATIONSHIPS BETWEEN TISSUE SOFTNESS AND OUT-OF-PLANE ULTRASONIC MEASUREMENTS

In the last PAC meeting report, we have discussed that subjective softness rankings of commercial tissue samples correlate well with out-of-plane ultrasonic tests. The preferred ultrasonic parameters for this purpose are the acoustic impedance and the apparent acoustic attenuation. The correlation coefficients were much higher with these quantities than with standard mechanical measurements (such as Young's modulus and ZD compressibility). Details of this investigation are included in the attached paper.

In hopes of gaining a more basic understanding on the ultrasonic measurements of tissue properties, a fundamentally oriented study was conducted during this period. We looked at the results of transmission and reflection measurements conducted on lab-prepared variable-controlled tissues.

INTRODUCTION

Softness of tissues is largely governed by paper-making variables such as pulp refining, wet-end additives, wet-pressing, drying, calendering, embossing and creping processes[1-4]. Changing the paper-making variables will change the sheet structures and hence the ultrasonic properties. Therefore, it would be interesting to know how these variables affect the out-of-plane ultrasonic properties.

In addition to the time-of-flight measurement of the out-of-plane ultrasonic waves through the paper, the reflection coefficient, R, from the paper-transducer interface can also be obtained by comparing the reflected signal with the incident one (see previous status report). The R is dependent

on the magnitude of acoustic impedance of paper, and also experimentally dependent on the coupling condition between the paper and the transducer. An advantage of the reflection coefficient measurement in that only one-sided coupling of the transducer to the paper surface is needed.

Although an investigation of panel softness would be of interest, this was not possible due to the limited supply of samples.

EXPERIMENTAL

Test Specimens

Table 3 is a description of the samples used in this study. The basis weight, caliper and the ratio of MD and CD in-plane Young's modulus are listed. In addition to regular handsheets, Formette Dynamique handsheets, and pilot machine-made tissues with creping and calendering information were also employed.

Handsheets were prepared with a mixture of 55/45 percent of hardwood and softwood pulps. The softwood pulp was beaten to 400 ml CSF and the unbeaten hardwood pulp was of a freeness level of 680 ml. All the handsheets were made without wet-pressing and air-dried on the blotter for at least 24 hours before testing. To investigate the effect of the fiber bonding on tissue property and ultrasonic measurements, two kinds of surfactants, Triton X-100 (a non-ionic surfactant) and Onyxsan HSB (a cationic surfactant, by Onyx Chemical Co., Jersey, NJ.) and Kymene (a cationic polymer) were added to the stock (Table 3).

Formette Dynamique handsheets were prepared from a commercially available tissue stock. The freeness was 580 ml CSF. Drum speed of the sheet former varied from 760 m/min to 1350 m/min to control the fiber orientation. Three different drying processes (Table 3) together with conventional steam

Table 3. Sample description.

Sample ID	Basis Weight (g/m^2)	Caliper (μm)	E_{md}/E_{cd}	Description
		Pilot Machine papers		
A	11.68	19.0	1.35	Control 1
B	12.37	51.8	0.56	Creped
C	12.38	44.0	0.50	Creped & Clnd*
A'	8.69	19.3	2.47	Control 2
B'	11.94	59.9	0.61	Creped
C'	11.99	51.3	0.64	Creped & Clnd*
		Handsheets		
D	22.63	90.8	1.0	Control 3
E	23.09	104.3	1.0	Triton 0.01%
F	22.95	92.9	1.0	Onyxsan 0.01%
G	22.01	80.8	1.0	Kymene 0.5%
F"	23.53	84.4	1.0	O-pulp 4 0.01%
G"	21.77	79.2	1.0	K-pulp 4 0.5%
		Formette Dynamique Handsheets		
H	21.38	69.5	1.27	Control 4
I	21.02	64.4	1.14	785 -40
J	21.87	64.7	1.84	810 -40
K	20.21	61.0	3.46	1250-40
L	23.77	67.4	3.57	1350-40
M	21.02	40.0	1.04	785-40/15**
N	20.50	67.0	1.45	Onyxsan 0.01%
O	19.65	61.6	1.20	Kymene 0.5%
H1	22.11	101.3	1.40	Free dry
H2	22.19	128.1	1.08	Air wire dry
H3	18.45	105.3	1.18	Oven wire dry

Control 1 and 2 differ in pulp and the wed-end conditions;
Control 3: pulp 3, no wet-pressing;
Control 4 (760-40): pulp 4, no wet-pressing and no additives.

*Clnd: Calendering.
**785-40/15: drum wire speed: 785 m/min.; dryer felt tension: 40 PSIG and wet-pressing pressure: 15 PSIG (181 PLI).

roll/felt drying were employed to vary the density of the paper. Onyxsan 0.01% and Kymene 0.5% were also used to alter the fiber bonding level of the Formette Dynamique handsheets. One grade of sheets was pressed at 181 PLI roll pressure to show the effect of wet-pressing.

Test Procedures

The soft platen caliper was determined by means of the caliper-measuring system built into the ZD longitudinal ultrasonic equipment[5]. The longitudinal velocity, the attenuation and reflection level of ultrasound were measured under a loading pressure of 20 kPa. The technique is described in the previous report and also in the last PAC meeting report (see appendix).

In-plane tensile tests were performed on the tissue samples using an Instron Load-Elongation Tester following TAPPI Standard Method T404 om-87 with cross head speed of 1 in./min. Extensional stiffness, Et (the product of the modulus of elasticity, E, and the thickness, t) was directly measured from the slope of the initial straight-line portion of the load-elongation curve. Then Young's modulus, E, was calculated using the soft platen caliper at 20 kPa.

RESULTS

Acoustic impedance, Z, was measured on the series of Formette Dynamique handsheets with varying paper-making conditions (Fig. 2). Compared with the paper dried by the conventional steam roll/felt drying system, the restricted air drying on the forming wire and the free air drying of the sheets reduced the Z dramatically. In addition, the restricted oven drying and the air drying process are significantly better in reducing Z than the free air drying process. Our previous work indicates that Z inversely correlates with softness.

Therefore, it is safe to conclude that the restricted drying processes are increasing tissue softness. This observation is more or less supported by the in-plane extensional Young's modulus measurement as shown in Fig. 3. The lower impedance tissues have smaller E values. In today's paper industry, the importance of drying on tissue softness has been established[4].

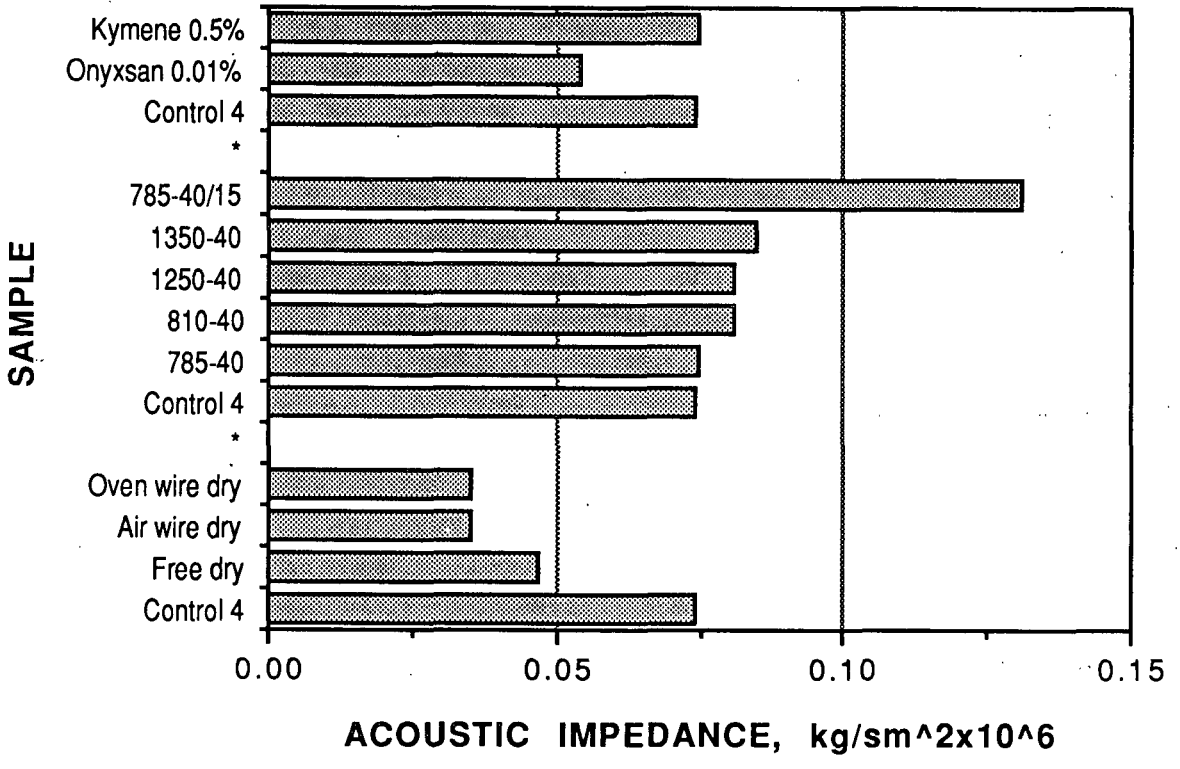

Figure 2. Acoustic impedance of Formette Dynamique handsheets.

As shown in Fig. 4, the drying processes also have large effects on the value of mass specific attenuation, A/BW, which is another parameter used in ultrasonic softness evaluation (see Appendix). Correspondingly, the one (oven wire drying), with the lowest Z value, gives the highest A/BW. Therefore, both Z and A/BW measurements indicate that this tissue is the softest of the four. As has been emphasized before, A/BW is more sensitive to the surface properties

of the sheets. So, a higher level of A/BW is thought to be associated with more open surface structures, which probably is a result of the restricted drying process.

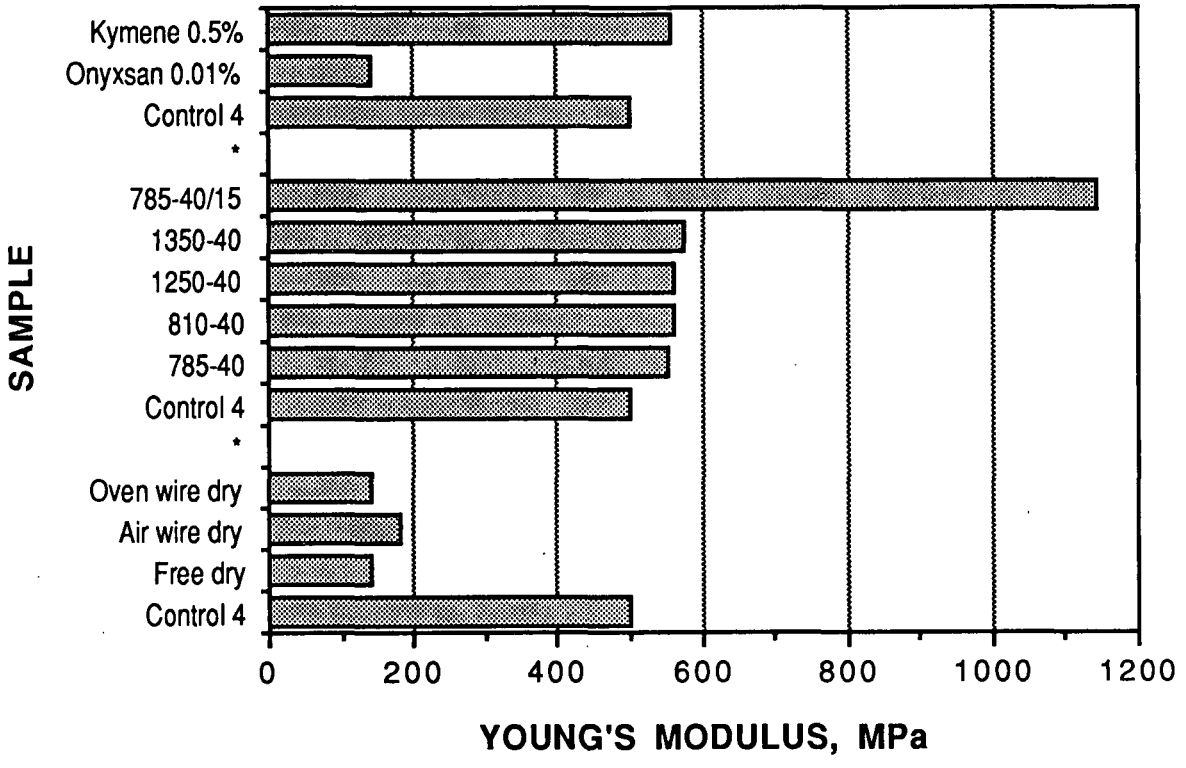

Figure 3. In-plane Young's modulus of Formette Dynamique handsheets.

The impact of fiber orientation and wet-pressing on Z and A/BW were investigated. The results are also shown in Figs. 2 and 4. The random fiber oriented (denoted by control in the figures) tissue gave slightly lower Z but higher A/BW values. Tensile tests on the same samples showed very similar tendencies (Fig. 3). These results indicate that fiber orientation has only minor influence on tissue softness. On the other hand, wet-pressing (181 PLI) changed the Z, A/BW and E values considerably since it greatly affects the densification of the sheet. Thus, wet-pressing control is important in the manufacture of soft papers.

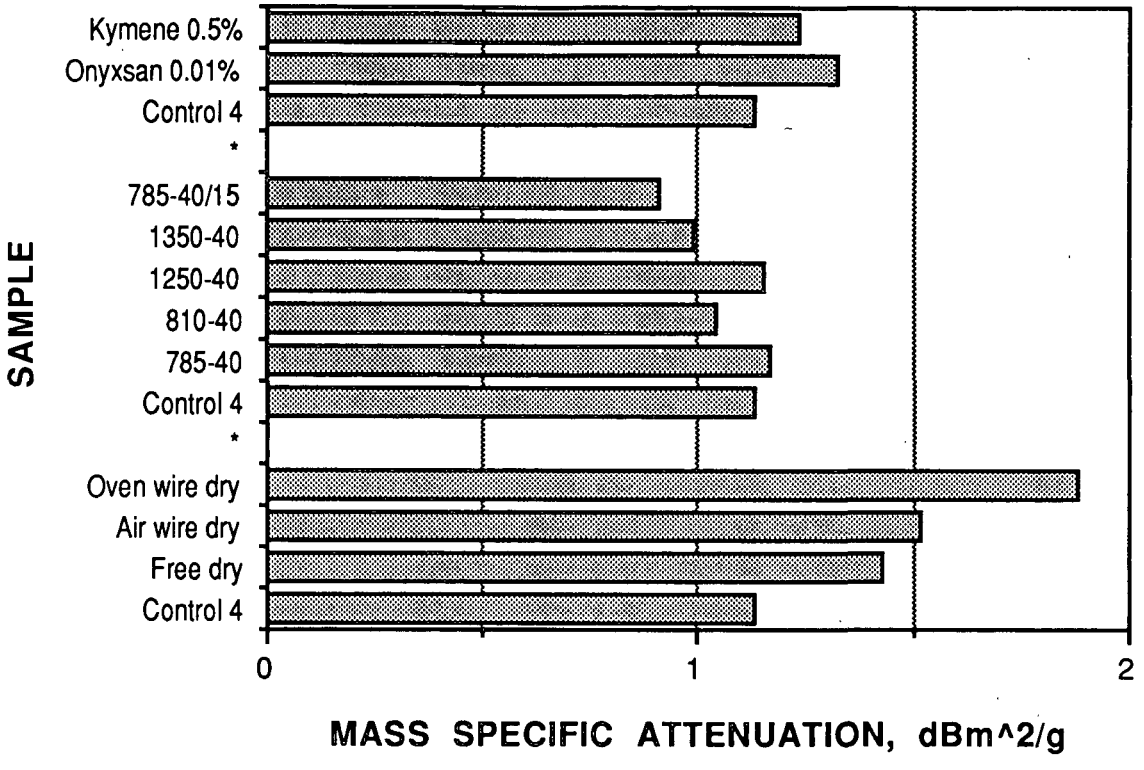

Figure 4. Out-of-plane mass specific ultrasonic attenuation measured on Formette Dynamique handsheets.

Effects of additives, creping, and calendering on Z are shown in Fig. 5. Compared with the control sample, the sample treated with strength additive (Kymene, a cationic polymer) showed a higher level of Z, while the paper with the addition of both non-ionic (Triton) and cationic surfactants (Onyxsan) exhibited lower impedance. Similar tendencies were also observed on in-plane Young's modulus (Fig. 6) and also in the case of Formette Dynamique handsheets (Figs. 2-4). These results are reasonable since the strength additive increases fiber bondings, while the surfactants reduce the surface tension of cellulosic fibers and thereby reduce bondings. Therefore, it is understood that a tissue paper with more fiber bonding will develop a higher Z, and will be harsher. On the contrary, a tissue paper with a lower level of fiber bondings will show a lower Z and appears softer.

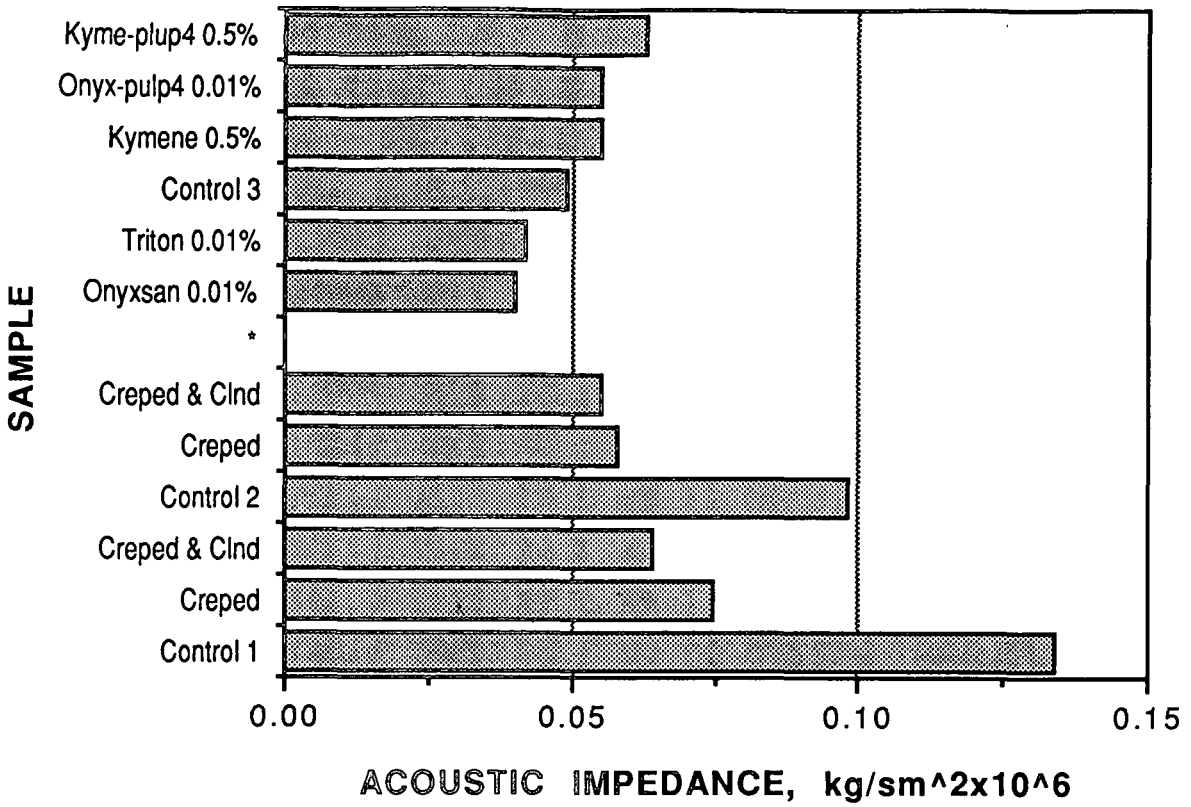

Figure 5. Out-of-plane acoustic impedance of handsheets and pilot machine made tissues.

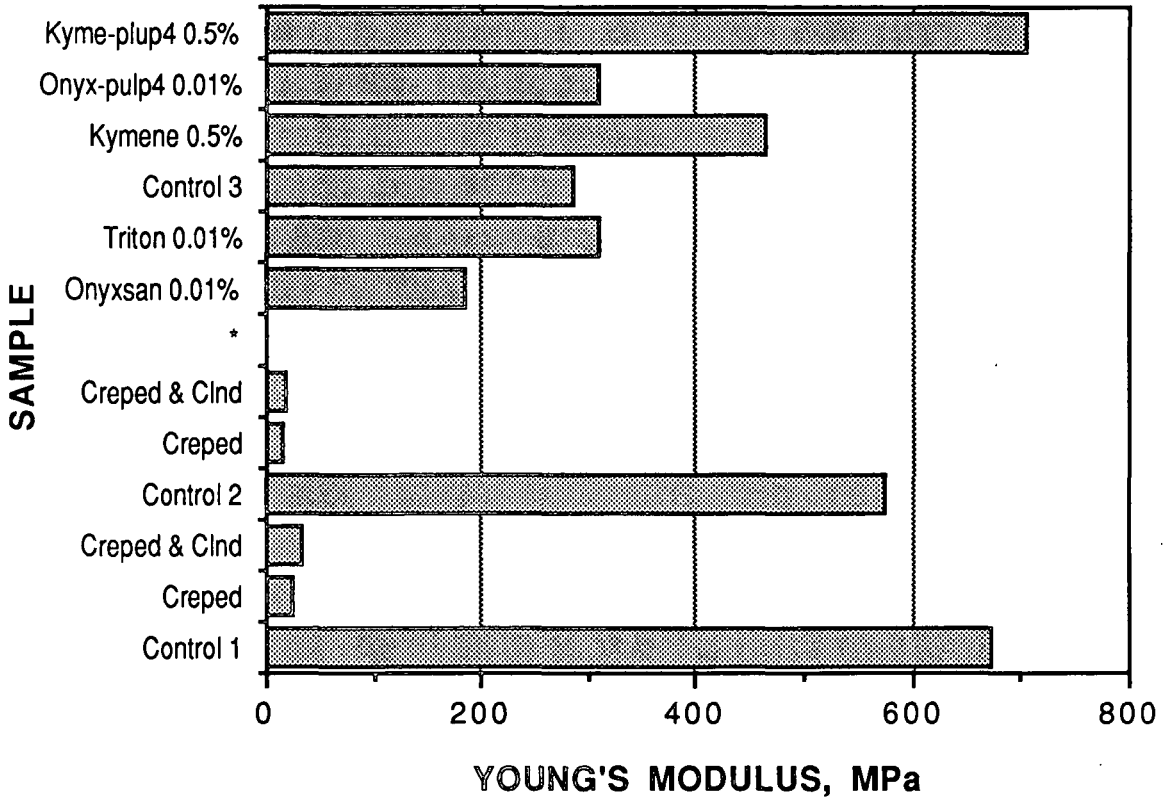

Figure 6. In-plane Young's modulus of handsheets and pilot machine made tissues.

Creping and calendering are very important processes for tissue manufacture. Effects of these processes on Z are also graphically shown in Fig. 5. Clearly, creping reduces the Z significantly. Calendering reduces Z, which probably indicates an increase in softness. Compared with out-of-plane ultrasonic measurements, in-plane tensile tests were more sensitive to the creping process (Fig. 6). From Figs. 5 and 6, it is clear that creping, a mechanical process, is much more effective in increasing tissue softness than are debonding agents, which chemically modify the fiber surfaces.

Although significant changes were observed on the impedance and in-plane Young's modulus of tissues, the impact of the additives on A/BW was minor as shown in Fig. 7. The reason appear to be that A/BW is dominated by surface effects, rather than the bulk properties which are more sensitive to the presence of both the polymer and surfactants. However, A/BW changed greatly with the processes of creping and calendering. As expected, creping increases significantly A/BW, which means that there is more energy loss at the transducer/paper interface. Calendering of the crepted sample decreased the level of A/BW slightly (Fig. 7). This is also probably associated with the change in surface smoothness.

Ultrasound reflection coefficient, R, of the samples was measured using the new IPC developed transducers (see Section II and Appendix 2). The plot of R vs. Z in Figs. 8 and 9, shows positive correlations. Therefore, it is possible that R might be used as a quick estimate of Z.

SUMMARY

Ultrasonic parameters and in-plane extensional Young's modulus were measured on lab-prepared tissues. The effects of several paper-making variables

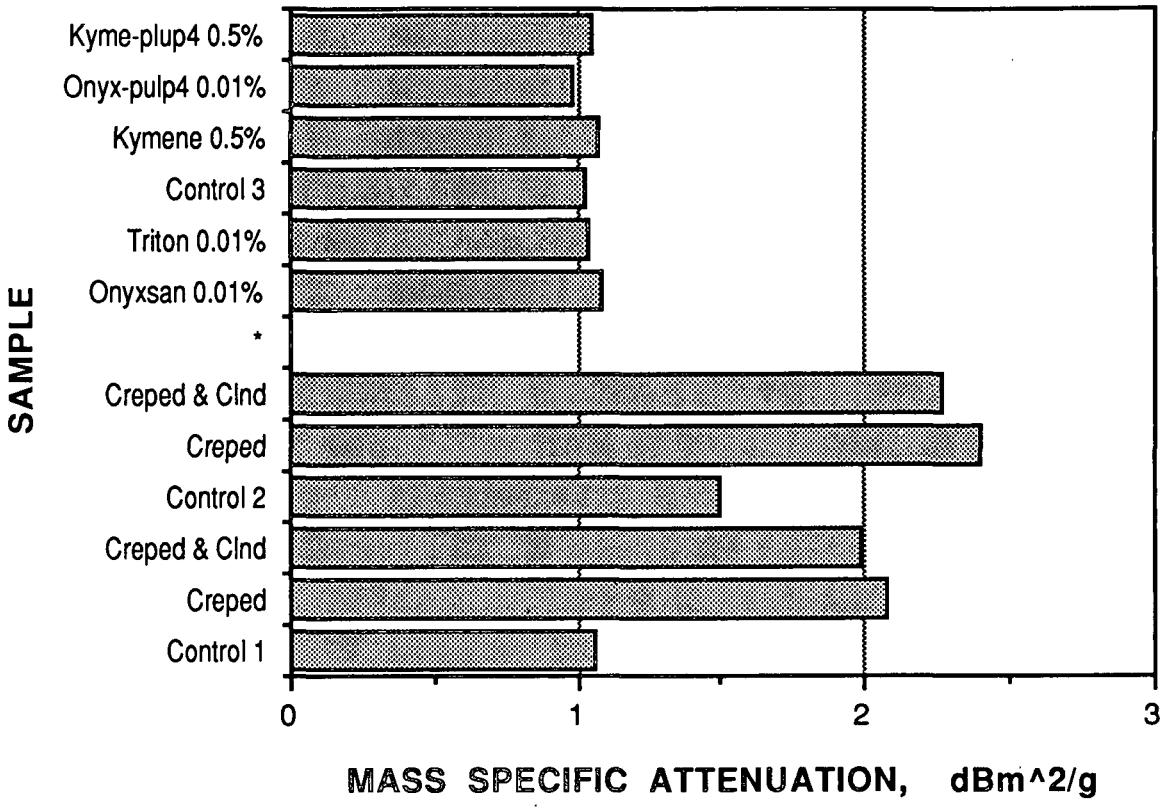

Figure 7. Out-of-plane mass specific attenuation determined on handsheets and pilot machine made tissues.

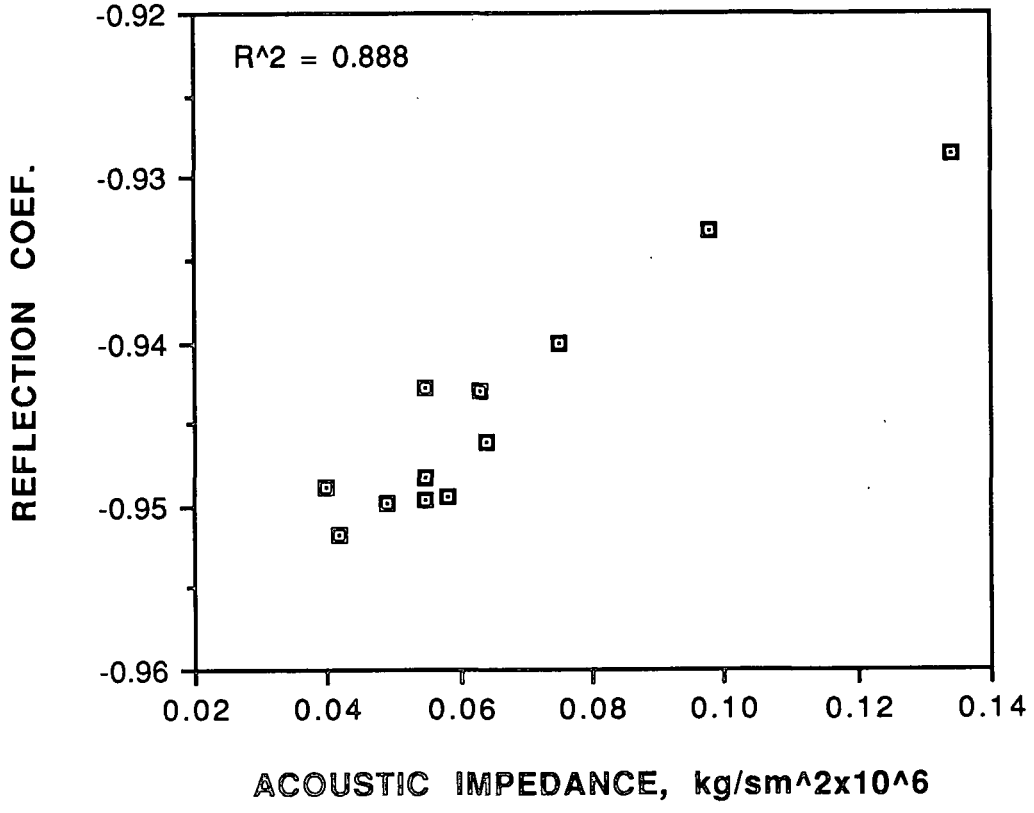

Figure 8. Correlation between ultrasonic impedance and reflection coefficient measured on handsheets and pilot machine made tissues.

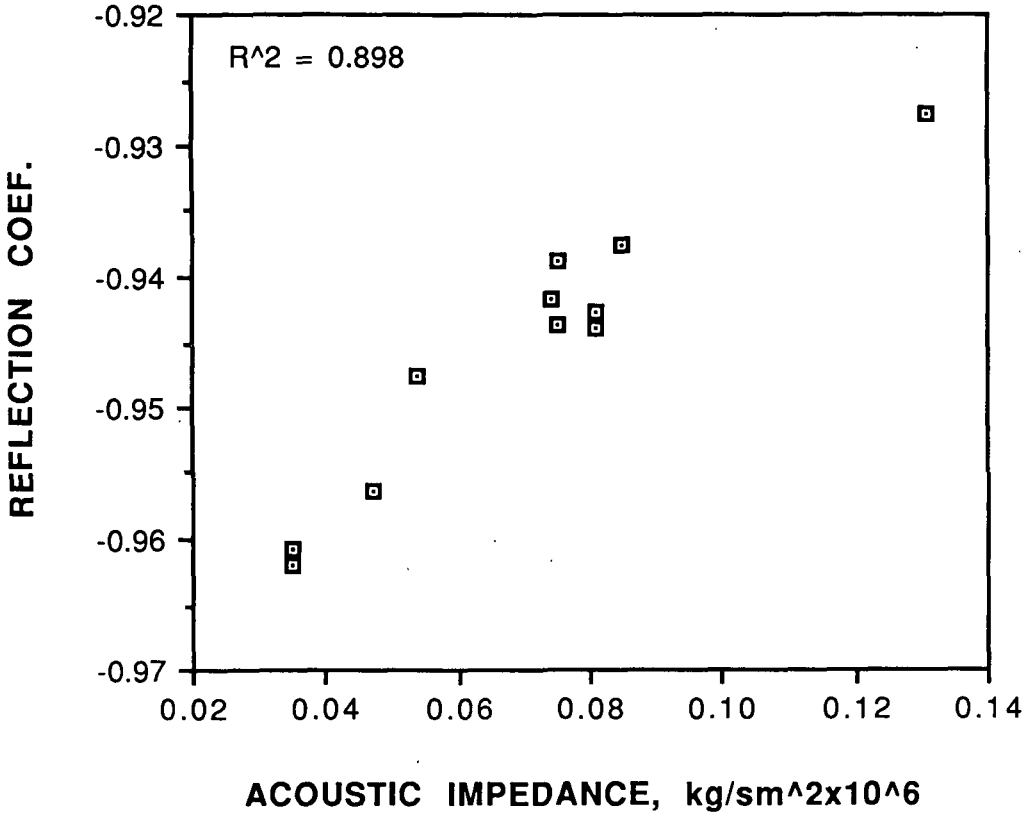

Figure 9. Correlation between acoustic impedance and reflection coefficient measured on dynamic format sheets.

on ultrasonic parameters and tissue softness were described. The results showed that acoustic impedance (Z), the mass specific attenuation (A/BW), and in-plane Young's modulus (E), are greatly affected by the drying (steam roll/drying, free drying and oven drying), creping and wet-pressing processes. Tissues with more open structures and lower densities (restricted drying and creping) tend to give lower Z or E but higher A/BW. However, fiber orientation (jet-to-wire ratios) only slightly affected these parameters, and probably has only limited effect on tissue softness.

The strength additives increase, while debonding agents decrease in-plane Young's modulus and the ZD impedance (Z) of tissue significantly. These

changes probably correlate with the changes in the bulk softness of the sheets. However, A/BW (the surface-effect dominated ultrasonic parameter) only experienced limited changes with different additives, which seems to indicate less change in the surface softness by the same additives.

Ultrasonic reflection coefficient, R, was also measured on tissues. The relationship between R and Z suggests that R is a new ultrasonic parameter that correlates with tissue softness. It may have an application in ultrasonic tissue softness evaluation because it eases the ultrasonic measurement.

IV. OPTICAL SCATTERING COEFFICIENT OF BOARD

INTRODUCTION

The degree of bonding of paper is commonly estimated from the light scattering coefficient determined from the reflectance of a single sheet on a black background (R_0) and the reflectance of a stack of sheets thick enough that addition of another sheet does not change the reflectivity value (R_∞). For high basis weight papers, however, there is little difference between R_0 and R_∞; consequently, the calculation is imprecise.

A way around the dilemma is provided by the Kubelka-Monk theory, which shows that the scattering coefficient can also be determined from one reflectance and one transmittance (T) value. IPC student B. J. Conor was assigned the design and construction of an instrument based on reflection and transmission values as a second-year research problem[6]. The instrument was later refined and evaluated by Knox and Wahren[7], who demonstrated that transmittance of heavy boards (to 699 g/m^2) could be measured, and that very good correlation was obtained for values of scattering coefficient of lighter weight paper calculated from measurements of R_0 and R_∞ and from measurement of R_0 and T.

In this instrument, the light source is a continuously-operated incandescent lamp. Photomultiplier tubes detect incident and transmitted light levels. The specimen is sandwiched between the Teflon diffusers, which become the top and bottom sheets of the "specimen stack". Specimen transmittance is calculated from the measured light transmission of the stack and the previously determined reflectances of the top and bottom "sheets"[7]. The reflectance of the sample is determined on a separate instrument, such as the TB-1 brightness tester.

The results obtained with the instrument are satisfactory, but getting valid measurements is a rather demanding operation. In view of an anticipated routine use for the measurements, it was decided to construct a new instrument, much easier to operate, and which measures both transmission and reflectance values. This instrument has been christened the Board Optical Transmission Meter, or BOTM.

NEW INSTRUMENT

In the new instrument, as has been reported previously, the specimen is placed between two integrating cavities. With the specimen to be viewed over a 15-mm diameter area, minimum integrating sphere size[8] is about 20 cm diameter. For easy, rigid attachment of source, detectors, and mounting means to the spheres, they have been made as spherical cavities inside cubic blocks. Figure 10 shows the arrangement.

The upper cube is fixed in place and has attached to it the flash lamp source, the source intensity detector, and the reflected intensity detector. An air actuator moves the lower cube up and down on linear bearings to permit insertion of and closing on a specimen. This lower cube supports the transmitted intensity detector. The sphere surfaces are lined with barium sulfate.

Illumination is provided by a xenon flash lamp discharging approximately 150 Joules. This gives the very high intensity level needed for sufficient light to pass through heavy specimens for detection. The very short duration (about 100 μsec) minimizes heating effects on the specimen. An infrared-removing filter in the port through which the illumination enters the upper sphere further reduces heating of the specimen. An additional filter is

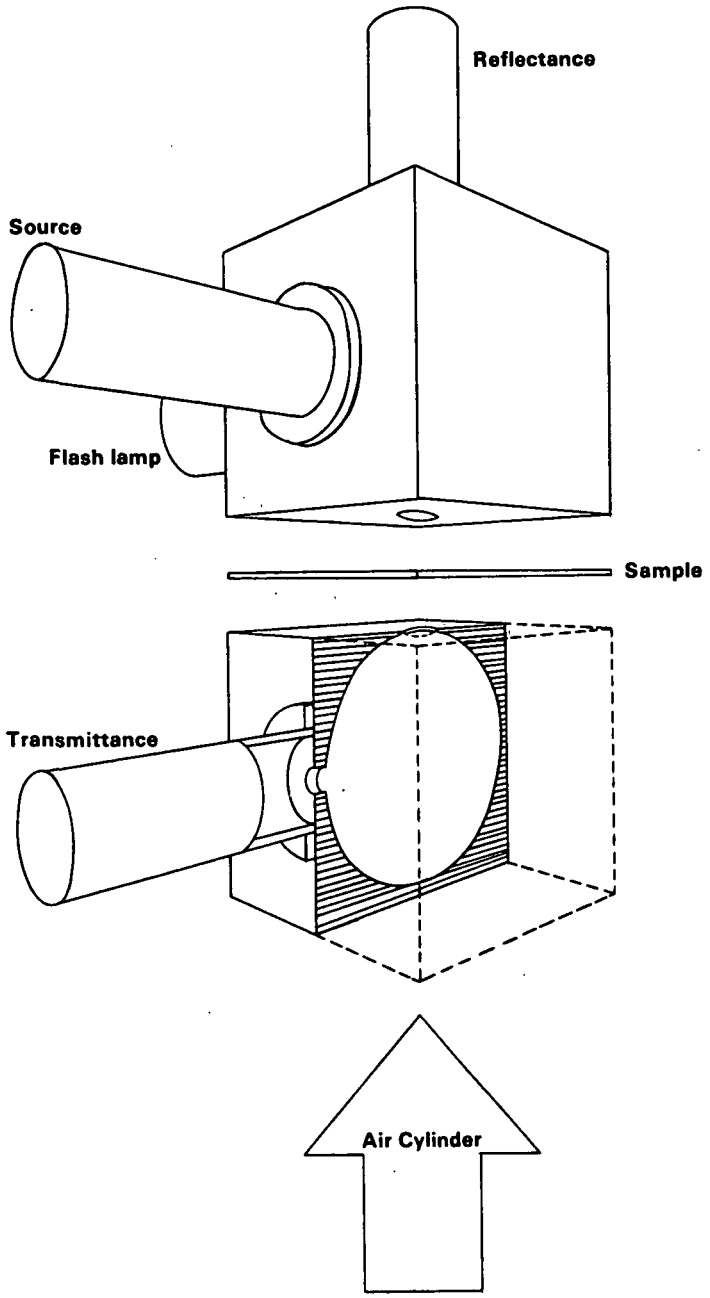

Figure 10. Schematic of the Board Optical Transmission Meter.

also placed here to remove ultraviolet radiation, which might otherwise induce fluorescence in the specimen.

Three photodetectors are used. Those sensing the light level in the upper sphere (reference) and that reflected from the specimen are silicon photo-

detectors, chosen for stability and ruggedness. This type was also tried for detection of the transmitted light, but it was found necessary to use a photomultiplier tube (PMT) in order to get the combined sensitivity and frequency response required. Optical filters are placed just ahead of the photosensors to give spectral responses approximating the CIE Y-function for illuminant A.

The output of each photodetector is a-c coupled to a peak-detector circuit. This peak value is then displayed on a digital panel meter in arbitrary units. Because of the a-c coupling, leakage of small amounts of room light do not affect the accuracy of the readings. Thus, use is considerably simplified over the elaborate light shielding required with the original instrument.

TRANSMITTANCE MEASUREMENT

The report for the previous meeting presented data which demonstrate very good agreement between values of the transmittance of light-weight papers as calculated from the R_0 and R_∞ values from the TB-1 brightness tester and from the TB-1 values of R_0 and the transmittance values calculated from the BOTM readings. It was also shown that transmittance measurements were easily made on a 90-pound unbleached kraft liner board.

Accommodating such a wide range of transmittances requires placing various sized apertures in the optical path of the transmittance detector. This has been accomplished by adding a manually adjusted, four-port, aperture wheel and mounting it in a flange bolted between the transmittance detector housing and the lower cube. Combining these apertures with two different voltages applied to the PMT (to change its sensitivity), permits reading over a transmission range of about 10^{-8}:1.

During the calibration of the ports and PMT gains, readings of the transmittance and source meters (T_m and S_m) were taken for stacks of 1-23 sheets of Sample A (Table 4). In Fig. 12, the logarithms of the calculated transmittances are plotted vs. the number of sheets in the stack. Transmittances as low as about 7×10^{-8} could readily be measured. It is interesting to note that the transmittance through the stacks of sheets very nearly follows the simple $I = I_0\varepsilon^{-kt}$ relationship of transmission through a transparent material.

Table 4. Sample descriptions.

Sample	g/m^2	Description
BB		black body
A	39.2	white bond
B	77.1	white bond
C	76.4	pink memo
D	69.7	deinked
E	75.1	yellow memo
F	162	cream tab card stock
G	250	blue cover stock
H	131	UK medium
I	159	semibleached medium
J	339	UK liner
L	163	buff cover stock
M	434	UK liner
N	72.4	copy machine paper (fluorescent)

REFLECTANCE MEASUREMENT

The samples described in Table 4 were used to check the reflectance measurement capability of the BOTM. Readings of these samples were made as:

1. R_o on the TB-1.
2. R_m/S_m on the BOTM, with a bare specimen (no Teflon diffusers) and backed with a black body.
3. R_m/S_m on the BOTM, with the specimen between the Teflon diffusers.

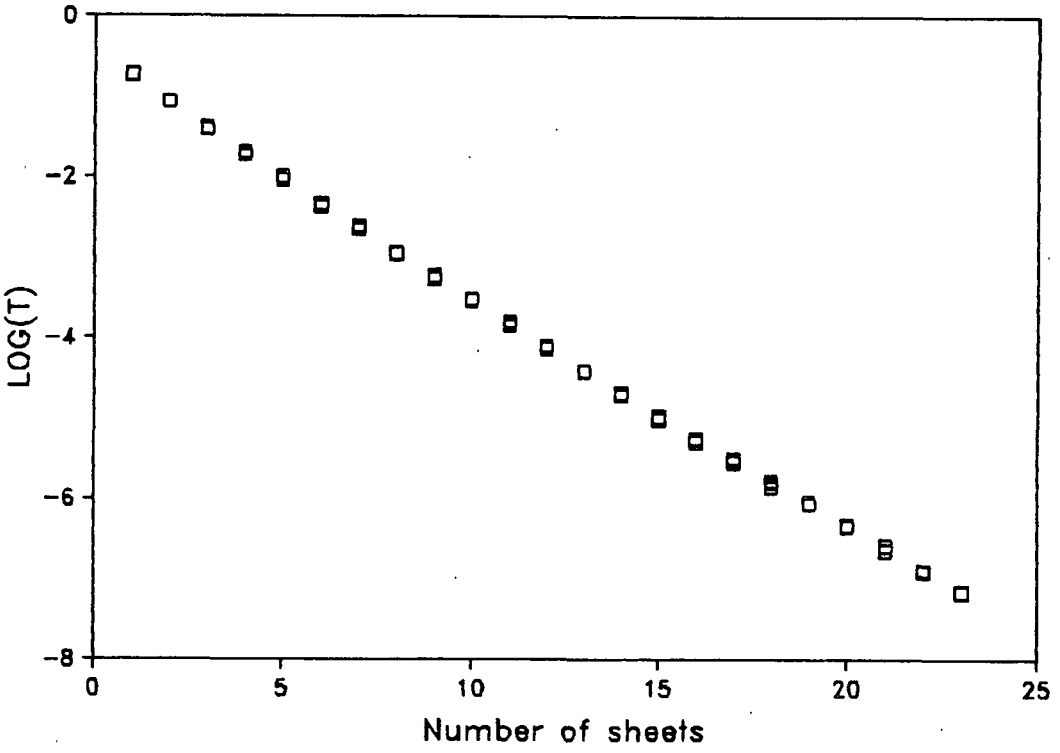

Figure 11. Logarithm of the calculated transmittance of stacks of Sample A (39.2 g/m^2) vs. the number of sheets in the stack. 162 readings, using the 4 T-ports and both PMT voltages.

Figure 12 is a plot of the black-body-backed specimen readings vs. the R_o [TB-1] values, which demonstrates that a specific calibration procedure can be used to get R_o values from the BOTM readings of bare specimens.

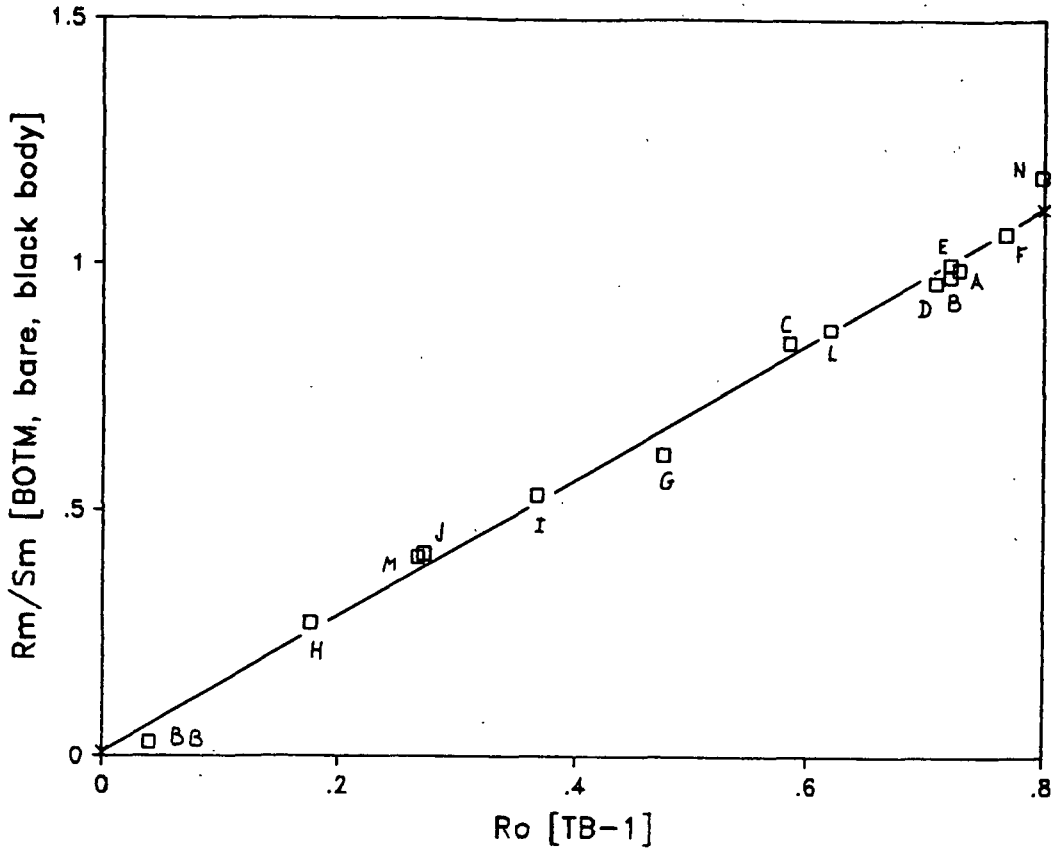

Figure 12. The relationship of the R_m/S_m BOTM readings of Table 3 specimens backed with a black body to the R_o readings from the TB-1 brightness tester.

Of special interest are the results from the BOTM readings made with the specimens in the Teflon sandwich. The relationship to the R_o [TB-1] values is not the same as for the bare specimens, but was found to be linear on using LOG[(R_m/S_m)-1] values. This is shown in Fig. 13. The white and unbleached kraft samples lie, essentially, on the regression line, but the colored samples show some departure (as is also the case in Fig. 12). Suspecting that this departure might be reduced by adjusting the spectral response of the reflectance detector, the filters were modified slightly. No improvement was noted and no

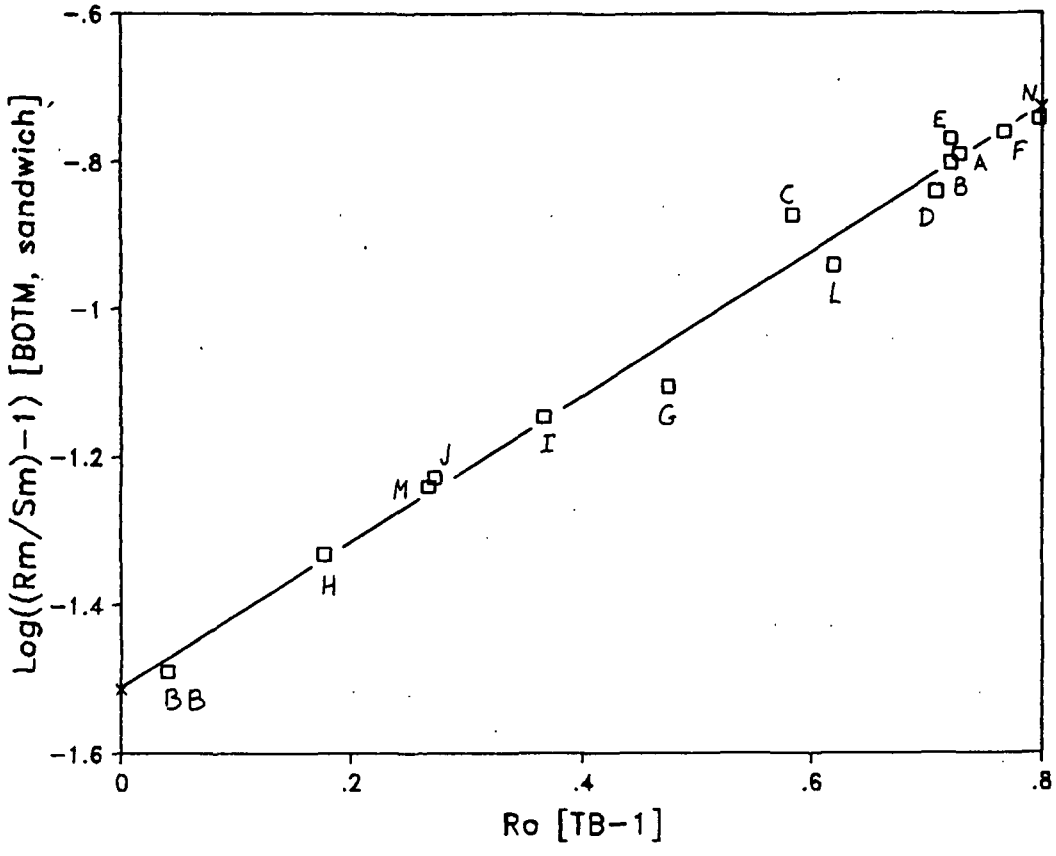

Figure 13. The relationship of the LOG[(R_m/S_m)-1] BOTM readings of Table 3 specimens in the Teflon sandwich to the R_o readings from the TB-1 brightness tester.

further attempts were made. (Perhaps some of the effect is due to the spectral characteristics of the Teflon diffusers.)

At a later time, another series of samples was measured. These were relatively light weight, white sheets of unknown composition and did not show a linear relationship between LOG((R_m/S_m)-1) [BOTM:Teflon] and R_o [TB-1]. It was found, however, that $(R_m/S_m)^4$ [BOTM:Teflon] vs. R_o [TB-1] was linear, so R_o values could be calculated easily from the BOTM readings. If R_o is to be calculated in this manner, a specific calibration must be performed for the sample types to be read.

Using the BOTM to measure both transmittance and reflectance of a sandwiched specimen simultaneously is desirable because specimen handling is reduced: the additional step of inserting and reading the black-body-backed specimen is not needed. Also, this procedure results in the reflectance and transmittance readings being taken on exactly the same area of the specimen. A disadvantage lies in the fact that the sensitivity to R_o (i.e., the range of R_m/S_m values) for the "sandwiched" readings of Fig. 13 is only about 13% that of the bare specimen/black-body backed readings of Fig. 12. Thus, for best accuracy, R_o should be determined from either the TB-1 or the bare specimen/black-body backed BOTM readings.

Since the transmittance measurements have been shown to be essentially independent of small air gaps between the specimen and the Teflon diffusers, the effect of the same air gaps on the reflectance measurements was checked. See Table 5.

Table 5. Effect of air gaps on calculation of Ro [BOTM: Teflon].

Specimen	g/m^2	Air gap per side	R_o
A	39.2	0 inch	0.729
		0.011	0.712
		0.022	0.690
H	131	0	0.172
		0.011	0.156
		0.022	0.160

Here, the presence of an air gap causes some change in the calculated value of R_o, so it must either not exist or be maintained constant during both the specific calibration and subsequent use.

SCATTERING COEFFICIENT

With the instrument now in working order, simple one-reading measurements were made of the samples listed in Table 4. The data and the results (R_o, T, and the scattering coefficient s) are shown in Table 6, using both R_o [TB-1] and R_o [BOTM:Teflon] values. These results are in the expected ranges, although those using the two R_o's for any one specimen are not always in good agreement. This latter is primarily due to the deviations of the colored specimens from the regression line shown in Fig. 13, and emphasizes the need to use either R_o [TB-1] or a specific calibration of R_o [BOTM] for the particular samples to be read.

FUTURE DEVELOPMENTS

If a more precise, universally applicable relationship is desired between the TB-1 and BOTM reflectance readings, further work should be done in tuning the color response of the BOTM.

At present, the BOTM readings are recorded manually, then keyed into a computer spreadsheet at a later time. It would be possible to attach a computer to the BOTM so that data entry of T-port size, PMT voltage, T_m, R_m, and S_m would be made automatically. Automatic adjustment of T-port size and PMT voltage might also be computer controlled to suit the specimen being read.

Further ahead, there is a strong possibility that an on-line instrument utilizing the measurement principles of the BOTM could be developed.

Table 6. Reflectances, transmittances, and scattering coefficients of samples.

Specimen	BW, g/m^2	T-Port	PMT-V	T Meter	R Meter	S Meter	R(0)	T	sW	s, cm^2/g
None	0	274	700	744	N/A	758	N/A	N/A	N/A	N/A
A Ro [BOTM]	39.2	274	700	327	891	748	.740	1.837e-1	3.643024	929
Ro [TB-1]	39.2	274	700	327	891	748	.728	1.903e-1	3.452941	881
B	77.1	274	700	337	893	752	.727	1.948e-1	3.391851	440
	77.1	274	700	337	893	752	.721	1.982e-1	3.302143	428
C	76.4	274	700	252	872	749	.639	1.945e-1	2.740823	359
	76.4	274	700	252	872	749	.585	2.225e-1	2.210217	289
D	69.7	274	700	236	890	758	.678	1.637e-1	3.356981	482
	69.7	274	700	236	890	758	.708	1.503e-1	3.816141	548
E	75.1	274	700	402	904	753	.772	1.966e-1	3.766972	502
	75.1	274	700	402	904	753	.721	2.280e-1	2.997161	399
F	162	274	700	280	907	754	.780	1.411e-1	4.808357	297
	162	274	700	280	907	754	.767	1.469e-1	4.525287	279
G	250	462	1000	488	833	749	.386	4.463e-5	8.930145	357
	250	462	1000	488	833	749	.475	3.681e-5	12.21171	488
H	131	462	700	198	806	745	.177	4.755e-4	2.778573	212
	131	462	700	198	806	745	.178	4.744e-4	2.801918	214
I	159	331	1000	296	824	746	.339	6.447e-3	3.771791	237
	159	331	1000	296	824	746	.367	6.098e-3	4.203370	264
J	339	664	1000	203	813	744	.259	7.279e-6	6.541989	193
	339	664	1000	203	813	744	.273	7.100e-6	6.948628	205
L	163	274	1000	300	852	743	.564	1.733e-2	6.080724	373
	163	274	1000	300	852	743	.619	1.502e-2	7.461840	458
M	434	664	1000	21	823	753	.261	7.416e-7	7.866177	181
	434	664	1000	21	823	753	.267	7.343e-7	8.078804	186
N	72.4	274	700	314	912	754	.801	1.454e-1	5.008570	692
	72.4	274	700	314	912	754	.798	1.468e-1	4.934179	682

V. OUT-OF-PLANE ULTRASONIC TECHNIQUES TO STUDY LIQUID PENETRATION

Out-of-plane ultrasonic techniques developed at IPC have found various uses in fast nondestructive testing of the Z-direction mechanical properties of paper products[5]. Recently, new equipment for ultrasonic evaluation of wetting and liquid penetration of paper has been constructed. Here, we would like to report on the status of this work.

BACKGROUND

Previous experiments have shown that the out-of-plane ultrasonic transmission coefficient changes with time (decreases at first and then increases) when a piece of paper was brought into contact with liquids[9,10] This phenomenon is observed when a sheet of paper is inserted between a pair of transducers which are immersed in water[9]. The experiment can also be conducted in a plexiglass cell as photographically shown in Figs. 14a and 14b. The cell accommodates the transducers and assures the repeatable contact of paper with liquids.

The reason for the changes in ultrasonic attenuation was thought to be mainly due to the changes in air content of the sample (air bubbles are driven out of the sheet layer by the penetrating liquid) as well as the distribution of air bubbles in the paper sheet (fiber swelling, replacing air by liquid and bubble coalescing). In addition, the viscoelastic properties of paper sheets change as the fiber absorbs fluids.

Useful information on the wetting and on liquid penetration properties of papers can be obtained by tracing the changes in ultrasonic attenuation with

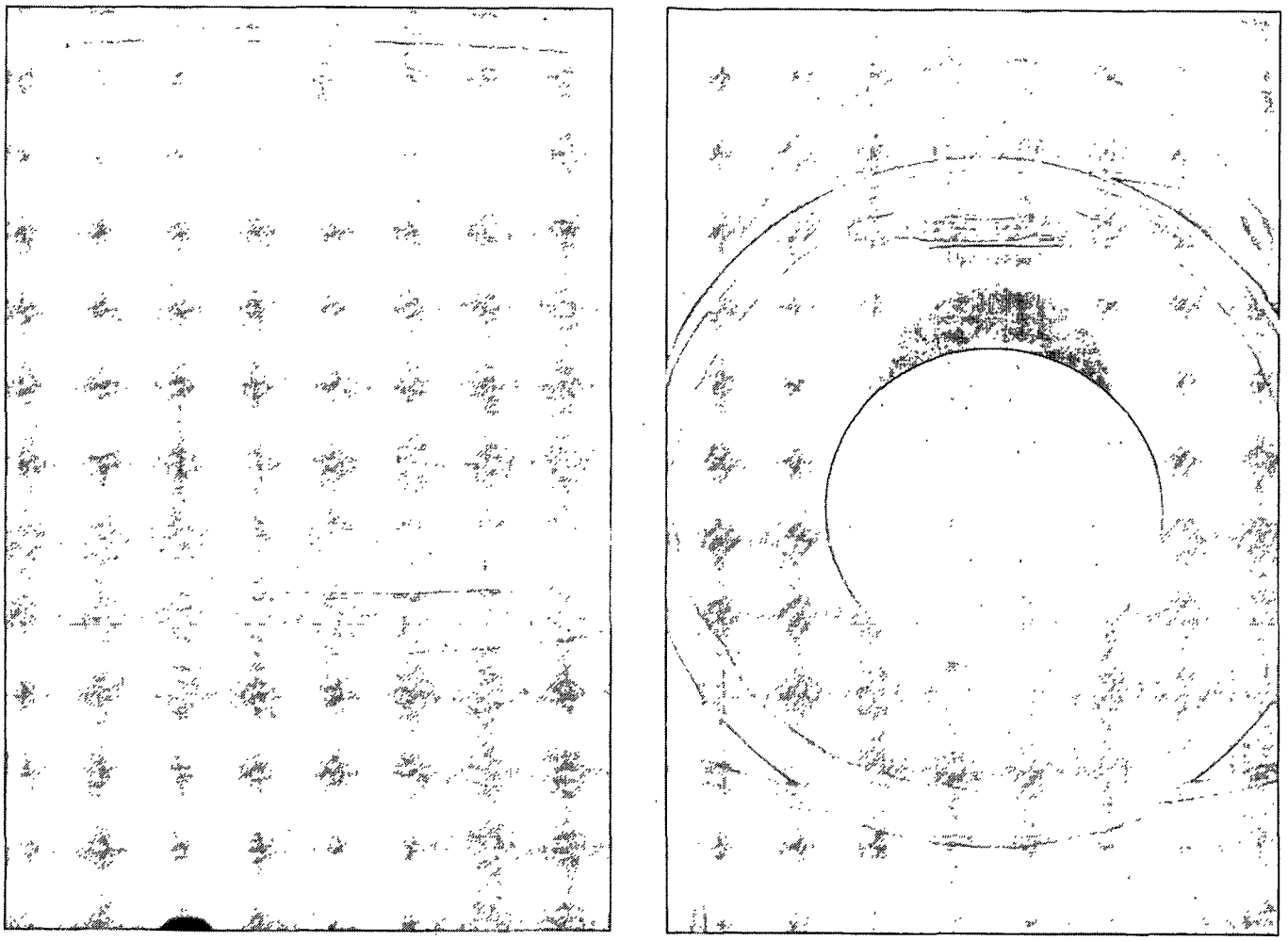

(a) (b)

Figure 14. A photograph of the plexiglass cell used for ultrasonic attenuation and phases change measurements. Figure 14a shows the arrangement of the transmitter, receiver and the position of sample holder. Figure 14b shows a paper sample attached to the sample holder.

time. The wetting delay of the paper surface corresponds with the initial increase in the attenuation level, and the subsequent rate of decrease of ultrasonic attenuation more or less reflects the penetration rate of liquid into paper sheets[9]. Compared with the conventional sizing tests, the ultrasonic technique is fast, simple and able to provide detailed information on the transient liquid/paper interactions of paper surfaces.

Previously, attention was focused on the ultrasonic attenuation during liquid/paper interactions[9]. However, there is good reason to believe that the delay time through the sample as a function of time will provide complimentary information on the liquid/paper interactions. Studies on this new phenomenon may give a new dimension to paper sizing evaluation.

Although the ultrasonic techniques can be used in evaluating wetting and liquid penetration properties of paper and the above-mentioned explanation for the changes in the attenuation upon liquid penetration are probably qualitatively valid, an adequate theoretical background has not been developed. Therefore, more studies in this area are necessary to understand the basic principles.

APPARATUS

Figure 15 shows the schematic diagram of the apparatus that we built recently for the ultrasonic measurement. The measuring cell is made of plexiglass tubes and aluminum plate. It consists of the upper (receiver) unit and lower (transmitter) unit which hold the transducers (Figs. 14a and 14b). An important feature of the design of the measuring cell is that the ultrasonic wave irradiates a stationary paper specimen through a liquid layer which is brought into contact with a dry specimen from below. The test liquid is fed into the cell by a gravity-controlled system.

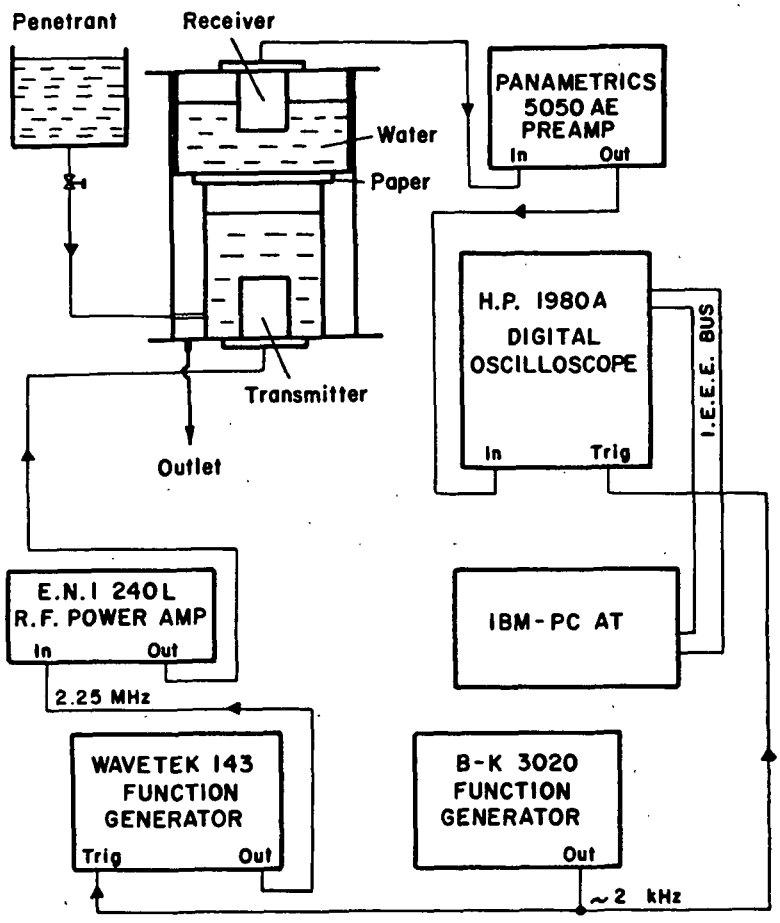

Figure 15. A schematic diagram for the apparatus of ultrasonic sizing measurements.

The inside diameter (45 mm) of the transducer mounting tube is selected based on the diameter of the transducers. The distance between the transducers was chosen to avoid interference from reflected waves. In order to obtain a discrete signal, a pair of broad-band PVDF transducers and a 5 mm-thick plexiglass sample holder (Fig. 14b) were selected.

As shown in Fig. 15, the transmitter is driven by a R.F. power amplifier which is excited by single cycle sinusoidal wave (2.25 MHz) from a

function generator. The repetition rate of the transmitter burst is set by another function generator used as a free running pulse generator. The repetition rate (usually about 2 kHz) is chosen as large as possible without incurring interference from the previous burst. The pulse generator also triggers a digital oscilloscope that displays the time history of the amplified receiver signal. An AT class personal computer analyzes the receiver signal.

The ultrasonic measurements are conducted in the following way. First, the lower tube is filled with water, and a reference signal is taken with no sample present. When the signal is received, the computer directs the oscilloscope to digitize the received signal. The trigger predelay of the oscilloscope has been set so that there is an expanded view of the main signal. A Fast Fourier Transform algorithm is performed on the reference signal, giving phase and amplitude numbers for integer multiples of 0.2441 MHz.

Sample testing begins with the attachment of the paper sample to the sample holder by means of a piece of double-sided adhesive tape (Scotch Brand Tape, 3M) as shown in Fig. 14b. The liquid level in the inner cell is below the sample. The gravity-controlled water filling system is then activated. When the paper comes into contact with the water, the computer directs the oscilloscope to digitize the sample signal. The digitized signal is stored and displayed on the C.R.T. below the reference signal. The computer calculates a "cross correlation delay time" by finding the offset time that maximizes the convolution integral of the reference and sample signals. Next, a Fast Fourier Transform is performed on the sample signal. Taking into account the different trigger predelays, the sample frequency domain amplitude and phase numbers are compared to the corresponding reference values. The time shifts (phase/$2\pi f$) are corrected by 2π times the integer that causes the time shift at that frequency

to be nearest the cross correlation time-of-flight. A new signal is analyzed by starting the program at pre-determined time. This process is repeated a controlled number of times. The time when receiver signal is taken, cross correlation time-of-flight, and frequency domain numbers are averaged, and the results are printed.

EXPERIMENTAL

A paper sheet to be tested is attached gently to one side of a double-sided adhesive tape, and test specimens of 1-inch diameter are prepared for the ultrasonic measurement. Distilled water is used as penetrant. The samples and liquids are conditioned and the tests are carried out under the TAPPI standard condition of 23°C and 50% RH.

RESULTS

Figure 16 is a photograph of oscilloscope traces of the received signals recorded on a computer paper at different penetration times. The first one was recorded 30 seconds after the water has contacted the sample. It has the highest amplitude and shortest phase width. As penetration time increases, the amplitude decreases and the phase width increases. The observed decrease in amplitude with time agrees well with the earlier observations[9].

Transmission coefficients of different frequency components (0.5 - 1.5 MHz resulted from FFT analysis of the receiver signal) as a function of penetration time are shown in Fig. 17. The transmission coefficient, R, here is defined as the ratio of the amplitude of the signal through sample to that of a reference signal. As expected, R initially decreases with time but increases after long time water penetration. The higher frequency components have smaller transmission coefficients and experience larger changes with time. This is

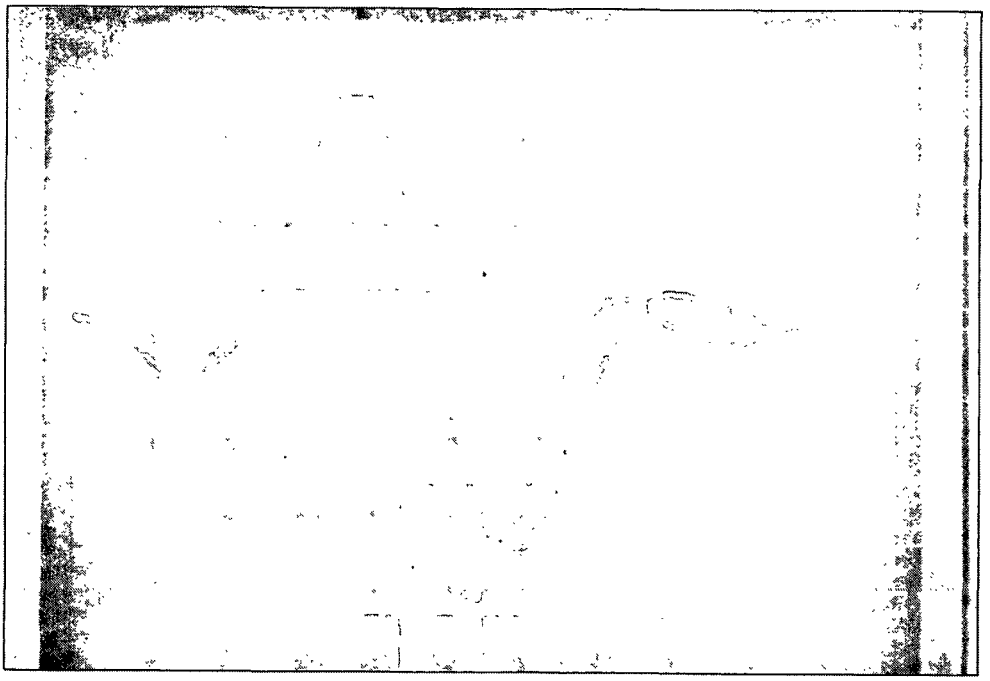

Figure 16. Oscilloscope traces of the transmitted signals at different water penetration times.

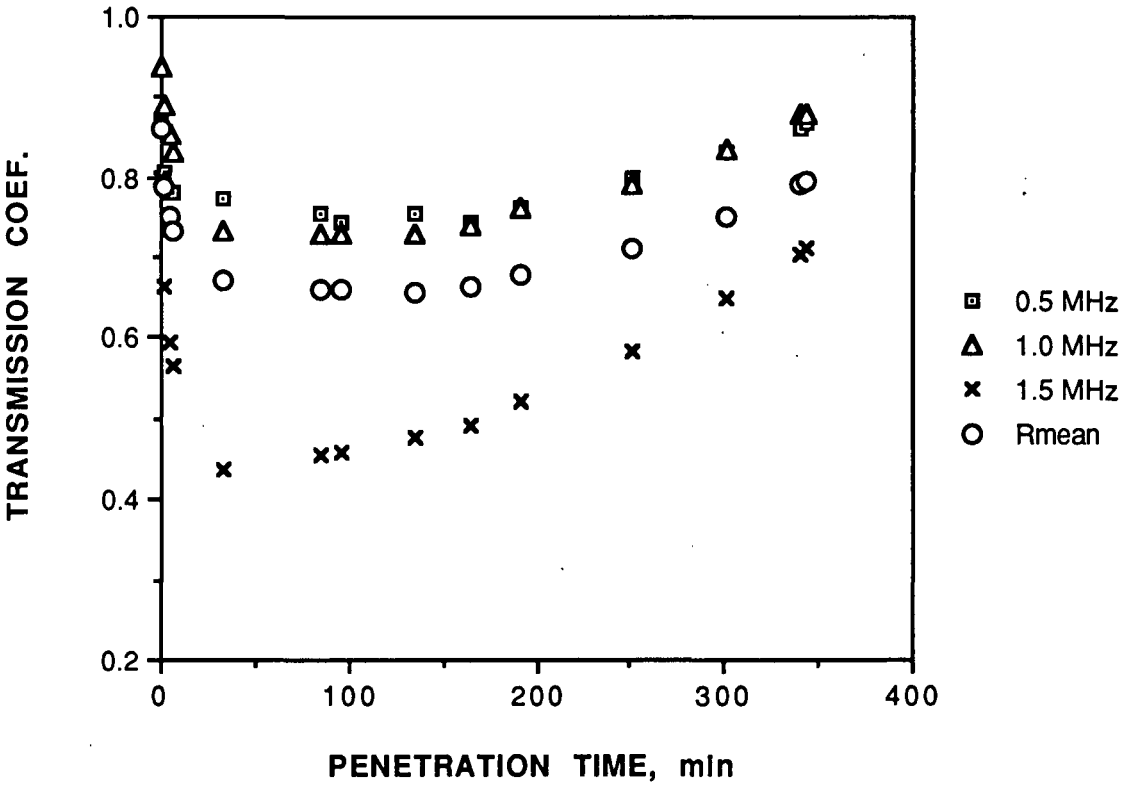

Figure 17. Transmission coefficients as a function of water penetration times (computer paper was used).

reasonable as the shorter wave length components are more effectively scattered by the paper structures. The frequency dependence of the responses are interesting, since they relate to the changes in pore-size distribution of the paper sheets.

Figure 17 indicates that delay time increases with time. This is another parameter which was investigated in this project. Figure 18 shows the delay time as a function of penetration time, obtained on the same computer paper. Delay time shows tendencies similar to the transmission coefficient. However, the delay times have sharper and earlier turning points. In general, the loss measurement is much more sensitive to the pore volume within the paper

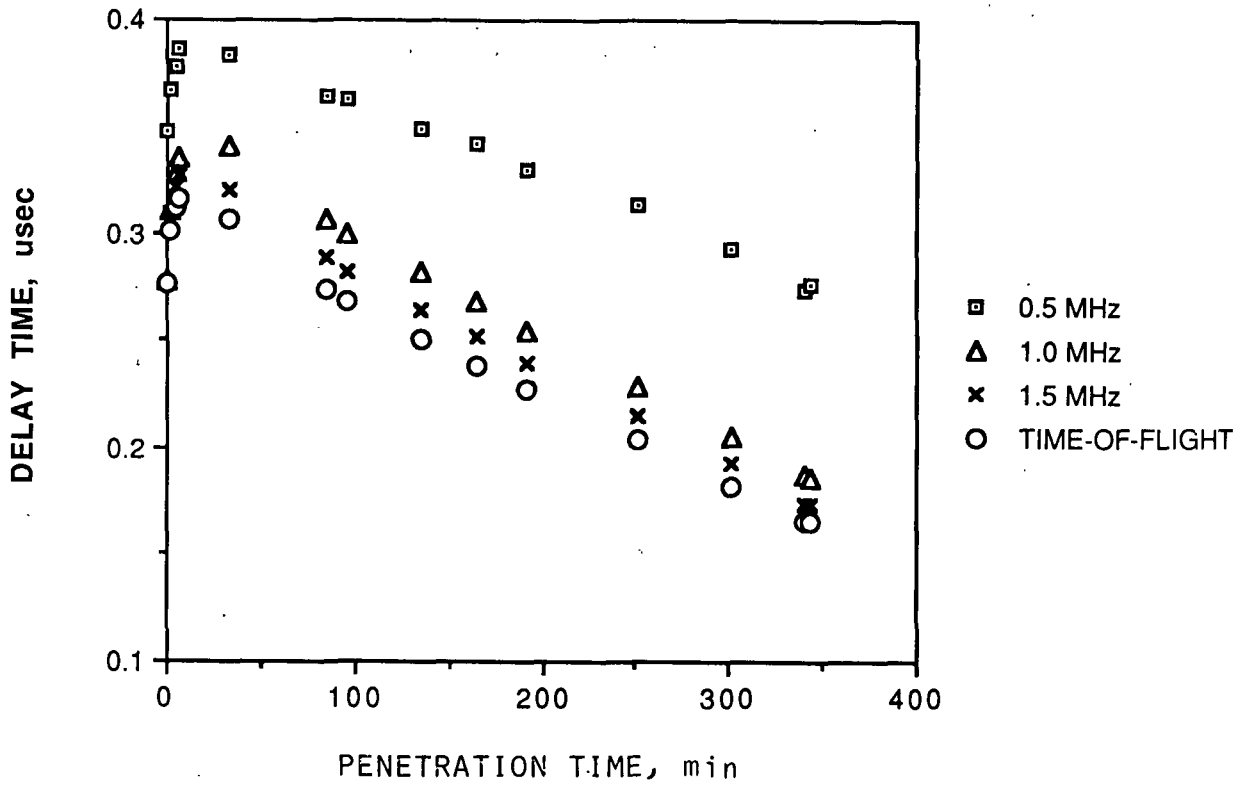

Figure 18. Delay times from phase shift of Fourier components and delay time from cross-correlation calculation (time-of-flight) as functions of water penetration time (computer paper).

(of course the pore-size distribution here is also important), than the delay time determination. The hypothesis here is that the turning point of the amplitude curve is governed by the process of air leakage, but that of delay time curve is related to the penetration of water through the paper. Water penetrating into paper has a higher velocity than the air driven out of the porous structures.

Summary

A new ultrasonic instrument for measuring the wetting and liquid penetration properties of paper was developed. The instrument, incorporating computer-control of the electronics and automated data analysis, has already shown promising results. The loss measurement correlates with the delay time determination, but the delay time curve experiences an earlier turning point than the loss curve. The higher frequency component respond more strongly to water penetration processes. The pore volume, pore-size distribution and the swelling of individual fibers are considered to be the governing factors.

At present, the apparatus can only test long time liquid penetration process because of the limited speed (about 30 seconds per signal) of the data acquisition system. Higher speed instrumentation suitable for the ultrasonic testing of wetting and liquid penetration property of paper is under development.

REFERENCES

1. Hollmark, B. H., in "Handbook of Physical and Mechanical Testing of Paper and Paperboard", Marcel Dekker Inc., Vol. 1: 497-521 (1984).

2. Oliver, J. F., Tappi 63(12): 91-95 (1980).

3. Scruton, H., Paper Trade J. P. 36-38 (May 31, 1965).

4. PPI P. 38-40 (August, 1981).

5. Habeger, C. C., Wink, W. A. and Van Zummeren, M. L., IPC Technical Paper Series No. 269 (Jan., 1988).

6. Conor, B. J. Development of a prototype instrument for measurement of diffuse light transmission properties of paper and board. A291 Research Problem. 30 p. The Institute of Paper Chemistry, Appleton, WI (June 21, 1982).

7. Knox, J. M., and Wahren, D. Determination of light scattering coefficient of light and heavy sheets. Tappi J. 67. no. 8:82-85 (Aug., 1984).

8. McNicholas, H. J. Absolute methods in reflectometry. J. Res. NBS 1; no. 1:29-74 (July 1928).

9. Pan, Y-L., Kuga, S. and Usuda, M. Tappi 71(5):119 (1988).

10. Pan, Y-L., Kuga, S., Usuda, M., and Kadoya, T. Tappi 68(9): 98 (1985).

Appendix 1

An Ultrasonic Technique for Testing the Orthotropic Symmetry of Polymeric Sheets by Measuring their Elastic Shear Coupling Coefficients

C. C. Habeger
Research Associate
Paper Physics Group
The Institute of Paper Chemistry
Appleton, WI 54912

Abstract

An ultrasonic method which allows one to determine the in-plane elastic stiffnesses of thin polymeric sheets is described. The determination is complete, as it includes the shear coupling coefficients. Sheets are often assumed to display orthotropic symmetry, which means that the shear coupling coefficients are zero along the principal axes. The shear coupling coefficients can now be independently calculated, and there is a test of the validity of the orthotropic assumption. A quantity called the nonorthotropic angle is presented as a coordinate-independent measure of the lack of orthotropic response. Results from a polyester sheet demonstrate that significant nonorthotropic behavior is encountered in commercial plastic sheets. Stiffnesses calculated from tests conducted on laminated sheets are shown to be in good agreement with stiffnesses predicted from measurements on individual plies. The technique is argued to be self-consistent and an attempt is made to convince the reader that this is a legitimate way to characterize all the in-plane elastic stiffnesses of thin sheets.

1 Introduction

The physical properties of commercial polymeric sheets are often anisotropic. In the case of paper, the fibers are preferentially aligned in the direction of manufacture (the machine direction of MD), and MD tension is applied to the web during drying. These factors cause the final product to be stronger and more rigid in the MD than in the direction perpendicular to manufacture (the cross direction or CD). Plastic films, extruded under MD tension, are also stiffer and stronger in the MD.

To simplify mathematical analyses of polymeric sheets, it is generally assumed that they exhibit orthotropic symmetry. This means that there are two perpendicular planes of reflectional symmetry. It is usually argued from the symmetries of manufacture that the reflectional symmetry planes are the plane determined by the MD and the thickness direction and the plane determined by the CD and the thickness direction. Sometimes, due to misalignment of a head box in paper manufacture or to off-axis tension in plastic film extrusion, the direction of greatest strength and stiffness is not along the MD. Nonetheless, it is still assumed that the principal axes of stiffness (wherever they may be) determine planes of orthotropic symmetry.

Under the orthotropic assumption, the elastic shear coupling coefficients are zero, when measured along a principal axis. This means that normal stresses along a principal axis do not produce shear strains and vice versa. The technique described below allows one to calculate the shear coupling coefficients and to test the orthotropic assumption. Results will be discussed for a polyester sheet and a polypropylene sheet. It will be argued that within the sensitivity of the measurement the polypropylene sheet is orthotropic. The

polyester sheet, however, will be shown to have shear coupling coefficients significantly different from zero along its principal axes, and it will thereby be deemed nonorthotropic. For the sake of increasing the confidence of the author and the reader, it will also be demonstrated, by testing polyester laminates, that the determinations are self-consistent.

2 Background

In the body of this paper, the time-of-flight velocity of in-plane ultrasonic waves in thin sheets will be discussed. A sheet can be considered thin if its thickness is much smaller than the acoustic wavelength. At the frequency of operation (about 80 kHz) wavelengths in polymers are over a centimeter, and this is a valid hypothesis for thin sheets. When the surfaces of a thin sheet are unconstrained (as will be the case), it is appropriate to assume that the sheet is in a state of plane stress and that there is no thickness direction variability in strain. For plane stress deformations the in-plane engineering strains, ε_i (i = 1,2,6), are related to the in-plane stresses, σ_i, through the planar elastic stiffnesses, Q_{ij}, as in Eq. (1).[1]

$$\begin{aligned} \sigma_1 &= Q_{11}\,\varepsilon_1 + Q_{12}\,\varepsilon_2 + Q_{16}\,\varepsilon_6 \\ \sigma_2 &= Q_{12}\,\varepsilon_1 + Q_{22}\,\varepsilon_2 + Q_{26}\,\varepsilon_6 \\ \sigma_6 &= Q_{16}\,\varepsilon_1 + Q_{26}\,\varepsilon_2 + Q_{66}\,\varepsilon_6. \end{aligned} \qquad (1)$$

The reader should be aware that Q_{ij}'s differ slightly from the in-plane portion of the bulk stiffnesses, C_{ij}'s, which relate in-plane stresses and strains when there is zero out-of-plane strain (rather than zero out-of-plane stress). In the description of acoustic wave propagation, it is convenient to introduce the mass specific planar stiffnesses, q_{ij}, where $q_{ij} = Q_{ij}/\text{density}$ (i,j = 1,2,6). The shear coupling coefficients, Q_{16} and Q_{26}, in Eq. (1) are zero for orthotropic

sheets when the 1 and 2 axes determine the planes of orthotropic symmetry. They are not in general zero off-axis in orthotropic sheets [Tsai and Hahn (1980)], or along any axis in nonorthotropic sheets.

It is straightforward to demonstrate [as Musgrave (1954) does in the analogous case of bulk stiffnesses] that the phase velocities, V_p, for plane harmonic waves in thin anisotropic plates are

$$V_p^2 = 1/2\ [A \pm (A^2 - 4B)^{1/2}], \tag{2}$$

where A and B are defined in terms of the q_{ij}'s and the angle, θ, of propagation of the plane wave with respect to the 1 axis as in Eq. (3) and (4).

$$A = \cos^2\theta q_{11} + \sin^2\theta q_{22} + q_{66} + 2\cos\theta\sin\theta(q_{16} + q_{26}) \tag{3}$$

$$B = (\cos^2\theta q_{11} + \sin^2\theta q_{66} + 2\cos\theta\sin\theta q_{16})\ (\sin^2\theta q_{22} + \cos^2\theta q_{66} + 2\cos\theta\sin\theta q_{26}) - [\cos^2\theta q_{16} + \sin^2\theta q_{26} + \cos\theta\sin\theta\ (q_{12} + q_{66})]^2 \tag{4}$$

The plus sign in Eq. (2) pertains to the phase velocity of the quasi-longitudinal mode, while the minus sign corresponds to the velocity of the slower traveling quasi-transverse mode [Musgrave (1954)].

From Eq. (2)-(4) it is clear that the phase velocity as a function of angle of propagation depends on all five independent planar stiffnesses. The planar stiffnesses could be determined by measuring the phase velocity of plane waves in many directions and adjusting the values of the q_{ij}'s to get a best fit of Eq. (2) to the experimental results. However, plane wave propagation can be experimentally approximated only if the lateral extent of the transducers is much greater than the transducer separation. Transducers of these dimensions are not practical for testing polymeric sheets. In fact, the better approach is to

employ transducers which can be modeled as point sources, since their contact dimensions are much less than the transducer separation. Musgrave (1954) has demonstrated that in anisotropic materials the phase velocities measured between point transducers is different from the phase velocity of plane waves as described by Eq. (2).

Musgrave calls the phase velocity, V_i, between point sources the velocity of information propagation, and he shows that there is a one to one graphical relationship between polar plots of V_i as a function of θ and polar plots of V_p as a function of θ. This is: a line drawn through a point on the plane wave polar plot perpendicular to the radial direction will be tangent to the information propagation polar plot. Using Musgrave's graphical construction, it is feasible to first experimentally generate the information propagation polar plot, to construct the plane wave polar plot, and to then find the q_{ij}'s that produce a best fit to the plane wave polar plot. This is the basic approach adopted in the analysis described below.

3 Experiment

The velocity measurements were performed with a robotic, in-plane, ultrasonic tester developed at The Institute of Paper Chemistry [Van Zummeren, Young, Habeger, Baum, and Treleven (1987); Habeger, Van Zummeren, Wink, Pankonin, and Goodlin (1989)]. This is comprised of a commercial laboratory robot (Mitsubishi RM 501), a specially designed end effector, and some external electronic instrumentation. The end effector mounts to the end of the robot arm and houses two specially-designed, miniature, bimorph transducers [Habeger, Van Zummeren, Wink, Pankonin, and Goodlin (1989)]. There are double-action air cylinders, as part of the end effector, which can rotate each transducer 90° about its axis.

This allows for the detection of both longitudinal and transverse waves with the same transducers. A third double-action air cylinder, also on the end effector, drives a carriage to which one transducer is mounted. By activating this cylinder, one of two different transducer separations (3 or 8 cm) can be selected. The robot arm is capable of dead-weight loading the transducers to a horizontal sample over a 4 by 5 inch span, with the displacement between transducers oriented at any in-plane angle. All mechanical motions of the robot and end effector are controlled by PC class AT personal computer.

A typical velocity measurement sequence begins with the computer instructing the robot to lower the end effector to the sample with the transducers in the "near" separation. The computer triggers a function generator to excite one of the transducers with a 20 volt, single-cycle, 80 kHz sine wave. This generates an ultrasonic wave in the sample which is detected by the other transducer. The received signal is amplified and applied to a digital oscilloscope, where it is digitized at a 10 MHz rate and communicated over a G.P.I.B. bus to the computer. This is repeated a preset number of times and the computer digitally averages the multiple received signals. The end effector is then lifted from the sample; the cylinder is fired to separate the transducers; and the transducers are returned to the sample. A composite "far" signal is generated in the same manner. The computer calculates the cross-correlation function for the two signals, and from the maximum in this function it determines the time-of-flight difference between the two signals [Bloch (1977)]. To avoid interference from edge reflections, only the first half cycle of the near signal is used in the calculation. The time-of-flight velocity is then calculated as the separation difference divided by the time difference. The robot raises the transducers and repeats the velocity determination at another location

on the sample. For more details on the operation and construction of the instrument the reader is referred to the earlier publications [Van Zummeren, Young, Habeger, Baum, and Treleven (1987); Habeger, Van Zummeren, Wink, Pankonin, and Goodlin (1989)].

The test procedure for the experiments reported in the paper is a three step process. Longitudinal velocity measurements are first made at 5° increments of the transducer orientation angle. At each orientation, tests are conducted at eight locations on the sample. About 45 minutes are required to perform the necessary 288 velocity measurements. After the longitudinal testing is complete, sixteen transverse velocity measurements are made along the minor principal axis of moment of inertia of the plane wave velocity squared polar plot. The computer prints the values of the information propagation velocities squared and constructs a polar plot. The results for a polypropylene sample are presented in Fig. 1.

Fig. 1 here

The next task is to use the Musgrave construction to create a plane wave polar plot. As demonstrated for the polypropylene sheet in Fig. 2, the computer does the required calculations, prints the values of the plane wave velocities squared at 5° increments, and produces a polar plot. Notice that along the principal axes the two figures display the same velocities, while the off-axis plane wave velocities are noticeably larger. These differences are exaggerated for sheets of higher anisotropy.

Fig. 2 here

Optimizing the stiffnesses to reproduce the plane wave polar plot is the last step. The specific shear stiffness, q_{66}, is set equal to the average of

the sixteen transverse velocities determined in the first step. To start with, the sample is assumed to be orthotropic. This means q_{16} and q_{26} are zero, when referred to the axes of reflectional symmetry. The axes for calculation of the elastic coefficients are taken as the principal axes of moment of inertia of the plane wave velocity squared polar plot. If the material is orthotropic, these are the reflectional symmetry axes. The computer now optimizes in a coordinate system aligned to the principal axes the three unknown parameters (q_{11}, q_{22}, and q_{12}) to produce a minimum value in the sum of the absolute relative differences between experiment and theory in the plane wave velocity squared polar plot. These results, along with the minimum average relative error, are reported as shown in Fig. 3. The optimization is then repeated. This time nonzero values of q_{16} and q_{26} are allowed. The new stiffnesses and error values are printed. By rotating the general stiffnesses tensor, the values of q_{11} are calculated as a function of θ, and a third polar plot is generated. Notice that for this sample the shear coupling terms are very small, and little improvement in the relative error is achieved by their addition. The minimum average relative error has been found to almost always be under 0.005 for a wide variety of papers and plastic sheets. This demonstrates that the theoretical framework fits the experimental data and is taken as evidence for the validity of the general approach.

Fig. 3 here

A parameter, called the nonorthotropic angle, is now presented as a quantitative indicator of the lack of orthotropic behavior. It is easily shown [Tsai and Hahn (1980)] that the derivatives of the stiffnesses with respect to orientation are as follows: $dq_{11}/d\theta = -4q_{16}$, $dq_{22}/d\theta = 4q_{26}$, $dq_{16}/d\theta = q_{11}-2q_{66}-q_{12}$, and $dq_{26}/d\theta = -q_{22} + 2q_{66} + q_{12}$. Notice that q_{16} is zero when q_{11} is an extremum

and that q_{26} is zero when q_{22} is an extremum. If a material is orthotropic, q_{16} and q_{26} are zero and q_{11} and q_{22} are extrema along the principal axes. If a material is not orthotropic, q_{16} and q_{26} are not zero at the same angle, the extrema of q_{11} and q_{22} do not coincide, and the extrema of q_{11} and q_{22} are not separated by 90°. The nonorthotropic angle, Φ, is defined as the angular separation between the null values of q_{26} and q_{16}. This, of course, also equals the angle between an extremum in q_{22} and an extremum in q_{11}. When Φ is small (ignoring derivatives of second order and higher in q_{16} and q_{26}), the nonorthotropic angle is

$$\Phi \approx -q_{16}/(q_{11}-q_{12}-2q_{66})-q_{26}/(q_{22}-q_{12}-2q_{66}). \qquad (5)$$

The nonorthotropic angle is a coordinate independent parameter which is directly related to the prominent behavioral peculiarities of nonorthotropic sheets. Therefore, it will be used as the principle measure of nonorthotropic response, and relatively large values of Φ [printed out according to Eq. (5) as in Fig. 3] are taken to mean that the orthotropic assumption is inappropriate for the sample in question.

4 Single Sheet Results

Pertinent values (with one standard deviation uncertainties) for a 75 μm thick polypropylene sheet and a 135 μm thick polyester sheet are listed in Table 1. The values of q_{16} and q_{26} are measured relative to the principal axes of the moment of inertia of the plane wave velocity squared polar plot. The symbol E_o represents the average relative error using the orthotropic assumption, and E_N is the error when q_{16} and q_{26} are allowed to vary.

Table 1 here

Each number reported in Table 1 is the average of eight different runs (the product of 2304 velocity measurements). The region of the sheet sampled at each angle is slightly different, and, on a single run, variations over the sample can lead to artifacts in the polar plots. This complication was addressed by rotating the sample 90° between runs and doing 50% of the runs on each side of the sample. In theory, turning a sheet over inverts q_{16} and q_{26}. This phenomenon was observed experimentally, and it is presented as evidence for self-consistency of the experiments. The results in Table 1 are taken relative to one side of the sample which was arbitrarily designated as the top.

The two plastic sheets are representative of orthotropic and nonorthotropic behavior. For the polypropylene sheet, the shear coupling coefficients and the nonorthotropic angle are extremely small and not significantly different from zero at a reasonable confidence level. Also, the fit of theory to experiment is little improved by adjusting q_{16} and q_{26}. The converse of all these observations are true for the polyester. The polyester sample is also interesting in that the axis of maximum stiffness deviates over 30° from the MD. The third page report for one of the polyester runs is included as Fig. 4. Notice that the nonorthotropic behavior is manifest in a slight asymmetry of the polar plot relative to the principal axes.

Fig. 4 here

5 Laminate Results

The reported shear coupling coefficients (even those of the polyester) are admittedly small, and it is legitimate to question their significance. Further demonstrations that they are not artifacts of the experiment are necessary before they can be taken seriously. An ideal approach would be to test sheets

with independently determined shear coupling coefficients. However, to the author's knowledge, there is no comparable method for measuring shear coupling coefficients in sheets.

Measurements on laminates was the method adopted here, to inspect the foundations of the technique. The laminates were made by bonding together plastic sheets whose general elastic constants had been measured. The effective stiffnesses of the laminates was calculated from the stiffnesses of their layers and compared to the values measured on the laminates. This approach can work only if the layers are well-bonded, with a very thin layer of adhesive. After considerable trial and error, a method was found which was successful with the polyester sheets, only. Polyester sheets were placed in contact, with a small amount of Locktite 447 "surface insensitive instant adhesive" applied inside, along one edge. This edge and the two adjacent edges were taped to keep the adhesive from escaping. The laminate was then turned through the nip of a heavily-loaded, rubber-rolled wringer. Then the laminate was sandwiched between flat metal plates, and the adhesive was allowed to cure for one day. The suitability of the lamination process was verified by making two ply laminates of polyester sheets. If the bonding was satisfactory, the q_{ij}'s of the laminate would equal those of the plies. Within one standard deviation, this was the case for all of the stiffnesses (including q_{16} and q_{26}).

The theoretical relationships between the elastic properties of the laminate and those of the plies are simple. Since the wavelength is large compared to the laminate thickness, the assumption of plane stress remains valid. Therefore, the effective elastic properties of the laminate are the average of the plies [Tsai and Hahn (1980)], and, as all plies have the same density, the

q_{ij}'s are merely the average of the layers. To predict the laminate stiffnesses, the ply stiffnesses are rotated to the axis of interest and averaged.

Four different laminates were fabricated from polyester sheets, taken from the same roll as that in Table 1 and tested. Two were "flip" laminates, and two were "rotation" laminates. An "off-axis flip laminate" was made by rotating one sheet 180° about the MD axis and bonding it to a similar sheet. The major principal axes were about 33° from the MD, making the principal axis of the plies about 66° apart. An "on-axis flip laminate" was also constructed. This time one sheet was rotated about a principal axis, and the principal axes of the plies were aligned. The plies of each laminate were chosen to have almost equal stiffnesses. Since flipping a sheet inverts its shear coupling coefficients and since the laminate stiffnesses are the average of the plies, the laminates approximate orthotropic behavior better than the plies. The on-axis flip laminate has roughly the same MD to CD stiffness ratio as the plies, while the off-axis laminate is a squarer sheet. The results for the flip laminates are presented in Table 2.

Table 2 here

In Table 2, the symbol, α, represents the angle between the rotation axis and the major principal axis of moment of inertia of the plane wave velocity squared polar plot. The α for the laminate is that determined by the measurements on the laminate, and the experimental stiffnesses are relative to that axis.

The agreement between experimental flip laminate stiffnesses and those calculated from the ply stiffnesses is impressive. Note particularly that, as predicted, very small shear coupling coefficients and Φ values were measured for the laminate.

A "two-ply rotation laminate" and a "three-ply rotation laminate" were also fabricated. The major principal axes of the layers in the two-ply sheet are at 90°. This produces a sheet with a decreased nonorthotropic angle and nearly cubic symmetry. The principal axes of the middle ply of the three-ply laminate is rotated 90° from those on the outside. This sheet should be squarer than a single ply, and it should have an even larger nonorthotropic angle. The results are in Table 3.

Table 3 here

The two-ply laminate in Table 3 is a very square sheet, and the determination of the principal axes is unstable. Therefore, there was much variability in the orientation of these axes as determined by the computer program. To get the results on a common basis, the stiffnesses from each run were rotated to the theoretical principal axis and averaged at that angle. The value of the principal axis listed in Table 3 is in parentheses to indicate that it was not found experimentally. Excellent agreement between the experimental and theoretical stiffnesses, with the possible exception of the shear coupling coefficients, was realized for the two-ply rotation laminate. Since the shear coupling coefficients are changing rapidly (in opposite directions) with angle near a principal axis, the difference between experiment and theory can be attributed to small errors in the orientation of the principal axes. The nonorthotropic angle is a coordinate-independent parameter, which is not influenced by the choise of principal axes. It therefore provides another (perhaps fairer) way to compare shear coupling results. Both values of Φ are extremely small. Thus theory and experiment agree that the two-ply rotation produces a nearly cubic sheet.

For the three-ply laminate, the values of q_{66}, the shear stiffness, do not compare as well as for the others. This may indicate that the lamination process is not as effective with three layers. Since the determination of q_{12} is very sensitive to q_{66}, the low shear stiffness as measured in the laminate results in a large disparity in q_{12} values. The three-ply laminate was the only highly nonorthotropic sheet produced, and although the shear values are in question, its results are included to show that theory and experiment are in concurrence on the lack of orthotropic symmetry. In this case, the values of Φ were too large to be calculated using Eq. (5), and instead they were obtained from complete plots of the shear coupling coefficients. Notice that both values of Φ are almost 20°. This means that the maximum in q_{11} and the minimum in q_{22} are nearly 20° apart. The effect of this was manifested in the raw experimental data which shows approximately a 70° spacing between a maximum and a minimum in the longitudinal velocity, see Fig. 5.

Fig. 5 here

6 Conclusions

It has been demonstrated that by using an automated ultrasonic apparatus it is possible to perform the large number of measurements necessary to make repeatable determinations of all the in-plane elastic stiffnesses (including the shear coupling coefficients) of a polymeric sheet. The results are shown to be consistent in that they yield the expected output when laminates are tested. To the author's knowledge, this is the first instrument developed to routinely measure the shear coupling coefficients on sheets.

Sheets without orthotropic symmetry can develop shear strain when normal stresses are applied along any axis. This can translate into out-of-plane

buckling and wrinkling and can cause numerous difficulties in handling and end-use performance. Measurements of shear coupling coefficients are clearly important for characterizing the response of thin sheets. The limited survey of plastic sheets done in conjunction with this study revealed that at least one commercially available polyester sheet displays shear coupling behaviors that are not consistent with orthotropic symmetry.

References

Bloch, S., Am. J. Phys., 45, 538 (1977).

Habeger, C., Van Zummeren, M., Wink, W., Pankonin, B., and Goodlin, R., Tappi, to be published, 1989.

Musgrave, M., Proc. Royal Soc., A226 (1166), 339 (1954).

Tsai, S. and Hahn, H., Introduction to Composite Materials, Technomic, Lancaster, PA, 1980.

Van Zummeren, M., Young, D., Habeger, C., Baum, G., and Treleven, R., Ultrasonics, 25, 288 (1987).

Table 1. Elastic parameters for single plastic sheets

Quantity	Polypropylene	Polyester
q_{16} (km^2/s^2)	0.000 ± 0.005	-0.036 ± 0.007
q_{26} (km^2/s^2)	0.002 ± 0.004	0.047 ± 0.012
Φ	0.01° ± 0.04	4.8° ± 1.1
E_o	0.00413	0.00406
E_N	0.0058	0.0027

Table 2. Elastic parameters for plastic flip laminates

OFF-AXIS FLIP LAMINATE

	Top Ply	Bottom Ply	Laminate Theory	Laminate Experiment
q_{11} (km^2/s^2)	6.51	6.55	5.80	5.78 ± 0.02
q_{22} (km^2/s^2)	4.36	4.34	4.92	4.91 ± 0.02
q_{66} (km^2/s^2)	1.75	1.75	1.85	1.84 ± 0.01
q_{12} (km^2/s^2)	1.63	1.65	1.73	1.72 ± 0.02
q_{16} (km^2/s^2)	-0.035	0.038	0.002	0.002 ± 0.007
q_{26} (km^2/s^2)	0.040	-0.050	-0.002	-0.002 ± 0.007
α	33.1°	-33.5°	-0.7°	-2.0° ± 1.0
Φ	4.2°	-5.0°	-0.5°	-1.3° ± 1.8

ON-AXIS FLIP LAMINATE

q_{11} (km^2/s^2)	6.50	6.56	6.53	6.48 ± 0.04
q_{22} (km^2/s^2)	4.38	4.36	4.38	4.34 ± 0.02
q_{66} (km^2/s^2)	1.75	1.75	1.75	1.76 ± 0.01
q_{12} (km^2/s^2)	1.65	1.65	1.64	1.62 ± 0.03
q_{16} (km^2/s^2)	-0.043	0.045	0.001	0.002 ± 0.004
q_{26} (km^2/s^2)	0.055	-0.058	-0.001	-0.004 ± 0.005
α	-0.9°	0.6°	-0.2°	-0.1° ± 0.6
Φ	6.0°	-6.1°	-0.0°	-0.4° ± 0.5

Table 3. Elastic parameters for rotation laminates

TWO-PLY ROTATION LAMINATE

	Top Ply	Bottom Ply	Laminate Theory	Laminate Experiment
q_{11} (km^2/s^2)	6.50	6.51	5.45	5.44 ± 0.02
q_{22} (km^2/s^2)	4.35	4.37	5.45	5.43 ± 0.02
q_{66} (km^2/s^2)	1.74	1.75	1.73	1.74 ± 0.03
q_{12} (km^2/s^2)	1.65	1.63	1.63	1.65 ± 0.06
q_{16} (km^2/s^2)	-0.046	-0.039	0.005	-0.006 ± 0.009
q_{26} (km^2/s^2)	0.060	-0.050	-0.003	0.006 ± 0.009
α	-0.4°	90.2°	8.9°	(8.9°)
Φ	6.3°	5.4°	-0.3°	-0.5° ± 2.8

THREE-PLY ROTATION LAMINATE

q_{11} (km^2/s^2)	6.53	6.47	5.80	5.79 ± 0.04
q_{22} (km^2/s^2)	4.34	4.34	5.05	5.04 ± 0.03
q_{66} (km^2/s^2)	1.75	1.76	1.75	1.73 ± 0.04
q_{12} (km^2/s^2)	1.61	1.61	1.61	1.71 ± 0.04
q_{16} (km^2/s^2)	-0.040	-0.045	-0.046	-0.061 ± 0.011
q_{26} (km^2/s^2)	0.051	0.059	0.049	0.065 ± 0.011
α	33.3°	-33.8°	33.3°	33.5° ± 1.1
Φ	5.4°	6.2°	18.4°	19.3°

THE INSTITUTE OF PAPER CHEMISTRY
ROBOTIC IN-PLANE ULTRASONIC VELOCITIES

POLAR PLOT OF LONGITUDINAL INFORMATION PROPAGATION VELOCITY SQUARED

OPERATOR: C. C. Habeger
PROJECT : 3467
SAMPLE : Polypropylene AA top corner 2 73°F

DATE: DECEMBER 6, 1988
TIME: 10:42:25

SIGNALS AVERAGED PER MEASUREMENT = 4
NUMBER OF TESTS PER ANGLE = 8
SIGNAL DISTANCE = 49.0 mm
SAMPLE HOLDER NUMBER = 2

ANGLE DEGREES	VEL SQR KM2/SEC2	COEF OF VARIATION	ANGLE DEGREES	VEL SQR KM2/SEC2	COEF OF VARIATION
0	10.12	0.015	90	5.08	0.010
5	10.00	0.008	95	5.12	0.007
10	9.78	0.008	100	5.19	0.008
15	9.32	0.010	105	5.29	0.009
20	8.92	0.011	110	5.41	0.009
25	8.33	0.011	115	5.59	0.008
30	7.86	0.008	120	5.80	0.011
35	7.38	0.004	125	6.04	0.006
40	6.98	0.009	130	6.33	0.010
45	6.62	0.004	135	6.63	0.007
50	6.27	0.005	140	7.03	0.009
55	6.02	0.006	145	7.46	0.007
60	5.76	0.008	150	7.86	0.004
65	5.55	0.008	155	8.37	0.006
70	5.40	0.007	160	8.88	0.010
75	5.29	0.004	165	9.37	0.005
80	5.17	0.004	170	9.82	0.010
85	5.11	0.007	175	10.02	0.009

ANGLE TO PRINCIPAL AXIS OF MOMENT OF INERTIA = -0.2° MD IS ALONG Tangent
AREA = 166.7 (km^4/sec^4) MD-CD STIFFNESS RATIO = 1.99

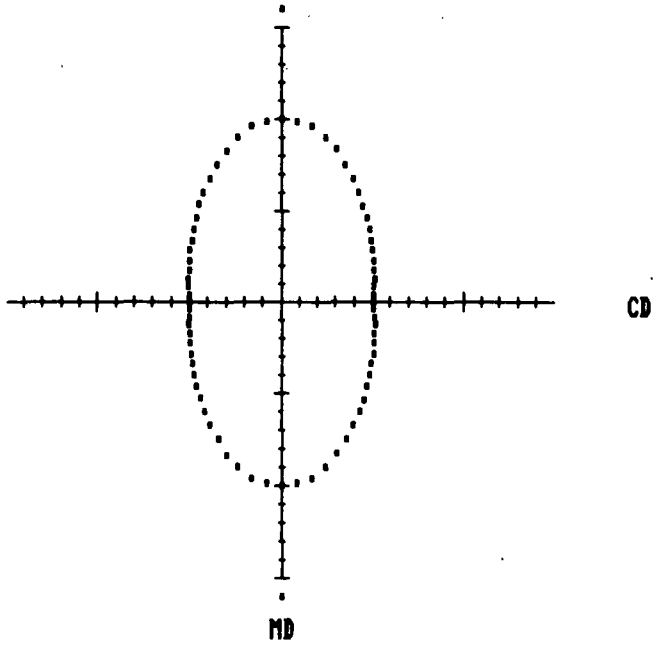

PLOT OF VEL SQR VS ANGLE
(Graph Scale = 1 km^2/sec^2/div)

Fig. 1. A computer printout of the measured values of the information propagation velocity squared for a polypropylene sheet as a function of clockwise angle from the MD.

THE INSTITUTE OF PAPER CHEMISTRY
ROBOTIC IN-PLANE ULTRASONIC VELOCITIES

POLAR PLOT OF LONGITUDINAL PHASE VELOCITY SQUARED

OPERATOR: C. C. Habeger
PROJECT : 3467
SAMPLE : Polypropylene AA top corner 2 73°F

DATE: DECEMBER 6, 1988
TIME: 10:43:30

SIGNALS AVERAGED PER MEASUREMENT = 4
NUMBER OF TESTS PER ANGLE = 8
SIGNAL DISTANCE = 49.0 mm
SAMPLE HOLDER NUMBER = 2

ANGLE DEGREES	VEL SQR KM2/SEC2	ANGLE DEGREES	VEL SQR KM2/SEC2
0	10.12	90	5.08
5	10.04	95	5.15
10	9.92	100	5.25
15	9.71	105	5.42
20	9.49	110	5.64
25	9.13	115	5.91
30	8.70	120	6.21
35	8.32	125	6.59
40	7.88	130	6.96
45	7.35	135	7.39
50	6.94	140	7.85
55	6.52	145	8.29
60	6.18	150	8.75
65	5.85	155	9.16
70	5.61	160	9.52
75	5.39	165	9.74
80	5.25	170	9.94
85	5.13	175	10.04

ANGLE TO PRINCIPAL AXIS OF MOMENT OF INERTIA = -0.2°
AREA = 186.8 (km^4/sec^4)
MD-CD STIFFNESS RATIO = 1.99

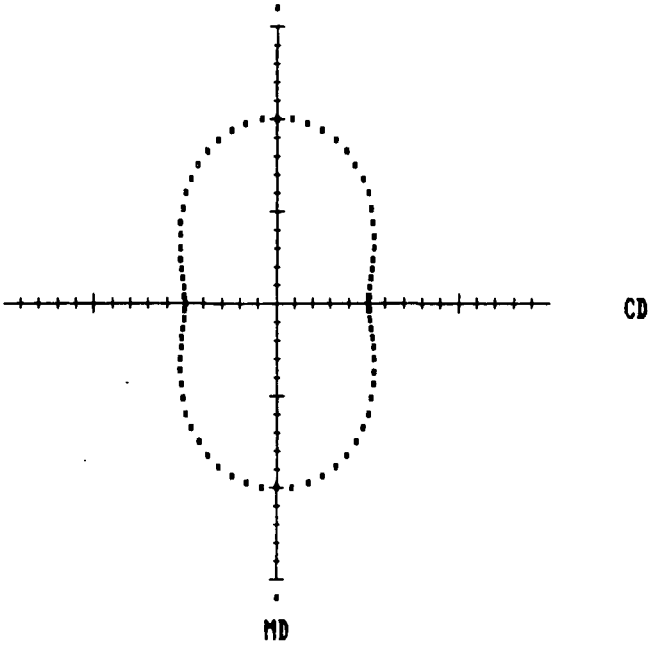

PLOT OF VEL SQR VS ANGLE
(Graph Scale = 1 km^2/sec^2/div)

Figure 2. Computer printout of the plane wave velocity squared values using Musgrave's construction and the results from Figure 1.

THE INSTITUTE OF PAPER CHEMISTRY
ROBOTIC IN-PLANE ULTRASONIC VELOCITIES

OPTIMUM MASS SPECIFIC STIFFNESSES FROM LEAST SQUARED FIT TO LONGITUDINAL PHASE VELOCITY

OPERATOR: C. C. Habeger
PROJECT : 3467
SAMPLE : Polypropylene AA top corner 2 73°F

DATE: DECEMBER 6, 1988
TIME: 10:44:31

ORTHOTROPIC STIFFNESSES
Q11 / rho = 10.094 KM2/SEC2
Q22 / rho = 5.136 KM2/SEC2
Q66 / rho = 2.226 KM2/SEC2
Q12 / rho = 2.128 KM2/SEC2

Average relative error = 0.003252
Stiffness ratio = 1.97

Poisson's Ratios
Vxy = 0.211
Vyx = 0.414
Geometric Mean = 0.296

GENERAL STIFFNESSES
Q11 / rho = 10.094 KM2/SEC2
Q22 / rho = 5.133 KM2/SEC2
Q66 / rho = 2.226 KM2/SEC2
Q12 / rho = 2.137 KM2/SEC2
Q16 / rho = 0.000 KM2/SEC2
Q26 / rho = 0.002 KM2/SEC2

Q66 / rho (Campbell) = 2.423 KM2/SEC2

Average relative error = 0.003225
NON-ORTHOTROPIC ANGLE = 0.07°

Poisson's Ratios
Vxy = 0.212
Vyx = 0.416
Geometric Mean = 0.297

ANGLE TO PRINCIPAL AXIS OF MOMENT OF INERTIA = -0.2°
INTEGRATED AREA = 179.8 (km^4/sec^4)

POLAR PLOT OF LONGITUDINAL MASS SPECIFIC STIFFNESS

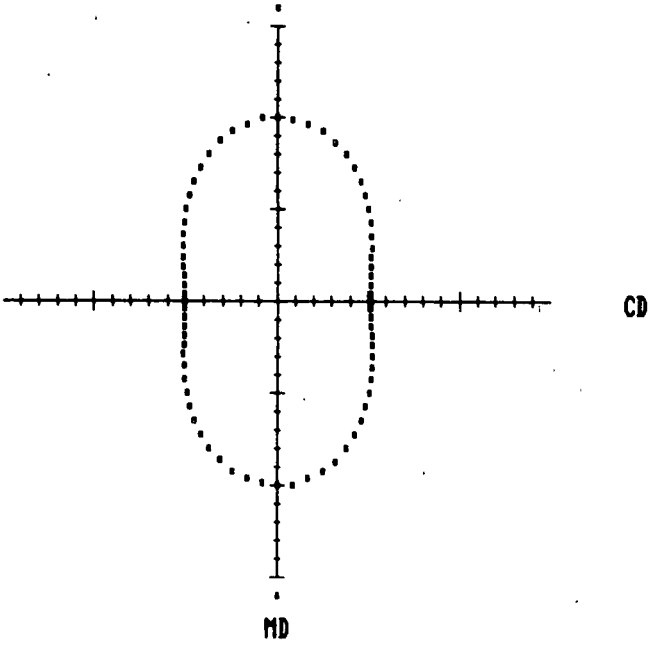

PLOT OF SPECIFIC STIFFNESS
(Graph Scale = 1 km^2/sec^2/div)

Figure 3. A computer printout of the elastic stiffnesses determined from a best fit to the Figure 2 polar plot.

THE INSTITUTE OF PAPER CHEMISTRY
ROBOTIC IN-PLANE ULTRASONIC VELOCITIES

OPTIMUM MASS SPECIFIC STIFFNESSES FROM LEAST SQUARED FIT TO LONGITUDINAL PHASE VELOCITY

OPERATOR: C. C. Habeger
PROJECT : 3467
SAMPLE : Polyester 121 top corner 2 73 °F

DATE: DECEMBER 6, 1988
TIME: 11:49:31

ORTHOTROPIC STIFFNESSES
Q11 / rho = 6.558 KM2/SEC2
Q22 / rho = 4.367 KM2/SEC2
Q66 / rho = 1.760 KM2/SEC2
Q12 / rho = 1.613 KM2/SEC2

Average relative error = 0.005669
Stiffness ratio = 1.50

Poisson's Ratios
Vxy = 0.246
Vyx = 0.369
Geometric Mean = 0.301

GENERAL STIFFNESSES
Q11 / rho = 6.554 KM2/SEC2
Q22 / rho = 4.372 KM2/SEC2
Q66 / rho = 1.760 KM2/SEC2
Q12 / rho = 1.636 KM2/SEC2
Q16 / rho = -0.034 KM2/SEC2
Q26 / rho = 0.045 KM2/SEC2

Q66 / rho (Campbell) = 1.830 KM2/SEC2

Average relative error = 0.002847
NON-ORTHOTROPIC ANGLE = 4.68°

Poisson's Ratios
Vxy = 0.250
Vyx = 0.374
Geometric Mean = 0.306

ANGLE TO PRINCIPAL AXIS OF MOMENT OF INERTIA = -34.1°
INTEGRATED AREA = 93.0 (km^4/sec^4)

POLAR PLOT OF LONGITUDINAL MASS SPECIFIC STIFFNESS

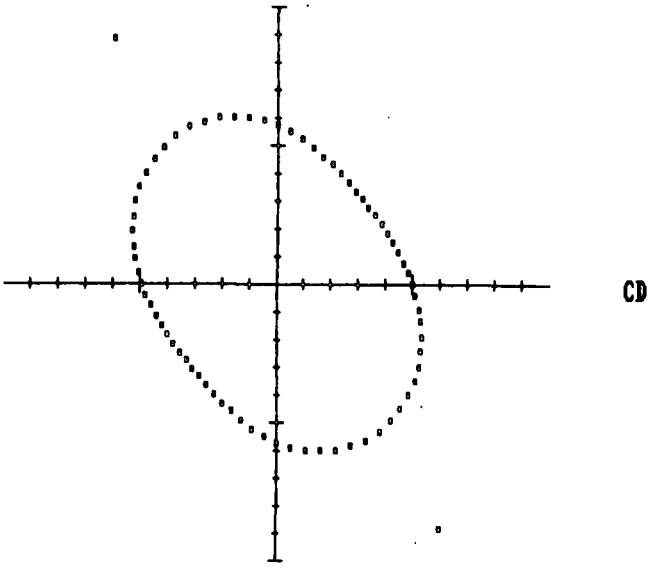

PLOT OF SPECIFIC STIFFNESS
(Graph Scale = 1 km^2/sec^2/div)

Figure 4. A computer printout of the elastic stiffnesses of a polyester sheet from a best fit to the plane waves velocity squared polar plot.

THE INSTITUTE OF PAPER CHEMISTRY
ROBOTIC IN-PLANE ULTRASONIC VELOCITIES

POLAR PLOT OF LONGITUDINAL INFORMATION PROPAGATION VELOCITY SQUARED

OPERATOR: C. C. Habeger
PROJECT : 3467
SAMPLE : Polyester trilaminate 104-106 90°-105 72.5°

DATE: DECEMBER 3, 1988
TIME: 8:45:25

SIGNALS AVERAGED PER MEASUREMENT = 4
NUMBER OF TESTS PER ANGLE = 8
SIGNAL DISTANCE = 49.0 mm
SAMPLE HOLDER NUMBER = 2

ANGLE DEGREES	VEL SQR KM2/SEC2	COEF OF VARIATION	ANGLE DEGREES	VEL SQR KM2/SEC2	COEF OF VARIATION
0	5.51	0.010	90	5.28	0.010
5	5.36	0.015	95	5.29	0.017
10	5.28	0.032	100	5.28	0.017
15	5.21	0.022	105	5.32	0.010
20	5.16	0.023	110	5.39	0.016
25	5.11	0.021	115	5.56	0.012
30	5.07	0.018	120	5.50	0.021
35	5.05	0.020	125	5.56	0.008
40	5.00	0.022	130	5.65	0.013
45	5.03	0.015	135	5.72	0.018
50	5.05	0.014	140	5.74	0.016
55	5.12	0.016	145	5.78	0.014
60	5.07	0.015	150	5.86	0.012
65	5.10	0.012	155	5.80	0.015
70	5.12	0.007	160	5.80	0.014
75	5.15	0.007	165	5.72	0.022
80	5.18	0.008	170	5.66	0.008
85	5.22	0.011	175	5.59	0.013

ANGLE TO PRINCIPAL AXIS OF MOMENT OF INERTIA = -34.8° MD IS ALONG Radius
AREA = 90.7 (km^4/sec^4) MD-CD STIFFNESS RATIO = 1.04

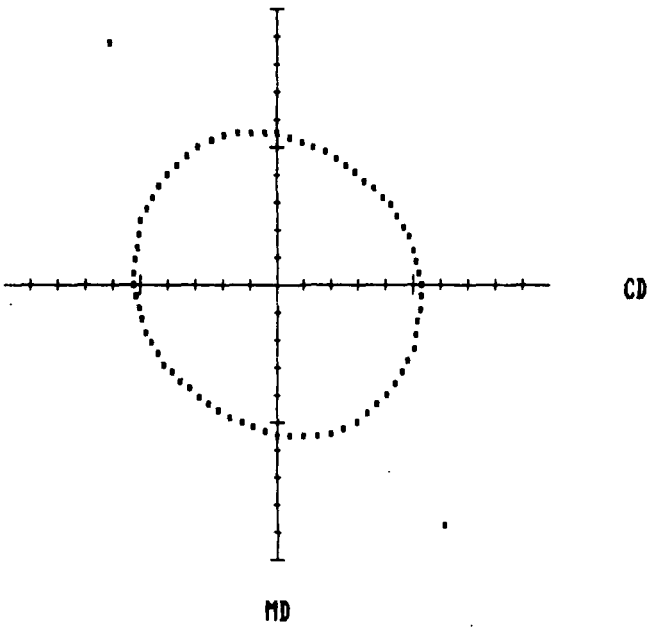

PLOT OF VEL SQR VS ANGLE
(Graph Scale = 1 km^2/sec^2/div)

Figure 5. A computer printout of the measured values of the information propagation velocity squared for the three-ply polyester laminate.

Appendix 2

THE DEVELOPMENT OF A DOUBLE ELEMENT, PULSE ECHO, PVDF TRANSDUCER

C. C. Habeger
W. A. Wink

ABSTRACT

This paper presents a simple way to use PVDF piezoelectric films to construct a multiple active element ultrasonic transducer. With this transducer, pulse echo measurements can be made using a separate transmitter and receiver. This eliminates the need for special electrical circuitry and provides the opportunity for individual design of receiver and transmitter response characteristics.

INTRODUCTION

Pulse echo techniques are widely used for ultrasonic inspection of materials.[1] Standard pulse echo techniques require the use of a single transducer for generation and detection of acoustic signals. In a typical application, the transducer is first coupled to the test object. The transducer is electrically pulsed, and an acoustic disturbance propagates into the test object. A signal, reflected back from an interface, produces a secondary signal in the transducer. Finally, the test object is characterized by analyzing the echo signal.

A limitation of the use of the same transducer for transmission and reception is that supplementary electrical circuitry must be introduced. In a straightforward employment, the excitation pulse is applied directly to the echo signal amplifier. Either the amplifier must be switched out of the circuitry during pulsing, or it must be designed to withstand high input voltages and recover quickly from saturation. If the pulse drive circuitry is not switched

out during echo reception, the input impedance of the amplifier should be lower than the drive circuitry to achieve efficient signal transfer.

Another drawback of the standard approach is that the transducer design must be a compromise between optimum transmitter and receiver characteristics. The piezoelectric element should both withstand large electric fields and be very sensitive. Different piezoelectric materials cannot be selected for transmission and reception, and the receiving and transmitting elements cannot employ different geometries.

One way to circumvent the difficulties of single transducer, pulse echo measurements is to simply place two active elements in the same housing. If standard ceramic piezoelectric materials were used, the construction could be bulky and cumbersome, and multiple reflections between elements could interfere with the echo signals. However, multiple element transducers are practical when polyvinylidene fluoride (PVDF or Kynar) plastic piezoelectric films are the active elements. Since they are thin films, a compact construction is easily achieved, and their natural broad band response allows straightforward suppression of internal reflections.

The double active element transducer design would be particularly useful in Barker-coded sequence, multilayer transducers.[2] The Barker code sequence of two multilayer elements could be opposite, allowing for straightforward pulse compression in single transducer pulse echo measurements.

TRANSDUCER CONSTRUCTION

The transducer described below has two PVDF elements. When used for pulse echo work, the need for special circuitry is precluded since there is a separate

transmitter and receiver within the same assembly. Although the transmitter and receiver elements are identical in this particular construction, different geometries could easily have been employed.

Figure 1 is a mechanical drawing of the transducer. The plastic piezoelectric elements are 110 μm thick PVDF copolymer films (VF2-VF3 from Pennwalt Corp.). Each element is a laminate of two films of opposite polarity. Electrical connection is made to the element center and the surfaces are grounded. This provides effective electrical shielding between elements and from the environment. The bottom side of the inner element is bonded to a disk of unpolarized Kynar. This provides a good impedance match with the film, thereby reducing backside reflections and producing broad band performance. The top side of the inner element is bonded to a short Kynar disk which, on its opposite end, is attached to the outer element. The Kynar provides an excellent impedance match to the films, and is an effective attenuator of ultrasound (loss tangent ≈ 0.08 at 1 MHz). This means that echos from reflections between the elements rapidly disappear. The top of the outer element is connected to a polystyrene delay line. The polystyrene acts as a low loss, impedance matching layer between the PVDF films and the neoprene front-face. The neoprene is used to couple energy into solid samples without the use of viscous fluids or bonding agents.

Figure 1 here

The assembly procedures for a similar, but single element, transducer are described elsewhere.[3] The rationale behind using soft neoprene to couple ultrasound into solids is also discussed in this paper.

TRANSDUCER PERFORMANCE

The operation of the transducer is presented below in the form of a series of oscilloscope traces of the signal received at the inner transducer resulting from a single-cycle 1.5 MHz pulse at the outer transducer. Figure 2 is a trace recorded during construction, before bonding of the neoprene front face to the polystyrene delay line. The very first signal is radio frequency communication between the two elements. Note that it is of lesser amplitude than some of the acoustic signals coming later, and it by no means causes amplifier saturation problems. The strong second signal comes from the acoustic wave directly between the elements. The inverted signal of slightly lower amplitude is the first reflection from the polystyrene-air interface. The second reflection, which is doubly inverted, lags the first reflection at a time interval equal to the delay between the direct signal and the first reflection. A low amplitude pulse follows each of these acoustic signals by about 4 μsec. These come from multiple reflections in the thin Kynar layer. The one associated with the direct signal is smaller than the others since it encounters two reflections at Kynar-film interfaces.

Figure 2 here

Figure 3 is a similar oscilloscope trace taken after assembly, with the neoprene front-face in place. Notice that the amplitude of the first reflection is decreased, as there is now a polystyrene-neoprene interface. The pulse following the first reflection is from the neoprene-air interface. In our application, this is the signal of interest since we are measuring the reflection coefficients between neoprene and paper board.

Figure 3 here

When the transducer is applied to a sample, a trace as shown in Fig. 4 is observed. In this case the sample is a sheet of paper board, and, since paper is very lossy in this frequency range, no signals from multiple reflections in the sample are observed. Some energy is, however, now coupled into the sample, and the front-face reflection is attenuated. The reflection coefficient at the neoprene-sample interface is minus the ratio of the front-face reflections in Fig. 4 and 3.

Figure 4 here

As demonstrated in the figures, the transducer is broad band, and delay line dimensions were chosen to isolate the front-face reflection. This provides an effective means to use pulse echo techniques to analyze sample interfaces without the special electrical circuitry used with standard pulse echo techniques.

REFERENCES

1. Truell, R., Elbaum, C., and Chick, B. Ultrasonic Methods in Solid State Physics, Academic Press, New York, Chapter 2, 1969.

2. Sung, K. Peizoelectric Multilayer Transducers for Ultrasonic Pulse Compression. Ultrasonics 22:61-68(1984).

3. Habeger, C., Wink, W., and Van Zummeren, M. Using Neoprene-Faced PVDF Transducers to Couple Ultrasound into Solids. J. Acoust. Soc. Am. 84(4): 1388-1396(1988).

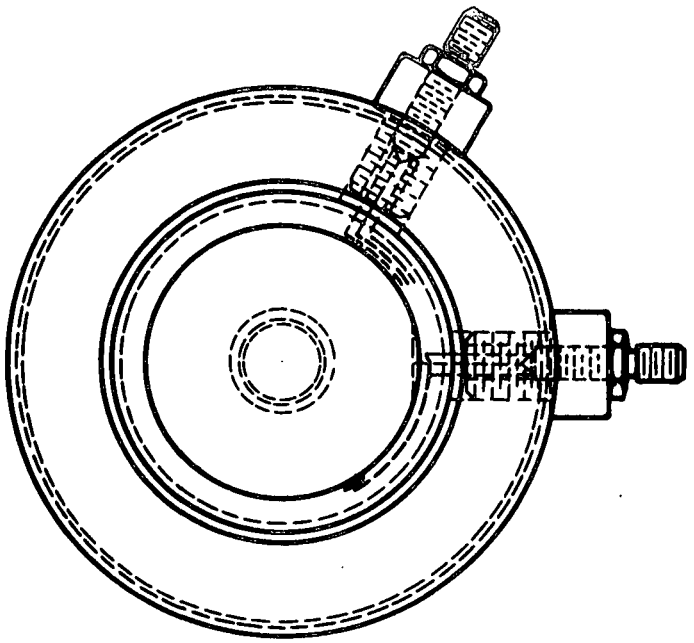

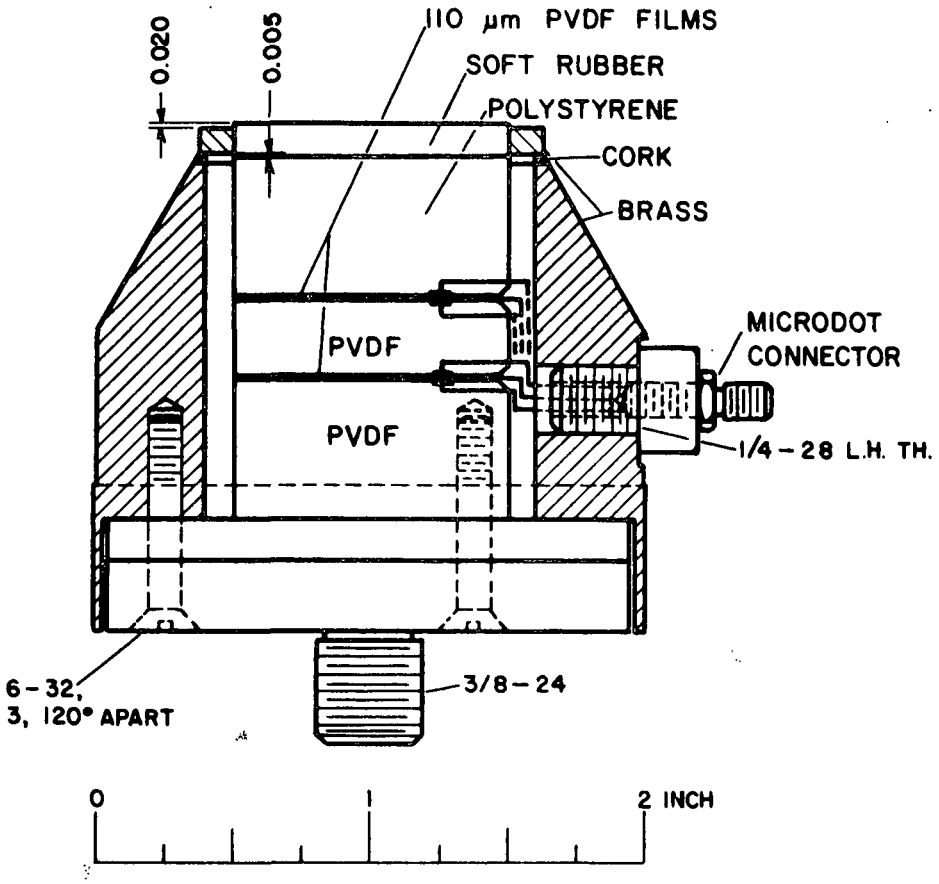

1 Mechanical drawing of the double element pulse echo transducer.

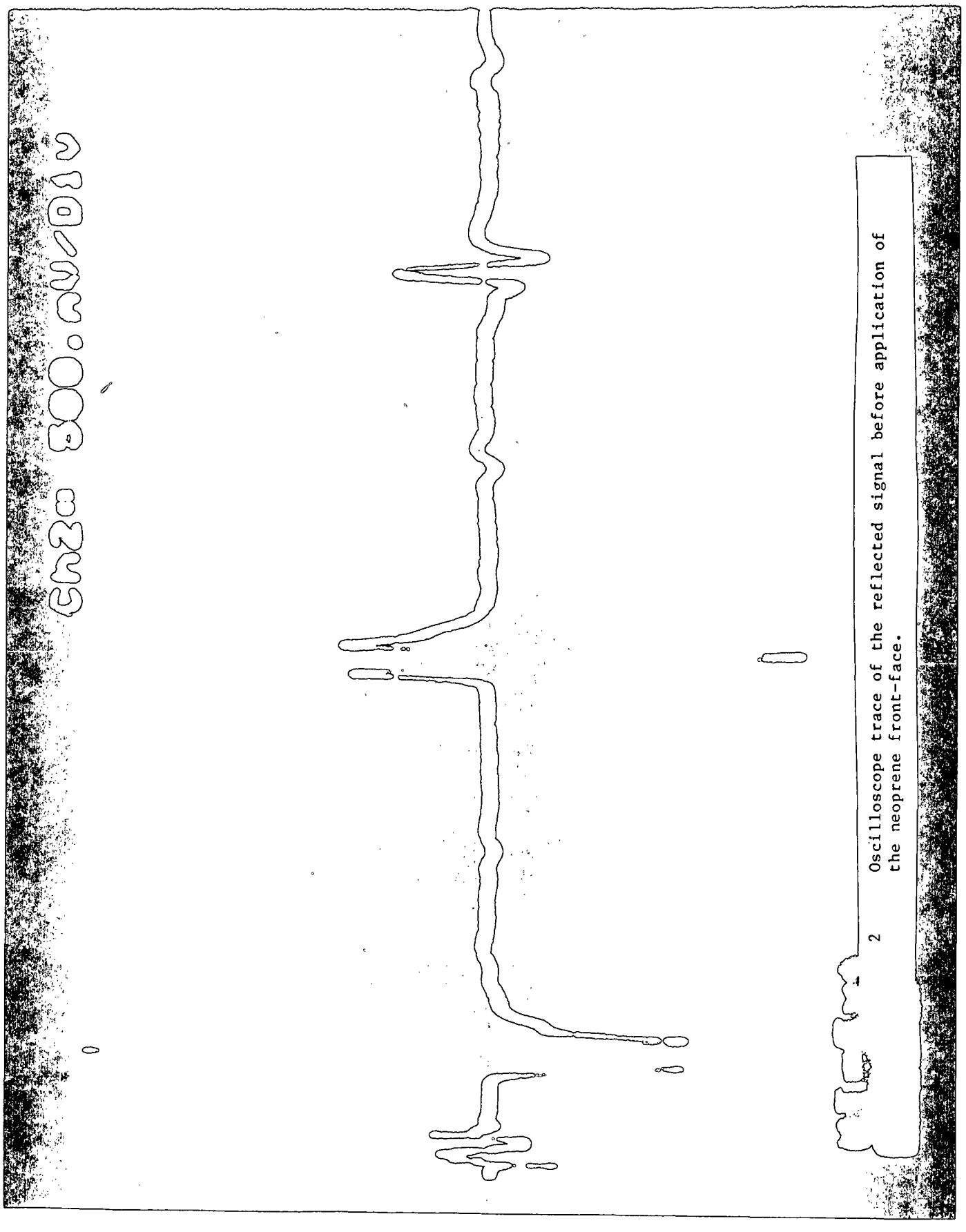

Oscilloscope trace of the reflected signal before application of the neoprene front-face.

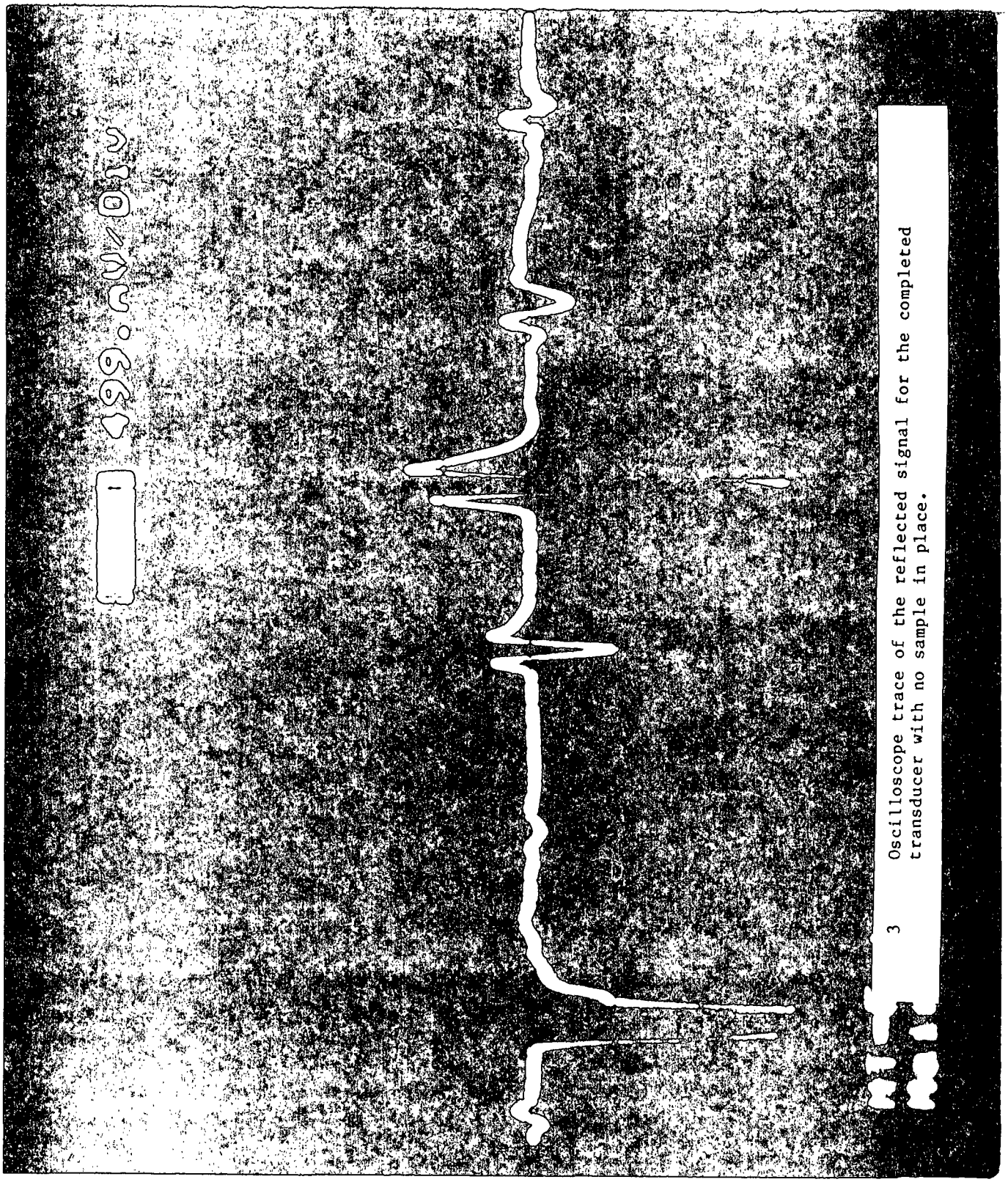

3 Oscilloscope trace of the reflected signal for the completed transducer with no sample in place.

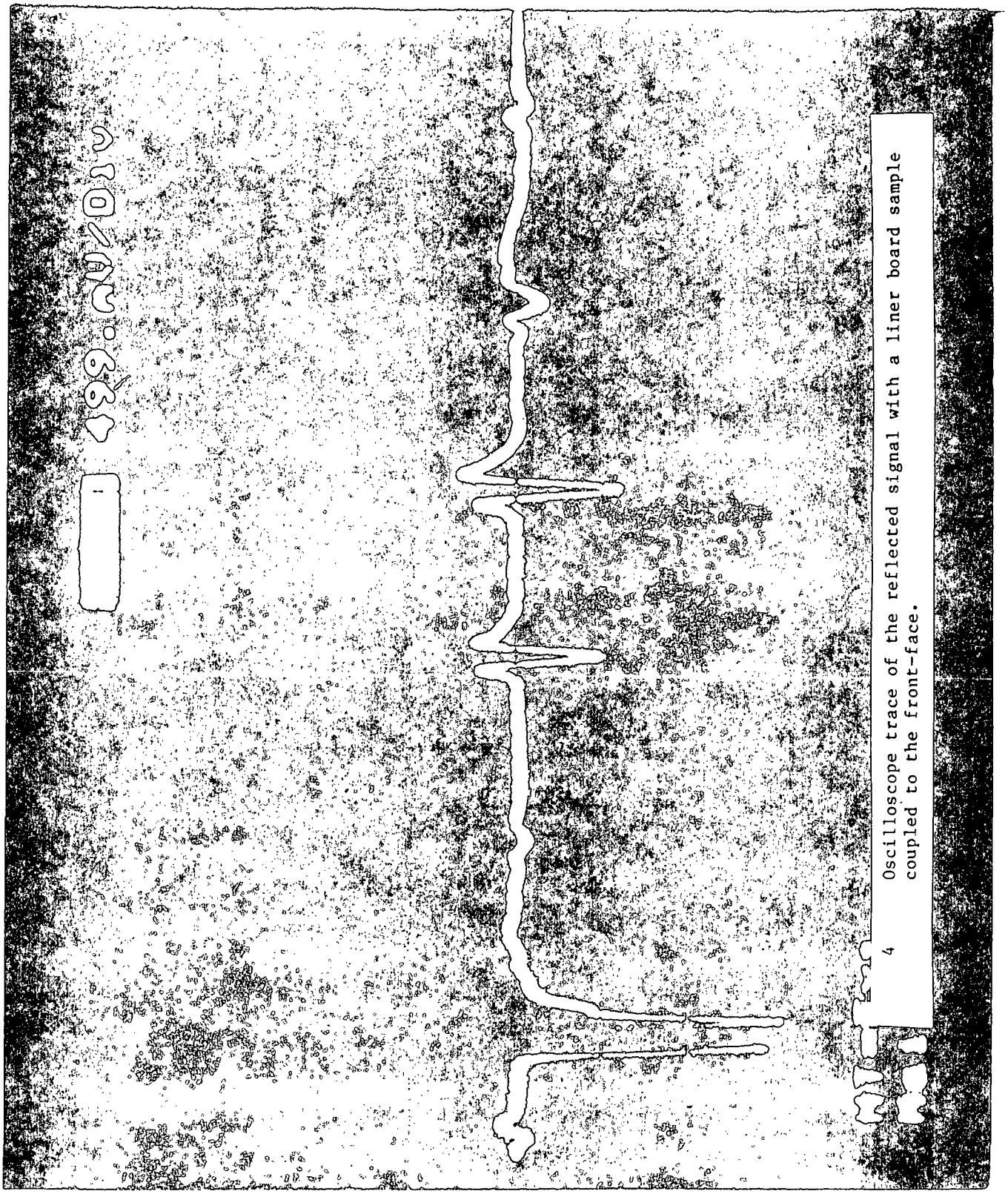

4 Oscilloscope trace of the reflected signal with a liner board sample coupled to the front-face.

Appendix 3

Empirical relationships between tissue softness and out-of-plane ultrasonic measurements

Y. Pan, C. Habeger, and J. Biasca
The Institute of Paper Chemistry
Appleton, WI 54912

ABSTRACT

In this paper, out-of-plane ultrasonic velocity and attenuation testing (1) is introduced for use on tissue. These measurements (along with in-plane extensional stiffnesses, basis weight, ZD compressibility, and caliper measurements) are conducted on a group of commercial tissue samples. Panel rankings for "bulk softness" and "surface softness" are also performed. Empirical correlations between the physical parameters and subjective softness rankings are examined. The three parameters which provide the best combined linear correlation to the softness rankings are the ultrasonic impedance, the mass specific ultrasonic attenuation, and the basis weight. Using these three quantities, the combined regression coefficients squared, r^2, are 0.884 for bulk softness and 0.785 for surface softness. When the facial tissues and bathroom tissues were analyzed separately, the r^2's are 0.997 and 0.970 for bulk softness and 0.971 and 0.896 for surface softness. Acoustic impedance is the most significant factor in the overall and facial tissue correlations, while specific attenuation is most significant when the bathroom tissues were analyzed alone.

Introduction

Softness is historically defined in terms of the subjective perceptions of a panel of human beings. It is basically a tactile perception, but panelists can also be influenced by such things as sample size, ply number, color, smell, and sound of crumpling (2-8). Softness, therefore, is an ill-defined, complex function of a multitude of physical and psychological interactions (3-5). Softness can be divided into bulk softness and surface softness (4,5). Bulk softness is normally judged by hand crumpling the tissues, while surface softness tests can be conducted by a light brushing of fingertips over the tissue surfaces (4,5).

The perception of softness is, of course, related to the physical properties of the tissue. Apparent density, basis weight, flexural rigidity, ZD compressibility, and surface smoothness all influence softness (9). These properties are closely related to the fundamental structures and the mechanical properties of fibers such as flexural rigidity of individual fibers, fiber length, the fiber bonding level and the distribution of the bonding inside the sheet. Flexural rigidity is the parameter most widely used in bulk softness correlations (4,8-11), while the magnitude and the distribution of surface irregularities appear to be more important in surface softness analysis (4,5).

There are several methods for performing the subjective panel assessments. These include magnitude estimation (3), multidimensional scaling (12), and pair-comparison techniques (3). Pair-comparison panel assessments, which are the simplest techniques, can be made by scaling, rating, or ranking the samples. The scaling and rating methods extract more information, but the panelists must be specially trained to assure repeatable results. The pair-comparison ranking method is used in this study.

Many people have studied the implications of tissue softness using subjective and instrumental approaches (3-22). It is generally agreed that the subjective assessments are necessarily tedious and time-consuming and are unduly influenced by human factors. For these reasons, numerous attempts have been made to develop instrumental techniques which, at least partially, supplant the ranking panels. Some of the methods [the Clark stiffness tester (13), the Brown method (14), the Peirce tester (15), and the torsion pendulum method (7)] are suitable for evaluating bulk softness. Others [the surface softness analyzer (5,6) and the Kato surface friction tester (16)] attempt to quantify surface softness. The Handle-O-Meter (17,18) is sensitive to a combination of surface and bulk properties. In spite of these worthy efforts, panel assessments remain the most commonly-used methods for tissue softness quality control.

The purpose of this paper is to introduce the use of ultrasound for measuring out-of-plane properties in tissue. In order to arouse interest by demonstrating a potential for practical application, the results are presented in terms of their correlations with panel softness rankings. Ultrasonic tests are rapid, nondestructive, and may have future application on-line. However, it is well understood that ultrasonic techniques (like the other instrumental approaches to softness) cannot reproduce or replace the panel tests. A more fundamental study is necessary to determine the effects of furnish and process variables on the propagation of ZD ultrasound through tissue, but, in the meantime, here are the softness correlations.

Experiment

As described in Table I, seven commercial bathroom tissues and seven commercial facial tissues were used for this study. From each of the 14 kinds of tissue

samples, eight single specimens were selected. The two-ply sheets were gently divided into single plies. Each sample was cut into a 4.5 x 8 inch rectangle for the panel testing. All testing was conducted in a room controlled at 50% R.H. and 73°F.

Table I here

The ultrasonic measurements were made using The Institute of Paper Chemistry's automated out-of-plane velocity tester (1). This is a computer-controlled apparatus which uses two specially developed, neoprene-faced, PVDF transducers to couple ultrasound into one surface of a paper board sample and detect it on the other face. The transducers are precisely aligned and mounted in a caliper gage (23). This allows simultaneous caliper and time-of-flight measurement at a repeatable time after contact of the neoprene face to the sample. A test sequence begins by placing a sample in the vertical gap between the two transducers. The computer (an IBM PC-AT® compatible) activates a motor that releases the top transducer, which becomes dead-weight loaded (50 kPa) to the lower one. After waiting a prescribed time for the neoprene to conform to the sample, one transducer is excited with a 1.5 MHz, single-cycle sine wave pulse. This produces a disturbance that propagates through the sample and into the other transducer. The resulting electrical signal is amplified, digitized at the rate of 100 MHz, and communicated to the computer. The computer calculates the cross-correlation function between this signal and one obtained during calibration from transit through a thin aluminum foil. The maximum in the cross-correlation function, along with the known transit time through the foil, allow the computer to determine the time-of-flight through the sample. This divided into the caliper (which is determined from the output of an

L.V.D.T.) is the time-of-flight velocity. The computer also performs a Fourier analysis of these signals, and it compares the foil and sample phases and amplitudes at each Fourier component.

Since paper strongly attenuates out-of-plane ultrasonic energy (especially at high frequency), it is difficult to generate pulses that are narrow compared to the ZD transit time through paper. This generally makes the apparatus inappropriate for testing low basis weight papers, as the transit time is less than the period of the pulse, and there is a danger of interference between multiple reflection at the sample-neoprene interfaces. For these reasons, the instrument was designed for operation on paperboard. However, it was later realized that if the loading pressure was lowered from 50 kPa to 20 kPa, meaningful measurements could be made on tissue. The ZD velocity of ultrasound in tissue is considerably lower than paper, and sufficiently long transit times are detected with a 20 kPa loading pressure.

The results of the ultrasonic time-of-flight measurements can be expressed in terms of several parameters. The velocity of sound (V_{ZD} = caliper/time-of-flight) is the most commonly used. However, the out-of-plane bulk elastic stiffness ($C_{33} = V_{ZD}^2$ multiplied by density) is also of interest. The ZD acoustic impedance of the sample, Z, is a third parameter. It equals the density multiplied by the velocity, which in terms of the measured quantities is simply basis weight divided by time-of-flight. This is a particularly appealing quantity, since it does not require a caliper measurement.

The amplitude results are presented in the form of an overall attenuation coefficient, A. In order to calculate A, the ratios of the amplitudes of the Fourier components through the foil signal to those through the sample signal

are calculated. These ratios are weighted according to the squared amplitude through the sample and averaged. Then, A is defined as 20 times the base ten logarithm of the average.

The amplitude ratios are influenced by reflections at the transducer-sample interfaces, by viscoelastic dissipation in the sample, and by scattering from the fibrous structure. Assuming that the coupling between surfaces is perfect, reflection losses alone would cause the ratio of sample signal to foil signal to be $4Z_NZ/(Z_N+Z)$, where Z_N is the acoustic impedance of the neoprene front-face. This is already a small number, since Z_N is much greater than Z. Perfect coupling means that the sample and neoprene move in unison at the interface. This is far from accurate at tissue-neoprene interfaces loaded to 20 kPa, and real interfacial losses are greater than $4Z_NZ/(Z_N+Z)$. The other two phenomena produce bulk losses which are dependent on the basis weight. Experiments performed at 20 kPa on liner board samples, with progressive amounts of surface grinding, demonstrate that there is little dependence of A on basis weight. This is taken as evidence that for tissue at 20 kPa interfacial effects dominate the A parameter.

The softness rankings were performed by a panel of two men and four women. Ratings for bulk softness (by hand crumpling) and surface softness (by fingertip feel) were obtained using a pair-comparison method. The panel results were conducted as follows. Each panelist compared each pair of samples in a random order. A positive 1 was tabulated for the softer sheet, and a negative 1 was tabulated for the harsher one. If the two sheets were judged equal, 0 was recorded for both. The numbers were totaled for each sheet. The softness ranking was then obtained by adding a constant, which gives the harshest sheet a ranking of 1, to each total.

Tensile load-elongation tests were also made. These were performed using an Instron tensile tester following TAPPI Standard Method T 404 om-87 with cross head speed of 1 inch/min. Extensional stiffnesses were calculated from the initial slope of the load-elongation curves, and the geometric mean of the MD and CD numbers was recorded. Young's moduli in the MD and CD were also calculated (using the caliper measured with soft platens at 20 kPa) and recorded.

The final physical parameter measured was the ZD compressibility. This is defined as one minus the ratio of the soft-platen caliper at 20 kPa divided by the soft-platen caliper at 9 kPa.

Results

The panel softness rankings are given in the form of a column graph in Fig. 1. The agreement between individual panelist values was good. When regression analysis was performed with the ranking of the individuals and the average ranking, the lowest correlation coefficient was 0.871. A slightly higher correlation coefficient was obtained for crumpling than fingertip feeling, indicating that the bulk softness is more repeatable. From Fig. 1, it is clear that there is a strong positive correlation between the bulk softness and surface softness rankings. Notice also that the lotion treated sample (no. 9) ranked first in the bulk and surface panel testing and that the highly embossed tissue (no. 1) ranked better in the bulk test than it did in the surface test.

Figure 1 here

To give the reader a feeling for the range of the ultrasonic, time-of-flight measurements, a bar graph of the impedance calculations is presented in Fig. 2. Included in the impedance testing were some other paper types: a fine

writing paper; a coated paper; a wax coated paper; a nonwoven rayon sheet; and three grades of linerboard. The additional samples provide a reference for the tissue impedances. By comparing Fig. 1 and 2, notice that softer tissues generally have lower impedances.

Figure 2 here

A bar graph is presented in Fig. 3 for the attenuation coefficients of the same samples. Since Z_N is larger than Z for all samples, interfacial reflection losses tend to increase with decreasing impedance, and some correlation between impedance and attenuation coefficients is expected. This is the case, but, by comparing Fig. 2 and 3, it will be noted that significant differences occur in the ordering of samples. It seems that the time-of-flight and amplitude measurements are contributing complementary information.

Table II is a list of the significance of the variance ratios (F-ratio) and correlation coefficients between softness rankings and individual physical properties. Notice that the ultrasonic parameters correlate better with softness than do the standard mechanical tests. It is particularly interesting that the high frequency ZD ultrasonic tests provide a much better correlation than the low frequency ZD compressibility tests, which are more directly related to the softness perception (9). The fact that there are good correlations between softness and a number of parameters which have some independent variation indicates that a multiple linear regression would be beneficial.

Table II here

In order to determine the physical tests that best account for the softness variations, a stepwise linear multiple regression analysis was conducted. Using a selection based on F-ratios, the combination of three parameters that gave the

best linear fit were chosen. Table III shows the results for the bulk softness analysis. Here, the favored quantities are listed in the left column, while the others, along with the appropriate statistical information, are in the right column. The three optimum quantities are the impedance, the mass specific attenuation, and the basis weight -- two ultrasonic parameters and a very basic mechanical property. The three combine to give an r^2 of 0.884 for bulk softness ranking, and 0.785 for surface softness ranking. Figures 4 and 5 are plots of the observed versus the predicted softnesses. Notice that points representing the embossed and lotion treated samples are relatively far from the line of one to one correspondence.

Table III and Figures 4 and 5 here

Table IV lists the regression parameters for bulk and surface softness and the three chosen parameters. Results are also given in Table IV for the regression analysis conducted separately on facial and bathroom tissues. When the two are treated separately, the squared correlation coefficients are 0.997 and 0.970 for bulk softness and 0.971 and 0.896 for surface softness. Notice, in Table IV, that the regression coefficients are quite different for facial and bathroom tissues. The facial tissues have a much larger coefficient for the impedance, and bathroom tissues have the larger specific attenuation coefficient. When multiple regression analyses were performed on the facial and bathroom tissues separately, the order of chosen parameters was Z, BW, A/BW for the facial tissues and A/BW, BW, Z for the bathroom tissues. It seems that A/BW plays a stronger role in bathroom tissues because of the greater surface effects, while Z is most important for creped facial tissues.

Table IV here

Conclusions

Out-of-plane ultrasonic time-of-flight and attenuation measurements can be applied to tissue grades. Using automated equipment developed at The Institute of Paper Chemistry, these tests are rapid, repeatable, and nondestructive. Over a range of commercially available samples, ultrasonic parameters correlate with subjective softness rankings. In fact, the ultrasonic tests are more highly correlated with softness than are the standard mechanical tests, conducted as part of this study. The use of a multiple linear regression with ultrasonic impedance (which is simply basis weight divided by time-of-flight), mass specific attenuation, and basis weight is demonstrated to be a simple and effective approach for predicting softness.

References

1. Habeger, C. C., Wink, W. A., and Van Zummeren, M. L., The Institute of Paper Chemistry Technical Paper Series No. 301, Aug., 1988.

2. Bates, J. D., Tappi 48(4): 63A-4A(1965).

3. Leporte, L. E., Project 2817, Report 2, The Institute of Paper Chemistry, March, 1970.

4. Hollmark, B. H., Tappi 66(2): 97-9(1983).

5. Hollmark, B. H., in "Handbook of Physical and Mechanical Testing of Paper and Paperboard", Marcel Dekker Inc., Vol. 1: 497-521(1984).

6. Hollmark, B. H., The Fundamental Properties of Paper Related to Its Use (Ed., F. M. Bolam), Technical Sec., BPBIF, p. 696, 1976.

7. Van Eperen, R. H., Hardacker, K. W., Wink, W. A., and Van den Akker, J. A., Project 2220, Report 5, The Institute of Paper Chemistry, Aug., 1962.

8. Van Eperen, R. H., Gander, J. W., and Wink, W. A., Project 2220, Report 7, The Institute of Paper Chemistry, Feb., 1967.

9. Lyne, L. M., Pulp Paper Can. p. 79-82, July, 1950.

10. Van Eperen, R. H. and Wink, W. A., Project 2220, Report 6, The Institute of Paper Chemistry, June, 1965.

11. Van Eperen, R. H., Gander, J. W., and Wink, W. A., Project 2220, Report 8, The Institute of Paper Chemistry, Jan., 1968.

12. Lyne, M. B., Whiteman, A. and Donderi, D. C., Pulp Paper Can. 3851(10): 43-50(1984).

13. Clark, J. d'A., Paper Trade J., TAPPI Sec., p. 169-172, March, 1935.

14. Brown, T. M., Paper Mill, p. 19-21 June, 1939.

15. Yang, C., Tappi 391(8): 146A-9A(1956).

16. A brochure of KES-SE Surface Friction Tester, Kato Tech Co., Kyoto, Japan 1988.

17. Wardwell, F. B., Tappi 48(4): 60A-1A(1965).

18. Lashof, T. W., Tappi 43(5): 175A-8A(1960).

19. Leporte, L. E., Project 2817, Report 1, The Institute of Paper Chemistry, Jan., 1970.

20. Leporte, L. E., Project 2817, Report 3, The Institute of Paper Chemistry, Jan., 1971.

21. Ray, J. E., Tappi 48(4): 57A-8A(1965).

22. Lyne, L. M., Pulp Paper Can. 51(7): 80-2(1950).

23. Hardacker, K. W., IPC Technical Paper Series No. 138, Jan., 1984.

I. Description of the tissue samples

Sample No.	Plies	Basis weight* kg/m^2	Type
1	1E	0.0248	B
2	1P	0.0292	B
3	2	0.0157	B
7	2P	0.0167	B
11	2	0.0218	B
12	2	0.0155	B
6	1	0.0419	B
4	2	0.0165	F
5	2	0.0155	F
8	2	0.0147	F
9	2L	0.0198	F
10	2	0.0143	F
13	2	0.0169	F
14	2	0.0145	F

E - highly embossed; L - lotion treated;
P - pattern printed.
B - Bathroom tissue; F - Facial tissue
* - Basis weight are all measured by a single ply.

II. Correlations between measured physical properties and both bulk and surface softness ranking

No.	Variables	Variance Ratio		Correlation Coefficient	
		Bulk Ranking	Surface Ranking	Bulk Ranking	Surface Ranking
1	Acoustic impedance	27.83	23.75	-0.836	-0.815
2	Mass specific attenuation coeff.	16.71	15.95	0.763	0.755
3	Basis weight	2.94	4.11	-0.444	-0.505
4	Tensile stiffness	5.54	5.92	-0.562	-0.575
5	Young's modulus	8.41	8.25	-0.642	-0.638
6	MD Young's modulus	8.09	7.86	-0.635	-0.629
7	CD Young's modulus	8.78	8.82	-0.650	-0.651
8	Out-of-Plane stiffness	13.06	14.45	-0.722	-0.739
9	Attenuation coeff.	4.75	2.52	0.532	0.417
10	Caliper	0.03	0.26	0.051	-0.144
11	Density	2.74	1.38	-0.431	-0.322
12	Time-of-flight	1.31	0.64	0.314	0.225
13	Out-of-plane velocity	1.98	2.88	-0.377	0.440
14	ZD compressibility	0.21	0.05	0.131	0.066

III. Bulk stiffness multiple regression analysis with stepwise selection of variables

$r^2 = 0.884$

Variables in Model		Coeff.	F-Remove	Variables Not in Model		P.Corr.	F-Enter
1.	Z	$-1.88\ m^2s/kg \times 10^{-4}$	10.06	4.	E_{mean}	0.480	2.70
2.	A/BW	$2.22\ m^2/kgdB \times 10^{-2}$	15.65	5.	Et	0.433	2.07
3.	BW	$6.66\ m^2/kg \times 10^2$	9.07	6.	E_{md}	0.534	3.60
				7.	E_{cd}	0.360	1.34
				8.	caliper	0.378	1.50
				9.	compressibility	0.053	0.03
				10.	C_{33}	0.361	1.35
				11.	time-of-flight	0.244	0.57

IV. Results of multiple regression analysis

		Regression Coefficient Z [$m^2s/kg \times 10^{-4}$]	A/BW [$m^2/kgdB \times 10^{-2}$]	BW [$m^2/kg \times 10^2$]	Constant	Correlation Coeff. of Multiple Regression (r^2)
Overall	Bulk	-1.88	2.22	6.66	-21.5	0.884
	Surface	-1.84	1.60	3.71	-6.1	0.785
Facial	Bulk	-4.42	0.12	5.94	30.5	0.997
	Surface	-4.12	-0.01	10.81	22.5	0.971
Bathroom	Bulk	-1.02	2.69	7.67	-36.5	0.970
	Surface	-0.93	1.97	4.37	-19.8	0.896

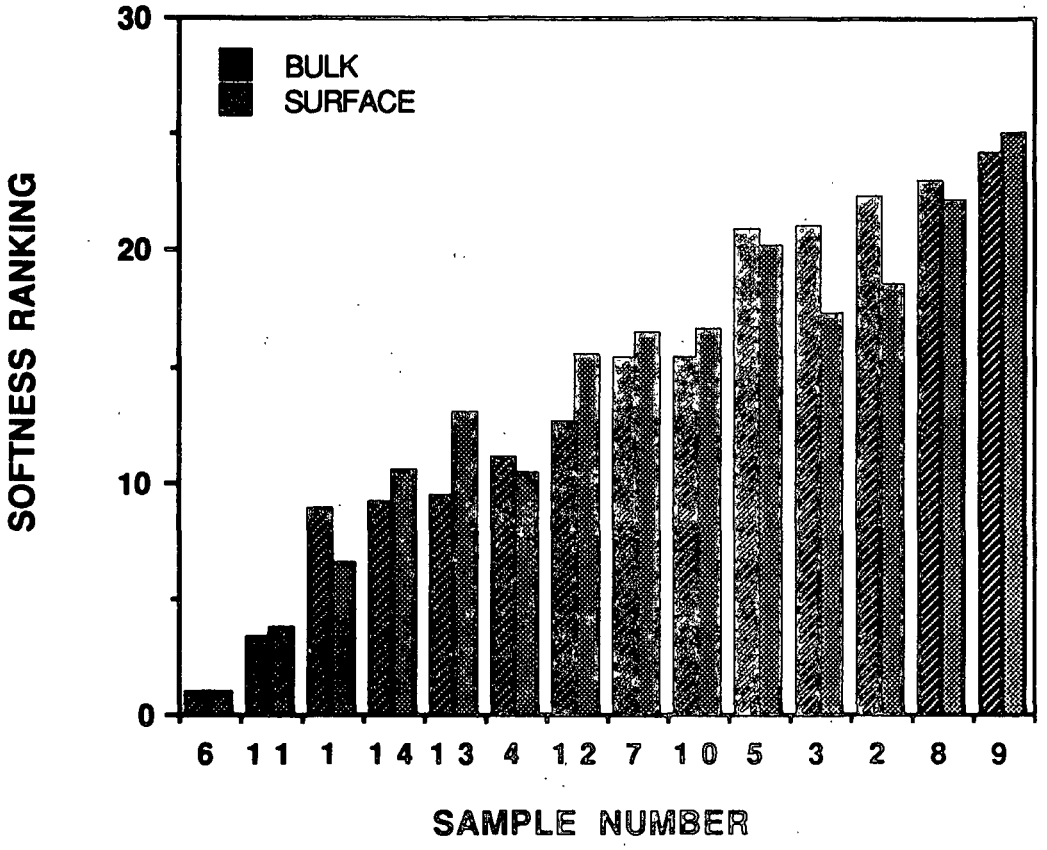

1. Softness rankings of commercial tissues.

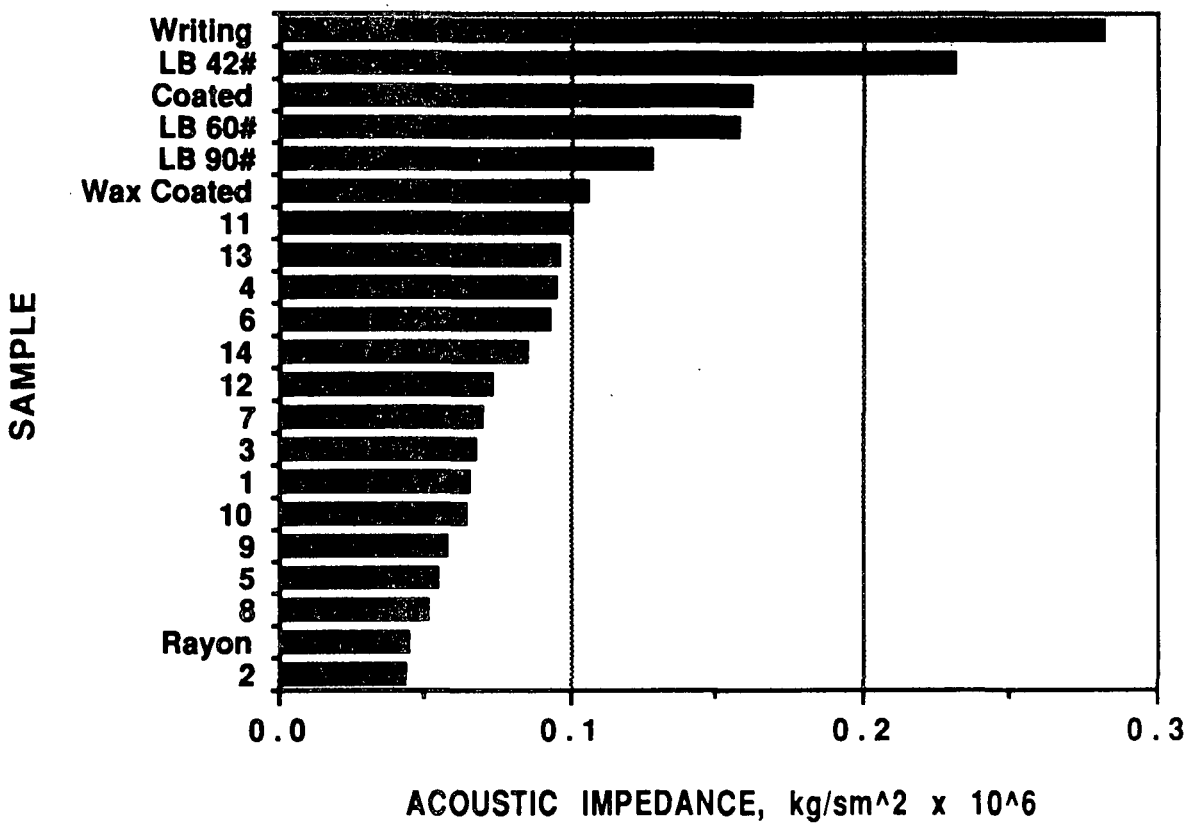

2. Acoustic impedance of regular papers and tissues.

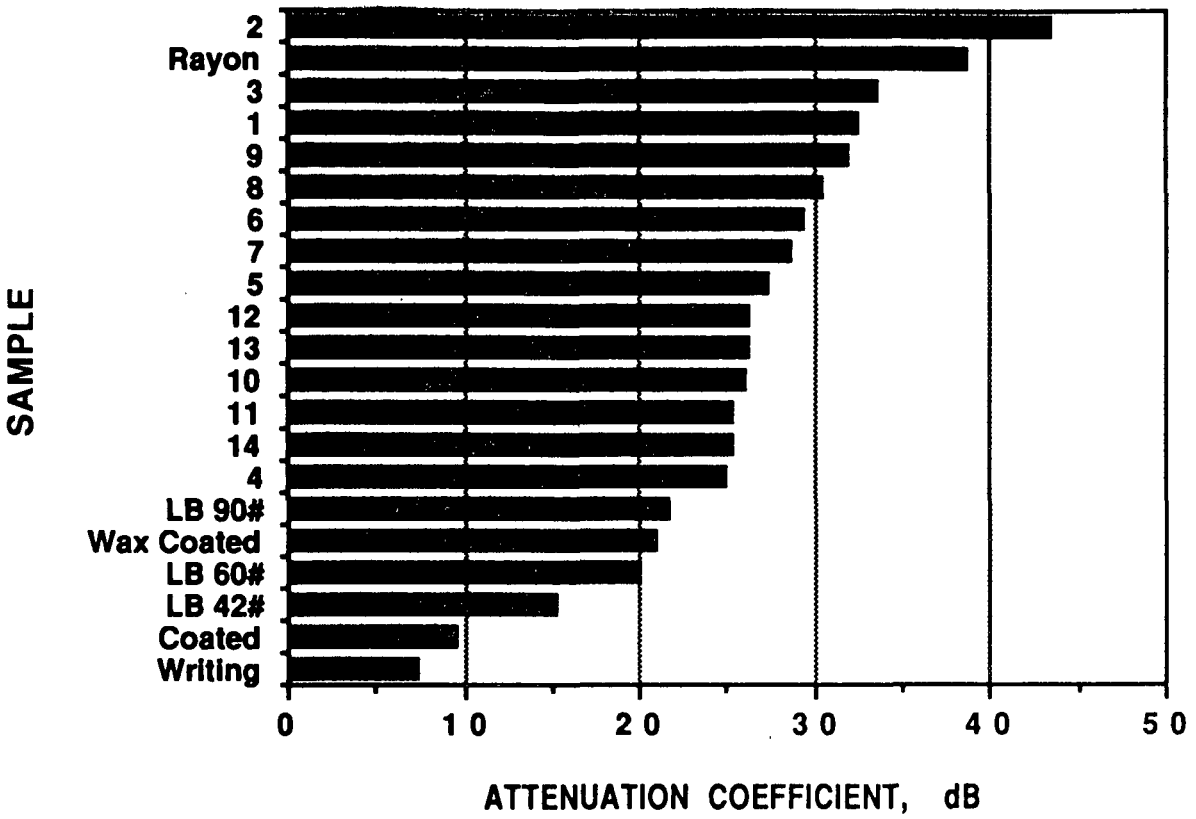

3. Attenuation coefficient of regular papers and tissues.

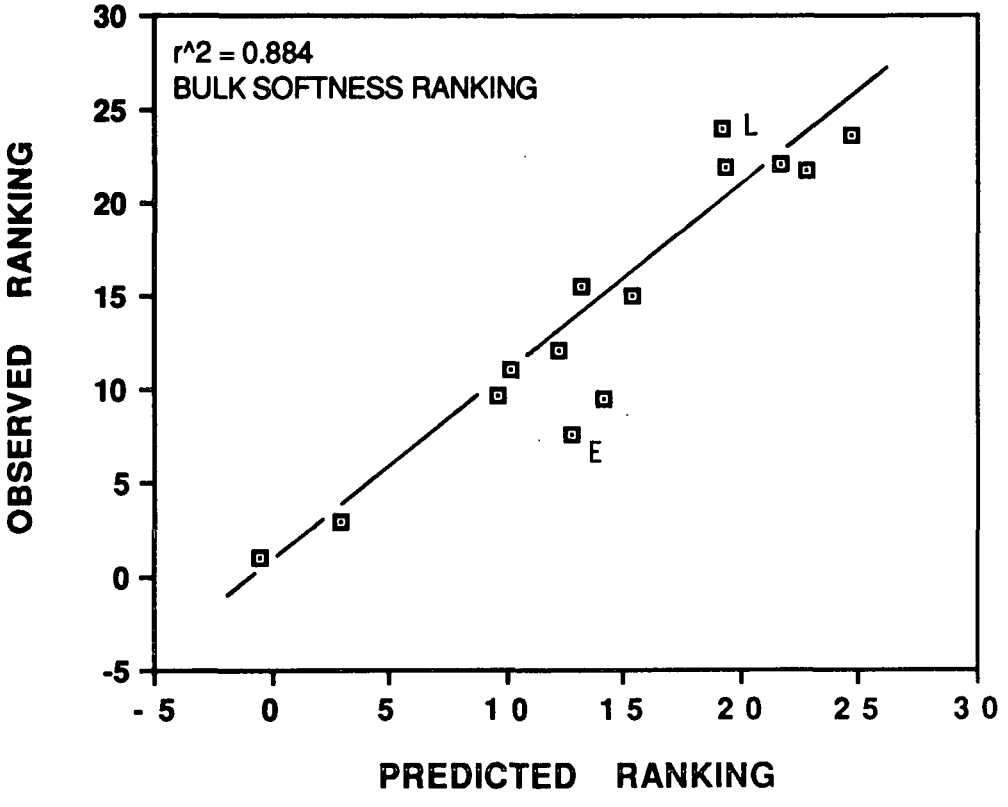

4. A plot of the predicted and measured bulk softness rankings.

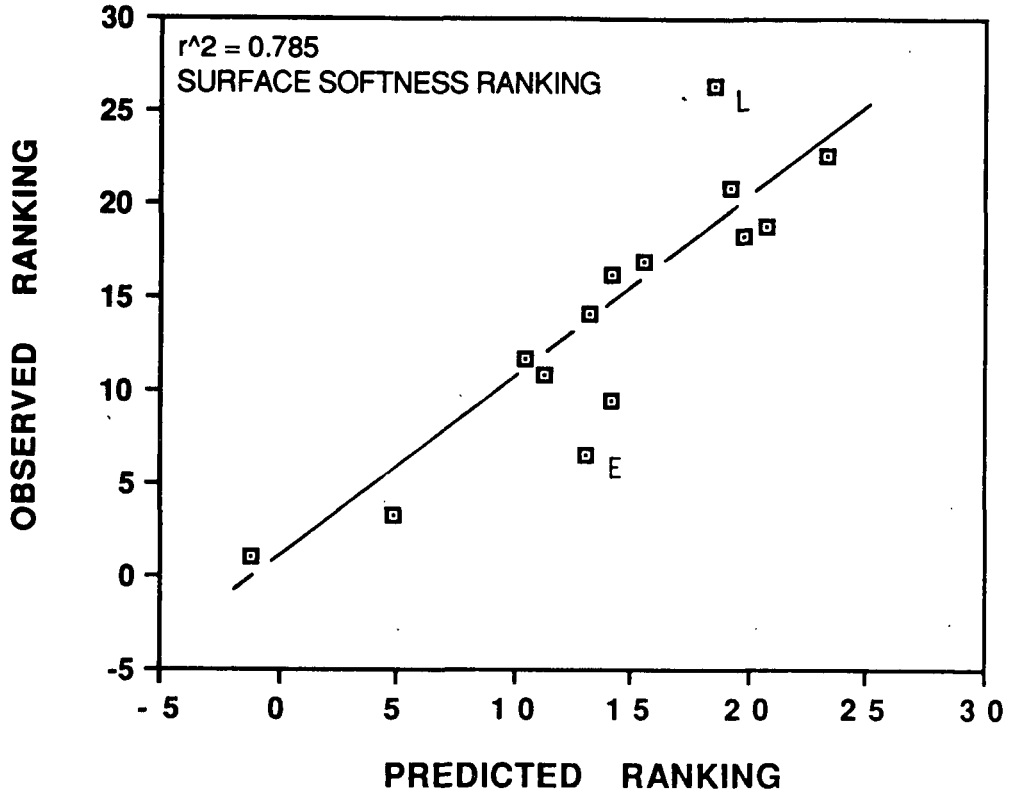

5. A plot of the predicted and measured surface softness rankings.

THE INSTITUTE OF PAPER CHEMISTRY

Appleton, Wisconsin

Status Report

to the

PAPER PROPERTIES AND USES

PROJECT ADVISORY COMMITTEE

Project 3646

FUNDAMENTALS OF PAPER SURFACE WETTABILITY

March 22-23, 1989

PROJECT SUMMARY

PROJECT NO. 3646: FUNDAMENTALS OF PAPER SURFACE WETTABILITY

PROJECT STAFF: F. Etzler/R. Stratton February 13, 1989

PROGRAM GOAL:

Develop an understanding of the interactions between liquids and the paper surface and their dependence on sheet properties.

PROJECT OBJECTIVE:

To improve our understanding of the influence of the structure and properties of paper and board on liquid absorption and penetration.

PROJECT RATIONALE, PREVIOUS ACTIVITY AND PLANNED ACTIVITY FOR FISCAL 1988-89 are on the project form that follows.

SUMMARY OF RESULTS LAST PERIOD: (March 1988 - October 1988)

(1) A survey of the literature concerning the state of water in cellulosic materials has been performed. It was found that many of the conclusions regarding the state of water adjacent to cellulosic surfaces reported in the paper, textile and forest products journals are probably in error as they conflict with the experimental observations made in model systems. The data can, however, be successfully reinterpreted so as to remove the apparent conflict. It is expected that these results will be published.

(2) Programs to be used for calculation of the the properties of Vornoi polyhedra have been written and tested on elementary systems. Calculations on simulated bulk water are presently in progress. These calculations will shed light on the structure of water near interfaces.

(3) Drop penetration times on kraft linerboard samples have been measured. The results indicate that the Washburn equation is useful in interpreting the drop penetration results. The Washburn equation suggests the the surface chemistry of the paper plays an important role in the printability of linerboards.

SUMMARY OF RESULTS THIS PERIOD: (October 1988 - March 1989)

(1) Initial calculations of Voronoi polyhedra for SPC/E water have been completed. These results suggest that the volume distribution of water molecules is bimodal. This calculation represents the first microscopic evidence supporting Roentegen's hypothesis (1982) suggesting that water exists in "bulky" and "dense" configurations. Furthermore, the calculations suggest that the model for vicinal water is microscopically robust.

(2) The Seteran DSC has been installed and initial calibration completed.

(3) Initial experiments on syntheses of chemically modified surfaces have been started.

(4) Experiments on kraft linerboard samples have shown that wettability is unrelated to lignin or benzene/alcohol extractives content.

PROJECT TITLE: Fundamentals of Paper Surface Wettability

PROJECT STAFF: F. Etzler/R. Stratton

PRIMARY AREA OF INDUSTRY NEED: Properties related to end uses

Date: 2/3/88
Budget: $75,000
Period Ends: 6/30/89
Project No.: 3646

PROGRAM AREA: Performance and Properties of Paper and Board

PROGRAM GOAL:

Develop an understanding of the interactions between liquids and the paper surface and their dependence on sheet properties.

PROJECT OBJECTIVE:

To improve our understanding of the influence of the structure and properties of paper and board on liquid absorption and penetration.

PROJECT RATIONALE:

Many converting and end uses of paper and board are associated with the application of a liquid to the surface. These include the processes of printing, coating, production of combined corrugated board, surface sizing, and exposure of the product in use to a variety of liquids. In many cases (printing, coating, etc.), the phenomena of interest occur at very short time scales, far removed from equilibrium. To improve these processes and to point the way for new products, it is important to understand the influence of the sheet structure and surface properties on the interactions with liquids.

RESULTS TO DATE:

New project.

PLANNED ACTIVITY FOR FY 1988-89:

Dr. Frank Etzler has recently joined the faculty and staff of IPC and will direct this project. A literature review will be conducted to ascertain the state of knowledge in the subject area. Based on the results of the review, a research program will be designed and implemented by Dr. Etzler to extend our knowledge in specific areas of liquid-sheet interactions.

Status Report

FUNDAMENTALS OF PAPER SURFACE WETTABILITY

Project 3646

The objective of this project is to understand the interaction of liquids with paper materials in a fundamental way. It appears important to assess the current state-of-the-art and suggest future research paths. The long-term objective of the project is to achieve a fundamental understanding of the role of liquid-paper interactions in paper making and in determining paper properties. The current work has been directed to: 1) reviewing the literature regarding the present understanding of water-cellulose interactions; 2) comparing results from model systems with that known for water-cellulose systems; 3) refining Etzler's statistical thermodynamic model for vicinal water, and 4) exploring the effect of paper surface chemistry on liquid penetration (particularly as related to flexographic printing).

The Structure of Water Near Surfaces

The nature of the liquid state, at the molecular level, continues to be a forefront topic of research in physics and chemistry. Despite the efforts of a considerable number of able researchers, much regarding the nature of the liquid state remains to be learned. Fortunately, much progress has been made in the last decade; this progress suggests that considerable advances will be made in the coming years. The nature of liquids near surfaces is, at present, receiving considerable attention by both experimentalists and theoreticians. A fundamental understanding of the processes important in determining the nature interfacial (vicinal) liquids has not been achieved. Indeed, considerable ignorance of the state of vicinal liquids exists. Many fundamental experiments are necessary in order for progress to be made.

As the state of water near cellulosic surfaces is of considerable importance to paper manufacture, it is important to discuss the current understanding of water near solid surfaces. A comparison of vicinal water in model substrates and in cellulosic substrates is also of importance.

It is known that the properties of water near surfaces are modified by propinquity to solid surfaces. To date the most comprehensive studies of interfacial water properties have been performed on water in silica and clays. Silicas and clays are nearly ideal substrates as water may be placed in pores of known size and geometry. It has been shown, for instance, that water in pores with a radii of 1-20 nm, exhibits a larger heat capacity, lower density and higher viscosity. [See for instance, Etzler, F.M., Langmuir, 4, 878 (1988).]

From studies of water in clays and from density measurements of water in silica gel, it appears that water is structurally modified to distances of 3-6 nm. It also appears that the structural modification decays in an approximately exponential manner with distance from the liquid-solid interface.

From work on a number of systems, it appears that the properties of vicinal water to a good first approximation are independent of the physicochemical details of the surface. For example, it has been shown that the heat capacity of water near a wide variety of surfaces is larger than the bulk. This aspect, however, deserves further attention.

The heat capacity of vicinal water appears to be a particularly useful quantity for understanding the nature of water in cellulosic systems; thus, this quantity is considered further. Stey (Ph.D. Thesis, University of Pittsburgh, 1967) has calculated the model independent distribution of single particle enthalpies for water and a number of other liquids. It was found that the

enthalpy distribution for water is unusual in that the distribution is bimodal. This type of distribution contrasts with the nearly Maxwell-Boltzmann type distributions found for more simple liquids. Some of Stey's results are seen in Fig. 1.

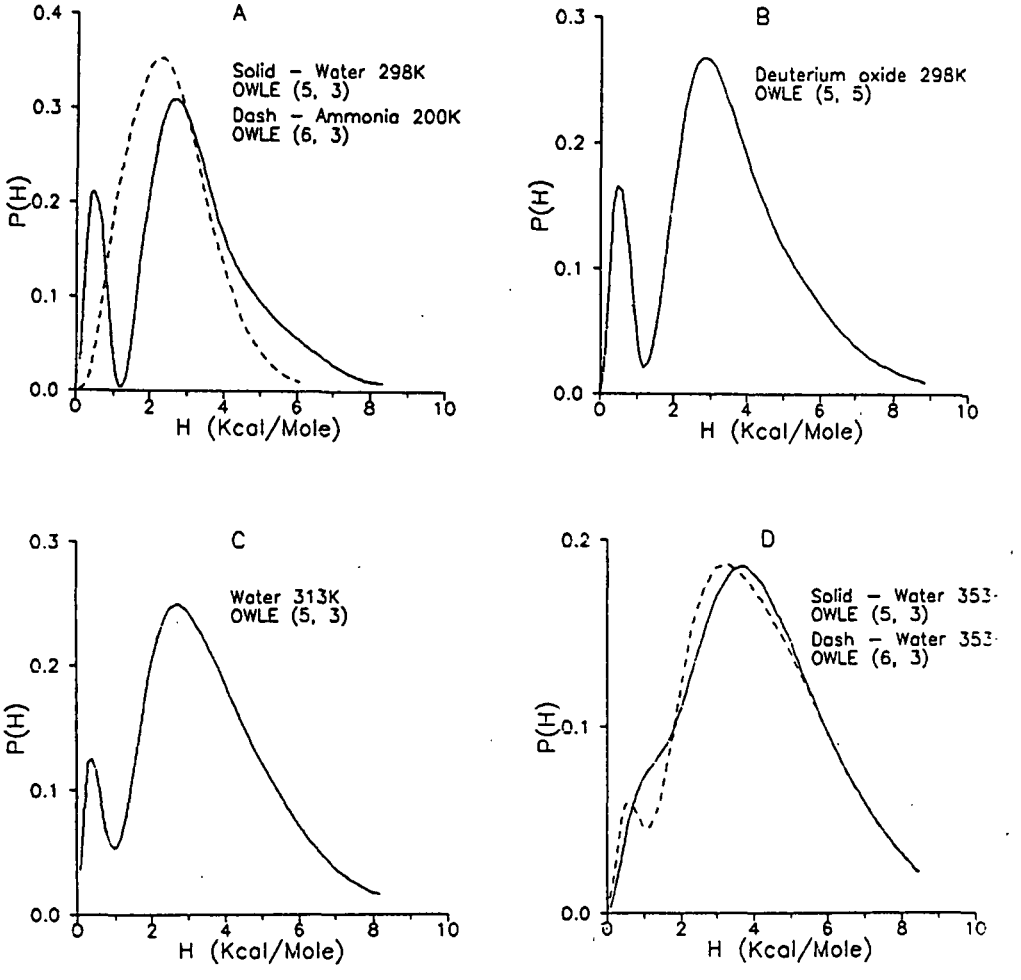

Figure 1. Stey's distribution functions. Probability, P(H), vs. enthalpy, H. (A) Water at 298 K and NH_3 at 200 K. (B) D_2O at 298 K. (C) H_2O at 313 K. (D) H_2O at 353 K.

It appears that the molecules represented by the low enthalpy peak in Stey's distribution are 4-hydrogen bonded water molecules while the high enthalpy peak represents molecules with 0,1,2 or 3 hydrogen bonds. The number of peaks in the distribution cannot be predicted from the number of hydrogen

bonding states. It is generally presumed that liquid state distributions would be nearly of the Maxwell-Boltzmann type.

The heat capacity, C_p, is related to the variance, σh^2, of single particle enthalpies, through the well-known statistical thermodynamic relation:

$$C_p = \sigma_h^2/RT^2 \qquad (1)$$

For a bimodally distributed liquid the heat capacity may be considered as follows:

$$C_p = x(1)C_p(1) + x(2)C_p(2) + x(1)x(2)\frac{\Delta H^2}{RT^2} \qquad (2)$$

Here x(1) refers to the fraction of 4-hydrogen bonded water molecules. If it is assumed that hydrogen bonding is non-cooperative then x(1) equals the fourth power of the hydrogen bond probability between adjacent water molecules. $C_p(1)$ it taken to be the heat capacity of ice and $C_p(2)$ is estimated using a variety of experimental data, including, for instance, the activation energy of the rotational correlation time. At 298K $C_p(2)$ = 16 cal/K mole. ΔH is the mean enthalpy of transfer between the two peaks in Stey's distribution or 2.55 kcal/mole. $C_p(1)$, $C_p(2)$ and ΔH for deuterium oxide may also be estimated. At 298 K approximately 6-10% of the water molecules in bulk water are 4 hydrogen bonded.

The heat capacity of water and deuterium oxide in silica pores of various diameters has been measured. The results are shown in Fig. 2. A significant feature of the graph is the presence of the maxima near 7 nm pore radius. Figure 3 shows C_p as a function of x(1) as calculated from Eqn. 2. Significantly, Fig. 3 suggests that vicinal water differs from the bulk in that hydrogen bond probability between adjacent molecules is enhanced by propinquity to

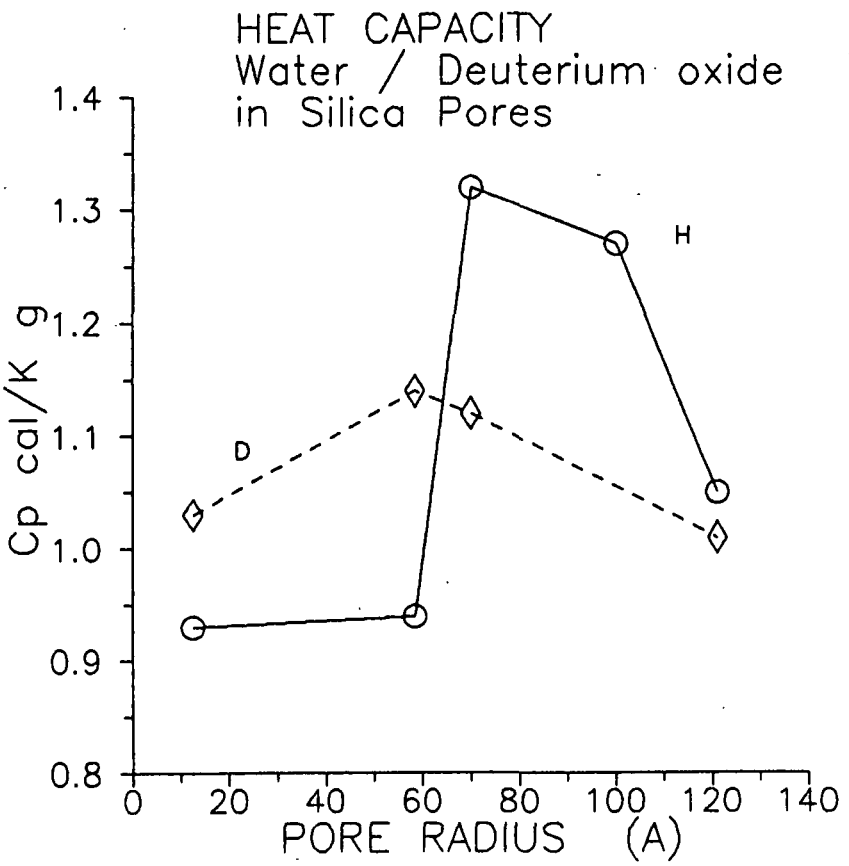

Figure 2. Heat capacities of water in silica pores as a function of pore radius at 298 K: o squares H_2O; diamonds, D_2O. Radius in Angstroms (10 A = 1 nm).

solid surfaces and that the magnitude of the experimentally observed maxima may be calculated on the basis of Stey's earlier calculations. Density measurements on water in silica pores are in agreement with the heat capacity measurements and suggest that hydrogen bond probability between adjacent water molecules decays to the bulk value in an approximately exponential manner. Significant structuring extends 3-6 nm. The density of water in 7 nm radius silica pores is 2-3% lower than the bulk at 298 K.

Water in Cellulosic Materials

Measurement of the properties of water associated with polymeric substances is difficult as it is often impossible to separate polymer properties

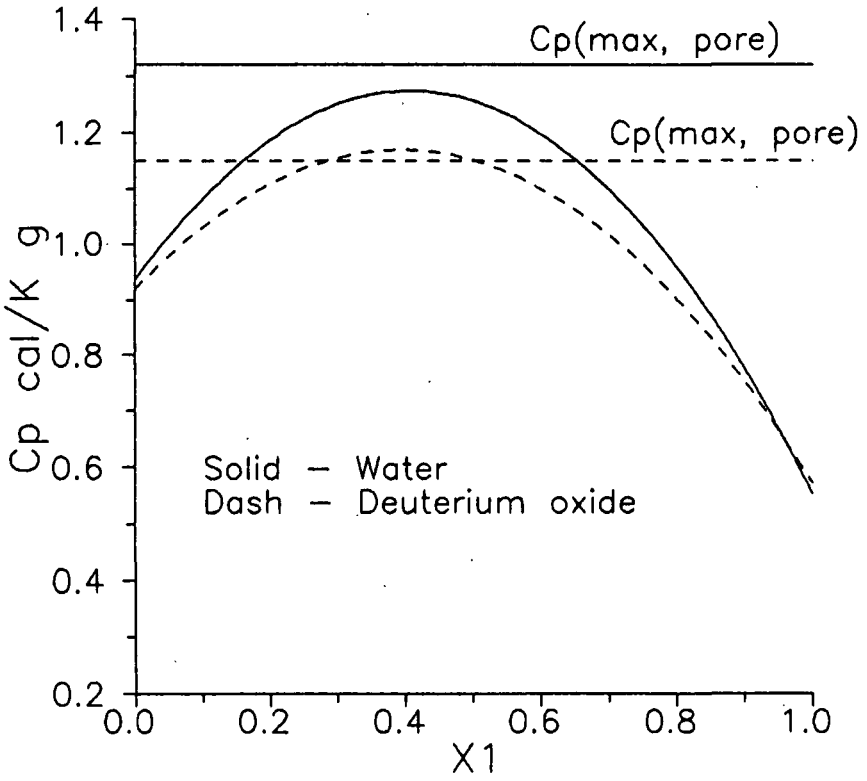

Figure 3. Hypothetical heat capacity of water and deuterium oxide as a function of x(1) at 298 K.

from water properties. Nonetheless several attempts have been made to measure the properties of water associated with cellulosic and other polymers. Early attempts to measure the density of water in wood suggested that the water had a density much larger than bulk water (Indeed much greater than the density of Ice VIII at 25 kbar!). Other measurements suggested that the expansivity of water was larger than the bulk. These results have been used to suggest that water associated with cellulosic materials is less structured than the bulk. This conclusion is in conflict with experimental evidence collected for water in clay and silica pores.

The use of thermal expansion as an indicator of vicinal water structure appears to be premature. It is not yet clear from statistical thermo-

dynamics what the effect of enhanced hydrogen bonding between water molecules in pores would have on the magnitude of the thermal expansion coefficient. Reexamination of the apparent specific volume data for liquids associated with wood collected earlier by Weatherwax and Tarkow suggests that the high apparent density of water is due primarily to the opening of new pores (This is also an earlier conclusion of Weatherwax and Tarkow.) and that the density of water in the pores is 0.98 or 2% lower than the bulk if ethanol is treated as an unmodified pore liquid (Pore density equal to bulk density). This assumption is consistent with density measurements of water and alcohols in silica pores.

Figure 4 shows the apparent heat capacity of water in two kinds of wood. Figure 5 shows the apparent heat capacity of water in gelatin and starch

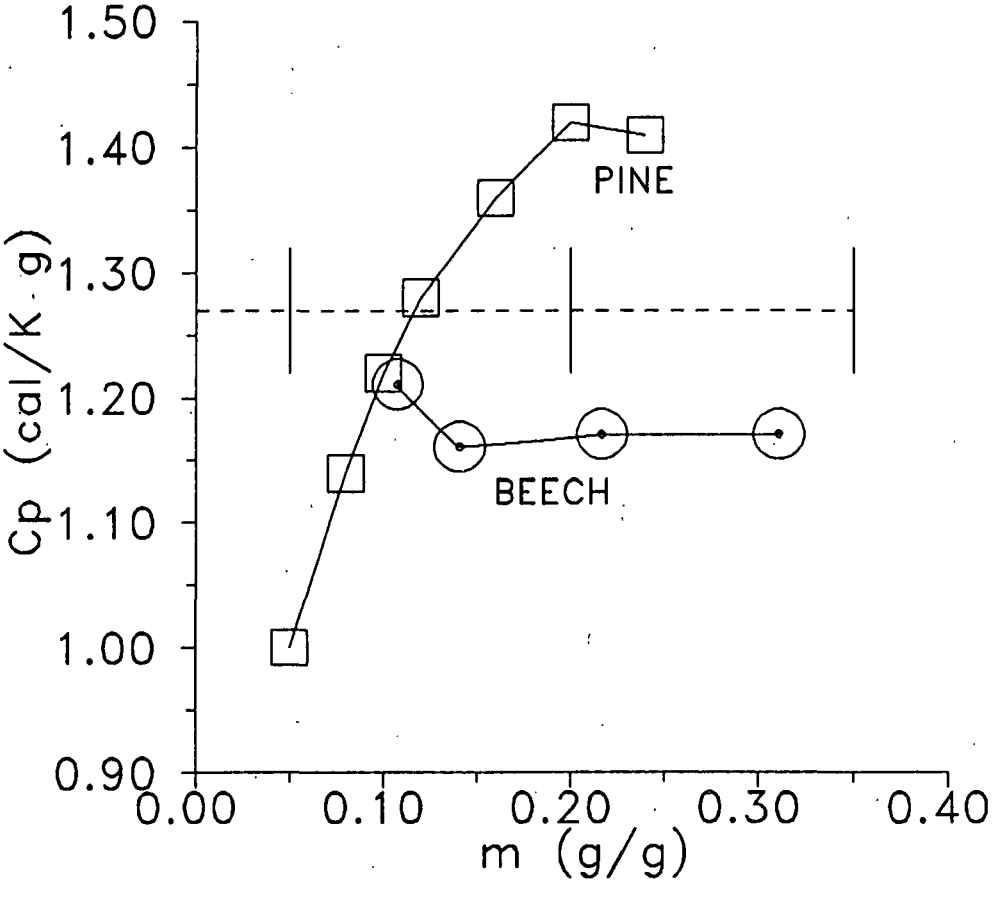

Figure 4. Apparent heat capacity of water in woods. Squares - pine; circles - beech; dashed line - maximum heat capacity as calculated from author's model.

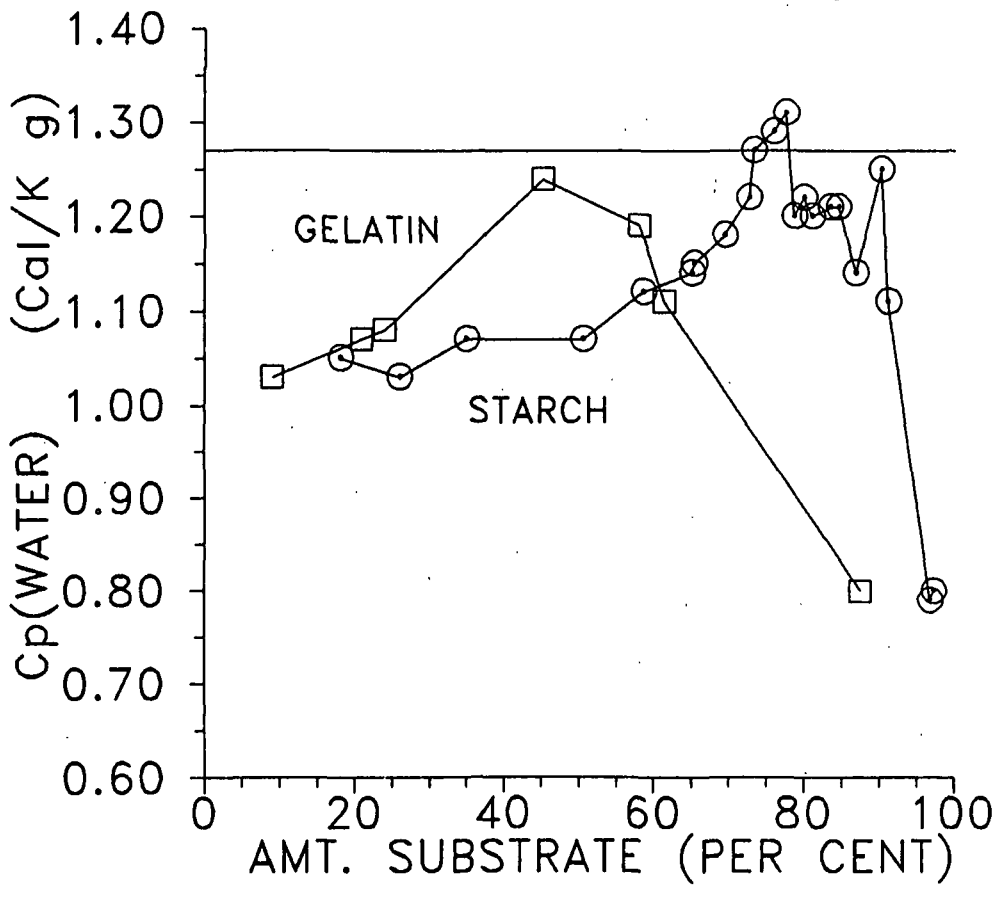

Figure 5. Apparent heat capacity of water versus per cent of substrate material in mixture. Squares - gelatin; circles - starch. Horizontal line - maximum heat capacity calculated from author's model.

suspensions. Both results are consistent with heat capacity measurements made in silica gel. In short, it appears that the properties of water associated with cellulosic materials and in silica gel are nearly identical and that water adjacent to either surface is more structured than the bulk.

VORONOI POLYHEDRA AND THE STRUCTURE OF VICINAL WATER

The results of Stey's calculations have been used successfully to correlate a number of thermodynamic properties of water near surfaces. Thus, it appears that Stey's calculated distribution can be used to make correct

predictions of and correlations between macroscopic properties. Stey's calculation also makes predictions regarding the microscopic or molecular behavior of water. From thermodynamics Enthalpy, $H = E + PV$, where P is pressure, V is volume and E is energy. The single particle enthalpies discussed by Stey can thus be broken into two parts - a volume part (Note: P = Constant) and an energy part. At present it is not clear whether energy or volume is the major factor in determining the form of Stey's enthalpy distribution.

It is not possible to calculate the distribution of molecular volumes in liquid via Stey's arguments without detailed knowledge of the intermolecular potential energy function. Knowledge of this function is not necessary, however, for the calculation of single particle enthalpies. It is possible, however, to estimate the distribution of molecular volumes from molecular dynamics calculations. The distribution of molecular volumes for liquid water is currently under investigation.

The volume of a molecule in a system can be regarded as the volume of the Voroni polyhedra whose center is the molecular center of mass. The Voroni polyhehra represents all points in space which are closer to the a given molecular center of mass (or other reference point) than to any other molecular center of mass. The temperature dependence of the isothermal compressibility for liquid water suggests that this distribution may have unusual features.

Our initial calculations concerning the properties of Voronoi polyhedra in computer-simulated water (SPC water) have been completed. Data on 30,000 polyhedra (3 sets of 10,000) have been collected. Figure 6 is a three-dimensional plot showing the probability of finding a polyhedron with a given number of faces and particular volume. The graph is unusual in a number of

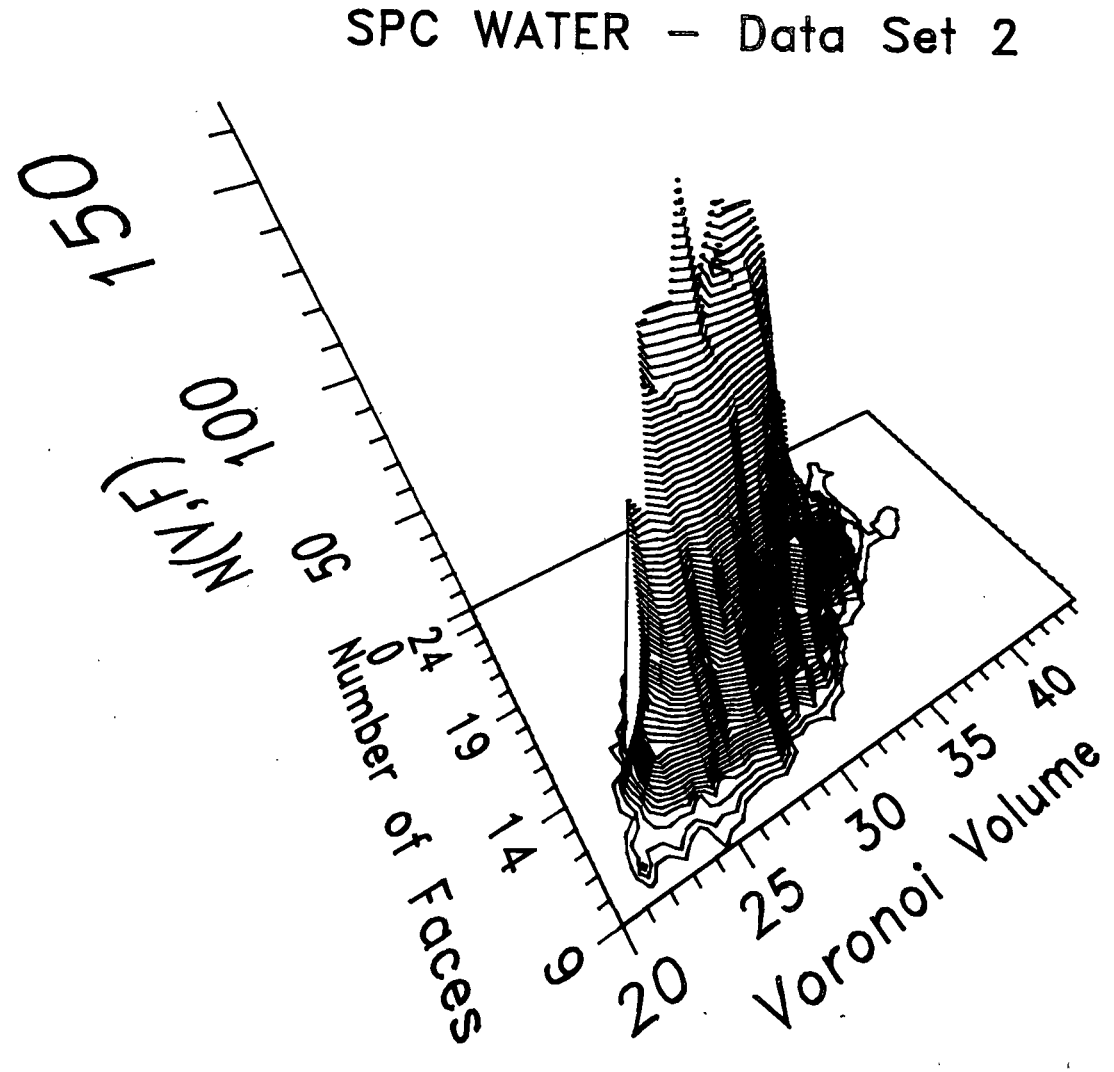

Figure 6. A three-dimensional plot showing the probability of finding a polyhedron with a given number of faces and particular volume.

respects when compared to simple liquids such as argon or Lennard-Jonesium. Two notable features are 1) the existence of two maxima in the distribution and 2) the high probability of 16-faced polyhedra. The abundance of 16-faced polyhedra is consistent with the existence of high-volume low-energy (i.e. "ice-like") states in liquid water. The number of faces can be increased by lengthening the first neighbor distances while leaving the second neighbor distances essentially

unchanged. The existence of two maxima give microscopic evidence which supports the earlier hypothesis of Roentgen and Frank suggesting simultaneous existance of "Bulky" and "Dense" regions in liquid water. The present calculation is important in that it presents the first microscopic evidence in support of Roentgen's hypothesis, first advanced nearly 100 years ago. It remains an important task to understand more clearly the interrelations between energy and volume which yield the bimodal enthalpy distribution calculated earlier by Stey.

It is hoped that this activity which is being cooperatively conducted between scientists at the University of North Carolina - Chapel Hill, AT&T Bell Laboratories, and IPC will attract some federal support.

Synthesis of Chemically Modified Surfaces

An understanding of the interaction of water with chemically modified surfaces will be undoubtedly important for achieving an understanding of a number of processes which occur at the liquid-paper surface.

Currently, the synthesis of silicas on which the normal surface hydroxyls are replaced by other chemical groups is underway. For instance it has been possible to place propyl amine groups on the surface. It is hoped that it will be possible to prepare chemically modified cellulosic surfaces.

Penetration of Liquids into Kraft Linerboard

The penetration of liquids into kraft linerboards has been measured. The penetration of liquids into a porous substrate is governed by the Washburn equation:

$$\frac{dh}{dt} = [r/4\gamma h]\gamma_{LV}\cos\theta \qquad (3)$$

Here η is the liquid viscosity, θ is the contact angle and γ_{LV} is the liquid vapor surface tension and (dh/dt) is rate of penetration. According to the Washburn equation if a surface is not wet (contact angle > 90°) then the rate of penetration is negative which in turn implies that the liquid will not penetrate. If surface is completely wet (contact angle = 0) then the Washburn equation becomes:

$$\frac{dh}{dt} = [r/4\eta h]\gamma_{LV} \qquad (4)$$

thus penetration is governed primarily by viscosity and not surface energetics when $\theta = 0$. Drop penetration time measurements made on a large number of kraft linerboard samples suggest that paper surface energy may play a significant role in flexographic printing. Linerboard samples which are not wet by typical inks have been found to exhibit poor print quality.

Recent experiments have shown the linerboard wettability is uncorrelated with lignin content and total benzene-alcohol extractives content. Investigations by Whitesides et al. have shown that the wettability of surfaces is strongly affected by the acidity of the surface groups. The effect of linerboard acidity on wettability is currently under investigation.

This work has also been supported by FKBG.

FUTURE WORK

It is planned to:

1. Begin calorimetric measurements of heat capacities of water in model substrates and in cellulosic materials in order to understand better the nature of pore water. Initial experiments are now in progress.

2. Continue to explore the distribution of Voronoi volumes in bulk water and to acquire and study data for simulations of water near solid surfaces.

3. Investigate possible experiments which may lead to an understanding of how the physico-chemical details of a surface may influence the structure of vicinal water.

4. Investigate the feasibility of making direct force measurements between cellulosic particles. It is hoped that such measurements would yield information regarding the effects of vicinal water on interparticle forces. (This may relate to paper strength etc.)

5. Investigate the suitability of thermoporometry for use on cellulosic materials. Thermoporometry is a technique for determining pore sizes for materials immersed in a liquid such as water. This technique will be important for detailed investigations of water in cellulosic materials. The analysis is performed on a differential scanning calorimeter.

THE INSTITUTE OF PAPER CHEMISTRY

Appleton, Wisconsin

Status Report

to the

PAPER PROPERTIES AND USES

PROJECT ADVISORY COMMITTEE

Project 3332/3613

ON-LINE MEASUREMENT OF PAPER MECHANICAL PROPERTIES

March 22-23, 1989

PROJECT SUMMARY

PROJECT NO. 3332: ON-LINE MEASUREMENT OF PAPER MECHANICAL PROPERTIES

PROJECT STAFF: C. C. Habeger, M. S. Hall February 13, 1989

PROGRAM GOAL: Develop ways to measure and control manufacturing processes.

PROJECT OBJECTIVE:

To develop the capability to measure elastic parameters on a moving paper web. Current emphasis is on out-of-plane measurements.

PROJECT RATIONALE, PREVIOUS ACTIVITY, AND PLANNED ACTIVITY FOR FISCAL 1988-89 are on the attached 1988-89 Project Form.

SUMMARY OF RESULTS LAST PERIOD: (March 1988 - October 1988)

(1) On-line operation of the IPC neoprene-faced wheel transducers has been simulated. The results are encouraging.

(2) A technique for molding neoprene to transducer front-faces is being developed.

(3) New out-of-plane wheel transducers, which we hope can withstand the temperature and wear experienced on-line, are under construction.

(4) Preliminary investigations of the fluid-filled wheels in an on-line measurement of out-of-plane properties have begun. These wheels should provide rugged, easily manufactured ZD velocity gage, once adequate temperature compensation is achieved.

(5) New, hopefully broader banded, immersion transducers have been designed for the fluid-filled wheels.

(6) The surface-hardened bimorph transducer have been tested for on-line, in-plane operation. With a better surface hardening procedure (now in development), they should provide significant advantages over the presently used extended, resonant transducers.

SUMMARY OF RESULTS THIS PERIOD: (October 1988 - March 1989)

(1) Software has been developed to handle the on-line fluid-filled wheel operation.

(2) Special homemade transducers have been constructed for the fluid-filled wheels.

(3) A procedure for sealing the immersion transducers has been adopted.

(4) Improvements in the mounting of the bender transducers have reduced their sensitivity to web tension.

(5) IPC, PVDF, on-line, wheels have been built. These should stand up to the rigors of operation on a moving web.

(6) The diamond coating, now in process, will hopefully lead to extremely wear-resistant bender transducers.

PROJECT TITLE: On-Line Measurement of Paper Mechanical Properties

DATE: 2/3/88
BUDGET: $50,000
PERIOD ENDS: 6/30/89
PROJECT NO.: 3332

PROJECT STAFF: M. Hall/C. Habeger

PRIMARY AREA OF INDUSTRY NEED: Properties related to end uses

PROGRAM AREA: On-Machine Uniformity -- Sensors and Control

PROGRAM GOAL:

Develop ways to make on-line measurement of product properties and process parameters in order to control manufacturing processes.

PROJECT OBJECTIVE:

To develop the capability to measure mechanical properties on a moving paper web. Current emphasis is on out-of-plane measurements. This project is concerned with the development of a laboratory instrument using wheel-type ultrasonic transducers. A related DOE-sponsored project is concerned with the development of sensors suitable for making measurements on the paper machine and subsequent control of the paper making process.

PROJECT RATIONALE:

The ability to measure mechanical properties on the paper machine will provide a means to continuously monitor product quality related to end-use performance. It also provides data needed to relate product characteristics to process variables for paper machine control.

RESULTS TO DATE:

A theory for the propagation of ultrasound in paper was developed. Devices were constructed to make on-machine measurement of the in-plane elastic parameters of paper and board. These devices were successfully tested in mill environments. Another version of the equipment for in-plane measurement was constructed and tested. This design used two receivers located at different distances from a transmitter, all mounted in a drum. Thus, this version was self-calibrating and could be used for on-machine measurement of light weight paper grades.

A cross correlation technique was implemented to improve the accuracy in measuring the transit time of an ultrasonic pulse for in-plane velocity measurements. Equipment was developed for measuring the effects of moisture and temperature on paper elastic properties. The feasibility of ZD signal transfer between rubber-faced, ceramic transducers at high paper speeds was demonstrated.

A high-frequency, low impedance, ultrasonic transducer was developed for out-of-plane measurements using a plastic (PVDF) piezoelectric material. This type of transducer is superior to commercial ceramic transducers for our applications.

The background information and experience provided by this project was the basis for obtaining a Department of Energy contract to develop "On-Machine Sensors to Measure Paper Mechanical Properties".

Wheel-type transducers for ZD measurement have been constructed with a continuous PVDF piezoelectric film around the circumference. Mechanical hardware and electronics have been assembled to provide a practical laboratory instrument for profiling caliper and ZD velocity by feeding a paper sample through the nip between two wheel-type transducers.

PLANNED ACTIVITY FOR FY 1988-89:

The laboratory instrument using wheel-type transducers to make ZD velocity and caliper measurements will be completed. Its performance and advantages relative to the present ZD laboratory instrument will be determined.

Most of the research activity in this program area will be performed under the closely related DOE project. The DOE project will be concerned primarily with transducer design selection and hardware design and construction to integrate in-plane and thickness-direction ultrasonic measurements into an assembly that can be used on a moving web and pilot paper machine.

STUDENT RELATED RESEARCH:

D. B. Macdonald, M.S.-1988.

Status Report

ON-LINE MEASUREMENT OF PAPER MECHANICAL PROPERTIES

Project 3332/3613

Work is continuing on new approaches for the on-line measurement of ultrasonic velocities in paper. We are attempting to develop out-of-plane, on-line capabilities using internally manufactured, neoprene-faced, PVDF wheel-transducers and using commercially available fluid-filled wheel-transducers. Our in-plane work is centered around the development of bender transducers, similar to those used in our laboratory testers, for on-line operation. The recent progress on each of these endeavors will be discussed separately below.

NEOPRENE FRONT-FACED, PVDF WHEEL-TRANSDUCERS

In the last PAC report, we presented the results of measurements made on narrow paper belts in the rotary out-of-plane laboratory instrument. These were encouraging, in that, with proper calibration, time-of-flight and caliper could be determined at the highest speed available (about 180 ft/min). The wheels in the laboratory instrument were not designed for the high speeds and temperatures routinely encountered on-line; therefore, our objective for this period was to design and build rugged wheel-transducers. As reported in the following paragraphs, these have been successfully constructed.

Compared to the wheel-transducers designed for laboratory use (see the appendix of the last PAC report), the new wheel design incorporates harder, more durable rubber front-faces, and higher temperature, more sensitive PVDF piezoelectric films. In addition, improvements were made in the uniformity of the piezoelectric element and the front-face. The wheel construction is essentially as before. A PVDF film is clamped between a Kynar core and an undersized Kynar ring, and an elastomer is applied to the contact surface of the Kynar

ring. Instead of the standard PVDF film, a new experimental PVDF copolymer film (VF2-VF3 from Pennwalt Corp.) was used. This provides for higher temperature performance, as the film can be subjected to 100°C without significant depolarization. It also has approximately a 50% higher coupling coefficient. Two wheels were fabricated, one with a stack of two 220 μm thick films, and one with a stack of four 110 μm films. The films were coupled with silicone grease, as before. However, rather than using flattened wires, inserted between the films and between the films and the Kynar, for electrical contact, lead wires were epoxied to tabs, extending out from the side of the film stack. This eliminated the nonuniformities created by the contacting wires and provided a more reliable, lower resistance coupling.

The major challenge in the development of the on-line transducers was the fabrication of the elastomer front-faces. The soft neoprene belts, used previously, would probably not withstand the frictional wear encountered on a moving web; therefore, we needed to develop a durable interface that efficiently coupled acoustic energy between the wheels and paper. We decided to use a hard polyurethane rubber, that is manufactured for repairing conveyor belts. Instead of bonding a belt to the Kynar wheel, the elastomer coupling was formed on the wheel. This produced a seamless tire that was not subjected to nonuniform stresses during application and bonding. Will Wink expended a good deal of effort and overcame a number of difficulties in perfecting a method for forming the polyurethane layer.

The polyurethane is a Devcon Flexane product. The molding fluid is produced by mixing Flexane 80 liquid resin with the Devcon curing agent. Flexane Flex-Add is also introduced into the mixture to achieve the desired durometer of the cured rubber. We targeted for a 50 durometer reading, which is

much harder than the 5-10 durometer neoprene used in the laboratory wheels. A cured elastomer that is well-bonded to the Kynar is achieved by first applying a thin layer of Devcon FL 20 Primer to a freshly machined Kynar surface. After a drying period of 5 minutes, a thin layer of Loctite Black Max adhesive is spread on top of the primer, and one minute later the molding fluid is poured onto the prepared surface.

The actual forming of the front-face, begins by combining the Flexane 80, the curing agent, and the Flex-Add in accordance with Devcon's instructions. The components are then mixed with a motor-driven stirrer inserted near the bottom of the mixing vessel. The mixture is next placed under vacuum to remove air bubbles. Infrared radiation is introduced to encourage the bubbles to break as they rise to the surface. In order to apply the molding fluid, the wheel, which is supported on an on-axis shaft, is placed between special sidewall fixtures and mounted in a lathe. As the lathe is slowly turned, the primer and Black Max layers are uniformly administered onto the Kynar rim. The viscous molding fluid is then carefully poured onto the turning rim. The sidewalls and a metering bar, fixed just out of contact with the sidewalls, maintain a fairly uniform thickness of the molding fluid. The lathe continues turning for 24 hours, allowing the polyurethane to cure. With the wheel still turning, the elastomer is trimmed to the width of the wheel with a surgical knife. The sidewalls are removed, and the elastomer surface is machined to a 1/8 inch thickness. This is done by mounting a grinding wheel attachment to the tool holder of the lathe. The grinding wheel automatically traverses the surface of the slowly turning transducer-wheel, gradually removing rubber layers. The result is a tough, uniform coupling layer that is free of air bubbles and is well-bonded to the transducer. Figure 1 is a photograph of the completed wheels.

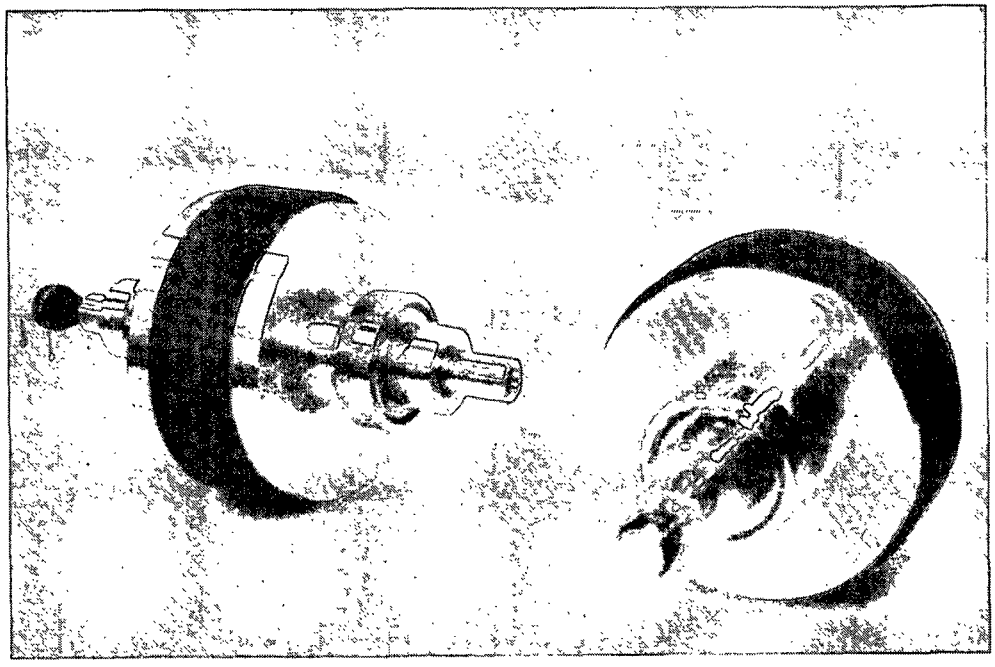

Figure 1. A photograph of the on-line, IPC, PVDF, wheel-transducer.

The on-line wheels proved to have approximately the same sensitivity as the laboratory wheels. They will be ready for testing on moving belts, when their mounting yokes are complete. These are under construction and should be ready in two weeks. The yokes will be bolted to a frame constructed for the fluid-filled wheels. The bottom yoke will be rigid, and the top one will be mounted on a plate attached to a linear bearing. The top wheel will be loaded with a spring-dashpot combination to the bottom wheel. This is similar to the mounting used for the rotary laboratory apparatus.

FLUID-FILLED WHEEL TRANSDUCERS

As discussed in the previous two PAC reports, we are using commercial, fluid-filled wheels to make out-of-plane velocity and caliper measurements in

paper. Here a transducer is mounted to a rigid frame which is encapsulated in a fluid-filled, rubber wheel. The paper sample runs in the nip between two such wheels, and the caliper and velocity of ZD ultrasound in the paper are calculated from a comparison of the arrival times of ultrasonic pulses between the two transducers with and without the sample present. We demonstrated that under static conditions it is possible to obtain reasonable values of velocity and caliper using this technique. We were also able to obtained good signal quality in dynamic tests.

In the last period, one of our tasks has been to write the software necessary to support the on-line operation of the fluid-filled wheels. This must first be capable of analyzing the reference signal obtained without a sample in-place. The three discrete pulses (described in earlier reports) must be detected and separated. Then they are individually gain controlled, signal averaged, and digitized. These references signals, along with the oscilloscope delay used in their digitization, are stored for comparison with the sample signals. After the wheels are applied to the web, the three sample pulses are consecutively digitized, averaged, and cross-correlated with the corresponding reference signals. As shown in Fig. 2, where measurements are simulated at a single point on a static sheet, the three time differences between the sample and reference pulses will be reported. Also, the time-of-flight through the sample (FF delay), the caliper (FF caliper), and the ZD ultrasonic velocity (FF velocity) in the sample will be calculated from the three time differences and printed out. Some work remains on improving the gain control and signal separation programs, but the software development is nearly complete.

Other work on this project concerns transducer development. The commercial transducers, originally used in the fluid-filled wheels, leaked fluid

THE INSTITUTE OF PAPER CHEMISTRY
Z-DIRECTION FLUID FILLED WHEELS RESULTS

OPERATOR: M. Kleiber
DATE: FEBRUARY 14, 1989
TIME: 11:50:08

PROJECT: 3613
SAMPLE : Liner Board #6469

SIGNALS AVERAGED = 32
TRANSDUCER DISTANCE = 0.1227(m)
FLUID VELOCITY = 1509.0(m/sec) @ 30.0°C

dT1 (µsec)	dT2 (µsec)	dT3 (µsec)	FF DELAY (µsec)	FF CALIPER (µm)	FF VELOCITY (m/sec)	TEMP (°C)	TIME
1.226	1.028	1.039	1.416	288	203	30.0	11:50:42
1.227	1.024	1.039	1.420	292	206	30.0	11:50:59
1.229	1.026	1.041	1.423	293	206	30.0	11:51:17
1.229	1.020	1.036	1.429	302	211	30.0	11:51:34
1.224	1.028	1.047	1.409	280	199	30.0	11:51:53
1.227	1.028	1.041	1.419	289	204	30.0	11:52:09
1.225	1.020	1.041	1.419	292	206	30.0	11:52:25
1.222	1.026	1.040	1.409	283	201	30.0	11:52:42
1.226	1.023	1.039	1.420	293	206	30.0	11:52:57
1.220	1.018	1.040	1.411	287	204	30.0	11:53:14
1.225	1.026	1.036	1.418	291	205	30.0	11:53:32
1.232	1.024	1.047	1.428	295	207	30.0	11:53:48
1.234	1.021	1.042	1.436	304	212	30.0	11:54:04
1.223	1.027	1.042	1.410	283	200	30.0	11:54:20
1.223	1.021	1.040	1.414	289	204	30.0	11:54:37
1.229	1.019	1.042	1.427	298	209	30.0	11:54:53
AVERAGES							
1.226	1.024	1.041	1.419	291	205	30.0	
STD DEV							
0.004	0.003	0.003	0.008	7	4	0.0	

Figure 2. Print-out format for on-line fluid-filled wheel operation.

after prolonged encapsulation in the wheels. This degraded and, in some cases, completely destroyed their sensitivity. After discussions with the manufacture, it was clear that the transducer were unacceptable for long-time immersion. We approached this problem in two ways. One was to build our own immersion transducers and the other was to find a way of sealing the commercial transducers.

Both of these remedies appear to have been successful. The IPC transducer is simply a PVDF film epoxied to one inch diameter Kynar rod. The housing is a hollow brass cylinder with a lip slightly less than one inch in diameter on one end. The PVDF film is epoxied to the lip of the brass rod. The backside of the film is wired to a connector, mounted to an end-plate at the opposite end of the brass housing. The interior of the housing is filled with potting compound through a small hole in the end-plate. The front-face is sealed from moisture penetration with a thin layer of two part epoxy, Epoxylite #8939-51. We are also using this material to seal the commercial transducers, and we are hopeful that it will prevent degradation. The IPC and commercial PVDF transducers provide roughly equivalent performance.

As mentioned in the last PAC report, temperature changes encountered in on-line operation appear to affect the three delay times. In order to monitor and correct for this, we have mounted a thermocouple in one of the wheels. This is part of a digital thermometer that is interfaced to the computer over an G.P.I.B. bus. This is now in operation and we will soon take a close look at the temperature influences.

At present, we are getting lower values for fluid-filled wheel calipers and velocities than previously reported. As soon as we understand and resolve these discrepancies, we will begin extensive dynamic testing.

ON-LINE BIMORPH TRANSDUCERS

There are two problems that require resolution before the use of bimorph transducers on-line will be practical. The first is to provide an durable contacting surface. The original plan of coating the transducer with Carborundum or alumina loaded epoxy has not proved to be satisfactory. We are

now hopeful that a commercial process, which uses a plasma discharge to apply a diamond wear-surface, will sufficiently protect the ceramic piezoelectric element. We have prepared a series of different elements and submitted them for diamond application. This has been a time consuming experience. We have waited three months to get our samples coated, but we are assured that they will soon be shipped.

The other major challenge is to mount the bimorphs in the wheel housing, so that the three transducer velocity measurement technique is not sensitive to web tension. We envisioned that insensitivity to tension would be a major advantage of a three transducer bimorph instrument. A custom-manufactured spring mounting fixture has been built to reduce variability in the loading of the transducers to the web. This has reduced tension sensitivity, compared to the results of the last PAC report. In fact, sometimes the velocity is stable over wide ranges of tension. However, performance, especially for the MD longitudinal mode, is not always sufficient. We will continue to investigate this situation until we have a uniformly satisfactory solution.

During the last period we also built a new wheel for mounting the bimorph transducers. This one is made of aluminum and is lighter than original steel wheel. It has the groove pattern that we feel is best for achieving strong, narrow acoustic pulses. It is more amenable to experimentation with different mounting procedures. It has transducer mountings arranged, so that measurements can be made at 45° from the principal axes. This we hope will allow us to make an on-line determination of the off-axis orientation of elastic stiffness.

THE INSTITUTE OF PAPER CHEMISTRY

Appleton, Wisconsin

Status Report

to the

PAPER PROPERTIES AND USES

PROJECT ADVISORY COMMITTEE

Project 3526

INTERNAL STRENGTH ENHANCEMENT

March 22-23, 1989

PROJECT SUMMARY

PROJECT NO. 3526: INTERNAL STRENGTH ENHANCEMENT

PROJECT STAFF: R. Stratton, K. Hardacker, D. Hollenberg February 13, 1988

PROGRAM GOAL: Bring new attributes to fiber based products

PROJECT OBJECTIVE:

To improve internal strength and moisture tolerance in paper and paperboard. The short term goals are to establish those parameters fundamental to inter-fiber and intra-fiber bonding in conventional and ultra high yield pulps and to control these parameters, if possible, by chemical or mechanical treatments.

PROJECT RATIONALE, PREVIOUS ACTIVITY, AND PLANNED ACTIVITY FOR FISCAL 1988-89 are on the attached 1988-89 Project Form.

SUMMARY OF RESULTS LAST PERIOD: (March 1988 - October 1988)

(1) The instrument to measure bond strength using sheets has been constructed. Improvements over previously used models include a frictionless air bearing in place of high precision ball bearings.

(2) Techniques have been developed to prepare sheets for use with this instrument, to operate the instrument, and to measure the scattering of the sheets before and after delamination.

(3) The effects of crosshead speed and basis weight on the bond strength determination have been characterized.

(4) A series of pulps with yields from 47 to 80% were produced by kraft cooking southern pine. These were beaten to several levels of freeness. A portion of each of the beaten pulps was then classified on the IPC Web Former. Some fines from each of the four yields were retained for later addition back to the pulp. This series of pulps will be used to study the effects of yield, refining, and fines on bond strength using the standard tests and the new instrument described above.

(5) Measurements on the whole pulps at the two lowest yields have been completed. The results are being analyzed.

(6) Adsorption experiments showed virtually all PAE is adsorbed on whole pulps at the usual dosages.

(7) Photomicrographs of ruptured tensile specimens treated at various levels with PAE/CMC revealed a shift in mode of failure from bond strength-controlled to fiber strength-controlled with increasing dosage.

(8) In preparation for joint experiments with Bill Whitsitt on the effect of strength additives on corrugated containers, several additive systems were screened for their effect on the wettability of the linerboard and medium. Two systems were found which should enhance the strength of the components, have little effect on glueability, and permit facile recycling of the corrugated board.

(9) A paper covering some of the work on this project presented at recent PAC meetings has been written and will be presented at the Paper Chemistry Symposium 1988 in Stockholm, September 27-29.

SUMMARY OF RESULTS THIS PERIOD: (October 1988 - March 1989)

(1) Measurements of the whole and the classified pulps at the four levels of yield have been completed. Analysis of this data is partially completed.

(2) Measurements on the effects of pulp fines are partially completed and the data are being analyzed.

(3) Extrapolation of results of scattering coefficient versus tensile strength, elongational modulus, or bond strength was used to evaluate the scattering at zero strength, i.e. the unbonded sheet. Only the modulus plot gave a single curve with small experimental scatter. From these results the relative bonded area (RBA) of the various sheets could be calculated.

(4) Several properties (bond strength, ultrasonic out-of-plane longitudinal velocity, tensile index, and TEA index) are directly proportional to the RBA.

(5) Two correlations (out-of-plane longitudinal velocity versus RBA and density versus RBA) clearly show a dependence on pulp yield. For the other properties the dependence on yield is weak or absent.

(6) Most of the property correlations showed a dependence on whether or not the stock was treated with a strength aid. However, correlations between bond strength and tensile index and between TEA index and tensile index are independent of treatment.

(7) The correlation between TEA index and tensile index is independent of pulp yield and strength aid treatment.

(8) At densities (or bond strengths) below a critical value, delamination of the sheet produced a negligible increase in scattering coefficient (increase in unbonded area). The critical value for the bond strength increases when a strength aid is used.

(9) The specific bond strength (or the ratio of the bond strength to the decrease in optical contact area) is a decreasing function of RBA or density.

(10) The status of a study by Industrial Research Fellow, Dave Hollenberg, "Influence of Retention Aid Addition on Sheet Properties," is included in this report.

PROJECT TITLE: Internal Strength Enhancement

Date: 2/3/88

PROJECT STAFF: R. Stratton/K. Hardacker

Budget: $200,000

PRIMARY AREA OF INDUSTRY NEED: Properties related to end use

Period Ends: 6/30/89

Project No.: 3526

PROGRAM AREA: Moisture tolerant, superior strength paper and board

PROGRAM GOAL: Bring new attributes to fiber based products

PROJECT OBJECTIVE:

To improve internal strength and moisture tolerance in paper and paperboard. The short term goals are to establish those fundamental parameters affecting inter-fiber and intra-fiber bonding in conventional and ultra high yield pulps and to control these parameters, if possible, by chemical or mechanical treatments.

PROJECT RATIONALE:

Major limitations of paper and board for many uses are low internal bond strength and poor moisture tolerance. Improved internal strength and enhanced moisture resistance would allow a number of present grades to be produced using less fiber and would also allow new end uses to be developed.

At present, commercial papers do not attain strength levels that realize the full potential of the wood fibers. Most paper mechanical properties are markedly degraded with increasing moisture content. We need to better understand the nature of fiber properties and fiber-to-fiber bonding and changes in them with increasing moisture content, if we are eventually to improve the moisture tolerance of paper.

RESULTS TO DATE:

The major areas of activity and results can be separated into two areas: handsheet studies of strength enhancement by chemicals; and bonding studies at the level of individual fibers. A number of polymers have been shown to be effective strength aids for a variety of chemical and mechanical pulps. In particular, combinations of a cationic polymer followed by an anionic polymer have provided substantial improvements in dry (50% RH), moist (92% RH), and wet tensile strength. Although fines contribute to strength, polymer adsorbed on long fiber is much more effective in improving strength than that adsorbed on fines. Use of a rigid SBR latex provided marked improvement in compressive strength measured at high humidity. Techniques have been developed to prepare, handle, and measure individual fiber/fiber bonds. Significant improvements in bond strength were achieved when strength aids were used. For unrefined fibers the location of bond failure (as observed in the scanning electron microscope) was shifted from between the fibers to within the fiber wall by the addition of a strength aid. Unrefined latewood fibers were found to produce stronger bonds than earlywood fibers. Comparison of lightly refined to heavily refined fibers

showed that the strength of individual bonds did not change with refining. When wet strength is not required, the use of strength aids acting by ionic interactions only allows the preparation of sheets that can be readily repulped.

Individual fiber bonds prepared using such additives were as strong as those made with covalently-bonding strength aids. Measurements of the loss of individual bond strength with increasing moisture content paralleled the similar losses in sheet strength and individual fiber axial strength.

PLANNED ACTIVITY FOR FY 1988-89:

An instrument will be constructed which will allow the measurement of bond strength using sheets.

This instrument will be used along with conventional tests to assess the effects of pulp yield, refining, type and level of addition of strength aid, and fines content on bonding. Correlations with in-plane and out-of-plane ultrasonic measurements will be sought to clarify the influence of bonding on these potentially on-line tests.

Methods will be developed to determine the relative contributions of fiber strength and bond strength when strength additives are employed.

Other additive systems will be explored as either internal or external treatments to enhance tensile and compressive strength under normal and high relative humidity conditions.

STUDENT RELATED RESEARCH:

J. E. Biasca, Ph.D.-1988; P. R. Proxmire, Ph.D.-1988; M. T. Goulet, Ph.D.-1989, C. O. Luettgen, Ph.D.-1990; C. E. Miller, Ph.D-1989; S. L. Molinarolo, Ph.D.-1988; D. L. Horstmann, M.S.-1989; M. W. Sachs, M.S.-1989; M. A. Friese, M.S.-1989.

Status Report

INTERNAL STRENGTH ENHANCEMENT

Project 3526

Introduction

During the past period we have been investigating the influence of pulp yield, refining, wet pressing, strength aid (PAE/CMC) treatment, and fines level on a variety of mechanical properties of handsheets. These properties include the conventional ones (tensile index, STFI compression strength, etc.) as well as in-plane and out-of-plane ultrasonic moduli, and the bond strength measured by delamination of the sheet[1,2]. Most of the measurements have been completed, and the results have been partially analyzed. This report will discuss the analysis to date. The latter should be understood to be preliminary with a great deal more data over a broader range of parameters to be forthcoming which will test the current conclusions. The results to be discussed here include those for the whole pulps at the two lowest yields.

Determination of the Relative Bonded Area (RBA)

This project is concerned with the effect of fiber-to-fiber bonding and with strength additives on sheet properties. An important parameter characterizing the amount of bonding in a given sheet is the relative bonded area. This is defined as

$$RBA = (A_u - A_s)/A_u \qquad (1)$$

where A_u and A_s are the total (external) area of the completely unbonded sheet and the unbonded area of the sample sheet, respectively. These areas have been measured by either gas adsorption or light scattering techniques but require a completely unbonded sheet to obtain A_u. To produce such a sheet with certainty is very difficult. Ingmanson and Thode[3] suggested an extrapolation to zero strength of a plot of scattering coefficient versus tensile strength for a

series of sheets formed with different amounts of wet pressing and from pulps with different degrees of refining. All the data should fall along a single curve and the curvature at low strength levels should be small enough so that an unambiguous extrapolation is possible. The scattering at zero strength corresponds to A_u and the scattering measured at finite strengths give the values for A_s. The implicit assumption that there is a direct proportionality between scattering and unbonded area in a sheet has been substantiated by Haselton and by others. The superposition of results for different freeness and different wet pressing amounts shown by Ingmanson and Thode[3] is not always found. The results of both Luner and coworkers[4] and of the present study produced a family of (nonsuperimposing) curves. Luner, Kärnä, and Donofrio[4] showed, however, that a plot of scattering versus tensile modulus did result in superposition of all the data. Moreover, the curvature of the plot was much less than that usually found when the tensile strength is used.

For our sheets linear correlations were found between scattering and tensile modulus. Results for different levels of refining and different amounts of wet pressing fell along the same line. Treated and untreated pulps gave slightly different intercepts suggesting a modification of the surface structure of the fibers by the strength aid. Increasing the pulp yield produced a lower scattering coefficient intercept (A_u). The values for A_u from the extrapolation were used to calculate the RBA of the various samples. The values ranged form 7 to 67%.

An attempt was also made to extract a value for A_u from plots of scattering coefficient against bond strength (from the delamination experiments). The experimental scatter in these plots prevented a satisfactory determination.

Correlations with RBA

Since the RBA is a direct measure of the amount of bonding in a sheet, it is of interest to determine which, if any, of the mechanical properties correlate directly with it. Both the bond strength (measured by the delamination technique) and the ultrasonic out-of-plane longitudinal velocity were found to be directly proportional to the RBA and to go to zero at zero RBA. Since these two mechanical properties should be related to Z-direction strength, it is reasonable to expect that they would be proportional to the amount of bonding in the sheet.

The tensile index and TEA index are also proportional to the RBA at low values of the RBA. Both are linear over the whole range of the RBA (0.07-0.5) for the untreated samples. For the samples treated with the strength aid, however, the linearity extends up to RBA's of 0.3 and 0.4 for the tensile index and TEA index, respectively. Beyond those RBA's the mechanical properties appear to have reached a plateau.

The density is also linearly correlated with RBA. The four curves (two pulp yields, treated and untreated) all extrapolate to approximately the same intercept (~ 0.25 g/cm^3) at zero RBA. The significance of this common intercept is not clear at present. At a given value of the RBA, the pulp with the higher yield has the higher density. Also, for both yields the untreated pulp has a higher density than does the treated one.

A final observation concerns the out-of-plane shear stiffness. The results to date suggest it may decrease with increasing RBA although the experimental scatter of the data preclude a definite conclusion.

Dependence of Properties on Pulp Yield

Since the pulp yield should affect the lateral compression of individual pulp fibers, it would be expected to also have an effect on bonding and properties dependent on bonding. Surprisingly, the following correlations were found to be independent of pulp yield:

Tensile index vs. RBA

TEA index vs. RBA

Et index vs. RBA

STFI index vs. RBA

Bond strength vs. RBA

On the other hand, plots of out-of-plane longitudinal velocity versus RBA and density versus RBA both clearly showed differing slopes depending on the pulp yield. Plots for the two yields of in-plane shear stiffness against tensile index also do not superimpose. Here, the differences are not so large as those for the two plots versus RBA just mentioned. It will be interesting to observe whether these findings will be substantiated as the data for the other two (still higher) yield pulps are analyzed.

Dependence of Properties on Treatment with a Strength Aid

It might be expected that the use of a strength aid would shift the sheet properties substantially and vitiate correlations between treated and untreated pulps. In general this is true. However, three correlations are independent of the strength aid treatment. These are:

Bond strength vs. tensile index

TEA index vs. tensile index

TEA index vs. bond strength

Apparently, these three mechanical properties are being affected to the same extent by the use of the strength aid.

Combined Dependence on Pulp Yield and Strength Aid Treatment

Only one correlation was found to be independent of both pulp yield and addition of strength aid. That is, all the data fell on one (linear) curve. This was a plot of TEA index against tensile index. Whether this correlation will continue with the data from the other pulp yields, and whether the correlation will yield to interpretation remains to be seen.

Correlations with the Change in Optical Contact Area (ΔC)

The increase in optical contact area (ΔC) when the sheet is delaminated is given by

$$\Delta C = LrG\Delta S \tag{2}$$

where ΔS is the difference in the light scattering coefficient measured before and after delamination, G is the grammage, and Lr is the test area. The magnitude of ΔC should be proportional to the loss in bonded area due to the delamination. A plot of ΔC against bond strength produces a linear correlation with a finite value of the latter parameter when ΔC is zero. The interpretation of this result is unclear. Skowronski and Bichard[1] define a specific bond strength (SBS) as the bond strength divided by the increase in optical contact area in the test area.

$$SBS = BS/(\Delta C/Lr) \tag{3}$$

where BS is the measured bond strength. Empirically, we find (above)

$$BS = BS_0 + a\Delta C \tag{4}$$

where BS_o is the intercept at ΔC equal to zero and a is the slope in the plot of BS against ΔC. Substituting equation (4) into (3) gives.

$$SBS = aLr + (BS_o)(Lr)/\Delta C \quad (5)$$

Equation (5) predicts that the specific bond strength (the amount of work necessary to create a unit increase in optical contact area) is not constant but decreases with increasing sheet strength (as measured by tensile strength, bond strength, density or RBA). Only when ΔC becomes very large does SBS approach a constant value (aLr). Further work will be necessary to understand this behavior.

Future Work

Additional work using the measurement of bond strength with the delamination test will examine the effects of

- oriented sheets (Formette and machine-made)
- calendering and supercalendering
- relative humidity (moisture)
- temperature
- additives between fibers
- changes in bonding outside the delamination zone
- additives in fiber walls
- mineral fillers

References

1. Skowronski, J., and Bichard, W., J. Pulp Paper Sci. 13(5), J165(1987).

2. Stratton, R. A., IPC Status Report, Project 3526, October, 1988.

3. Ingmanson, W. L., and Thode, E. F., Tappi 42(1), 83(1959).

4. Luner, P. Kärnä, A. E. V., and Donofrio, C. P., Tappi 44(6), 409(1961).

PROJECT TITLE

Influence of Retention Aid Addition on Sheet Properties

PROGRAM GOAL

To demonstrate whether addition of retention aid to the components of pulp will influence the level of retention and the sheet properties.

PROGRAM OBJECTIVES

To determine if differences in addition of retention aid to either the whole pulp or just to the fines fraction of a pulp will change the level of retention of the fines and whether the difference in point of addition will change the strength, bulk, porosity, or other properties of the sheet.

PROJECT RATIONALE

Controlling retention on paper machines impacts productivity. Retention aids are finding increased use, improving first-pass retention. Typically, these cationic polymers are added to the whole furnish prior to the headbox. With the advent of twin wire machines, particularly in tissue applications, the potential for reduced first-pass retention has increased. In the past it has been amply demonstrated that cationic polymers preferentially absorb onto the fines of a pulp. This results from a combination of surface charge and surface area. In many present papermaking operations, fines obtained from the safe-all are added back to the virgin furnish going to the headbox. Addition of retention aid to this relatively pure fines fraction should improve overall retention but might also change the properties of the subsequently formed sheet. The work reported here was done to determine whether addition of retention aid to the fines only might be a viable alternative to retention aid addition to the whole furnish.

RESULTS

A pulp was beaten to three different levels of freeness; 600 CSF, 400 CSF, and 200 CSF. These were then individually fractionated by running them over the web former. The respective long fiber and fines portions were retained. Britt Jar studies were done to assess retention where the simulated furnishes were made by mixing specific amounts of fines with long fiber. The efficiency of retention aid performance was assessed as a function of amount of cationic polymer added (1/2 lb and 1 lb/ton), as well as by addition of polymer to either the fines only or the long fiber only. Measurements of the electrophoretic mobility of the fines from the Britt Jar studies were made with the Zetasizer. Finally, handsheets were made from the simulated furnishes where cationic polymer was added only to the fines, or to the whole furnish.

Addition of retention aid to the different pulp components had little effect on the physical properties of handsheets. When added to the fines, the retention aid provides minor reductions in strength (3-7%) relative to addition of the retention aid to the whole pulp. Addition of polymer to the fines only also increased the density (2-7%).

The changes in electrophoretic mobility of the fines were generally consistent with expected trends. Addition of cationic polymer resulted in fines with less negative charge.

The Britt Jar studies of retention indicated that addition of polymer to the fines only was at least as efficient for retention as addition to the whole furnish and, in most instances, was more efficient. The least efficient application of the polymer was to the long fiber fraction. Retention, in this instance, was no better than retention with no polymer added.

THE INSTITUTE OF PAPER CHEMISTRY

Appleton, Wisconsin

Status Report

to the

PAPER PROPERTIES AND USES

PROJECT ADVISORY COMMITTEE

Project 3469

STRENGTH IMPROVEMENT AND FAILURE MECHANISMS

March 22-23, 1989

PROJECT SUMMARY

PROJECT NO. 3469: STRENGTH IMPROVEMENT AND FAILURE MECHANISMS

STAFF: J. Waterhouse February 13, 1989

PROGRAM GOAL:

Identify critical parameters which describe converting and end-use performance and promote improvements in cost/performance ratios.

PROJECT OBJECTIVE:

Establish practical methods for enhancing strength properties (especially compressive strength) during paper manufacture and to evaluate deformation behavior as it relates to sheet composition and structure.

PROJECT RATIONALE, PREVIOUS ACTIVITY and PLANNED ACTIVITY FOR FISCAL 1988-89 are on the attached 1988-89 Project Form.

SUMMARY OF RESULTS LAST PERIOD: (March 1989 - October 1988)

(1) Software development is in progress for the IPC Formation Tester: coefficient of variation, histograms, scan line, and image maps have been developed.

(2) The Promethium 147 beta source has been installed in the Formation Tester.

(3) The formation characteristics of a variety of paper samples have been measured including newsprint, tissue, fine paper, offset, and medium grades.

(4) Formette Handsheets containing different blends of NSSC pulp and synthetic fiber have been saturated with various binders and characterized.

(5) An out-of-plane biaxial device for measuring the deformation behavior of paper and board when subjected to combined stresses has been designed and fabricated.

(6) Student Related Work - Tom Bither has made fracture toughness and pore size distribution measurements as a function of wet pressing and refining.

(7) Student Related Work - Mikko Jokkio has completed a research study, "The Interaction of Base Paper and Coating on Coated Paper Properties".

SUMMARY OF RESULTS THIS PERIOD: (October 1988 - March 1989)

(1) Improvement of circuitry for light transmission and reflectance measurement on the IPC Formation Tester.

(2) Failure stress measurements have been made on the recently fabricated out-of-plane biaxial tester.

(3) A limited set of handsheets, containing blends of NSSC pulp and synthetic fiber, have been saturated and dried under restraint after saturation to determine the effects of such restraint on forming losses.

(4) Differences in "wire side" and "felt side" fiber orientation on lean angle (polar plot diagram) and curl have been investigated.

(5) Student Related Work - Robert Aloisi has investigated the effects of felt type and formation on surface roughness using a profilometer.

PROJECT TITLE: Strength Improvement and Failure Mechanisms

Date: 2/3/88
Budget: $100,000
Period Ends: 6/30/89
Project No.: 3469

PROJECT STAFF: J. Waterhouse

PRIMARY AREA OF INDUSTRY NEED: Properties related to end use

PROGRAM AREA: Improved converting processes and converted products

PROGRAM GOAL:

Identify critical parameters which describe converting and end-use performance and promote improvements in cost/performance ratios.

PROJECT OBJECTIVE:

To evaluate deformation behavior and its relationship to sheet composition and structure, and to establish practical methods for enhancing strength properties (especially compressive strength).

PROJECT RATIONALE:

Deformation and strength properties are important in predicting end use performance. An improved understanding of failure mechanisms and ways to improve certain strength properties are important to nearly all grades. The recognized importance of compressive strength in linerboard and corrugating medium to box performance provides impetus for research in this area. The approach is to meet the objectives through new papermaking strategies.

RESULTS TO DATE:

We have shown that compressive strength of paper is highly related to a product of in-plane and out-of-plane elastic stiffnesses. The relationship holds for commercial and experimental sheets made under a variety of conditions. This development suggests it will be possible to monitor compressive strength in the mill using ultrasonic techniques.

Compressive strength is enhanced by high densification, which increases bonding, and high fiber axial compressive stiffness. Thus compressive strength increases with refining and wet pressing. Within a practical range, higher CD compressive strength can be achieved by decreased fiber orientation, loose draws, and/or increased CD restraint during drying. Where limitations to increased refining and wet pressing exist, low levels of polymer addition could be used as a viable means to improve compressive strength. The effect of pulp type and additives on the stiffness-compressive strength correlation has been investigated. A technique involving small wood coupons and mini handsheets has been developed to measure the compressive strength potential of wood fibers.

We have developed a torsion mode technique for measuring the out-of-plane shear stress-strain behavior, and studied ZD shear straining on compressive strength. Internal stress variations have been determined in the thickness direction

together with the variation of in-plane and out-of-plane properties. Measurements of the relative losses in elastic and strength properties due to supercalendering have been made. A procedure for determining the residual stress distribution in paperboard has been developed using a layer removal method.

A formation tester with the capability of making light transmission and reflectance, and mass density measurements has been designed and fabricated.

Commercial and laboratory formation samples of fine, tissue, newsprint and medium papers have been obtained and extensively characterized.

PLANNED ACTIVITY FOR FY 1988-89.

Formation - Continue development of IPC formation tester and evolve a menu of formation related parameters. Determine how the relationship between optical and mass density is affected by certain papermaking variables.

Compressive Strength - Develop fiber and polymer reinforcement strategies to improve compressive strength and also minimize losses due to forming and conditioning.

Internal Stresses - Determine how internal stress distribution is affected by refining and wet pressing and certain drying strategies.

Combined Stresses - Explore techniques for measuring the deformation behavior of paper and board when subjected to combined out-of-plane stresses.

STUDENT RELATED RESEARCH

T. W. Bither, Ph.D.-1988; H. R. Cedergren, M.S.-1988; M. H. Jokio, Special Student-1988

Status Report

STRENGTH IMPROVEMENT AND FAILURE MECHANISMS

Project 3469

INTRODUCTION

Project 3469 "Strength Improvement and Failure Mechanisms" embraces the following areas: Compressive Strength Improvement, Formation Meaurements, Combined Stress Measurements and Internal Stresses in Paper and Board.

1. COMPRESSIVE STRENGTH IMPROVEMENT

Forming processes in converting can have an adverse effect on the strength properties of paper and board. A better understanding of these forming losses, and strategies to reduce them, should lead to a more effective utilization of the raw material and process improvements we have discussed in previous work. This understanding may further affect raw material selection and process requirements.

The forming of corrugating medium is one area where forming losses can have a significant impact on combined board compressive strength and flat crush. We have therefore been seeking ways to improve medium performance to reduce these losses. A complex stress situation is imposed on the medium during forming, however it is believed that the large bending strains and "calendering" of the medium are primarily responsible for the large losses in MD and CD compressive strength. Another strength requirement aspect of corrugating is flute fracture. It is suspected that the medium requirements to avoid flute fracture may, to some extent, be in conflict with those required to minimize forming losses. Therefore a compromise will ultimately have to be sought.

To better understand the forming process, and evolve a medium more tolerant of the forming process, we have been investigating various model

systems. Our attempts to evolve a medium more tolerant of the forming process have so far been based on incorporating high modulus fibers suitably positioned in the medium, and then activating them during the forming process. Activation might be achieved by the addition of a polymer or bicomponent fiber system which will go through its softening temperature during flute formation.

In our last progress report we investigated the behavior of several synthetic fiber/corrrugating medium and binder combinations shown in Tables 1 and 2.

Table 1. Fiber furnishes.

Fiber Series 1

1. NSSC pulp
2. NSSC/Kevlar "pulp" blends

Fiber Series 2

1. NSSC pulp
1. NSSC pulp/Kevlar staple blends
2. NSSC pulp/Kevlar "pulp" blends
3. NSSC pulp/1/4 in. glass fiber blends
4. NSSC pulp/1/8 in. glass fiber blends

Table 2. Binder series 1.

A. Carboxylated SBR	T_g = 42°C
B. Carboxylated SBR*	T_g = 42°C
C. Styrene latex	
D. Styrene latex	T_g = 105°C
E. SBR latex (99% styrene)	
F. SBR latex (85% styrene)	T_g = 54°C

*Plasticized version of A, T_g Glass Transition Temperature as supplied by manufacturer.

In summary we found, because of unrestrained drying (after polymer addition by saturation and before heat treatment), a large loss in in-plane elastic properties. Heat activation of the various binder systems was effective in increasing both in-plane and out-of-plane elastic properties. These increases were also reflected by significant improvements in compressive strength.

Specific compressive strength results after heat activation (3 mins at 125°C and 7 Kpa) for Fiber Series 1 and 2 are given in Tables 3 and 4. Also shown in parenthesis in Tables 3 and 4 is the percentage increase in compressive strength with respect to the water only saturated sheet for each fiber type. The average binder content for Fiber Series 1 and 2 is 10.9% and 8.37% respectively. This is mainly due to the fact that the Formette handsheets comprising Fiber Series 1 were wet pressed at a lower press load than Fiber Series 2, and therefore the saturant pick up was greater. Although there is a significant loss in compressive strength with synthetic fiber addition, the increase in compressive strength per % of binder added, is greater than the control sheets (100% NSSC) in most cases, as shown in Table 5 below.

Forming losses by corrugating have been investigated using the concora fluter. After characterization of the various fiber binder systems shown in Tables 3 and 4, 4 in. x 1/2 in. samples with no previous heat treatment were fluted at a mean temperature of 177°C. The approximate sample temperature during fluting was 166°C which had been previously measured using temperature sensitive crayons. After conditioning, STFI compressive strength measurements were made at four positions along the flute, i.e., leading flank, upper tip, trailing flank and lower tip. Flat crush measurement comprising first and

Table 3. Fiber Series 1, Mean Specific Compressive Strength Nm/g.

Furnish: Latex:	100% NSSC	8% Kevlar Pulp	8% 3-ply Kevlar Pulp	16% Kevlar Pulp	3-ply 16% Kevlar Pulp
A	25.9 (50.6)	21.7 (59.6)	20.8 (41.5)	19.7 (66.9)	21.3 (61.4)
B	23.8 (38.4)	20.7 (52.2)	21.7 (47.6)	19.6 (66.1)	20.5 (55.3)
C	22.7 (32.0)	19.7 (44.9)	19.3 (31.3)	19.2 (62.7)	18.9 (43.2)
D	22.2 (29.1)	18.2 (33.8)	18.2 (23.8)	16.1 (36.4)	18.9 (43.2)
E	22.4 (30.2)	- -	19.9 (35.4)	17.3 (46.6)	18.6 (40.9)
F	25.7 (49.4)	- -	21.8 (48.3)	19.5 (65.3)	20.7 (56.8)
H_2O	17.2 -	13.6 (-20.9)	14.7 (-14.5)	11.8 (-31.4)	13.2 (-23.3)

Note: The numbers in parenthesis are % increase or decrease in compressive strength with respect to the water saturated controls.

second peak loads were made on another set of samples using six flutes. (Note: the normal number of flutes is ten, but we have found that the flat crush load is proportional to the number of flutes.)

Table 6 shows the effect of wet pressing on tip and flank forming losses for the 100% NSSC control sheets. The tip values are averages of the upper and lower tip values, and the flank values are averages of the leading and

Table 4. Fiber Series 2, specific compressive strength, Nm/g.

Furnish:	100% NSSC	8% Kevlar Staple	8% 3-ply Kevlar Staple	8% Kevlar Pulp	8% 3-ply Kevlar Pulp	8% 1/4 in. Glass	8% 3-ply 1/4 in. Glass	8% 1/8 in. Glass	8% 3-ply 1/8 in. Glass
Latex:									
A	30.3 (22.2)	27.1 (30.9)	27.4 (42.0)	27.5 (29.7)	27.5 (32.2)	30.1 (37.4)	28.3 (33.5)	29.8 (41.2)	29.4 (42.7)
B	32.0 (29.0)	27.3 (31.9)	27.3 (41.5)	29.5 (39.2)	27.4 (31.7)	29.8 (36.1)	28.0 (32.1)	29.6 (40.3)	29.1 (41.3)
C	26.2 (5.6)	23.8 (15.0)	23.3 (20.7)	23.4 (10.4)	23.9 (14.9)	25.2 (15.1)	25.3 (19.3)	25.6 (21.3)	25.2 (22.3)
D	29.3 (18.1)	24.8 (19.8)	23.7 (22.8)	25.0 (17.9)	24.8 (19.2)	26.6 (21.5)	25.1 (18.4)	26.3 (24.6)	24.3 (18.0)
E	29.3 (18.1)	25.7 (24.2)	25.4 (31.6)	25.8 (21.7)	25.6 (23.1)	26.7 (21.9)	26.2 (23.6)	26.4 (25.1)	26.7 (29.6)
F	32.2 (29.8)	27.1 (30.9)	27.1 (40.4)	29.0 (36.8)	28.0 (34.6)	32.2 (47.0)	27.9 (31.6)	30.0 (42.2)	30.2 (46.6)
H_2O	24.8* -	20.7* (-16.5)	19.3 (-22.0)	21.2* (-14.5)	20.8* (-16.1)	21.9 (-11.7)	21.2 (-14.5)	21.1 (-14.9)	20.6 (-16.9)

*Estimated

Note: The numbers in parenthesis are % increase or decrease in compressive strength with respect to the water saturated controls.

Table 5. % Increase in compressive strength per % binder added.

Furnish:	100% NSSC	8% Kevlar Staple	8% Kevlar Pulp	16% Kevlar Pulp	8% 1/4 in. Glass	8% 1/8 in. Glass
Fiber Series 1	4.58	-	5.10	6.05	-	-
Fiber Series 2	3.50	3.64	4.29	-	5.0	5.18

Table 6. Average tip and flank forming losses for Binder Series 1 for 100% NSSC at two levels of wet pressing.

	Low W.P. = 0.540 g/cm^3		High W.P = 0.738 g/cm^3	
	t	f	t	f
Binder	%	%	%	%
A	46	34	35	16
B	43	32	35	16
C	40	34	35	6
D	40	35	27	12
E	47	32	34	16
F	46	28	34	12

t: tip
f: flank

trailing flank values. The main effect is a significant reduction of both tip and flank forming losses as the medium is densified by wet pressing, confirming the earlier findings of W. Whitsitt. The losses in general are not greatly affected by binder type. The effect of synthetic fiber addition (i.e., Fiber Series 2) on forming losses is given in Tables 7 and 8.

The forming losses shown in Tables 6, 7, and 8 are with respect to flat samples which have been heat treated (i.e., 3 mins at 125°C, and 7 kPa). Generally the tip forming losses shown in Table 7 for the 3-ply structures are lower than the uniform sheets. We also note that the tip forming losses for the glass containing sheets are considerably higher than the 100% NSSC controls. Part of this higher forming loss may be due to the greater MD orientation which is found when glass fibers are incorporated into the furnish. The glass containing sheets also have a higher flank loss as shown in Table 8. Also surprising is that the forming losses for water saturated only sheets have such a high forming loss.

Table 7. Average tip forming losses for Binder Series 1 and Fiber Series 2.

	100% NSSC %	8% Kevlar Staple %	8% Kevlar Staple 3-ply %	8% Kevlar Pulp %	8% Kevlar Pulp 3-ply %	8% 1/4 in. Glass %	8% 1/4 in. Glass 3-ply %	8% 1/8 in. Glass %	8% 1/8 in. Glass 3-ply %
Binder	t	t	t	t	t	t	t	t	t
A	35	31	28	32	32	46	38	47	44
B	35	34	30	34	27	44	41	48	43
C	35	29	29	38	29	50	39	49	37
D	27	38	27	28	21	44	34	39	31
E	34	42	34	36	30	39	40	40	36
F	34	36	29	38	27	44	37	41	46
H_2O	-	-	32	-	-	52	36	50	45

Table 8. Average flank forming losses for Binder Series 1 and Fiber Series 2.

	100% NSSC %	8% Kevlar Staple %	8% Kevlar Staple 3-ply %	8% Kevlar Pulp %	8% Kevlar Pulp 3-ply %	8% 1/4 in. Glass %	8% 1/4 in. Glass 3-ply %	8% 1/8 in. Glass %	8% 1/8 in. Glass 3-ply %
Binder	f	f	f	f	f	f	f	f	f
A	16	11	14	15	16	24	23	28	25
B	16	19	17	19	12	18	24	25	23
C	6	16	18	17	14	21	24	18	20
D	12	21	18	19	15	26	24	26	24
E	16	21	14	21	18	18	25	18	15
F	12	20	12	19	15	20	18	20	23
H_2O	-	-	13	-	-	26	17	22	17

Despite the high percentage forming losses in the tip and flank regions of the glass containing sheets, the flat crush values as shown in Table 9 are marginally better than the controls for binders A, B, and F. In this instance the film forming latices give a better performance than the 100% styrene binders C, D, and E.

The effects of drying restraint after saturation on forming losses have recently been investigated for a limited sample set.

Table 9. Flat crush for Binder Series 1 and Fiber Series 2 (lbs/6 flutes).

Binder	100% NSSC	8% Kevlar Staple	8% Kevlar Staple 3-ply	8% Kevlar Pulp	8% Kevlar Pulp 3-ply	8% 1/4 in. Glass	8% 1/4 in. Glass 3-ply	8% 1/8 in. Glass	8% 1/8 in. Glass 3-ply
A	44	33	32	40	39	45	40	47	42
B	45	27	29	40	34	46	42	45	43
C	44	22	23	34	27	30	30	35	31
D	43	22	24	29	28	32	31	31	33
E	42	27	25	33	31	39	34	37	36
F	42	32	32	46	41	46	42	48	41
H_2O	-	-	20	-	-	25	26	-	29

2. FORMATION

The recently fabricated IPC Formation Tester is shown in Fig. 1. It has the capability of making light transmission and reflectance measurements in the wavelength range of 400 - 700 nm, as well as beta particle absorption measurements. An aperture of 1 mm x 1 mm is used for both light transmission

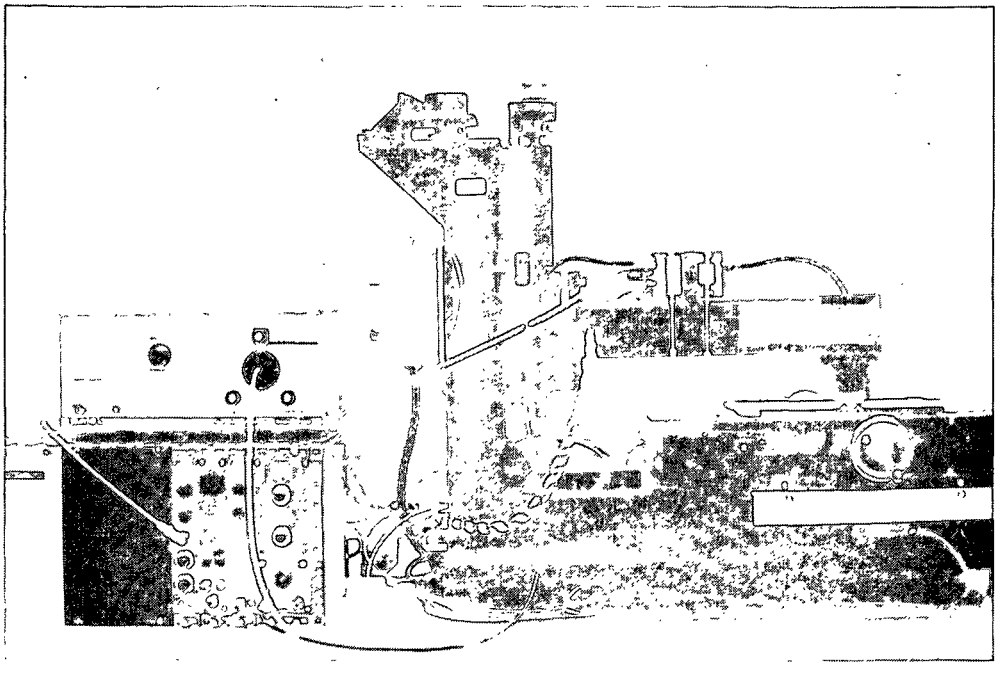

Figure 1. General view of IPC formation tester.

and beta measurements. The respective circuits are shown in Fig. 2. Formation samples of various sizes can be measured and are held in place with magnetic strips.

With the skilled assistance of Keith Hardacker, the circuitry for mass density measurements has been improved and installed together with the promethium 147 source. The circuitry seems to be working in a satisfactory manner although the particle count level is not as high as anticipated. Work is in progress to identify the source of the problem.

Significant noise level reductions have been made in both the transmitted and reflected light photodiode circuitry by Keith Hardacker. A comparison of formation measurements made on a series of commercial samples using both the single and bifurcated light guide are shown in Fig. 3.

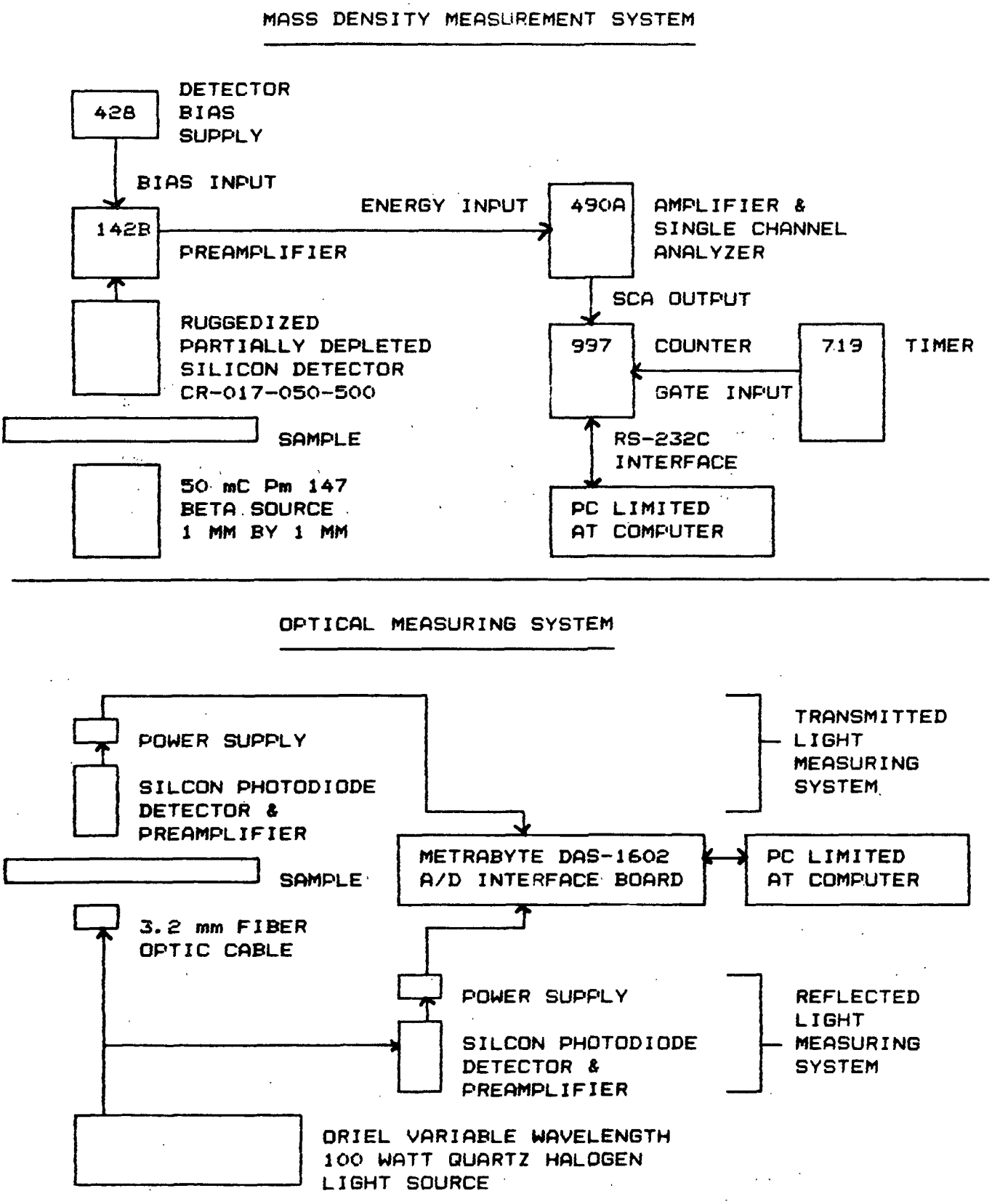

Figure 2. Schematic layout of mass density and optical measuring system for IPC formation tester.

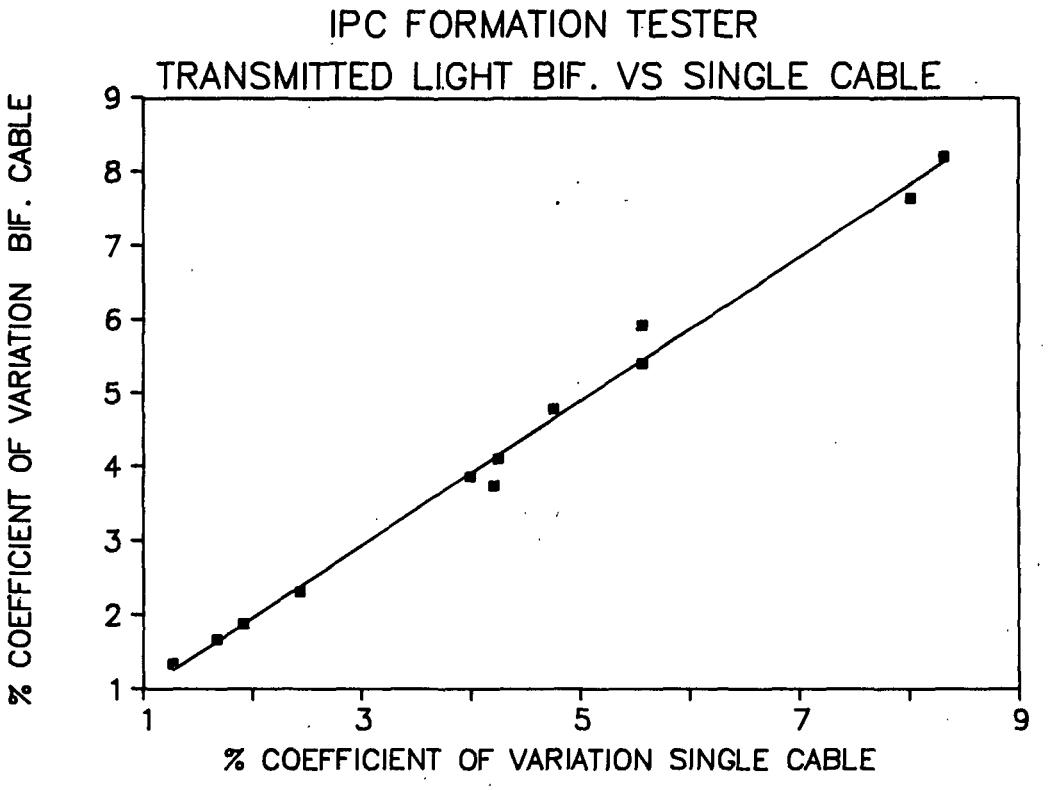

Figure 3. Correlation of formation measurements using the single and bifercated light guide system.

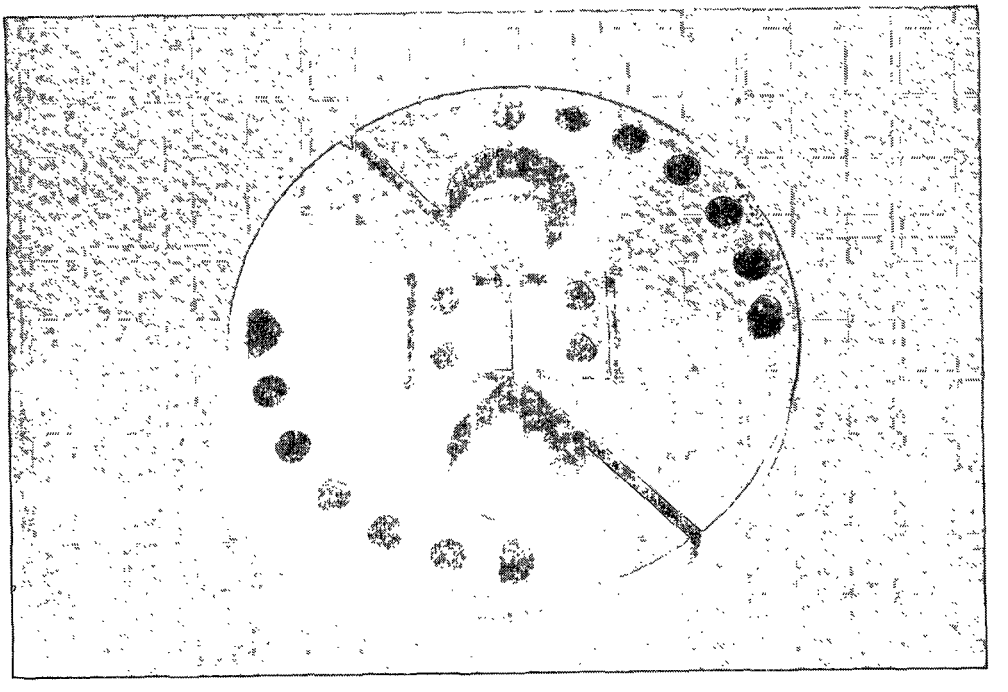

Figure 4. Out-of-plane biaxial fixture with sample and holder in place.

3. COMBINED STRESS MEASUREMENTS

Combined out-of-plane stresses arise in a number of converting and end uses of paper and board such as corrugating, calendering, and adhesive joints.

An out-of-plane biaxial device for measuring the failure envelope of paper and board when subjected to combined out-of-stresses has recently been designed and fabricated. The biaxial fixture together with the sample holder and sample is shown in Fig. 4. This assembly is then installed in an Instron as shown in Fig. 5. Also shown in Fig. 5 are balancing arms which are required to ensure that there are no resultant moments on the sample during testing. Alternative support pillars are also being evaluated, and if successful, should be more convenient to use. The sample holder is also being improved, and a new set are currently being fabricated.

The preferred method of sample mounting is the use of photographic mounting tissue as used for making out-of-plane shear measurements (Waterhouse J. F., Tappi 67(6) June 1984). However to save time, and since we currently have a limited supply of sample holders, we are using double sided adhesive tape for development work. This appears to be suitable for a limited range of testing, i.e. 0° to 30°.

Commercial 42-lb linerboard is being used for the development work and its properties are summarized in Table 10 below. Formette handsheets have also been made to investigate the effects of refining and wet pressing on the out-of-plane biaxial failure envelope. The properties of these sheets are given in Table 11 below.

The variation of failure stress with Instron cross-head speed is shown in Fig. 6 for an angle of 0°, to the z direction using 3-M double sided tape.

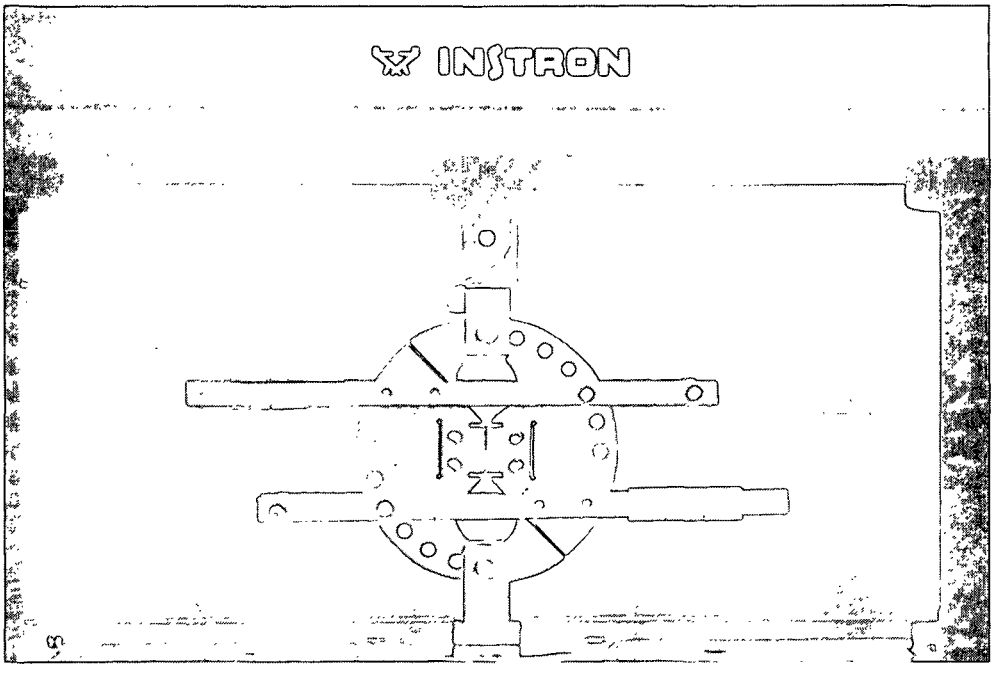

Figure 5. Biaxial fixture with balancing arms installed in Instron.

Table 10. Commercial linerboard properties.

Grammage g/m^2	Caliper µm	Density g/m^3	E/ρ $(k/sec)^2$	R	E_z/ρ $(k/sec)^2$	E_{XZ}/ρ (k/sec^2)	E_{YZ}/ρ (k/sec^2)	Z.D.T. mPa
206.2	295.6	0.698	7.76	2.27	0.053	0.138	0.112	49.2

Table 11. Formette handsheet properties.

Freeness C.S.F.	Grammage g/m^2	Caliper µm	Density g/m^3	E/ρ $(k/sec)^2$	R	E_z/ρ $(k/sec)^2$	E_{XZ}/ρ (k/sec^2)	E_{YX}/ρ $(k/sec^2$
667	313	642	0.487	6.51	2.26	0.144	0.236	0.151
640	310	454	0.682	7.46	2.11	0.226	0.278	0.201
-	312	411	0.759	7.79	2.13	0.264	0.266	0.211
433	299	557	0.537	7.13	1.75	0.163	0.269	0.178
436	288	395	0.730	8.29	1.71	0.245	0.300	0.239
-	295	371	0.796	8.50	1.71	0.265	0.334	0.270

Also shown in Fig. 6 is the ZDT result at 2.4 in./min. Some preliminary failure stress measurements at 0° (pure Z-direction stress) and 90° (pure out-of-plane shear stress) are shown in Table 12. The failure stress at a given cross head speed is higher using the photographic mounting tissue than the double-sided tape. In pure shear, tape rather than sample failure always occurs. The MD failure stress in pure shear, using the MTS mounting tissue, is about a factor of 7:1 higher than the normal failure stress. It is interesting to note that the ratio of MD shear modulus to Z-direction longitudinal modulus is 2.6:1 and the ratio of CD shear modulus to Z-direction longitudinal modulus is 2.1:1. Further measurements will be required to determine if the maximum in failure stress at a cross head speed of 0.10 ins./min is real or some artefact. It does, however, occur for both methods of sample mounting.

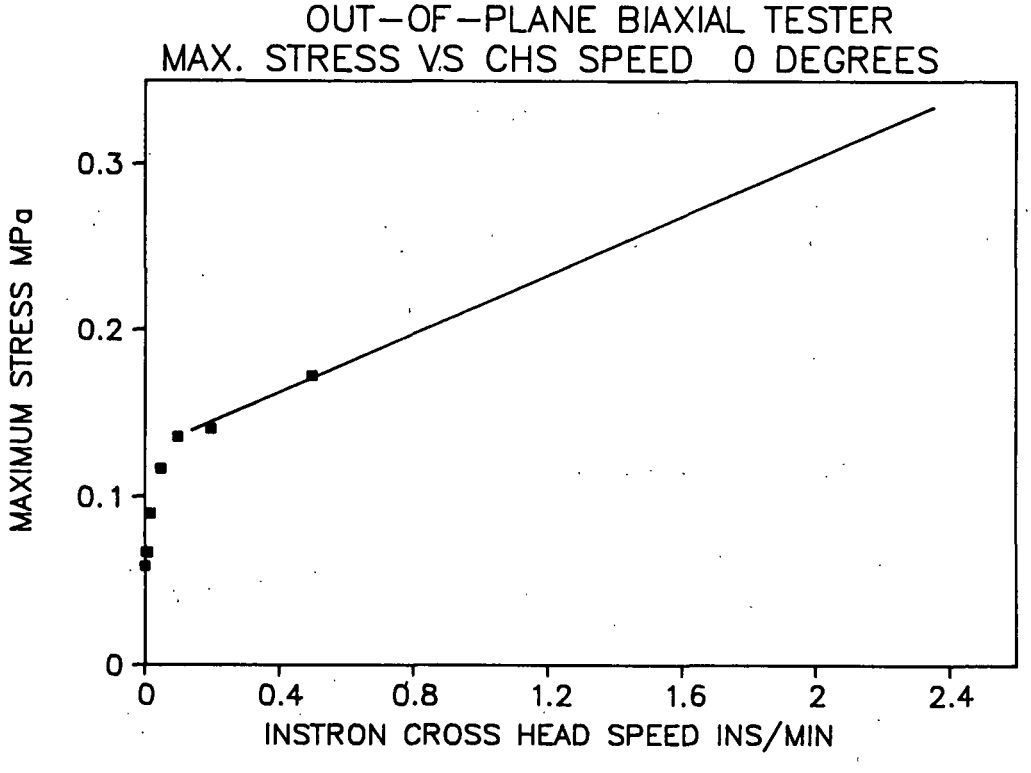

Figure 6. Variation of failure stress with Instron cross head speed at 0°, using 3-M double sided tape.

Table 12. Failure stresses at 0° (normal stress) and 90° (pure shear stress) for different Instron cross head speeds.

C.H.S. in/min	θ	MTS Photographic Mouting Tissue, Failure Stress MPa	3-M Double Sided Tape, Failure Stress MPa
0.002	0°	0.120	0.0590
0.02	0°	0.116	0.0903
0.10	0°	0.275	0.150
0.20	0°	0.207	0.138
0.002	90°	1.26	-
0.02	90°	1.28	-
0.10	90°	1.33	-
0.20	90°	1.24	-

4. INTERNAL STRESSES IN PAPER AND BOARD

The curl of paper and board is a critical problem area in the converting and end use of paper. It is primarily related to differences in hygroexpansivity, from layer to layer in the thickness direction of paper. Factors affecting hygroexpansivity include furnish, bonding, and fiber orientation. Irreversible changes in curl are due to changes in the residual stress distribution induced either through large moisture changes or other stress relaxation processes. A further complexity is the phenomenan of off-axis curl. This mode of curl can arise when the principal elastic axes do not coincide with the MD and CD axes from layer to layer in the thickness direction of paper. The development of the in-plane ultransonic robotic tester is an important new tool for analyzing and understanding off-axis curl.

To better understand the off-axis curl problem and the suitability of the robotic tester in analyzing it, a series of laminated formette handsheets were made. The individual layers were characterized, as well as the laminates, which included a cross laminate of 10°. The sheet properties are summarized in Table 13 below. A possible difference in fines distribution was checked by measuring the freeness of the whole sheet and the individual layers. As is evident from Table 13 C.S.F. differences between the various layers are negligible.

Table 13. Formette handsheet properties for off-axis curl simulation.

#	Grammage g/m^2	C.S.F. ml.	Condition	Density g/m^3	C_{11}/ρ $(k/s)^2$	C_{22}/ρ $(k/s)^2$	C_{33}/ρ $(k/s)^2$	Polar Angle	Polar Area	R $(=E_x/E_y)$
60	-	556	(stock chest)	-	-	-	-	-	-	-
62	-	588	(redispersed sheet)	-	-	-	-	-	-	-
63	-	585	(wire side of sheet)	-	-	-	-	-	-	-
64	71.2	-	(single ply)	0.740	8.26	3.26	0.103	-0.5	107.8	2.53
65	35.6	-	(single ply)	0.627	7.15	2.96	0.077	-0.8	82.4	2.41
70	-	-	(2-ply aligned MD)	0.643	8.28	3.36	0.086	0.8	108.4	2.46
72	-	-	(2-ply 10° to MD)	0.685	7.58	3.07	0.119	-5.9	92.1	2.47

With the large number of transducer impacts required to obtain the polar diagrams, trials were conducted (by C. Habeger and W. Wink) to determine the minimum pressure required to obtain good ultrasonic transducer coupling but avoid "calendering" of the sheet. When these adjustments had been made it was possible to replicate the measurements without affecting the area of the polar

diagram or its symetry. The measurement of the inclination of the elastic axis to the MD of -5.9° is in close agreement with the predicted value of 5°.

Curl measurements were also made using MD, CD and +45° samples taken from sheet #'s 70 and 72. The results are given in Table 14 below for a relative humidity change of 50% to 16.5%. The curl characteristics are different for each sheet and suggest a complex rather than a simple curvature change. The data indicates that even with sheet #70 there is some degree of off-axis curl since $k_3 = k(45°) - 1/2*(k_1 + k_2)$ the twisting curvature is not equal to zero. (Ueasaka, T., Kodaka, I., Okushima, S., and Fukuchi, R. "Curl in Paper (1) A New Approach to the Evaluation of Curl Shape" Japan Tappi 39(10) 953 1985.)

Table 14. Curl measurements, 50% - 16.5% RH.

Direction	Sheet # 70 m^{-1}	Sheet # 72 m^{-1}
MD	3.8	0
CD	-2.5	-2.5
-45°	3.2	-0.3
+45°	-0.5	1.0

A series of commercial fine papers which had exhibited significant off-axis heat set curl were also examined. Polar plots were made on the whole sheet, and on the wire and felt sides which had been produced by surface grinding. It is not only important to know if asymetry is present in the polar diagram, but its origin with respect to the wire and felt sides of the sheet. The results of this investigation are shown in Table 15 below.

Table 15. Summary of polar plot results for whole and surface ground commercial fine papers.

Position Number	Polar Angle	Polar Area $(k/s)^4$	E_{MD}/E_{CD}	Curl Angle	Polar Angle	Polar Area $(k/s)^4$	E_{MD}/E_{CD}
	Whole Sheet				Sections		
161 wire	0.7°	253.1	1.87	-29.0°	1.5°	174.8	1.93
161 felt					-3.3°	160.5	1.98
167 wire	-5.0°	251.4	1.86	27.0°	-7.3°	165.2	1.77
167 felt					0.6°	164.3	1.96
165 wire	-5.5°	252.8	1.84	31.0°	-9.8°	185.6	2.05
					-------- damaged ------		

There are several interesting things to note from these results. The first is that small changes in lean angle can result in large curl angles. This has been predicted by Uesaka, T. (private communication), e.g., for a simple cross laminate of 10° the curl angle is predicted to be ±45°. We note that a negative curl angle is related to a negative polar angle on the felt side of the sheet, while a positive curl angle is related to a negative polar angle on the wire side of the sheet. Asymmetry in fiber orientation distribution due to shake induced cross flows (leading to asymmetry in polar diagrams) was predicted by Finger, E. R. and Majewski, Z. J., Tappi 37 (5) 1954.

We also note in the above table the large change in polar area (i.e. a reduction in mean specific stiffness) of the wire and felt side sections. This may in part be due to damage induced by surface grinding and the release of residual stress. The sheets were intitially flat before surface grinding, but

significant curvature developed after grinding of approximately $12m^{-1}$, which is evidence of internal stress release.

STUDENT RELATED WORK

Titles and brief comments on student related work are given below. It is anticipated that several of the students will present their work at the forthcoming PAC meeting.

A190 Research Projects

1. "Effect of papermaking process variables on Surface Roughness Measurements" - Robert Aloisi.
   This investigation uses a stylus type profilometer to measure surface roughness. The papermaking variables which have been investigated include the level of wet pressing and the influence of wet press felt type. The effects of formation are also being investigated.

2. "A Comparison of Hard Nip and Soft Nip Calendering" - Eero Palogankas.
   This study is mainly concerned with the effects of formation on the response of hard and soft nip calendering. It will also seek to determine if there is a difference in how properties are affected at a given level of densification by these modes of calendering.

3. "Non-destructive Measurement of Aging" Andrew Gau.
   This study will be concerned with how aging (and other degradation mechanisms) can be monitored using ultrasonic and other non-destructive testing methods.

A490 Doctoral Research

1. "Strength Development through Internal Fibrillation and Wet Pressing" - Thomas Bither.

Tom's work has been focussed on trying to determine if a Fracture Mechanics approach can be used to explain the differences in strength development between refining and wet pressing. In particular he is exploring the validity of Griffith's formula to paper. To date he has found envelopes (when apparent density is used as the independent variable) for elastic modulus, average pore size, fracture toughness, and tensile strength. Calculated critical crack sizes are orders of magnitude larger than the average pore size. A strength correlation for refining and wet pressing was found, which only involves the product of elastic modulus and fracture toughness.